# MINERAL PARAGENESIS, GEOCHEMISTRY AND FLUID CHARACTERISTICS OF THE KARA SCHEELITE-MAGNETITE SKARN DEPOSIT, NORTHWESTERN TASMANIA

By

**Blackwell Singoyi**
B. Min. Sc. (University of Zambia, Zambia), P. G. Dip. (ITC, The Netherlands)

A thesis submitted in partial fulfilment for the degree of Master of Economic Geology

University of Tasmania
Centre for Ore Deposit and Exploration Studies, Geology Department
Hobart

September 1995

Dedicated to my mother Siliya Dainess Namukoko, my wife Florence and my children Shirley Nakamba, Mumba and Twiza.

# DISCLAIMER

This thesis contains results of research undertaken at the University of Tasmania from February 1993 to September 1995. It contains no material that has been accepted for the award of a higher degree or graduate diploma in any tertiary institution and contains no material previously published or written by another person, except when due reference is made in the thesis.

Blackwell Singoyi

University of Tasmania
September 1995

# ABSTRACT

The Kara scheelite-magnetite deposit is located in northwestern Tasmania 40km south of Burnie at latitude 41°18' S and longitude 145° 48'E. The deposit consists of several skarn bodies with total remaining mineable ore reserves estimated at 1.7 Mt magnetite @ >30% Fe, and 0.3 Mt scheelite @ 0.52 % $WO_3$ by 1992. The major orebodies at Kara are hosted by limestone or calcareous sandstones of the Ordovician Gordon Limestone Subgroup which are in contact with the Devonian Housetop Granite or separated from it by the Ordovician Moina Sandstone or Owen Conglomerate.

The predominant skarn minerals display a zonation that ranges from epidote-quartz to garnet, magnetite-amphibole, vesuvianite and clinopyroxene zones away from the granite contact. Mineral paragenetic studies reveal at least four stages of skarn formation and ore deposition:

1) Stage I —clinopyroxene-garnet-vesuvianite±wollastonite±quartz±scheelite,

2) Stage II —garnet-vesuvianite-magnetite±scheelite±apatite±quartz,

3) Stage III —magnetite-amphibole-epidote-fluorite±quartz±garnet±vesuvianite ±chlorite±scheelite±sphene±hematite±pyrite±clinopyroxene, and

4) Stage IV —hematite±fluorite±calcite±quartz.

Stages I and II mineral assemblages represent early skarn formation and are dominated by anhydrous minerals of clinopyroxene and garnet. Stages III and IV minerals represent late skarn-forming phases and pervasively replace early mineral assemblages. Scheelite occurs in Stages I-III and generally shows a close spatial association with hydrous minerals (vesuvianite in Stage I/II and amphibole in Stage III). Abundant scheelite is found in Stage III where it forms very coarse grains up to >5cm. Magnetite occurs in Stages II and III but is also more abundant in Stage III.

Microprobe analyses indicate that the majority of the skarn minerals are calcic, and have high $Fe^{3+}/Fe^{2+}$. Clinopyroxene is diopside-rich generally having a mole composition

of >80% diopside and <25% hedenbergite, while garnet composition from Stages I to III are andradite-rich, displaying mole proportions of >70% andradite and <30% grossular. Garnet appears to have the highest levels of tin (up to 0.37 wt. % $SnO_2$) and may be the major carrier of tin in the skarn. Amphiboles are largely of hastingsite and magnesian hastingsite composition. Scheelite contains moderate amounts of molybdenum (<3 wt. % $MoO_3$) which give powellite mole proportions of up to 6% and is unaccompanied by molybdenite.

Fluid inclusion microthermometric measurements of primary fluid inclusions for skarn minerals reveal systematic declining temperatures from early mineral assemblages to later stages, but salinity values are variable. Stage I clinopyroxene yielded a homogenisation temperature range of 460° to 620°C (modes at 520°C and 600°C). The Stage II minerals gave a homogenisation temperature range of 350° to 570°C (mode at 500°C). The Stage III mineral assemblage yielded homogenisation temperatures ranging from 240° to 360°C (mode at 300°C). Stage I clinopyroxene gave salinity values from 2.0 to 10.0 equiv. wt. % NaCl . The Stage II mineral assemblages showed salinities of 12.0 to 16.0 equiv. wt. % NaCl. The Stage III mineral assemblage yielded salinity values of 0.2 to 19.8 equiv. wt. % NaCl (modes at 5 and 15 equiv. wt. % NaCl).

Isotopic measurements of the protolith Gordon Limestone reveal $\delta^{13}C$ composition from -1.6 to -4.4 ‰ (PDB) and $\delta^{18}O$ composition of 10 to 23‰ (SMOW) which are both depleted with respect to the unmetamorphosed Gordon Limestone values ($\delta^{13}C$ = -1.5 to 1.8‰, PDB; $\delta^{18}O$ = 22 to 27 ‰, SMOW). The isotopic compositions of the Stages III and IV skarn calcite range from -1.7 to -7.3‰ (PDB) (mean -4.5‰) for carbon and 3.4 to 14.0‰ (SMOW) (mean 11‰) for oxygen. Calculated isotopic compositions yield $\delta^{13}C_{CO2}$ values of 0.0 to -5.0‰ (PDB) (mean -3‰) and $\delta^{18}O_{H2O}$ values of 0.0 to 10.0‰ (SMOW) (mean 7‰). Depletion in isotopic values for the protolith marble are interpreted to be dominantly due to interaction with magmatic fluids from the nearby granite which are also responsible for the formation of skarn calcite. The values below the magmatic range in the skarn calcite are interpreted to be due to minor contribution from meteoric fluids. Oxygen isotope values of Stages II to III magnetite vary from 2.7 to 4.7‰ (SMOW) and yield $\delta^{18}O_{H2O}$ values of 12.3 to 13.9‰, whereas oxygen isotopic compositions of Stages II to III

scheelite vary from 5.2 to 6.4‰ (SMOW) and yield $\delta^{18}O_{H2O}$ values of 6.0 to 9.0‰. These $\delta^{18}O_{H2O}$ values are generally in agreement with the isotope values from skarn calcite and confirm a magmatic source for the fluids.

The geological, mineral paragenesis, mineral chemistry, fluid inclusion and stable isotope studies indicate that the Kara deposit formed in stages as a proximal skarn assemblage in carbonate host rocks following the emplacement of the Devonian Housetop Granite and was characterised by early, high temperature (up to >600°C) mineral assemblages dominated by anhydrous minerals, and late low temperature (300°C) assemblages with abundant mineralisation (scheelite, magnetite) and hydrous minerals. Fluid inclusion and stable isotope data indicate that early skarn formation was probably solely due to magmatic fluids, while later skarn formation and ore deposition was developed from magmatic fluids mixed with minor meteoric fluids. Chemistries of clinopyroxene, garnet and scheelite (unaccompanied by molybdenite) suggest that the Kara skarn deposit was formed under highly oxidised conditions. The deposit differs significantly from other scheelite deposits such as CanTung in the abundance of magnetite (up to >90 vol. %) and lack of sulphides (eg. pyrrhotite).

# CONTENTS

# LIST OF FIGURES

# LIST OF TABLES

# ACKNOWLEDGMENTS

I wish to acknowledge the assistance and generosity of the following people and institutions:

• AusAID for the scholarship which allowed me to undertake this research.

• Dr. Khin Zaw, my supervisor, for his excellent guidance and discussions throughout the project. I also thank him and his family for his generosity towards my family.

• Dr. J. Bruce Gemmell for helpful discussions during the early stages of the project.

• Dr. Paul Kitto for his ideas, guidance and critical reading of some of the thesis Chapters.

• Mr. Mick McKeown and other staff of Tasmania Mines N. L. Limited, operators of the Kara Mine, are acknowledged for allowing me access to their records and mine area.

• Dr. R. Berry for the discussions and ideas on skarn mineral chemistry.

• Mr. Simon Stephens for preparing thin/polished and fluid inclusion sections.

• Mr. Wieslaw Jablonski for assisting with the microprobe analysis.

• Dr. Noel Davies for helping with fluid inclusion gas mass spectrometry.

• Dr. Gerrit Kuipers and Mr. Mike Power for the oxygen and carbon isotope analyses.

• Prof. Ross R. Large and Staff, postgraduate and honours students of CODES and the Geology Department, too numerous to mention, are thanked for their friendliness and willingness in sharing their ideas and knowledge.

• I must also thank all lecturers and participants of the CODES short courses for their contributions from which I benefited greatly.

• Staff of the International Student Office are thanked for welcoming me to Hobart.

• Ms. Robin Bowden of AusAID, Hobart Office, for her kindness and assistance on social and cultural matters.

• Mrs. Louise Oxley of the International Student Office for proof-reading this thesis.

• Mrs. Vina and Mr. Reg Gee, my Australian host-family, for giving me and my family a wonderful and memorable time in Australia.

• Mrs. Lilian Wilson and Mr. Ken Hayes of Hobart were very generous to my family, for which I am very appreciative.

• I also wish to thank my wife, Florence, my children, Shirley Nakamba, Mumba and Twiza for the good company and for standing by during my time in Australia. I am also very grateful to Florence for typing parts of the thesis.

• Other international students including Mr. Elkana Ngwenya (Zimbabwe) and Ms. Tuelo Nkwane (Botswana) are thanked for their moral support especially during my first months in Hobart.

# CHAPTER 1: INTRODUCTION

## 1.1. LOCATION AND FIELD CONDITIONS

The Kara deposit is located 40 km south of Burnie in northwestern Tasmania at latitude 41°18' S and longitude 145° 48' E (Fig. 1.1). The area is characterised by an undulating topography, a dense cover of eucalypt and rain forest, and thick weathering soil profiles of up to 15 m or more. Good rock exposures are mostly found in open cuts. The area is easily reached by a nine kilometre tarred and gravel road from Hampshire which is situated on the Burnie-Queenstown Highway.

## 1.2. EXPLORATION HISTORY

The exploration and mining history at Kara and the surrounding region have been reported by various workers including Barrett (1980), Richards and Jones (1981) and Whitehead (1990). The Kara deposit area was first pegged in 1968 by Tasminex NL Limited (now Tasmania Mines NL limited). Since then, the company has investigated the prospect jointly with ANZECO (Australia New Zealand Exploration Company) and McIntyre Mines (Australia) Pty Limited. The initial exploration involved a combination of geological mapping, stream sediment sampling (panning) and aeromagnetics. The metals sought included W, Cu, Pb, Zn, Bi, Mo, Au and Ag. Exploration companies used the concept that scheelite mineralisation was related to magnetite-bearing skarns in formulating their exploration models. Ground magnetics and soil sampling techniques were employed in follow-up surveys. The skarns were located mainly by stream sediment panning and airborne and ground magnetic techniques. Drilling campaigns involving several diamond drill holes varying in depth from about 40m to 140m have been undertaken to establish ore reserves at Kara.

Mining at Kara is by open cut and has concentrated on the Kara No. 1 orebody since its commencement in 1977. To June 1989, a total of 1.6 million tones of ore had been

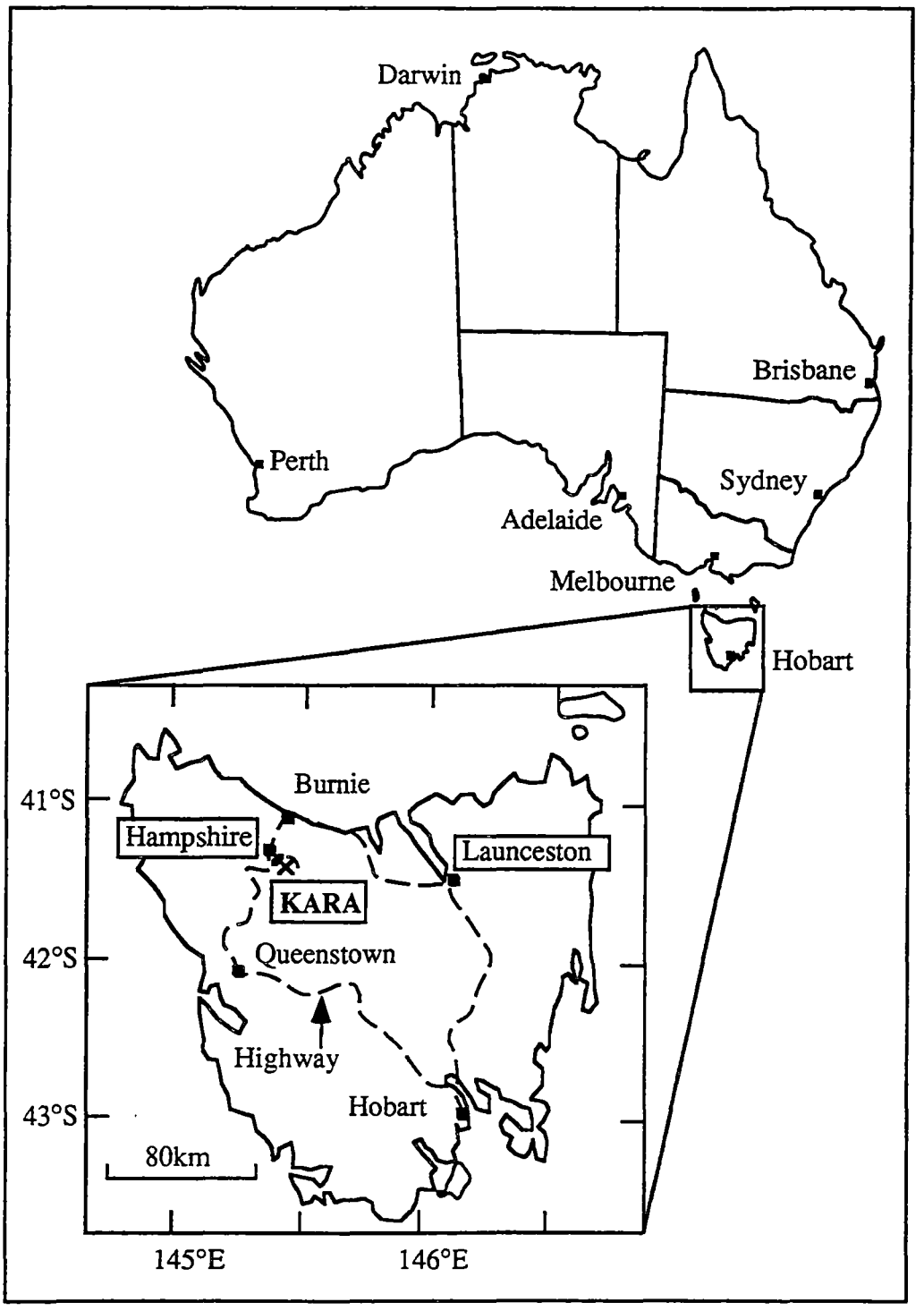


Fig. 1.1. Map showing the location of the Kara skarn deposit, northwestern Tasmania.

mined giving 2 958 tonnes of high grade concentrates containing >65% $WO_3$ and 1.8% Mo (Whitehead, 1990). The Kara skarns have been re-assessed several times (e.g. Whitehead, 1985 and 1992) and are becoming increasingly more important for magnetite resources. Estimates from company reports to 1992 show total remaining mineable reserves of 1.7 Mt magnetite ore @ >30% Fe, and 0.4 Mt scheelite ore @ 0.75% $WO_3$. Potential scheelite reserves from Kara North 266 Zone, Bobs' Bonanza, Eastern Ridge and L5 Zone are 0.7 Mt scheelite ore @ 0.9% $WO_3$. Plumbridge (1986) considers that the full potential of the Kara skarn system has not been determined due to combined effects of basalt cover and destruction of scheelite during chemical weathering.

## 1.3. PREVIOUS STUDIES

The Kara area has been investigated and mapped by staff of the Mines Department (now Mineral Resources of Tasmania) and geologists from private exploration companies. Many previous workers have undertaken geological studies on the deposit and the associated granitoid. Reports and detailed geological maps of the area are available at the Mineral Resources of Tasmania and from Tasmania Mines NL Limited which is currently operating the deposit. The reports and papers include those by Reid (1924), Hughes (1950), Longman (1961), Baillie et al. (1986), Collins et al. (1989) and Whitehead (1990). An honours research thesis examining conditions of skarn formation has also been undertaken by Barrett (1980).

These early investigations have shown that the majority of skarn orebodies at Kara are developed within Ordovician sedimentary units (calcareous sandstone and limestone) close to the Devonian granitoid. The rocks in the area range in age from Cambrian to Recent. Early works also show that prior to the Devonian granite intrusion, the rocks were deformed largely by folding during the Mid-Palaeozoic Tabberaberran Orogeny (Williams, 1989). The deposit is considered to be genetically related to the Devonian Housetop Granite. Although mineralogical studies by company consultants and Barrett (1980) indicate that there is a variety of skarn assemblages from garnet, clinopyroxene, vesuvianite, epidote, amphibole to fluorite, no detailed paragenesis has been established. Barrett (1980) also

reported fluid inclusion salinity and temperature data, but no detailed relationship with the formation of skarn assemblages was shown.

## 1.4. REVIEW OF SKARN TERMINOLOGY AND SCHEELITE/MAGNETITE SKARN DEPOSITS

The terminology and genetic processes associated with skarns have been discussed and reviewed in numerous papers (eg. Sato, 1980; Einaudi et al., 1981; Kwak and Askins, 1981; Kwak, 1986; Newberry and Swanson, 1986; Meinert, 1992; Kwak, 1994). In this section, a summary of skarn terminology and the skarn-forming processes with emphasis on tungsten and iron skarn deposits will be presented.

Many skarn deposits form under changing physical and chemical conditions. This has been demonstrated for many skarn deposits including the following: King Island scheelite deposit (Large, 1972; Kwak, 1978; Kwak and Tan, 1981), Renison Bell tin deposit (Patterson et al., 1981; Kitto, 1994), Moina fluorite-tin-tungsten skarns (Kwak and Askins, 1981), Cleveland tin deposit (Collins, 1983) and Mt. Lindsay tin-tungsten-fluorite-beryllium skarns (Kwak, 1983) in Tasmania; Fujigatani tungsten mine (Sato, 1980) in southwest Japan; Lost River tin-tungsten-fluorine deposit, Alaska (Dobson, 1982) and Pine Creek tungsten deposit, California (Brown et al., 1985; Brown and Essene, 1985) in USA; CanTung E Zone Orebody, Northwest Territories (Khin Zaw, 1976; Khin Zaw and Clark, 1978; Mathieson and Clark, 1984), JC tin deposit, Southern Yukon Territory (Layne and Spooner, 1991) in Canada and Sangdong scheelite deposit (Moon, 1983) in South Korea.

### 1.4.1. Skarn terminology

Skarns have been classified using various criteria which include the following:

(1) Contained dominant minerals.

(2) Contained dominant economic metal.

(3) Sedimentary or igneous protolith (exoskarn or endoskarn).

(4) Calcium and magnesium content of protolith carbonate.

(5) Genetic criteria such as reduced and oxidised conditions, and depth of formation.

(6) Distance from igneous contact (proximal or distal).

(7) Metamorphic and ore skarn. For this criterion, Kwak (1994) describes metamorphic skarns as those formed by isochemical metamorphism and ore skarns as skarns formed by metasomatism. Metamorphic skarns pre-date ore skarns.

In this study the term skarn refers to replacement rocks formed as a result of metasomatic reaction caused by hydrothermal fluids. The protolith may be a sedimentary or an igneous rock. Hydrothermal fluids may be sourced from a variety of reservoirs (e.g. igneous, metamorphic, meteoric and marine). The term skarn is used as a descriptive term based on the contained dominant mineralogy, and is free of genetic implications as suggested by Einaudi et al. (1981). Exoskarn and endoskarn are used to indicate a sedimentary and granite (intrusive) protolith respectively as defined by Meinert (1992). Skarn deposits are skarns that contain economic mineralisation and are subdivided into several main types as defined by Meinert (1992) who divided them into the following types: W, Fe, Cu, Sn, Zn and Au.

The Kara skarns contain scheelite (tungsten) and magnetite (iron) as the dominant economic commodities and can therefore be classified as scheelite and magnetite skarn deposits on the basis of the dominant economic metal. Scheelite and magnetite skarn deposits are discussed below.

### 1.4.2. Scheelite skarn deposits

Skarns form one of several classes of tungsten deposits. Tungsten occurs principally as tungstates in form of scheelite ($CaWO_4$) and wolframite ($Fe,MnWO_4$). The principal scheelite skarn deposits are associated with plutons that are emplaced at moderate crustal levels (hypabyssal) (e.g. the Pine Creek skarn deposit, California, U.S.A, Newberry and Einaudi, 1981; Brown and Essene, 1985). Newberry and Swanson (1986) and Meinert (1992) have also argued that relatively deep environments favour the formation of scheelite skarn deposits and pointed out that these deposits are found in continental environments that are associated with the following tectonic settings:

(1) continental subduction environment with accreted oceanic terrain and

(2) continental rifting environment.

Scheelite skarn deposits are largely developed within carbonate protoliths and are commonly associated with calc-alkaline plutons (Meinert, 1992). The tungsten sources in most of these scheelite deposits are believed to be felsic intrusions. For example, Kwak (1978) and Dick and Hodgson (1982) demonstrated that for many scheelite skarn deposits such as King Island in Tasmania and CanTung and MacTung in Canada, host rocks do not contain enriched tungsten levels relative to average sedimentary rocks. They concluded that the source of the bulk tungsten in these deposits is magmatic in origin. However, in some scheelite skarn deposits, the tungsten is considered to originate from the intruded host rocks (e.g. Otjua scheelite-fluorite skarn in Namibia, Steven and More, 1994). These scheelite plutons neither possess a particular chemical composition nor are they rich in tungsten, but they are however highly fractionated (Newberry and Swanson, 1986).

### 1.4.3. Magnetite (iron) skarn deposits

Iron (magnetite) skarn deposits form the largest skarn deposits (e.g. >50Mt @ 45% Fe, Mojave Desert Region, Eagle Mountain, U.S.A., Hall et al., 1988) and are chiefly mined for their magnetite (Meinert, 1992). They contain minor silicate gangue minerals predominantly of garnet and pyroxene and can be divided into two types: 1) calcic iron skarns that occur in oceanic island arcs, and which are associated with iron-rich plutons that intrude limestone and volcanic wall rock, and 2) magnesian iron skarns which are associated with diverse plutons in a variety of tectonic settings from continental subduction to oceanic island arc settings. In the magnesian iron skarn, the iron is used up in magnetite crystallisation causing gangue minerals to be impoverished in iron. Meinert (1992) has also reported that iron skarns may contain appreciable levels of gold as well.

## 1.5. AIMS AND SCOPE

The purpose of the present study is to undertake mineralogical and geochemical investigations to:

(1) document the temporal and spatial distribution of the skarn minerals,

(2) establish a comprehensive paragenetic relation of skarn and ore (scheelite and magnetite) minerals,

(3) characterise the mineralogical and geochemical controls on the skarn- and ore-forming processes,

(4) place tight constraints on the source(s) of skarn and ore fluids during skarn development,

(5) determine factors or features controlling ore deposition,

(6) generate a genetic model of skarn formation and ore deposition and compare the deposit with other skarn deposits, and

(7) propose an exploration model for the scheelite skarn-type deposit based on the genetic model generated.

## 1.6. METHOD OF STUDY

The present study includes field and laboratory investigations and employs the following methods and phases to achieve the aims of the research:

(1) a re-logging of the previous drill cores, detailed studies of outcrops and sampling.

(2) an examination of the distribution of metals along drill holes and on sections to understand the ore element relation with variation in skarn type,

(3) mineralogical and paragenetic studies,

(4) electron microprobe analysis of individual skarn and ore minerals to determine their compositional variations and infer conditions of skarn formation and ore deposition,

(5) fluid inclusion studies to determine the homogenisation temperatures, salinities and volatile contents during skarn development.

6) oxygen isotope analysis of scheelite and magnetite to constrain the source(s) of ore-forming fluid, and

(7) carbon and oxygen stable isotope studies of carbonates to evaluate source(s) of carbon and oxygen and infer skarn and ore fluid histories.

# CHAPTER 2: REGIONAL AND DEPOSIT GEOLOGY

## 2.1. INTRODUCTION

The Kara magnetite-scheelite deposit is one of many replacement deposits associated with Devonian granitoids in northwestern Tasmania (Fig. 2.1). The regional geology of the area has been described and summarised by many authors including Barrett (1980), Baillie et al. (1989), Banks and Baillie (1989), Brown (1989), Collins (1989), Turner (1989), Williams et al. (1989), Green (1990) and Kitto (1994). The geological setting of the deposit area has been mapped in detail by staff from Mineral Resources of Tasmania, and personnel from Tasmania Mines Limited and their predecessor companies. A brief description of the regional geological setting and deposit-scale geology of the area is given below.

## 2.2. REGIONAL GEOLOGY

The regional geology of the Kara deposit area is characterised by Late Pre-Cambrian to Recent volcano-sedimentary sequences and Devonian granitoids. The Kara deposit area occurs between two PreCambrian blocks: Rocky Cape to the north and the Tyennan block to the south. The Pre-Carboniferous regional geology of the Kara deposit area is shown in Fig. 2.1.

### 2.2.1. Sedimentary and volcanic sequences

Late Pre-Cambrian to Quaternary sedimentary and volcanic rocks are widely exposed in the area. Pre-Cambrian rocks form the basement of the area and consist of interbedded quartzose lithic wacke, phyllite, and minor dolomite that are correlated to the Burnie and Oonah Formations. These rocks crop out to the west, north, and south of the area. The Pre-Cambrian rocks are unconformably overlain by Cambrian to Lower Devonian units. Cambrian rocks are divided into the Success Creek Group and the Creemson Creek Formation. The Success Creek Group contains siliceous sandstone, mudstone, dolomite

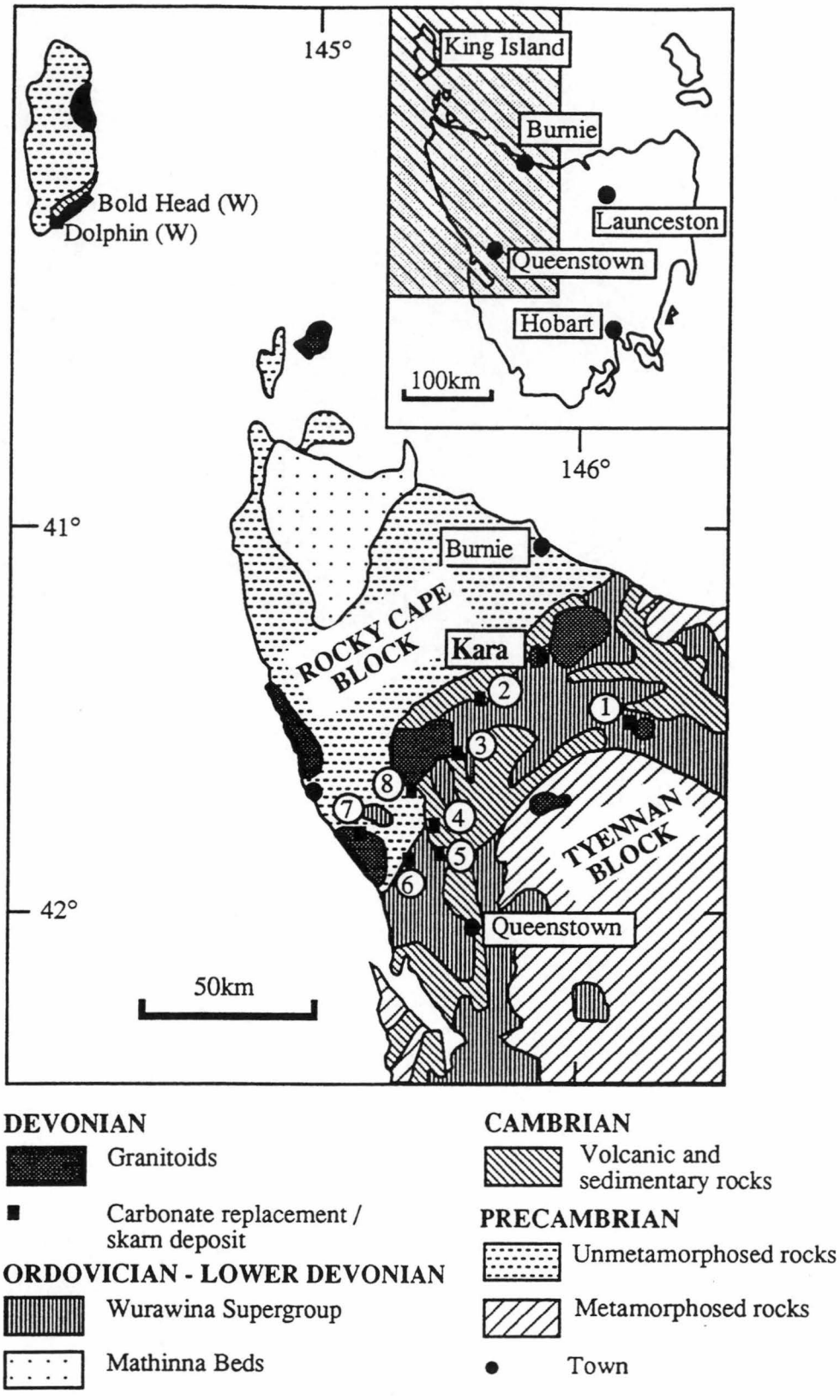


Fig. 2.1. Pre-Carboniferous geology and location of the Kara skarn deposit, together with other Devonian replacement deposits of northwestern Tasmania. 1, Moina, Sn-W-F; 2, Mt. Bischoff, Sn; 3, Cleveland, Sn-Cu; 4, Renison, Sn; 5, Razorback, Sn; 6, Zeehan, Sn; 7, St. Dizier, Sn-Fe; 8, Mt. Lindsay, Sn-W-F. Adapted from Collins et al. (1989).

andbreccia, whereas the Creemson Creek Formation consists of mafic volcanic and volcano-sedimentary rocks. Ordovician to Lower Devonian rocks comprise the Mathinna beds and the Wurawina Supergroup. The Wurawina Supergroup crops out at Kara and the adjacent area. Banks et al. (1989) divided the sequence into the Denison, Gordon and Tiger Groups from lower to higher stratigraphic level. The Denison Group (locally Moina Sandstone and Owen Conglomerate) is made up of conglomerate, sandstone, siltstone and argillite. The Gordon Group (locally known as Gordon Limestone) consists of carbonates, whereas the Tiger Group comprises grotty quartzite with limestone fragments.

Tertiary and Recent rocks are widespread and form a cover that conceals most of the older geology including mineralisation. Tertiary rocks consist of basalt and sedimentary units of sand and gravel. Recent sediments consist of transported and insitu gravel to clayey materials.

### 2.2.2. Devonian granitoids, deformation and ore deposits

The Housetop Granite is an important granitoid body in the area and is one of a series of Devonian granitoids of northwestern Tasmania (Fig. 2.1). These granitoids intrude volcano-sedimentary successions ranging in age from Pre-Cambrian to Lower Devonian and are spatially associated with many carbonate replacement deposits. Gee and Groves (1971) considered the mechanism of the intrusion to have been passive, mainly by upward displacement. McClenghan et al. (1989) noted that the Devonian granitoids have been emplaced at high crustal level with narrow contact aureoles. For the Housetop granitoid, gravity and magnetic interpretations by Leaman (1989) indicate that the intrusion is characterised by intermediate slopes, with depths of up to >5km (Fig. 2.2). McClenghan et al. (1989) reports Late Devonian ages (Rb/Sr) of 367±10 Ma to 319± Ma. Sawka et al. (1990) have also reported $^{40}K/^{39}Ar$ ages of 369.4 Ma for the Housetop Granite. The Devonian Granitoids of western Tasmania (including the Housetop Granitoid) represent a diverse assemblage of highly fractionated intrusions (Sawka et al., 1990). Regional studies from the Housetop Granite by Sawka et al. (1990) and studies from the Kara deposit by Barrett (1980) show that the granitoid is highly fractionated with $SiO_2$ values of 70-77%.

The Housetop Granite exhibits compositional affinities to a fluorine-rich I-type magma (Sawka et al., 1990).

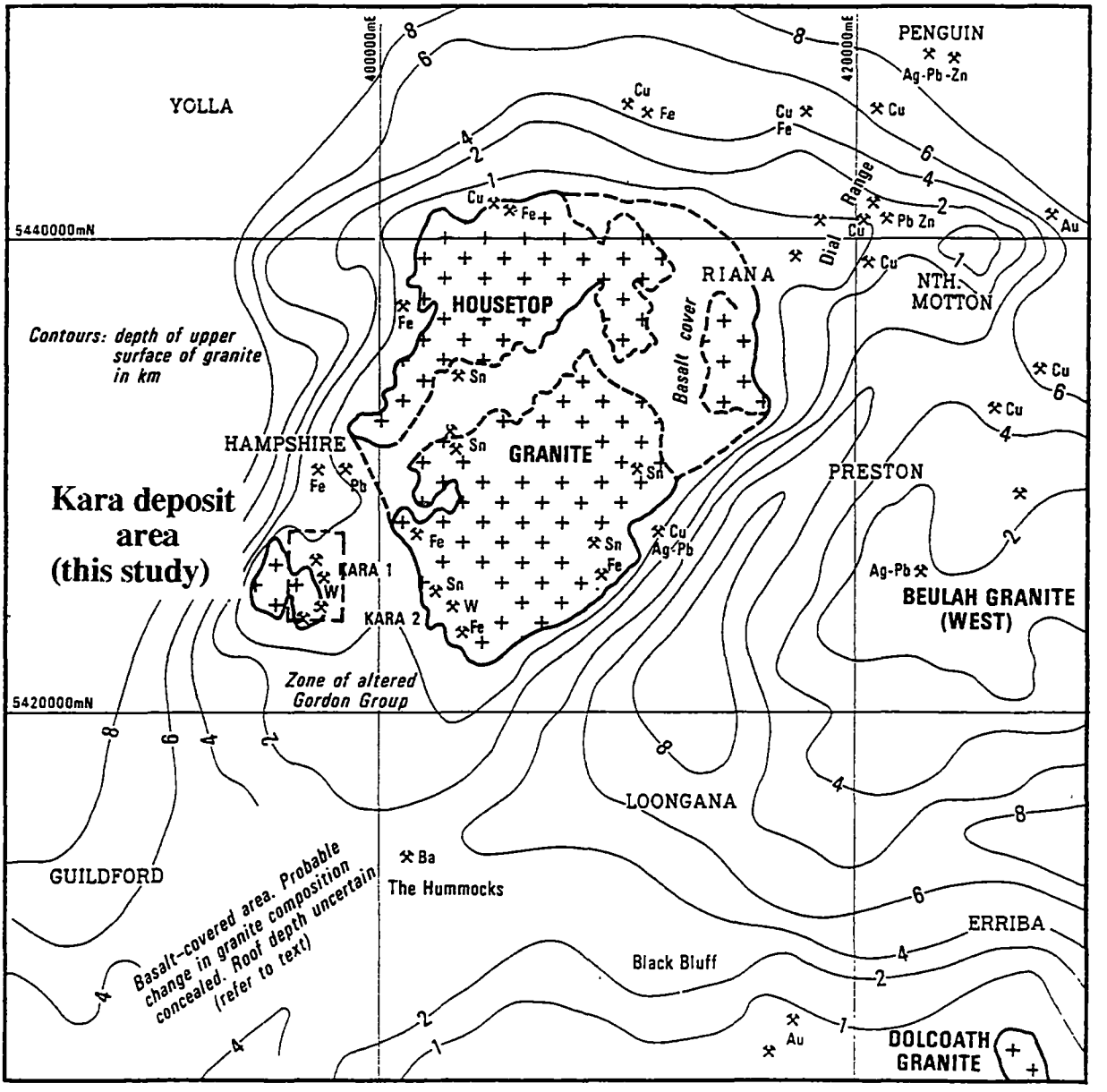


Fig. 2.2. Geophysical interpretation of subsurface form of the Housetop Granite and spatially associated mineral occurrences including the Kara deposit area, northwestern Tasmania. After Leaman (1989).

Leaman (1980) suggests that the Devonian granitoids of western Tasmania form a NNW trending zone from the southern part of the State to King Island on the far northwestern part of the State. In contrast, the Devonian granitoids comprising the Pieman,

Meredith, Heemskirk, Granite Tor and the Housetop in northwestern Tasmania reveal an ENE trend that is also supported by aeromagnetics. This ENE trend generally coincides with an area of Mid-Palaeozoic deformation lying between the Rock Cape and Tyennan blocks which is largely occupied by Cambrian, and Ordovician to Lower Devonian lithologies (Fig. 2.1). The major Mid-Palaeozoic structures are folds, and these deformation structures have been correlated to the Tabberabberan deformation of eastern Australia (Williams et al., 1989). Emplacement of Devonian intrusions postdates and truncates the Mid-Palaeozoic structures. The spatial association of the west Tasmanian Devonian granitoids with the Mid-Palaeozoic deformation zone appears to suggest that the intrusions were focussed by a structurally weak zone that resulted from the Tabberabbaran tectonic event or other earlier events in the Cambrian period. The cause of the melting that resulted in the formation of the Devonian granitoids is not well understood. Coney (1992) has suggested that the emplacement of the Lachlan granitoids in eastern Australia was triggered by continental-oceanic collision of the proto-Pacific plates to the east of the Lachlan fold belt. Wesolowski et al. (1988) also attributed the emplacement of the Devonian granitoids that are associated with the King Island scheelite skarn deposits to a Mid-Palaeozoic subduction event. Emplacement of the Housetop Granite together with other western Tasmanian Devonian granitoids can also be ascribed to the continental-oceanic collision of the proto-Pacific plates to the east of the Lachlan fold belt as pointed out by Berry (1995, Pers. Comm.).

Williams et al. (1989) also indicates that the Mid-Palaeozoic granitoids are associated with the Mid-Palaeozoic ore deposits of scheelite skarns, cassiterite-stannite-pyrrhotite carbonate replacement bodies, argentiferous lead-zinc veins and probably gold deposits. Around the Housetop granite, numerous mineral occurrences are found in close proximity to the granite (Fig. 2.2), and Leaman (1989) points out that these occurrences are found within a distance of 1-1.5km from the intrusion.

## 2.3. DEPOSIT GEOLOGY

The geological setting of the magnetite-scheelite deposit at Kara has been studied by

geologists from Tasmania Mines Limited and the predecessor companies, staff of the Minerals Resources of Tasmania (e.g. Baillie et al., 1986; Reid, 1924) and other workers (e.g. Barrett, 1980; Hopwood, 1985). The Kara deposit area is characterised by a volcano-sedimentary sequence varying in age from Cambrian to Recent and a Devonian granitoid intrusion (Fig. 2.3.). The Cambrian to Ordovician sequence is deformed, and has been intruded by Devonian granites. Several skarn bodies are found in the Pre-Carboniferous sedimentary rocks adjacent to the Devonian Granite. Tertiary to Recent rocks form a cover which has hidden much of the older geology in the mine area. Here, a summary of the deposit geology based on the earlier works and the author's own observations made during this study is presented.

### 2.3.1. Cambrian - Ordovician sequence

Cambrian rocks form the oldest rock units, and are exposed to the north-west of the deposit area. The Cambrian sequence consists of laminated cherty mudstone interbedded with carbonates (Baillie et al., 1986), with contact rocks that are commonly transformed to hornfels, marble and in places to metamorphic skarn assemblages. This sequence may also contain pyrrhotite (Barrett, 1980). The Ordovician units comprise conglomerate (Owen Conglomerate), sandstone and argillite (Moina Sandstone correlate), and limestone and impure limestone (Gordon Subgroup correlate). The Owen Conglomerate and the Moina Sandstone correlate forms the Denison Group of Banks et al. (1989). Hopwood (1985) reported Cambrian cherts passing to the Owen Conglomerate, to a sequence of quartzite (Moina Sandstone) and to sandstone and quartzite containing calc-silicate units (basal parts of the Gordon Limestone) in the northwestern part of the deposit area and correlated this sequence to that observed at the Cleveland tin deposit, northwestern Tasmania.

The Owen Conglomerate unit is massive, poorly bedded, largely consisting of quartz, and rounded to subrounded quartzite pebbles and cobbles in argillite matrix. Barrett (1980) also recorded volcanic clasts in the unit. The Owen Conglomerate unit varies from being pebbly to matrix-supported. The Moina Sandstone unit is extensively exposed in the mine area and lies stratigraphically above the Owen Conglomerate. The Sandstone unit is

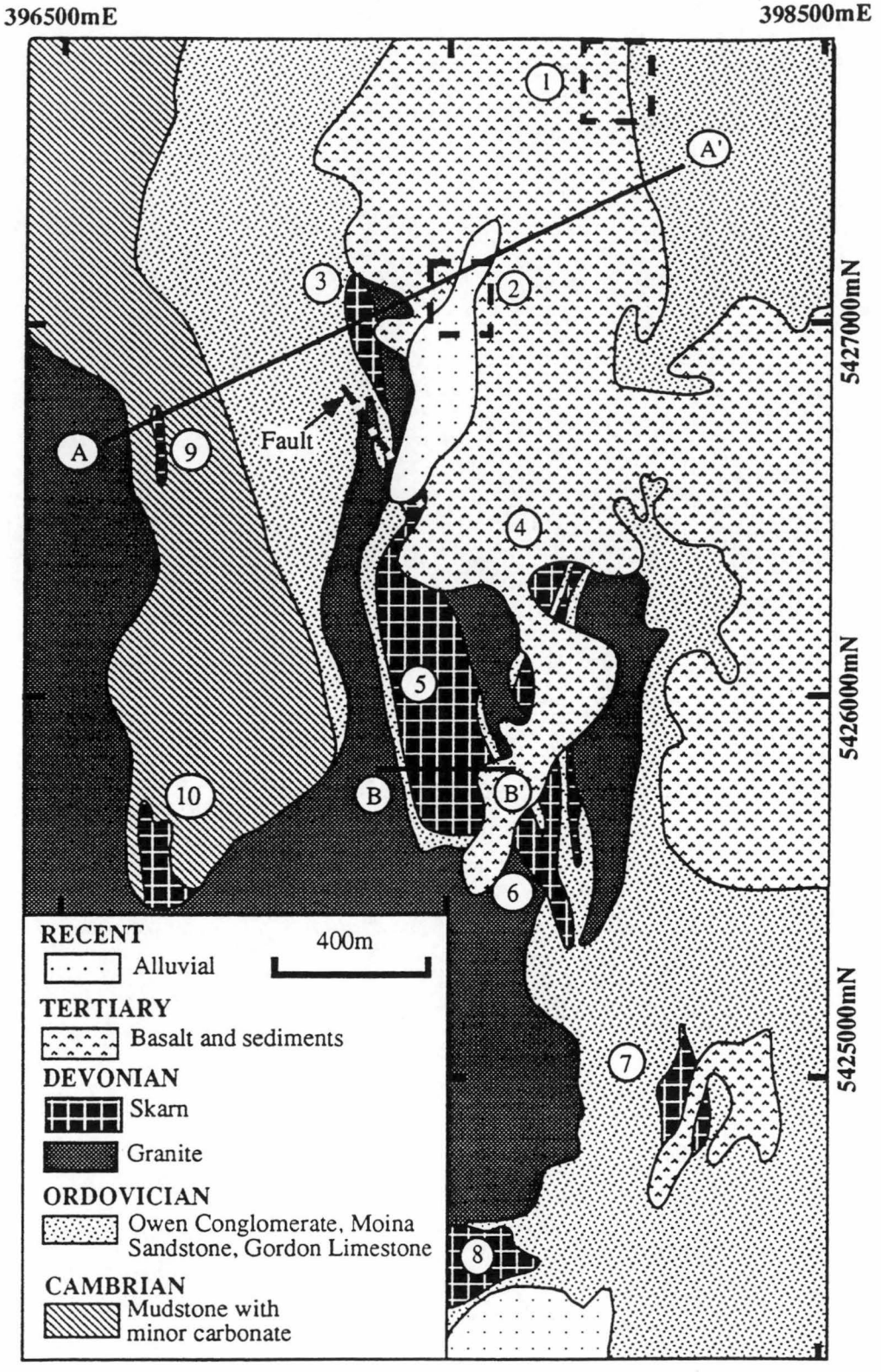


Fig. 2.3. Deposit geology and skarn bodies of the Kara area, northwestern Tasmania. 1, L5; 2, Kara North Magnetic Zone; 3, Kara North 266 Zone; 4, Eastern Ridge; 5, Kara No. 1; 6, Bobs Bonanza; 7, Lohreys Pit; 8, Kara south; 9, L10; 10, L9.). Adapted from geological maps of Tasmania Mines Limited. A-A' and B-B' are locations of cross-sections given as Figs. 2.5, 4.2 and 4.5.

massive to weakly bedded, coarse- to fine-grained and argillaceous. It is predominantly composed of quartz clasts with a matrix of finer quartz and clays, and shows reddish colouration of iron oxide and hydroxide. Close to the granite contact, the rock is massive, compact and hornfelsed. Thin section studies reveal the development of epidote and chlorite within the matrix of quartz clasts in hornfelsed sandstone (Fig. 2.4A). The Gordon Limestone is restricted to the north of the deposit area, and appears to have been converted to skarns in the south where carbonate rocks are not intersected by drilling. The impure limestone overlies the Moina Sandstone and is known in the Tasmania Mines Limited literature as Transitional Series (e.g. Whitehead, 1985).This impure limestone consists of sandstone intercalated with carbonates, and is overlain by limestone which commonly occurs as recrystallised marble. This marble is massive and coarse-grained.

### 2.3.2. Granite

Granite is exposed in open cuts (Kara No. 1, Bob's Bonanza and Lohreys' Pit) and on the surface in places. The granite may occur in contact with skarns (Fig. 2.4B) and is intersected in drill cores from several skarn bodies. It is pink, massive, coarse-grained and equigranular, although porphyritic and medium-grained varieties are observed in places (Figs. 2.4C1-2.4C3). The granite is composed of K-feldspar (~35 volume %), quartz (~35 volume %), plagioclase (~25 volume %) and accessory minerals (~5 volume %) consisting of biotite, muscovite, epidote, hornblende and magnetite. Epidote, black to green amphibole (hornblende to hastingsite) and some of the magnetite occur as secondary minerals in the granite. Amphibole appears to replace biotite. The granite generally shows increasing intensity of alteration towards its margin, with feldspars being altered to sericite or epidote (Figs. 2.4C2 and 2.4D). Calcite and fluorite are also noted as veins in the altered zone. The contact zone between the granite and the Moina Sandstone is commonly fractured and consists of broken granite and sandstone fragments. This fragmentation is probably due to hydraulic pressures induced by late hydrothermal fluids emanating from the granite intrusion. Within the granite, the fragments contain matrix or linings of skarn minerals (epidote, quartz, and amphibole).

Fig. 2.4. Micro- and macro-photographs of rocks from the Kara skarn deposit, northwestern Tasmania.

**A.** Contact metamorphosed sandstone composed of clasts of quartz (Qtz) within fine-grained altered matrix (Alt) of epidote and chlorite.

**B.** Granite intrusion (Gra) adjacent to banded skarn (skarn) at Kara No. 1.

**C1.** Medium-grained equigranular feldspar - quartz granite with veins and replacements of epidote (Ep) and amphibole (Amp).

**C2.** Coarse-grained equigranular feldspar-quartz granite. Note greenish sericitic material (Alt) surrounding feldspar.

**C3.** Feldspar-quartz phyric granite.

**D.** Microphotograph of an altered coarse-grained feldspar (Fsp)-quartz (Qtz) granite. Note preferential alteration (Alt) of feldspar to epidote (Ep).

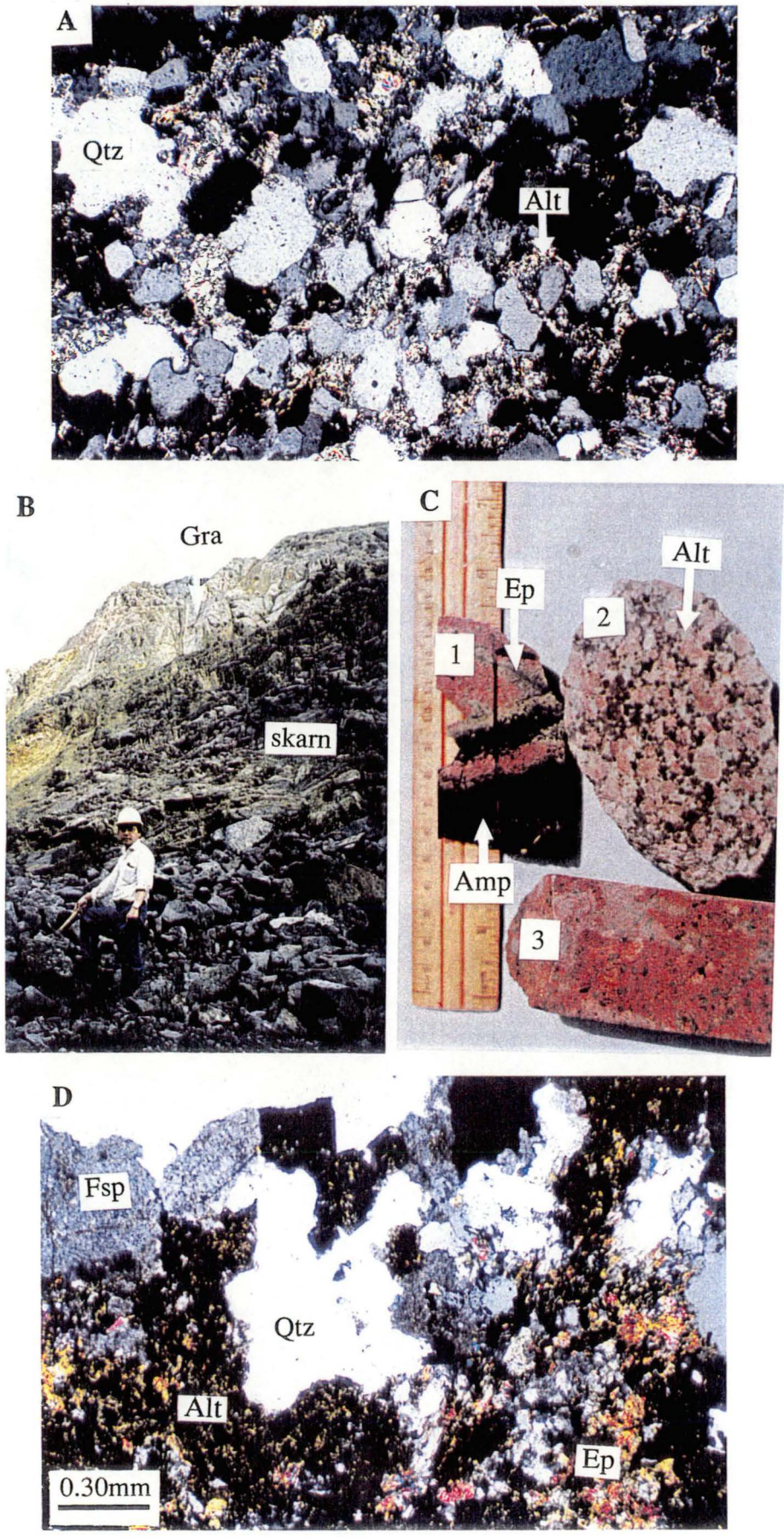


Fig. 2.4

### 2.3.3. Skarn bodies

The Kara magnetite-scheelite deposit consists of several skarn bodies that include: Kara South, Kara No. 1, Bobs Bonanza, Kara North 266 and Magnetic Zone, and L5 (Fig. 2.3). The majority of these bodies have developed within the Ordovician sequence of the Gordon Limestone Subgroup which is stratigraphically above the Moina Sandstone. They occur in the lower part of the Gordon Group and comprise carbonates and sandstone (impure limestone or Transitional beds); and are also considered to have developed in the upper part of the Gordon Subgroup which is mostly comprised of limestone in the southern skarn bodies (e.g. Kara No. 1 and Bob's Bonanza) where no carbonates are found. The skarns are in direct contact with the granite but may be separated from it by a thin layer of the Owen Conglomerate or Moina Sandstone away from the contact (Figs. 2.3 and 2.5). Subordinate skarns are found within the Cambrian sequence (e.g. L9 and L10, Figs. 2.3 and 2.5) and are considered by many workers (e.g. Hopwood, 1985) to have developed in calcareous horizons of the Cambrian sedimentary sequence which has not been differentiated at Kara.

### 2.3.4. Tertiary - Recent sequence

Tertiary to Recent units are widespread and have concealed much of the Devonian to Cambrian or older geology and related mineralisation. The Tertiary units consist of basalt, sand and gravel. The basalt is a massive, feldspar-olivine phyric rock with matrix of fine feldspar, olivine and pyroxene. In places, the rock is vesicular and amygdaloidal. Barrett (1980) has reported zeolite in some of the vesicles. The Recent cover is composed of eluvial and alluvial materials.

### 2.3.5. Structure

The major structural feature of the deposit area is folding of Cambrian and Ordovician sequences (Fig. 2.5) related to the Mid-Palaeozoic deformation of northwestern Tasmania described earlier in section 2.2.2. The fold structures have been intruded by Devonian granite, and the beds in the folded strata are either semi-concordant to the granite intrusive

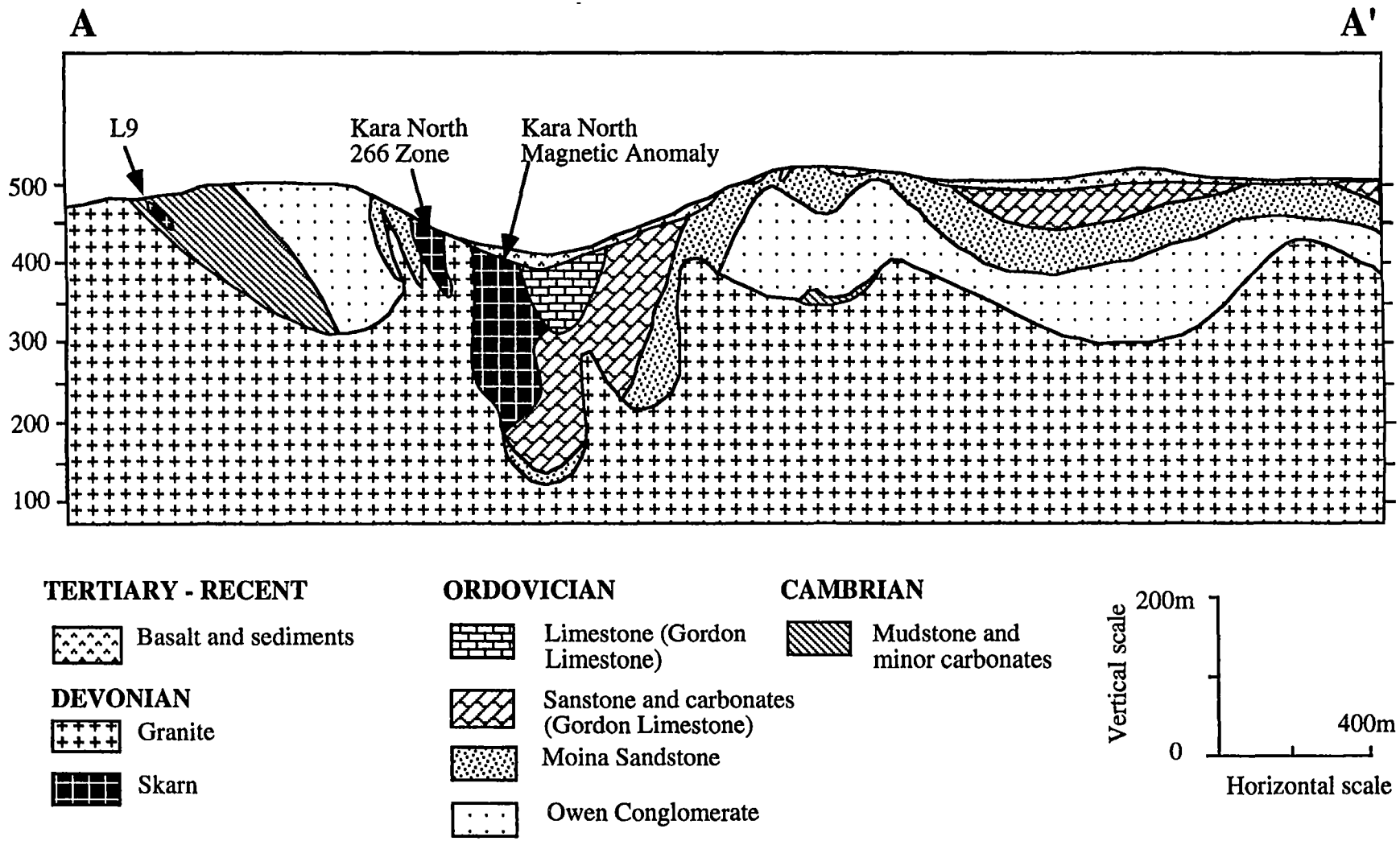


Fig. 2.5. Cross section showing the geological structure on line A-A' of Fig. 2.3. Adapted from geological maps of Tasmania Mines Limited.

or truncated by it. The folds generally trend N-S and have limbs that are shallow- to very steep-dipping, and locally overturned. At the Kara No. 1 orebody, Ordovician sandstone beds on the western side of the pit are nearly vertical to overturned, and dipping to the east, indicating that a syncline is situated to the east of the pit. This syncline has been extrapolated to extend northwards and is enveloped by the underlying granite intrusive, and contains skarns (Fig. 2.5). Mine geologists consider the syncline to plunge at small angles (15°C) towards the north. Faults do not constitute a major deformation feature at the Kara deposit area though minor faults have been mapped and interpreted by mine geologists. Most of the faults tend to displace the granite and therefore post-date granite emplacement. Fault styles include dextral and thrust faults which commonly have small displacements, generally of a few metres.

# CHAPTER 3: SKARN MINERALOGY AND PARAGENESIS

## 3.1. INTRODUCTION

Mineralogical studies of the Kara skarn deposit have been undertaken by previous workers (e.g. Barrett, 1980; numerous company reports such as Fander, 1972, 1979, and Cowan, 1981). Some of their work contains excellent descriptions of the Kara skarn mineralogy but there are no detailed studies on mineral paragenesis of the Kara skarn system. Einaudi et al. (1981), Meinert (1992), Kwak (1994) and others have emphasised the importance of undertaking detailed mineral paragenetic studies in trying to understand the genetic evolution of skarns. In this study, a detailed petrological and mineralogical study has been undertaken to understand the following:

(1) the distribution of the skarn minerals in time,

(2) the relationship between the skarn formation and ore mineralisation, and

(3) the physico-chemical conditions prevailing during the evolution of the Kara skarn deposit.

## 3.2. PETROLOGY AND TEXTURES

The principal skarn minerals at Kara are magnetite, garnet, vesuvianite, clinopyroxene, epidote and amphibole together with fluorite, calcite, quartz, scheelite, hematite, chlorite, wollastonite, sphene, pyrite, chalcopyrite and apatite as subordinate or accessory minerals.

Paragenetic studies based on macro- and micro-textures show that skarn formation at Kara occurred in a number of stages similar to other skarns (see Einaudi et al., 1981; Meinert, 1992; Kwak, 1994). There are early skarn mineral facies which are entirely or partially replaced by later mineral phases. The textural features further indicate that later minerals have developed largely by pervasive and diffusive replacement of earlier minerals and to a minor extent by filling vugs, veins and fissures. Early mineral facies are largely

anhydrous, whereas later ones are predominantly hydrous. At least four stages of skarn formation and ore deposition have been recognised at Kara and are as follows:

Stage I — Clinopyroxene-garnet-vesuvianite±wollastonite±quartz±scheelite,

Stage II — Garnet-vesuvianite-magnetite±scheelite±apatite±quartz,

Stage III — Magnetite-amphibole-epidote-fluorite±quartz±garnet±vesuvianite ±chlorite±scheelite±sphene±hematite±pyrite±clinopyroxene, and

Stage IV — Hematite±flurite±calcite±quartz.

A brief, slightly different description of mineral paragenesis from the preliminary work of this study was given in Singoyi and Khin Zaw (1994a, 1994b). A comprehensive description of the skarn mineral paragenesis is given below, and textural and petrographic features are shown in Figs. 3.1 to 3.3.

### 3.2.1. Clinopyroxene±garnet±vesuvianite±wollastonite±quartz±scheelite (Stage I)

The Stage I mineral assemblage represents the earliest skarn-forming phase at Kara and consists of minerals that are typically anhedral, fractured and fragmented. The Stage I mineral assemblage is altered and replaced by later skarn stages and is dominated by clinopyroxene with subordinate amounts of garnet, vesuvianite, wollastonite, and quartz.

***Clinopyroxene:*** In hand specimens, clinopyroxene is pale green and mostly fine-grained. It commonly shows pervasive replacement (Fig. 3.1A) and contains minor veins which may be 3cm wide (Fig. 3.1B). Under the microscope, the average grain size of clinopyroxene is about 0.2mm across but some clinopyroxene may be up to 4mm long. The fine clinopyroxene grains commonly occur as shattered short prismatic or anhedral crystals (Figs. 3.2A, 3.2B and 4.2C) and may exhibit granoblastic textures (Fig. 3.2D). Fragmental or prismatic grains may be separated by altered material or later minerals ( Figs. 3.2A, 3.2B and 3.2E). The fine-grained clinopyroxene may be found as relict inclusions in later mineral phases, such as vesuvianite (Fig. 3.2.F), magnetite (Fig. 3.2G) and garnet. Coarse-grained clinopyroxene crystals are generally anhedral, fractured, and sometimes with a set of cleavages at perpendicular angles to each other. The mineral is corroded along the fractures

Fig. 3.1. Photographs of outcrop and core samples from the Kara skarn deposit, northwestern Tasmania.

**A.** Stage I clinopyroxene (Cpx) being overprinted by Stage III magnetite (Mag) and amphibole (Amp), Kara No. 1 open cut.

**B.** Stage I clinopyroxene (Cpx) being transected by veins containing euhedral crystal of magnetite (Mag) and calcite (Cc) of Stage III.

**C.** Stage III magnetite (Mag) replacing Stage II (Gar), Kara No. 1 open cut. Note magnetite vein in garnet.

**D.** Massive Stage garnet (Gar) with fractures and veins of amphibole (Amp), magnetite (Mag) and calcite (Cc) of Stage III.

**E.** Massive Stage III magnetite (Mag) with bands and pockets of relict Stage II garnet (Gar). Note occurrence of epidote (Ep, Stage III) along margins of garnet fragments.

**F.** Stage III veins and fractures of scheelite (Sch) and amphibole (Amp) within Stage II magnetite (Mag).

**G.** Stage II magnetite cut by vein of fluorite (Flu) and minor amphibole (Amp) of Stage III.

**H.** Magnetite (Mag)-amphibole (Amp)-scheelite (Sch) assemblage (Stage III) displaying grains that are mutually intergrown.

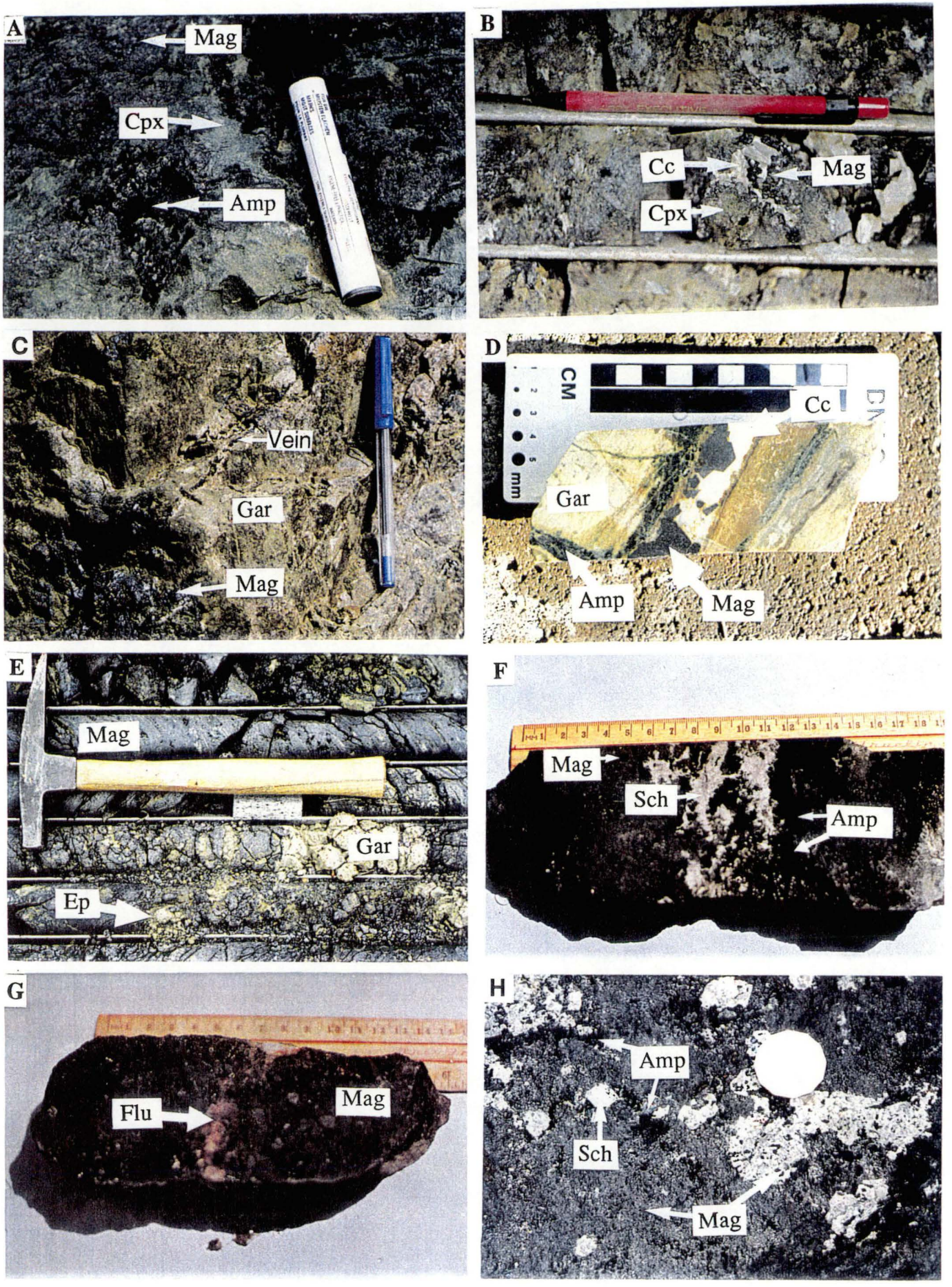
A
Mag
Cpx
Amp
B
Cc
Mag
Cpx
C
Vein
Gar
Mag
D
CM
mm
Cc
Gar
Amp
Mag
E
Mag
Gar
Ep
F
Mag
Sch
Amp
G
Flu
Mag
H
Amp
Sch
Mag

Fig. 3.1

Fig. 3.2. Photomicrographs showing textural relations of skarn minerals from the Kara skarn deposit, northwestern Tasmania.

**A.** Stage II magnetite (Mag) overprinting and filling spaces in fine grained Stage I clinopyroxene (Cpx).

**B.** Stage I clinopyroxene (Cpx) with corroded fractures of oxide material (Ox) that are accompanied by Stage II vesuvianite (Ves) overprint.

**C.** Stage III amphibole (Amp)-magnetite (Mag) assemblage transecting fine-grained Stage I clinopyroxene (Cpx).

**D.** Stage III amphibole (Amp) encroaching on granoblastic clinopyroxene (Cpx) of Stage I.

**E.** Subhedral magnetite (Mag) and vein/vug quartz (Qtz) of Stage II overprinting clinopyroxene (Cpx). Note alteration rim (brown material) along clinopyroxene margins.

**F.** Poikiloblastic vesuvianite (Ves) with inclusions of Stage I clinopyroxene (Cpx).

**G.** Zoned poikiloblastic vesuvianite (Ves) and magnetite (Mag) of Stage II. The inclusions are relict clinopyroxene (Cpx) grains.

**H.** Stage II magnetite (Mag) filling fractures within coarse-grained Stage I clinopyroxene (Cpx).

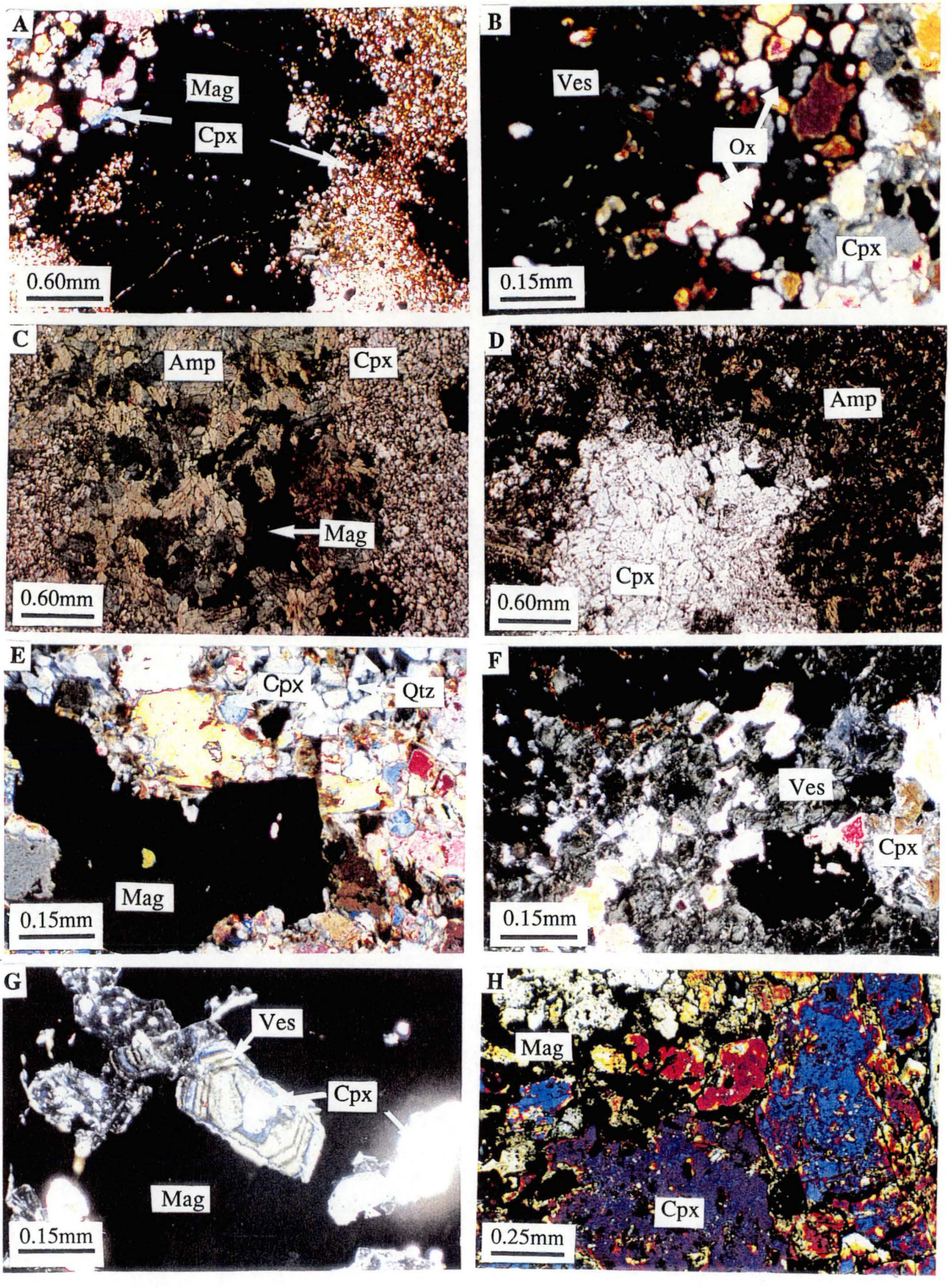
A
Mag
Cpx
0.60mm
B
Ves
Ox
Cpx
0.15mm
C
Amp
Cpx
Mag
0.60mm
D
Amp
Cpx
0.60mm
E
Cpx
Qtz
Mag
0.15mm
F
Ves
Cpx
0.15mm
G
Ves
Cpx
Mag
0.15mm
H
Mag
Cpx
0.25mm

Fig.3.2

Fig. 3.3. Photomicrographs showing textural relations of skarn minerals from the Kara skarn deposit, northwestern Tasmania

**A.** Alteration (Alt) of Stage I clinopyroxene (Cpx) to chlorite (Chl).

**B.** Fractured early garnet (Gar II) overgrown and cut by later garnet (Gar III) which coexists with quartz (Qtz)± amphibole (Amp, needle-like) of Stage III.

**C.** Coexisting Stage III scheelite (Sch)-magnetite (Mag)-amphibole (Amp)-fluorite (Flu) assemblage. The brown material (Ox) is iron oxide.

**D.** Stage III scheelite (Sch)-magnetite (Mag)-amphibole (Amp) assemblage replacing granoblastic Stage I clinopyroxene (Cpx).

**E.** Zoned Stage III garnet overgrowing early poikiloblastic garnet (Gar II, Stage II) in mutual existence with vein calcite (Cc) of Stage III.

**F.** Stage III fluorite (Flu)-amphibole (Amp) vein transecting Stage III quartz (Qtz)-epidote (Ep) assemblage.

**G.** Euhedral Stage III epidote (Ep) with interstitial quartz (Qtz).

**H.** Veinlet of calcite (Cc, Stage IV) transecting early mineral assemblages of amphibole (Amp) -magnetite (Mag) -fluorite (Flu) of Stage III and garnet (Gar) of Stage II.

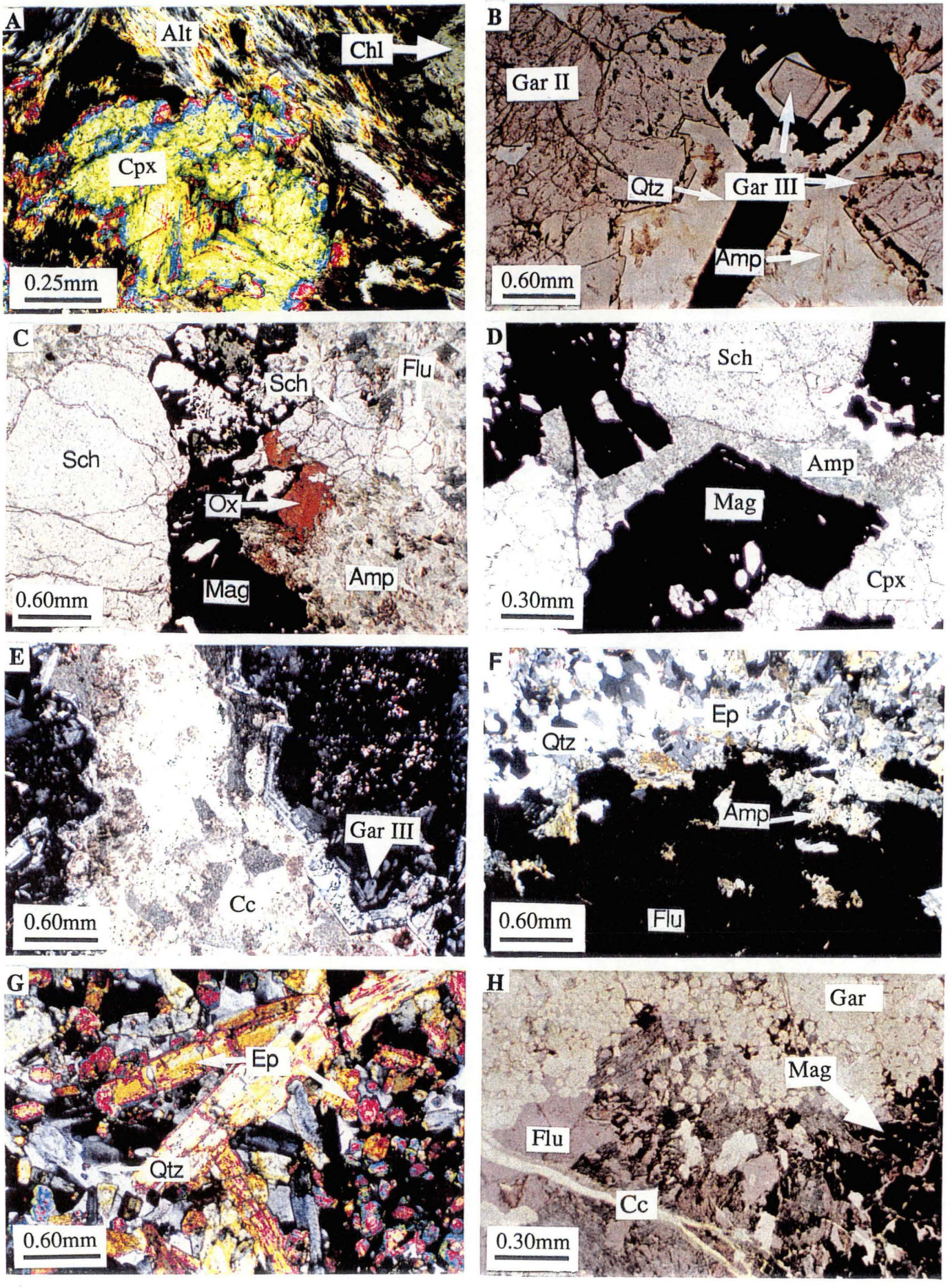
A
Alt
Chl
Cpx
0.25mm
B
Gar II
Qtz
Gar III
Amp
0.60mm
C
Sch
Flu
Sch
Ox
Mag
Amp
0.60mm
D
Sch
Amp
Mag
Cpx
0.30mm
E
Gar III
Cc
0.60mm
F
Ep
Qtz
Amp
Flu
0.60mm
G
Ep
Qtz
0.60mm
H
Gar
Mag
Flu
Cc
0.30mm

Fig. 3.3

which are filled with later minerals (Figs. 3.2E and 3.2H). Stage I clinopyroxene may be partially or completely altered to later minerals. The partially altered clinopyroxene grains typically exhibit fibrous textures (Fig. 3.3A).

***Garnet, vesuvianite, wollastonite, quartz and scheelite:*** Garnet, vesuvianite, wollastonite, quartz and scheelite occur as accessory minerals in Stage I. These minerals show mutual grain boundaries with clinopyroxene. Quartz is fine-grained (about 1mm across) with polygonal grain boundaries. Vesuvianite and garnet grains are anhedral, generally about 2-4mm across and commonly fractured. Scheelite in the Stage I assemblage is disseminated, fine-grained and very rare.

### 3.2.2. Garnet-vesuvianite-magnetite±scheelite±apatite±quartz (Stage II)

The Stage II mineral assemblage principally comprises garnet and vesuvianite. Magnetite, scheelite, apatite, and quartz are found in subordinate quantities. Where the Stage II minerals are found together, the grain boundaries are mutual, suggesting that growth took place under equilibrium conditions or during the same period. The mineral facies in Stage II are commonly coarse, anhedral and poikiloblastic containing relict grains of Stage I clinopyroxene, and overprinting the Stage I minerals. This assemblage is also overprinted by later mineral facies which may form veins.

*Garnet:* In hand specimens, the Stage II garnet is brown and shows numerous fractures. It is generally coarse-grained (up to 5mm across), anhedral and contains veins of later minerals (Figs. 3.1C and 3.1D). In thin section, the garnet is commonly isotropic and reveals numerous fine relict clinopyroxene grains which display corroded edges. The Stage II garnet is often overgrown by later garnet (Fig. 3.3B) or overprinted by epidote (Fig. 3.1E)

*Vesuvianite:* In hand specimens, vesuvianite is green and often forms coarse tabular subhedral crystals about 5mm long. In thin section, vesuvianite generally displays platy, poikiloblastic grains containing inclusions of clinopyroxene relicts from Stage I (Fig. 3.2F, 3.2G). In places, the mineral replaces clinopyroxene grains from earlier Stage I (Fig. 3.2B). Under cross polarised light, the mineral shows low order interference colours of varying shades of blue and grey along the crystallographic Z-axis.

***Magnetite:*** In hand specimens, Stage II magnetite may be distinguished from later magnetite phases by its spatial association with early vesuvianite (Fig. 3.2G) and garnet. In places, it is transected by later mineral assemblages such as scheelite, amphibole, fluorite, epidote, garnet, and magnetite (Fig. 3.1F). In thin section, the magnetite is typically anhedral displaying a number of textures. It may exhibit a dendritic structure overgrowing clinopyroxene and exsolution lamellae of hematite. It fills spaces within fragmented and veined clinopyroxene (Figs. 3.2A, 3.2B and 3.2E).

***Scheelite:*** Scheelite is white to greyish white, and displays light blue fluorescent colours under ultraviolet light. Stage II scheelite is generally fine-grained (mostly <0.1mm across) and generally detected in hand specimens by means of ultraviolet light radiation. It is disseminated, sometimes concentrated within interstices of different minerals such as vesuvianite and garnet. Coarse grains up to 5mm do occur but are rare.

***Apatite and Quartz:*** Apatite occurs as an accessory mineral and was only observed in thin section. Apatite exhibits subhedral to euhedral, prismatic, and elongated form. Prismatic grains are small, <0.5mm in diameter, whereas elongate grains may be larger, up to 2mm in length. The equant grains are isotropic to moderately anisotropic, whereas the elongate grains are anisotropic with parallel extinction angles. The mineral is intergrown with the Stage II garnet and magnetite. Quartz forms a minor constituent and commonly displays an equigranular texture and fills veins or vugs (1mm across) together with magnetite (Fig. 3.2E). The grains are typically small (<0.5mm).

### 3.2.3. Magnetite-amphibole-epidote-fluorite-quartz±chlorite±garnet±vesuvianite ±clinopyroxene±sphene±scheelite±pyrite (Stage III)

The Stage III mineral facies are widespread and represent a period of major skarn formation. This assemblage is characterised by the appearance of hydrous minerals (green and black amphibole, epidote and chlorite). The minerals may be intergrown (Fig. 3.1H) and generally show mutual grain boundary relationships (Figs. 3.3C, 3.3D and 3.3E). The Stage III minerals pervasively or diffusively replace earlier mineral assemblages (Fig. 3.1A) and fill veins/vugs (Figs. 3.1B and 3.1F).

***Magnetite:*** Magnetite is the principal skarn mineral at Kara and has mostly developed during Stage III. The Stage III magnetite commonly occurs with amphibole, replaces earlier mineral assemblages of clinopyroxene, garnet, vesuvianite, and forms as massive aggregates, fractures or veins (Figs. 3.1A-3.1D, 3.2C, 3.3B). Grain sizes vary from fine (about 0.2mm) to coarse (15mm). In thin section, magnetite is often massive, poikiloblastic with relict clinopyroxene. It may show euhedral grains intergrown with other Stage III mineral species such as scheelite, epidote, garnet, vesuvianite, (Figs. 3.1E, 3.3C and 3.3D) and overprinting earlier minerals (e.g. Stage I clinopyroxene, Fig. 3.3D). Atoll and granoblastic magnetite textures are also found.

***Amphibole:*** Amphibole is the principal hydrous mineral associated with most of the magnetite and scheelite minerals. It is common in the Stage III mineral assemblage. There are bluish-green (hastingsite) and black (hornblende) amphibole varieties, the former is by far more common. In hand specimens, the amphibole occurs as aggregates forming patches or zones diffusively intergrown with magnetite (Fig. 3.1A) or in veins (Fig. 3.1D). These aggregates may consist of fine- to coarse-grained amphibole, sometimes with bladed grains up to 5mm across. The mineral may also be intergrown with other stage III minerals such as scheelite, fluorite and calcite (Figs. 3.1F, 3.1G and 3.1H). The mineral commonly replaces early clinopyroxene as exemplified in thin sections (Figs. 3.2C and 3.2D) and may also overprint early garnet as well as the protolith marble. Thin section studies further show the mutual existence of amphibole with other Stage III mineral assemblages such as magnetite, fluorite, scheelite, epidote and calcite (Figs. 3.1D, 3.1G, 3.2G, 3.2F and 3.2H). Needle-like amphibole grains, about 0.3mm across, are sometimes associated with Stage III vug quartz within Stage II garnet.

***Epidote:*** Epidote commonly shows mutual existence with other Stage III minerals (e.g. fluorite, Fig. 3.3F) but is mostly observed forming a persistent layer above the granite and at the base of the skarn together with interstitial quartz (Fig. 3.3G). Epidote has variable grain sizes from fine-grained (0.2mm) to coarse-grained (10mm) and displays anhedral grains that are partially developed from the alteration of earlier skarn minerals (e.g. garnet, Fig. 3.1E) as well as granite feldspar (Fig. 2.4D) to euhedral crystals (Fig. 3.3G). Along the

margins of the epidote-quartz layer, epidote together with amphibole, fluorite and quartz may occur as alteration products, matrix materials or fracture fill within earlier garnet, magnetite and the underlying granite.

***Fluorite:*** Fluorite is a common mineral within the Stage III assemblage. It is almost always found together with the hydrous minerals of amphibole, epidote and chlorite (Figs. 3.1G, 3.3C, 3.3F and 3.3H). Fluorite varies in colour from greenish white to purple. The purple variety appears to be restricted to the epidote-rich facies. Fluorite ranges in grain size from 0.1mm to 10mm but is mostly coarse-grained (>5mm across). In amphibole-rich zones, fluorite may be associated with scheelite (Fig. 3.3C).

***Quartz, carbonate, chlorite, and sphene:*** Quartz occurs as an interstitial or vein mineral. It is typically fine-grained, <0.1mm across, and shows polygonal grain boundaries. Quartz is more common in epidote-rich facies where it occurs predominantly as an interstitial mineral (Fig. 3.3G). Stage III quartz is recognised by its mutual grain relationship with other Stage III minerals such as epidote, fluorite and amphibole. It may fill veins together with needle-like tremolite-actinolite (?) (Fig. 3.3B).

The carbonate minerals are predominantly of calcite and often fill vugs and veins where they show a temporal association with other Stage III minerals, eg. garnet, amphibole, magnetite (Figs. 3.1B, 3.1D and 3.2E) The calcite veins range in size from a few mm to a few cm across, with larger veins and vugs containing large well-formed crystals of calcite which exhibit rhombic cleavages.

Chlorite also occurs in Stage III, but is not widespread. It forms as aggregates of platy minerals with irregular grain boundaries and individual grains of about 1mm across. The mineral typically occurs as a replacement mineral of clinopyroxene (Fig. 3.3A) and other earlier mineral facies. Chlorite is found in close association with amphibole and fluorite, and may be accompanied by scheelite.

Sphene was only observed in thin section. It is a rare skarn mineral and was found to occur in close association with epidote and amphibole. Sphene commonly occurs as an anhedral equant mineral of about 0.2mm across.

***Garnet, Vesuvianite and Clinopyroxene:*** These minerals are less common in the

Stage III mineral assemblage than in the earlier assemblages. Stage III garnet is brown-red and forms veins in earlier mineral assemblages including Stage II magnetite and garnet. Stage III garnet is typically coarse-grained (10mm across) and zoned. In thin section, the mineral is anisotropic and exhibits well-developed oscillatory zoning (Fig. 3.3E). It may occur as overgrowths on Stage II garnet or fill veins where it shows mutual grain boundaries with quartz and amphibole (Fig. 3.3B) and calcite (Fig. 3.3E).

The occurrence of vesuvianite in Stage III is localised. The mineral is tabular as in the Stage II assemblage but is intergrown with euhedral magnetite and epidote.

Minor clinopyroxene is observed in this stage. It is medium- to coarse-grained, subhedral to euhedral. The Stage III clinopyroxene is observed in vugs or veins where it displays mutual grain contacts with other Stage III minerals, notably amphibole and calcite.

***Scheelite:*** Scheelite predominantly occurs in Stage III where it is remarkably coarse-grained with an average size of 5cm. The mineral typically exhibits mutual grain boundaries against other Stage III mineral species (Figs. 3.3C and 3.3D). It shows an intimate spatial association with amphibole. Magnetite is also always present but is too widespread to deserve any special mention.

***Pyrite and chalcopyrite:*** Pyrite occurs in Stage III. Minor amounts of chalcopyrite may be present in association with pyrite. Pyrite is abundant in magnetite-bearing skarn facies where it commonly forms blebs up to 5mm long. It is intergrown with magnetite; some grains appear to replace magnetite, whereas others are replaced by the magnetite. Occasionally, well-formed cubic pyrite crystals are found within epidote-quartz assemblages. The crystals may be about 10mm across.

### 3.2.4. Hematite±fluorite±calcite±quartz (Stage IV)

The skarn minerals in Stage IV occur locally and constitute a small proportion of the entire skarn assemblages at Kara. Hematite is relatively more abundant and may form massive bodies.

***Hematite and fluorite:*** Stage IV hematite and fluorite are commonly observed in the epidote-quartz zones where they fill fissures or open spaces, and overprint the Stage III

epidote skarn assemblages. Hematite also develops in magnetite (Stage II) as exsolution lamellae and replacement phases.

***Calcite and quartz:*** These minerals typically occur as veins or veinlets that traverse Stage III mineral assemblages and earlier ones (Fig. 3.3H). The veins are narrow (typically <5mm). Within each vein there are generally successive zones of quartz- and calcite-rich areas.

## 3.3. SUMMARY AND DISCUSSION

The textural studies of skarn mineral assemblages at Kara show that skarn evolution occurred in stages. Four stages have been recognised and are summarised in Table 3.1. The Stage I and II mineral assemblages are dominated by anhydrous minerals of clinopyroxene and garnet with subordinate amounts of the vesuvianite hydrous mineral. These two stages are considered to represent prograde anhydrous skarn development, whereas the Stage III which is dominated by hydrous minerals (amphibole, epidote, chlorite, vesuvianite), together with Stage IV which comprises chiefly hematite, fluorite and calcite are considered to represent retrograde hydrous skarn development. This conclusion is in line with many observations from other skarns as documented by Einaudi et al. (1981), Meinert (1992) and Kwak (1994).

The epidote-quartz assemblage persistently found at the base of the skarn along the granite contact appears to have developed largely from the granite protolith through the interaction of the granite and deuteric fluids. Part of it is however due to the replacement of earlier skarn mineral facies. Abundance of scheelite in Stage III indicates that scheelite deposition was at its peak during the late hydrous phases of skarn formation, although scheelite deposition has been reported to develop equally well or better in early skarn assemblages in other skarn deposits, such as King Island scheelite deposit (Kwak and Tan, 1981) and Southern Cordillera deposits (Newberry and Einaudi, 1981). The observed spatial association of altered, fractured early skarn minerals such as clinopyroxene with later minerals (e.g. chlorite, amphibole, magnetite) suggests that the formation of later skarn minerals was largely pervasive. This pervasive replacement was probably promoted

by initial creation of fluid channelways through hydraulic fracturing of early-formed skarn zones caused by advancing hydrothermal fluids. These fluids not only had the capacity to dissolve early formed minerals as they percolated through fissures, they also carried

Table. 3.1. Mineral paragenesis of skarn minerals from the Kara skarn deposit, northwestern Tasmania.

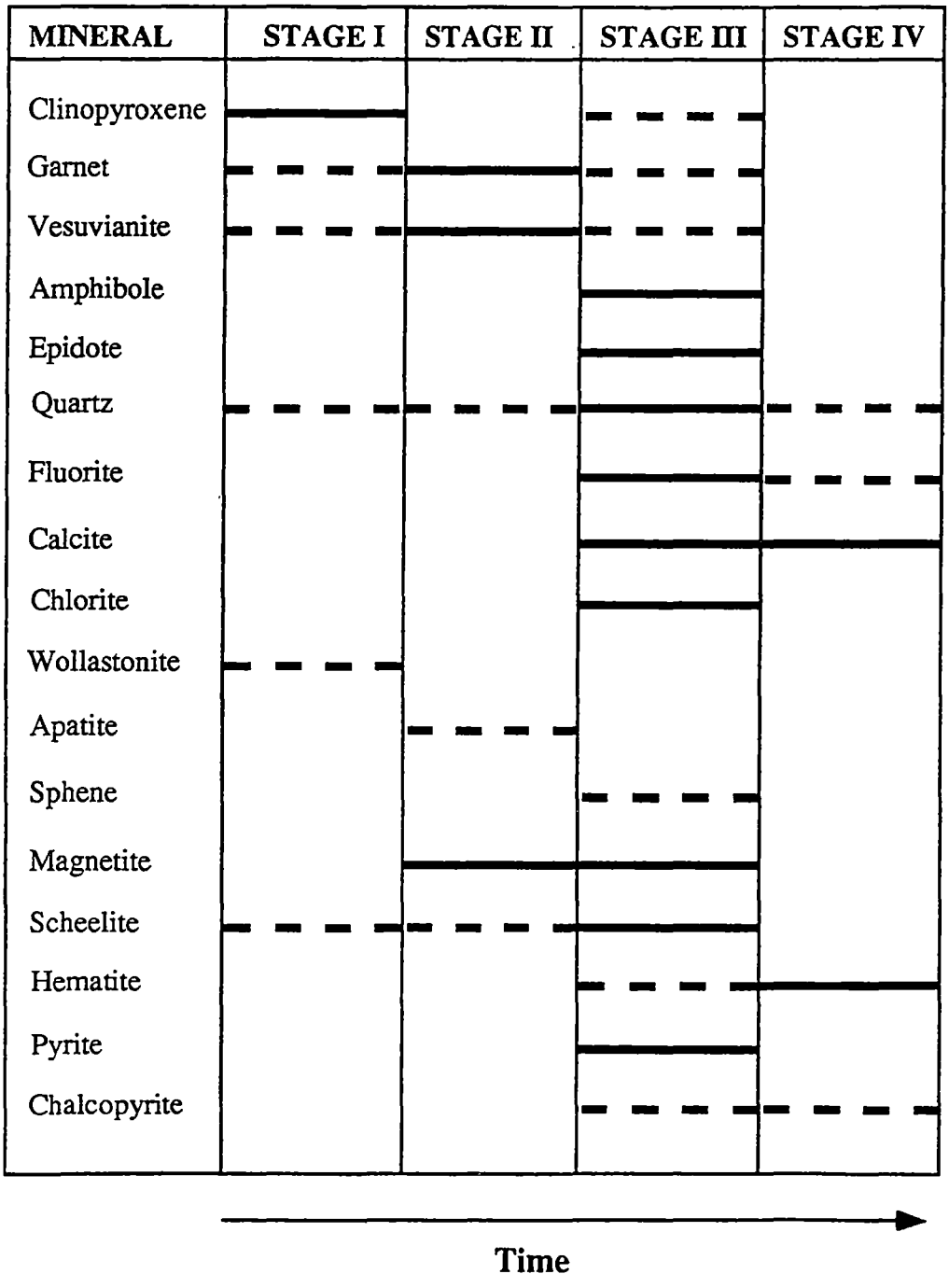

elements or material so that early minerals either could be transformed, eg. clinopyroxene to chlorite or epidote, or could provide a site for deposition of completely a new mineral such as magnetite or scheelite.

# CHAPTER 4: SKARN MINERAL AND METAL DISTRIBUTION

## 4.1. INTRODUCTION

The study of the distribution of skarn minerals and metals at Kara was undertaken to:

(1) define the nature of the skarn and ore metal zonation, and

(2) establish the relationship between skarn mineral facies and ore metal zonation.

## 4.2. MINERAL DISTRIBUTION

Field investigations together with thin section studies indicate that the Kara skarn mineral assemblages described in Chapter 3 generally display mineral zonation consisting of simple mineral assemblages made up of nearly one mineral facies or complex assemblages where the proportion of other mineral facies is relatively high and variable. These complex zones contain one or two mineral facies that are dominant over the other minerals. A dominant skarn mineral is defined as the mineral that forms greater than 35-40% (by volume) of the total skarn minerals present within a mappable zone. Estimates of the proportions of skarn minerals were based on visual examination of diamond drill core samples.

The skarns at Kara show that the zonal arrangement changes from an epidote-quartz zone along the granite margin at the base of the skarn to other skarn units away from the granite contact. The epidote-quartz zone is overlain by zones of garnet, vesuvianite, clinopyroxene, magnetite, epidote, amphibole and hematite away from the granite contact (Figs. 4.1A, 4.1B and 4.2). Within the skarn zones, remnant marble may be found (e.g. at the Kara North Magnetite Anomaly orebody, Fig. 4.3). The magnetite zone is the most widespread unit containing very high magnetite proportions (>80 vol. %, eg. Fig. 3.1E). Scheelite is found in nearly all skarn zones. It is low or absent in clinopyroxene-rich zones and typically absent in the proximal epidote-quartz zone, though it occurs in epidote-

Fig. 4.1. Photographs of outcrop and drill core samples of skarn rocks from the Kara deposit, northwestern Tasmania.

**A.** Mineral zonation in skarn away from granite (Gra) contact starting with the epidote-quartz zone (Ep), Kara No. 1 skarn . Note calcite (Cc) vein within the epidote-quartz zone. DDH113, 90.0-81.0m. Core box length is 80cm.

**B.** Mineral zonation continuing from the epidote-quartz zone to vesuvianite(Ves) to magnetite (Mag) zones, Kara No. 1 skarn. DDH113, 81.0-76.0m. Core box length is 80cm.

**C.** Clay material, with remnant weathered magnetite (Mag). Kara No. 1 skarn, Kara skarn deposit.

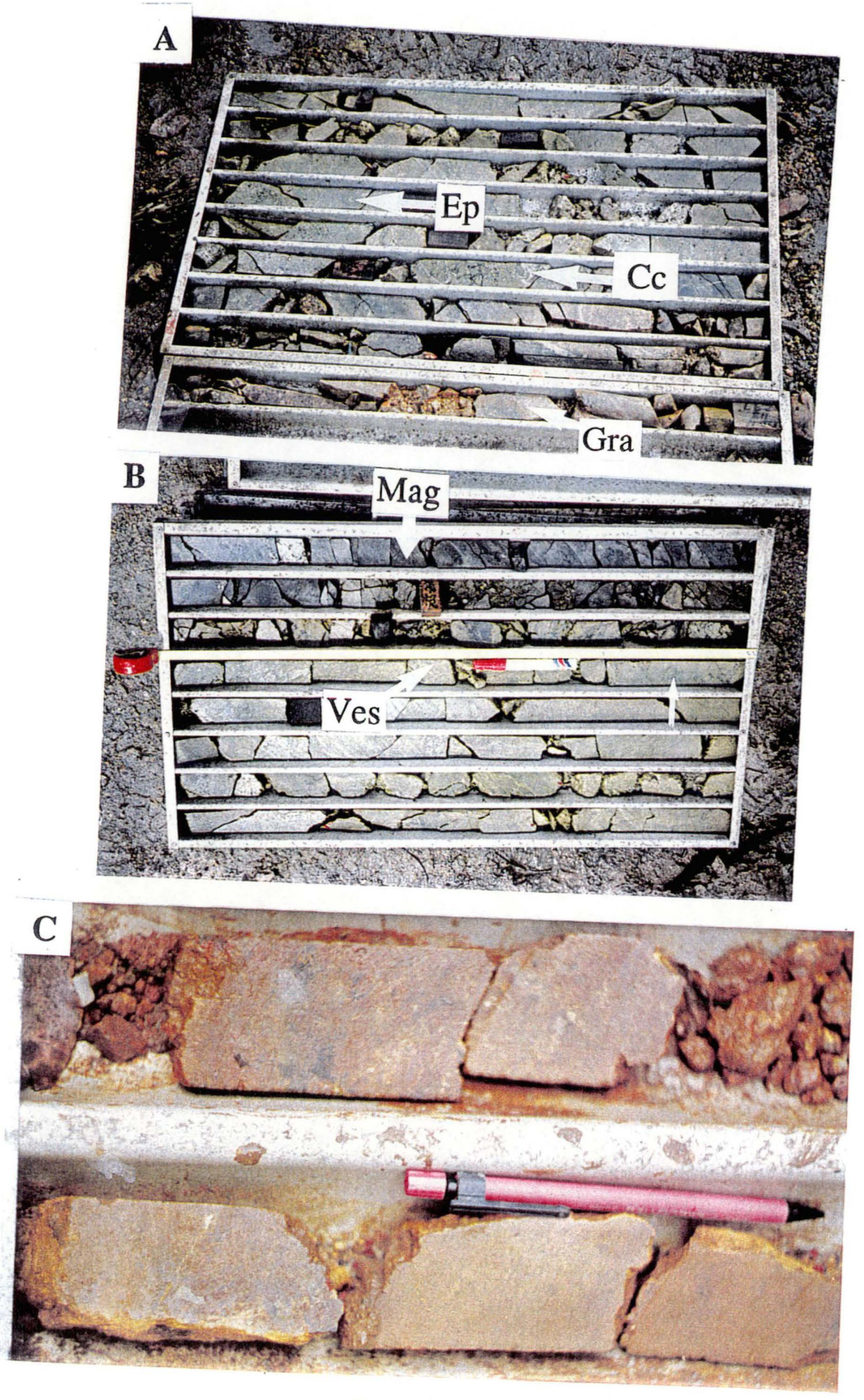


Fig. 4.1

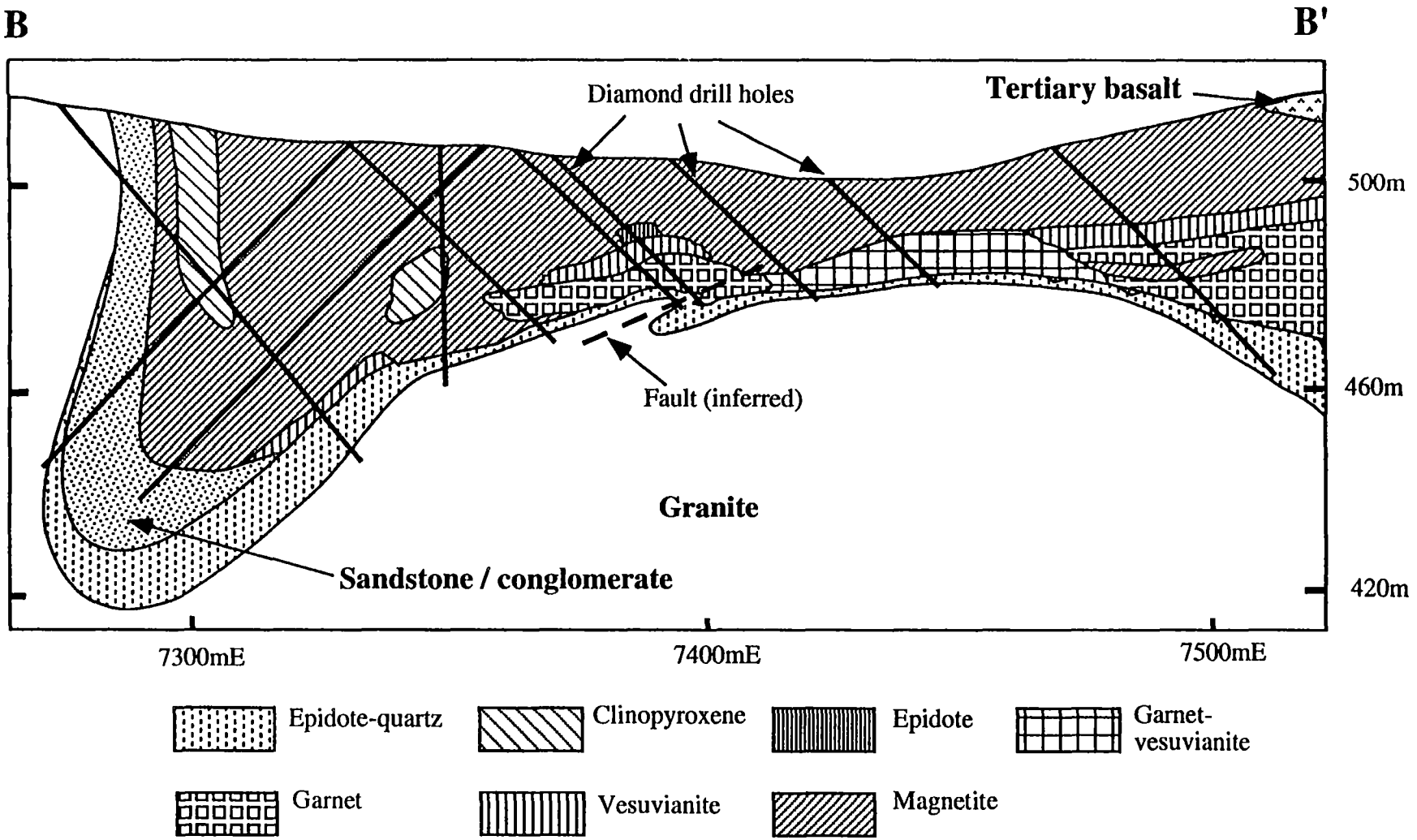


Fig. 4.2. Cross section showing mineral zonation at the Kara No. 1 on line B-B' of Fig. 2.3.

Fig. 4.3. Relationship between skarn type and grade distribution of tungsten and tin along diamond drill hole DDH287, Kara North Magnetite Anomaly.

**Basalt.**

**Clay (plus weathered skarn):** clay, sand and gravel (>75%) + remnant weathered magnetite (<15%) and clinopyroxene (<15).

**Magnetite skarn:** magnetite (>40%) + clinopyroxene (<40%) + garnet (<20%) + amphibole (<15%) ± calcite (5-10%) ± epidote (<5%); Marble: recrystallised limestone ± calcsilicates.

**Garnet skarn:** garnet (>50%) + clinopyroxene (<15%) ± magnetite (<10%) ± amphibole (<10%) ± calcite (<5%).

**Clinopyroxene skarn:** clinopyroxene (>80%) ± magnetite (>15%) ± calcite (<5%) ± garnet (<10%).

**Epidote-quartz skarn:** epidote (50%) + interstitial quartz (40%) + blocky (remnant granite) quartz (10%).

**Granite.**

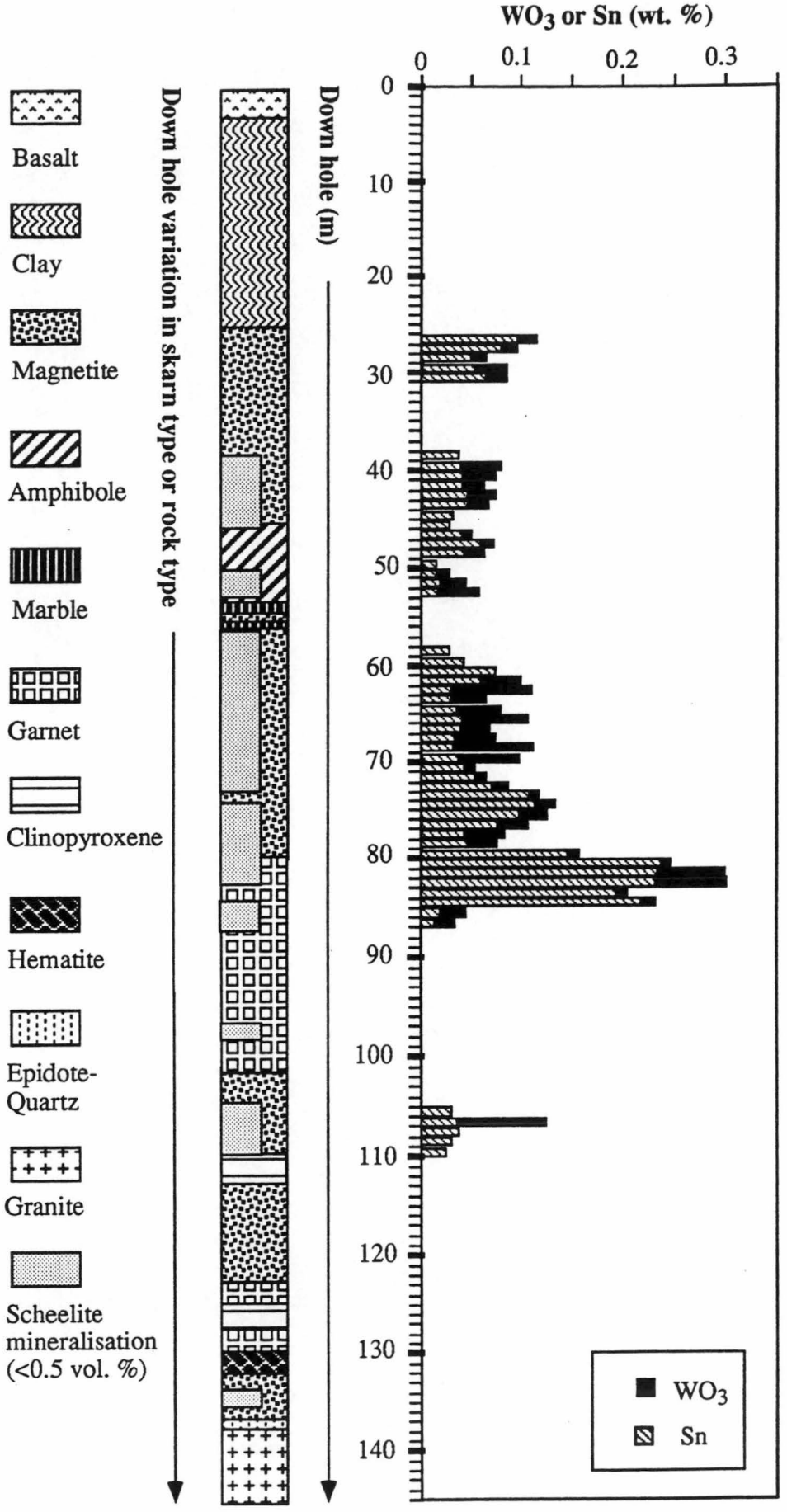
WO3 or Sn (wt. %)
0
0.1
0.2
0.3
Down hole (m)
0
10
20
30
40
50
60
70
80
90
100
110
120
130
140
Down hole variation in skarn type or rock type
Basalt
Clay
Magnetite
Amphibole
Marble
Garnet
Clinopyroxene
Hematite
Epidote-Quartz
Granite
Scheelite mineralisation (<0.5 vol. %)
WO3
Sn

Fig. 4.3

bearing zones located distal to the granite contact. Because of surface weathering, the skarn has been transformed to clays (Fig. 4.1C) and soils close to the surface (10 to 15m).

## 4.3. RELATIONSHIP OF METAL DISTRIBUTION WITH SKARN MINERALS

In this study, assay data from Tasmania Mines N. L. Limited and its predecessor companies were used. The assays are from drill core samples that were analysed by commercial laboratories. Magnetite (iron) and scheelite (tungsten) are the only commodities currently being produced from the Kara skarn deposit. Other metals in the skarn that show elevated concentrations are molybdenum, tin, lead and bismuth. Gold, silver and fluorine contents have also been determined in a few selected core and surface samples, but do not constitute mineable ore reserves . Metal concentration and distribution are shown in Fig. 4.4 and are discussed in relation to skarn mineral assemblages below:

### 4.3.1. Iron

Iron occurs predominantly as magnetite upon which current mining is operating. Minor amounts are found in the form of hematite. Iron has not been routinely analysed for in drill core samples. The distribution of iron is therefore examined from the proportion of magnetite present. Magnetite is widespread in the Kara skarn orebodies. The magnetite may form skarn zones which are massive with up to 90% magnetite by volume in places. Magnetite forms mineable ore reserves with grades greater than 30% Fe.

### 4.3.2. Tungsten

Tungsten grades range from <0.01 to as high as 6% $WO_3$ (Fig. 4.4A). 90% of assay results are below the ore grade of about 0.7% $WO_3$. There is a zonation of tungsten grades within the skarn, with highest grades developed away from base of the skarn. This zonation is depicted in Fig. 4.5. Poor tungsten grades along the skarn margin coincide with the epidote-quartz zone which is typically poor in scheelite. Scheelite mineralisation generally occurs in all the skarn types which have developed away from skarn contact and leads to the high grades which are found about 20-30m away from the granite contact (Fig. 4.5).

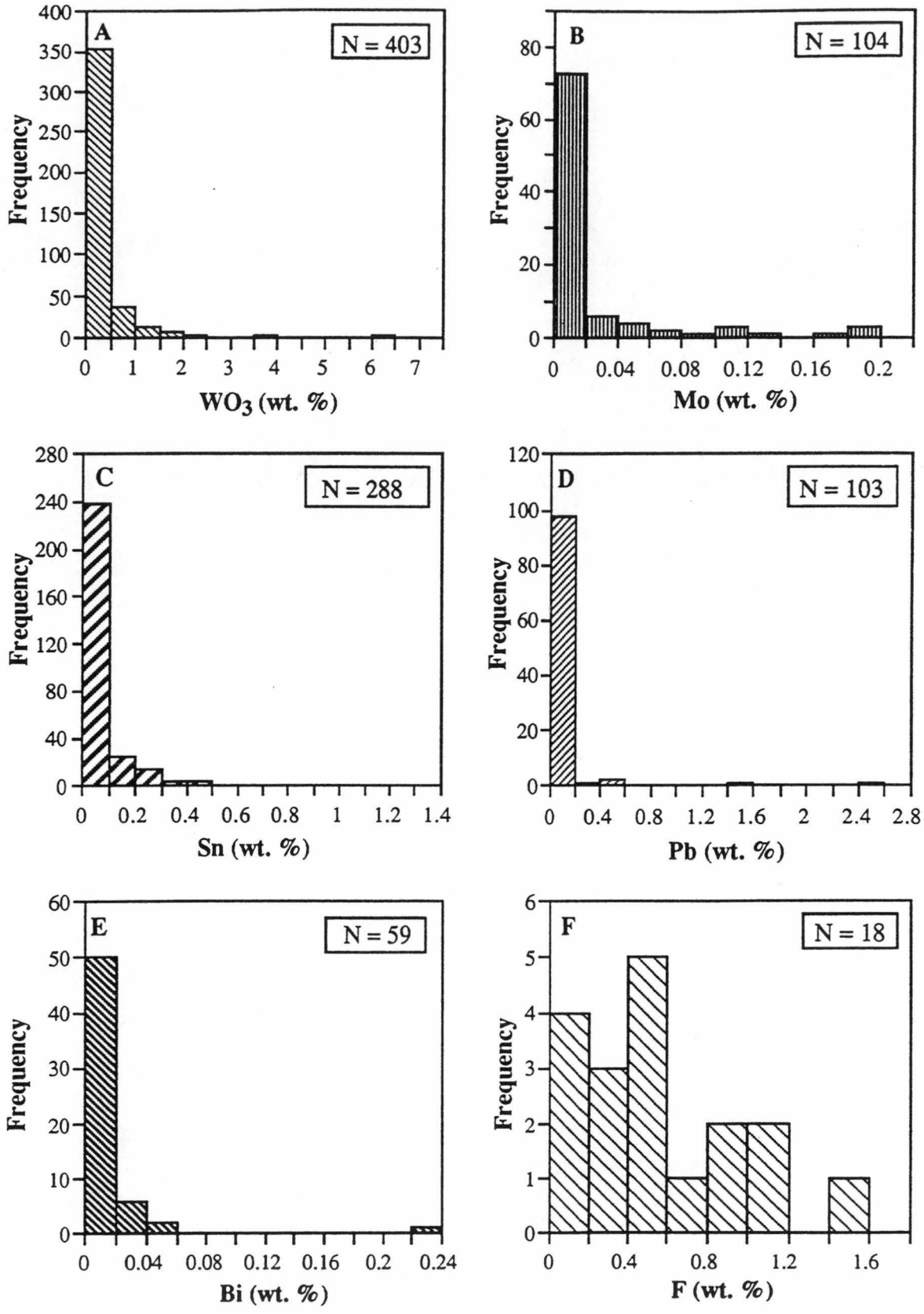


Fig. 4.4. Histograms showing frequency distribution of tungsten (**A**), molybdenum (**B**), tin (**C**), lead (**D**), bismuth (**E**) and fluorine (**F**) concentrations of drill core samples from the Kara skarn deposit..

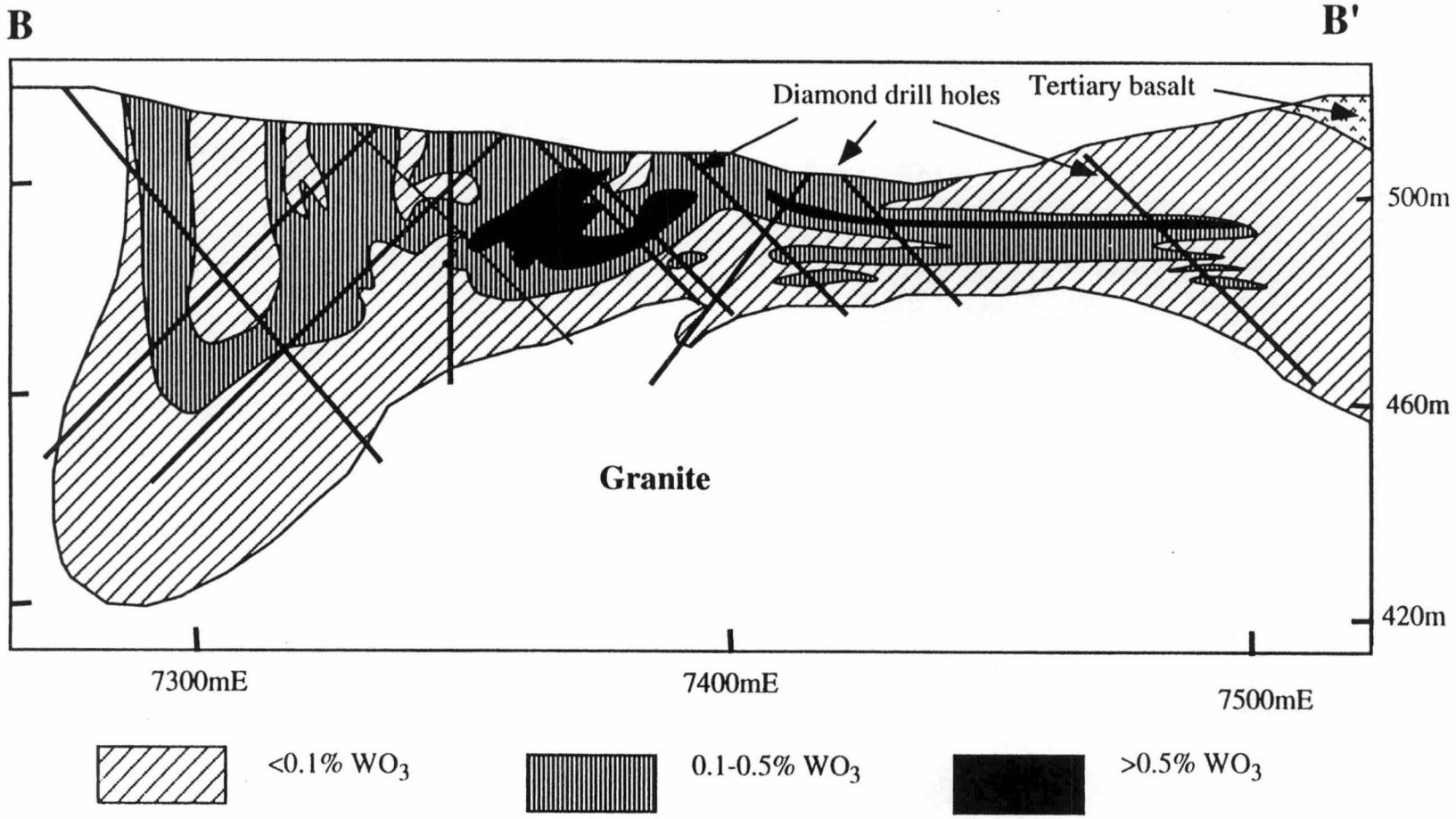


Fig. 4.5. Zonation of tungsten grades on line B-B' of Fig. 2.3, Kara No. 1 skarn body, Kara deposit, northwestern Tasmania. The geology of this section is shown in Fig. 4.2

Abundant scheelite mineralisation, often very coarse-grained, commonly occurs in close spatial association with amphibole and magnetite of Stage III. Subordinate amounts of scheelite mineralisation are associated with vesuvianite, chiefly of Stage II. Scheelite is often found in assemblages containing hydrous minerals. However, increasing the proportions of hydrous minerals (amphibole, vesuvianite) in the skarn does not necessarily lead to increasing tungsten grades (e.g. the amphibole zone in drill hole DDH287) (Fig. 4.2). The same is true for the vesuvianite skarn zone. In fact, in places, these hydrous phases are absent or lacking, and the scheelite mineralisation is accompanied by the Stage III garnet.

In comparison, the association of scheelite mineralisation with hydrous minerals appears to be common in other skarn systems. For example, Turnbull (1991) observed an apparent association of tungsten distribution and chlorite-actinolite (hydrous mineral) skarn assemblages at Colebrook Hill, western Tasmania.

### 4.3.3. Molybdenum

Molybdenum at Kara occurs in levels below economic grades. Concentration of up to 1.8% Mo is obtained from scheelite concentrates but no significant amount of molybdenite or other molybdenum-bearing mineral occurs. Molybdenum assay values are typically very low; 90% of the results are below 0.07% Mo, occasionally up to 0.2% Mo (Fig. 4.4B). The molybdenum distribution is similar to that of tungsten. Scatter diagrams of drill core assays of molybdenum against tungsten show a positive correlation between the two metals (Fig. 4.6A). An example of the spatial distribution of molybdenum is shown in Fig. 4.7.

The positive correlation of molybdenum and tungsten and the high molybdenum contents of 1.8% $MoO_3$ in scheelite concentrates suggest that scheelite is the source of molybdenum at Kara.

### 4.3.4. Tin

Tin assays in the skarn are typically between 100ppm (0.01%) and 1000ppm (0.10%) Sn (Fig. 4.4D). Anomalous values up to 1.4% Sn are recorded. Tin bears a complex relationship with tungsten and appears to show an exponential decay with increasing

tungsten conentration (Fig. 4.6B). The distribution of tin appears to be variable. Although tin appears to occur in all skarn zones (Figs. 4.2, 4.7 and 4.8), closer examination shows that tin levels are higher in some skarn mineral facies. The highest levels generally coincidewith garnet-rich skarns (e.g. DDH287; Fig. 4.2). Only minor amounts of cassiterite (tin ore) have been reported from the Kara skarn deposit and are not generally found where relatively high tin assays are revealed. The spatial association of elevated tin with garnet appears to confirm the results of microprobe analyses which show enhanced tin in garnet.

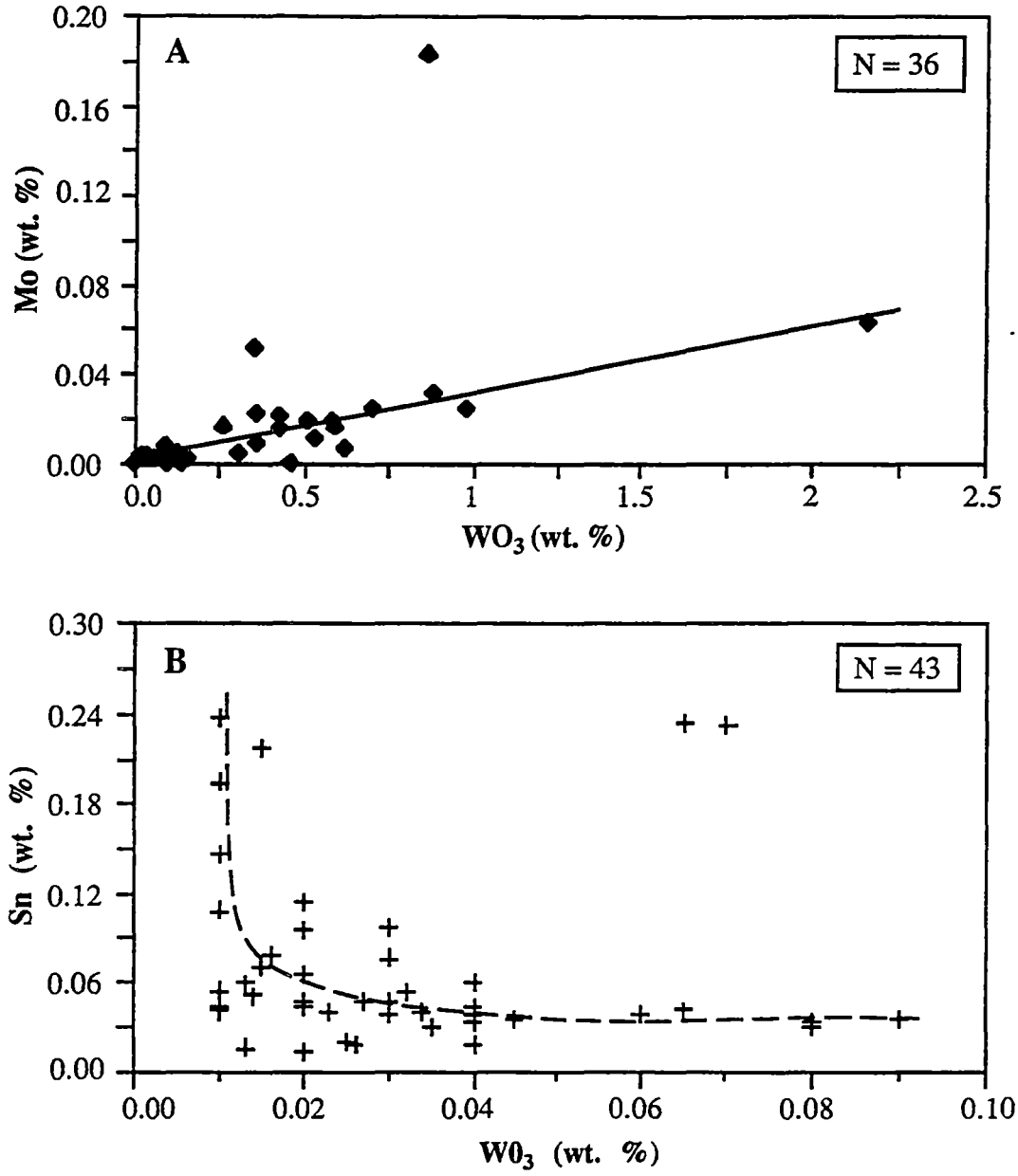


Fig. 4.6. Scatter diagrams showing relationships of metals from the Kara skarn deposit, northwestern Tasmania. **A.** Molybdenum versus tungsten. **B.** Tin versus tungsten.

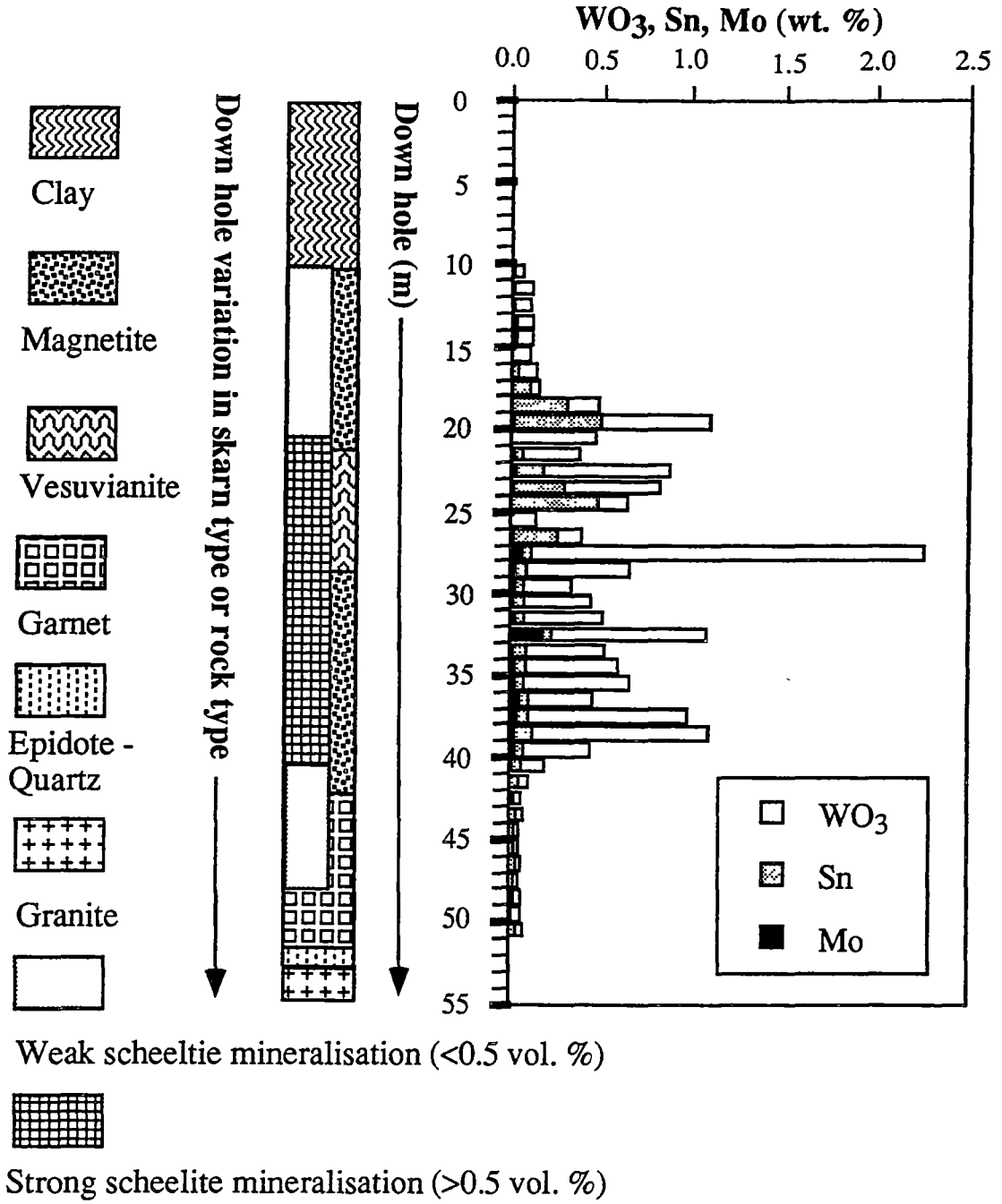


Fig. 4.7. Relationship between skarn type and the distribution of tungsten, tin and molybdenum along drill hole DDH231, Kara No. 1 orebody. Clay: clay and soil (>75%) + remnant weathered magnetite and clinopyroxene (<10%); Epidote-magnetite skarn: epidote (>50%) + magnetite (20-30%) + clinopyroxene (10-20%); Magnetite skarn: magnetite (>75%) + amphibole (20%) + clinopyroxene (<10%) ± garnet; Garnet skarn: garnet (>60%) + magnetite (20%) + amphibole (10-15%) ± clinopyroxene; Epidote-quartz skarn: epidote (>60%) + interstitial quartz (20-30%) + relict granite quartz (10-20%).

### 4.3.5. Lead, bismuth and fluorine

Lead assays are available from a selected number of drill holes. Typical assays vary from <20ppm (0.002%) to 200ppm (0.02%) (Fig. 4.4D). Occasionally values of up to 2.5% Pb are encountered. Lead distribution in the skarn is erratic and bears no relationship with other skarn metals. No lead mineral have been found in the skarn.

Bismuth has not been routinely analysed for, and only a few bismuth assay data are available. The grades are consistently low; 90% are less than 40ppm (0.004%) Bi (Fig. 4.4E). Bismuth concentrations show no apparent relationship with other metals. Barrett (1980) reported bismuthinite in magnetite-rich facies at Kara. The bismuthinite encountered is presumed to be the source of the bismuth.

Fluorine results are only available from one drill hole at the L5 orebody. The fluorine assays vary from 0.05 to 1.50% F (Fig. 4.4F). The fluorine concentration can be attributed to fluorite and hydrous minerals (vesuvianite and amphibole) present in the skarn.

### 4.3.6. Gold and silver

Tasmania Mines N.L. limited has been selectively carrying out analyses for gold and silver on drill core and surface samples of skarn rocks. The assayed samples are mostly from magnetite skarns or magnetite-bearing skarns. This exercise is aimed at assessing the economic potential of these commodities, however, the results reveal mostly low concentrations (<0.05ppm for Au and <5ppm for Ag). Few anomalous gold values have been reported at Kara No. 1: 0.27ppm Au from DDH316 and DDH113; 0.18ppm Au from DDH204; and 0.12ppm Au from DDH205. Higher levels of gold have recently been reported from weathered skarn zones, and are attractive for further investigations.

The source of the anomalous gold has not been determined but is most likely associated with pyrite which is the rare but dominant sulphide in the Kara skarn. Gold may be present as inclusions in the pyrite structure or minute isolated native gold grains.

## 4.3. CONCLUSIONS

The skarns at Kara display mineral zonation consisting of simple or complex mineral assemblages dominated by one or two minerals. The mineral zonation changes from an

epidote-quartz zone proximal to the granite to garnet, vesuvianite, clinopyroxene, magnetite, epidote, amphibole and hematite zones distal from the granite. The proximal skarn (epidote-quartz) is interpreted to have developed largely from the granite protolith, whereas the distal assemblages represent exoskarns that are due to the replacement of the Gordon Limestone. In places, calcareous rocks (Gordon Limestone) have been preserved as marble within exoskarn assemblages.

Magnetite is the principal mineral of the skarn and forms widespread skarn units. Scheelite mineralisation is commonly associated with zones containing hydrous minerals, chiefly amphibole and vesuvianite, in all exoskarn zones. It is low in clinopyroxene-rich zones. Increased amounts of hydrous minerals in a zone do not necessarily correspond to increased tungsten grades. In places, zones of anhydrous minerals (mostly garnet of Stage III) contain enhanced scheelite mineralisation and tungsten grades. Tungsten grades vary from low (<0.01 wt. % $WO_3$) to ore grade (>0.7 wt. % $WO_3$) and show a crude zonation with high grades developed in the exoskarn away from the endoskarn. Molybdenum concentrations are low (<2 wt. % Mo), accompany tungsten in scheelite and are positively correlated with tungsten. Tin is generally low, <0.10 wt. % Sn, and appears to occur throughout the entire skarn facies though the highest values coincide with garnet-rich facies and thus may be attributed to garnet since cassiterite or other tin ores are absent or insignificant.

# CHAPTER 5: SKARN MINERAL CHEMISTRY

## 5.1. INTRODUCTION

In this chapter, mineral chemistry of skarn minerals will be presented and discussed. Most skarn minerals have compositional variations that can yield significant information about the environment of formation and can subsequently be used to differentiate between skarn types. Garnet and pyroxene compositions in skarns are particularly very important as they indicate the oxidation/reduction conditions of a skarn. Sato (1980), Einaudi et al. (1981), Meinert (1992) and Kwak (1994) have suggested that the relative abundance of ferric to ferrous iron in skarn minerals, especially those with end-member equilibria or in solid-solution series (Brown and Essene, 1985), can be used to determine the oxidation/ reduction condition of a skarn. Knowledge of the oxidation/reduction condition of a skarn may have important exploration implications. For example, Meinert (1992) also points out that there is a tendency for oxidised tungsten skarns to form small deposits, whereas reduced ones generally form large deposits.

Previous mineral compositional determinations on the Kara skarn minerals were undertaken by Barrett (1980) on clinopyroxene, garnet, vesuvianite, amphibole, epidote, chlorite, calcite and sphene mainly to identify the minerals and were not corroborated with detailed mineral paragenesis.

In this study, chemical analyses of major and trace elements were undertaken on skarn minerals from stages I to IV representing the early prograde to late retrograde skarn phases to:

(1) determine compositional variations,

(2) constrain physical and chemical conditions during skarn evolution, and

(3) classify the skarn types.

The skarn minerals on which the analyses were carried out were clinopyroxene, garnet, vesuvianite, amphibole, epidote, chlorite, calcite, sphene and apatite.

## 5.2. ANALYTICAL TECHNIQUES

Compositional variations of skarn minerals were determined using a Cameca SX50 electron microprobe at the Central Science Laboratory of the University of Tasmania. For most minerals operating conditions were: accelerating voltage at 15kv, beam current at 15nAm, counting time of 30 seconds and a beam diameter of 5μm. The conditions were varied for analyses involving trace or heavy elements to: accelerating voltage, 20kv, beam current, 20nAm, and counting time of 60 seconds.

## 5.3. RESULTS

Analytical results for clinopyroxene, garnet, vesuvianite, amphibole, epidote, chlorite, calcite, sphene, apatite, magnetite and scheelite are briefly described below.

### 5.3.1. Clinopyroxene

Microprobe analyses were undertaken for the Stage I clinopyroxene. The compositional variation of the clinopyroxene is given in Table 5.1 and plotted on a ternary diagram, diopside ($CaMgSi_2O_6$), hedenbergite ($CaFeSi_2O_6$), johannsenite ($CaMnSi_2O_6$) (Fig. 5.1). The microprobe data indicate $SiO_2$ (51.4 to 54.90 wt. %), CaO (26.0±1.0 wt %), $FeO_{total\ iron}$ (2.5±1.0 wt. %), $Al_2O_3$ (1.0 wt. % ), MnO ( <1.0 wt. %), and $Na_2O$ (<0.10 wt %). The Kara skarn clinopyroxene is largely diopside with mole composition of $Hd_{0-22}$ - $Di_{68-97}$ - $Jo_{1-2}$ (Fig. 5.1). Fig. 5.1 also shows pyroxene compositions from other scheelite skarn deposits. The Kara clinopyroxene distinctly falls in the diopside field, whereas clinopyroxene from the King Island scheelite deposit falls in a wider field ranging from the hedenbergite to the diopside, and clinopyroxene from Otjua and MacTung distinctly plot in the hedenbergite field (Figs. 5.1A-5.1D). The Kara clinopyroxene shows Mn/Fe ratios of 0.0 to 0.3 with an arithmetic average of 0.17.

### 5.3.2. Garnet

Microprobe analyses were undertaken for the garnets from Stages I, II and III. The compositional variations of the Kara skarn garnets are shown in Table 5.2 and graphically

Table 5.1. Representative microprobe analysis of Stage I clinopyroxene from the Kara skarn deposit, northwestern Tasmania. Element site allocation based on computer programme by Afifi and Essene, University of Michigan.

| | Clinopyroxene | | | | | | | | | |
|---|---|---|---|---|---|---|---|---|---|---|
| S. No. | 105399 | 105341 | S1 | S4A | S16 | S19 | S37 | S37 | S199 | S199 |
| An. No. | 5 | 1 | 5 | 4 | 1 | 3 | 1 | 6 | 1 | 4 |
| | Oxide composition (wt. %) | | | | | | | | | |
| $SiO_2$ | 53.26 | 53.44 | 54.88 | 54.27 | 53.74 | 53.14 | 52.46 | 51.32 | 51.44 | 52.25 |
| $TiO_2$ | 0.00 | 0.00 | 0.04 | 0.00 | 0.02 | 0.00 | 0.00 | 0.00 | 0.05 | 0.03 |
| $Al_2O_3$ | 0.35 | 0.29 | 0.47 | 0.13 | 0.72 | 0.80 | 0.92 | 1.25 | 1.87 | 0.55 |
| $Cr_2O_3$ | 0.00 | 0.04 | 0.03 | 0.02 | 0.00 | 0.00 | 0.00 | 0.00 | 0.00 | 0.00 |
| $Fe_2O_3$ | 0.00 | 0.00 | 0.00 | 0.00 | 0.00 | 0.00 | 0.00 | 0.00 | 0.00 | 0.00 |
| FeO | 4.60 | 3.67 | 0.52 | 2.73 | 2.04 | 3.66 | 5.44 | 7.74 | 5.68 | 9.57 |
| MnO | 0.68 | 0.56 | 0.03 | 0.55 | 0.62 | 0.60 | 0.93 | 0.92 | 0.74 | 0.74 |
| NiO | 0.00 | 0.00 | 0.00 | 0.00 | 0.00 | 0.00 | 0.00 | 0.00 | 0.00 | 0.00 |
| MgO | 15.38 | 15.77 | 18.20 | 16.62 | 16.71 | 15.73 | 14.70 | 13.24 | 14.43 | 12.23 |
| CaO | 25.69 | 26.22 | 26.41 | 25.56 | 26.14 | 26.07 | 25.54 | 25.52 | 25.76 | 25.54 |
| $Na_2O$ | 0.01 | 0.00 | 0.07 | 0.01 | 0.00 | 0.00 | 0.01 | 0.01 | 0.02 | 0.07 |
| $K_2O$ | 0.00 | 0.00 | 0.00 | 0.00 | 0.00 | 0.00 | 0.00 | 0.00 | 0.00 | 0.00 |
| Total | 99.97 | 99.99 | 100.65 | 99.89 | 99.99 | 100.00 | 100.00 | 100.00 | 99.99 | 100.98 |
| | Cation allocation based on six oxygen atoms | | | | | | | | | |
| Si IV | 1.97 | 1.97 | 1.98 | 1.99 | 1.97 | 1.96 | 1.95 | 1.93 | 1.92 | 1.96 |
| Al IV | 0.02 | 0.01 | 0.02 | 0.01 | 0.03 | 0.03 | 0.04 | 0.06 | 0.08 | 0.02 |
| T site | 1.99 | 1.98 | 2.00 | 1.99 | 2.00 | 2.00 | 1.99 | 1.99 | 2.00 | 1.99 |
| Al VI | 0.00 | 0.00 | 0.00 | 0.00 | 0.00 | 0.00 | 0.00 | 0.00 | 0.00 | 0.00 |
| Ti | 0.00 | 0.00 | 0.00 | 0.00 | 0.00 | 0.00 | 0.00 | 0.00 | 0.00 | 0.00 |
| Cr | 0.00 | 0.00 | 0.00 | 0.00 | 0.00 | 0.00 | 0.00 | 0.00 | 0.00 | 0.00 |
| $Fe^{+3}$ | 0.00 | 0.00 | 0.00 | 0.00 | 0.00 | 0.00 | 0.00 | 0.00 | 0.00 | 0.00 |
| $Fe^{+2}$ | 0.14 | 0.11 | 0.02 | 0.08 | 0.06 | 0.11 | 0.17 | 0.24 | 0.18 | 0.30 |
| $Mn^{+2}$ | 0.02 | 0.02 | 0.00 | 0.02 | 0.02 | 0.02 | 0.03 | 0.03 | 0.02 | 0.02 |
| Ni | 0.00 | 0.00 | 0.00 | 0.00 | 0.00 | 0.00 | 0.00 | 0.00 | 0.00 | 0.00 |
| Mg | 0.85 | 0.87 | 0.98 | 0.91 | 0.91 | 0.87 | 0.82 | 0.74 | 0.80 | 0.68 |
| Ca | 1.02 | 1.04 | 1.02 | 1.00 | 1.03 | 1.03 | 1.02 | 1.03 | 1.03 | 1.03 |
| Na | 0.00 | 0.00 | 0.00 | 0.00 | 0.00 | 0.00 | 0.00 | 0.00 | 0.00 | 0.01 |
| K | 0.00 | 0.00 | 0.00 | 0.00 | 0.00 | 0.00 | 0.00 | 0.00 | 0.00 | 0.00 |
| M1,M2 | 2.03 | 2.04 | 2.02 | 2.01 | 2.02 | 2.03 | 2.03 | 2.05 | 2.04 | 2.04 |
| O | 6.00 | 6.00 | 6.00 | 6.00 | 6.00 | 6.00 | 6.00 | 6.00 | 6.00 | 6.00 |
| Mn/Fe | 0.14 | 0.18 | 0.00 | 0.25 | 0.33 | 0.18 | 0.18 | 0.13 | 0.11 | 0.07 |
| Clinopyroxene components (mole fraction) | | | | | | | | | | |
| Di | 0.89 | 0.92 | 1.00 | 0.92 | 0.97 | 0.92 | 0.87 | 0.82 | 0.91 | 0.74 |
| Hd | 0.09 | 0.05 | 0.00 | 0.06 | 0.01 | 0.05 | 0.10 | 0.14 | 0.07 | 0.24 |
| Jo | 0.02 | 0.02 | 0.00 | 0.02 | 0.02 | 0.02 | 0.03 | 0.03 | 0.02 | 0.02 |

An. No.: Serial number of analysis in a sample
Di: Diopside
Hd: Hedenbergite
Jo: Johannsenite

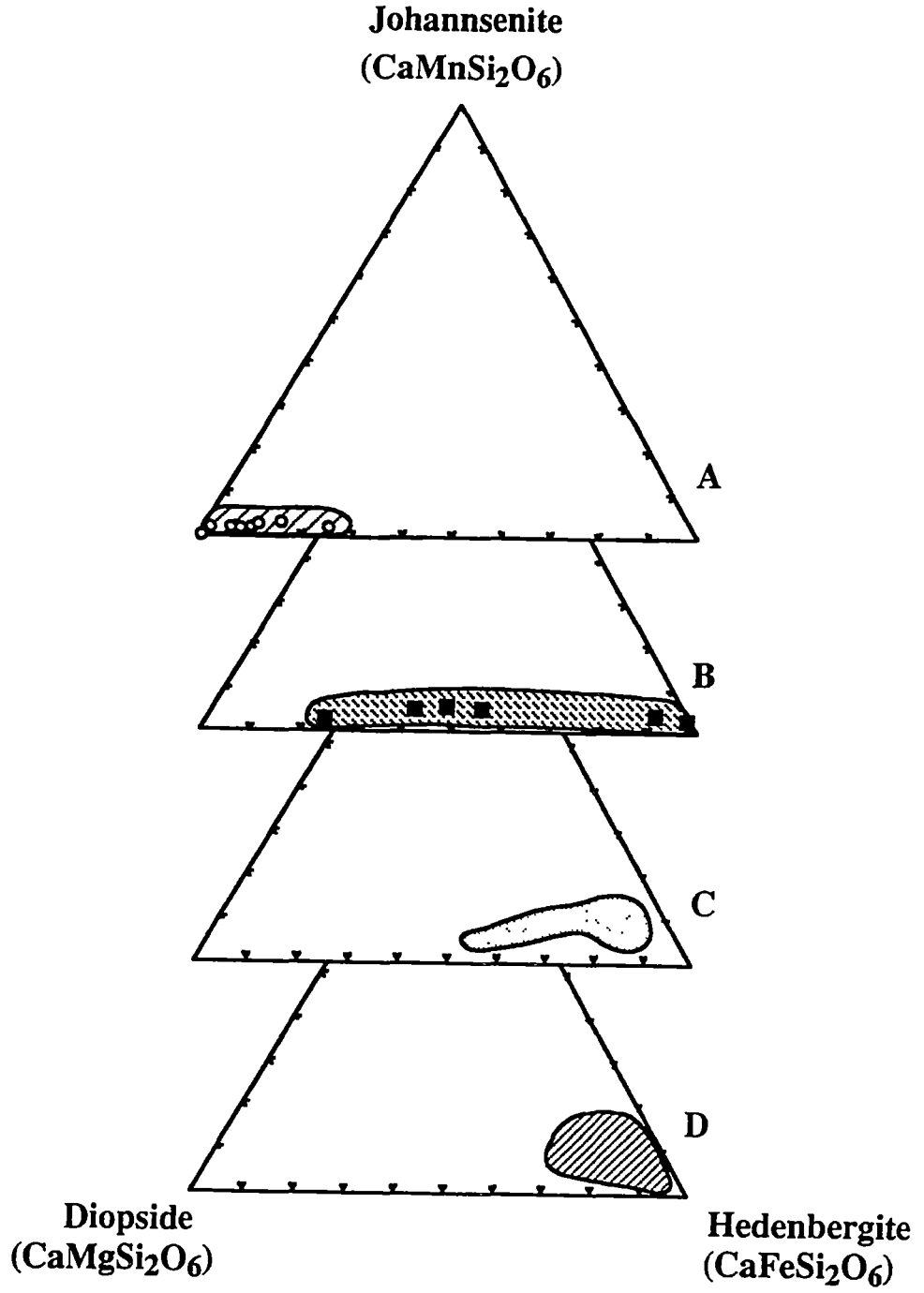


Fig. 5.1. Ternary diagrams showing compositional variations of clinopyroxene from the Kara skarn deposit, northwestern Tasmania (**A**) and other scheelite skarn deposits. **B:** King Island scheelite deposit, Tasmania (compositions from Kwak and Tan, 1981); **C:** Otjua scheelite prospect, Namibia (compositions calculated from data of Steven and Moore, 1994); **D:** MacTung scheelite deposit, Canada (plot adopted from Dick and Hodgson, 1982).

presented in Fig. 5.2 together with garnets from the King Island scheelite deposit in Tasmania, Otjua scheelite prospect in Namibia and MacTung scheelite deposit in Canada. The major oxide contents of the Kara skarn garnet are relatively uniform with $SiO_2$ (33.4 - 36.7 wt. %), CaO (34.0±1.0 wt. %), $FeO_{total\ iron}$ (19.1-23.1 wt. %), $Al_2O_3$ (0.2 - 7.6 wt. %), MnO (<1.0 wt. %) and MgO (<0.1wt. % MgO). Garnets contain elevated tin contents and seem to show decreasing tin contents from Stages I and II to III. Garnets from Stages I and II have 0.10 - 0.37 wt. % $SnO_2$ averaging 0.25 wt % Sn, whereas those from Stage I have 0.01-0.1 wt. % $SnO_2$.

Mole fraction calculations of the microprobe data show that the garnets are andradite. Stages I and II garnets are andradite-rich, with low to intermediate levels of grossular and little or no spessartine-almandine-pyrope components. The Stage III garnet is generally the same but can manifest pure andradite. Zoned garnets (typically Stage III) also show narrow compositional variations (Fig. 5.3).

Garnet microprobe data reveal that the skarn garnets contain high iron contents and low alumina. Stoichiometry calculation (Table 5.2) shows that nearly all the iron is in the oxidised state ($Fe^{3+}$) hence resulting in the formation of andradite-rich garnets which plot in the andradite field in a ternary plot, and are similar to those from King Island though the latter extends to the grossular field (Figs. 5.2A and 5.2B). The Kara garnets differ significantly from garnets from Otjua and MacTung which plot in the grossular-pyrope+almandine+spessartine field away from the andradite field (Figs. 5.2A, 5.2C and 5.2D). Estimates of the log $f(O_2)$ values for skarn formation at Kara were attempted using garnet and clinopyroxene compositions. Temperature-log $f(O_2)$ diagrams of Gustafson (1974) give log $f(O_2)$ values of >-25, while garnet-clinopyroxene composition diagrams of Brown and Essene (1985) reveal log $f(O_2)$ values of >-20.

### 5.3.3. Vesuvianite

Representative results of the present microprobe analyses of vesuvianite from the Kara deposit are presented in Table 5.3. Barrett (1980) also reported results of vesuvianite microprobe analyses from the Kara deposit, some being analysed, erroneously, as

Table 5.2. Representative microprobe analyses of garnet from Stages I , II and III mineral assemblages, Kara skarn deposit, northwestern Tasmania. Element site allocation based on computer programme by Afifi and Essene, University of Michigan.

| | Garnet | | | | | | | | | |
|---|---|---|---|---|---|---|---|---|---|---|
| S. No. | S32-3 | S35-2 | S10-8 | S11-9 | S16-1 | S18B | S19-11 | S8-A1 | S8-A7 | S35-8 |
| An. No. | 3 | 2 | 8 | 9 | 1 | 1 | 11 | 1 | 7 | 8 I |
| Stage | I | I | II | II | II | II | II | III | III | III |
| | Oxide composition (wt. %) | | | | | | | | | |
| $SiO_2$ | 35.90 | 33.99 | 35.90 | 35.86 | 35.81 | 36.12 | 35.93 | 35.94 | 34.42 | 33.99 |
| $TiO_2$ | 0.17 | 0.02 | 0.26 | 0.38 | 0.21 | 0.20 | 0.21 | 0.09 | 0.10 | 0.02 |
| $Al_2O_3$ | 4.51 | 0.20 | 5.40 | 7.63 | 4.06 | 6.46 | 6.98 | 4.94 | 4.65 | 0.20 |
| $Cr_2O_3$ | - | - | 0.00 | - | - | - | 0.00 | 0.00 | 0.00 | - |
| $Fe_2O_3$ | 24.66 | 30.94 | 23.83 | 20.93 | 24.48 | 22.33 | 21.41 | 24.03 | 25.16 | 30.94 |
| FeO | 0.00 | 0.00 | 0.00 | 0.00 | 0.00 | 0.00 | 0.00 | 0.00 | 0.00 | 0.00 |
| MnO | 0.47 | 0.70 | 0.61 | 0.35 | 0.43 | 0.95 | 0.70 | 0.58 | 0.49 | 0.70 |
| MgO | 0.17 | 0.02 | 0.06 | 0.19 | 0.11 | 0.14 | 0.08 | 0.12 | 0.10 | 0.02 |
| CaO | 34.10 | 33.86 | 33.94 | 34.61 | 34.28 | 34.14 | 34.45 | 33.94 | 33.98 | 33.86 |
| $SnO_2$ | 0.27 | 0.01 | - | 0.03 | - | - | 0.10 | 0.23 | 0.12 | 0.01 |
| $WO_3$ | 0.00 | 0.00 | - | 0.00 | - | - | 0.00 | 0.00 | 0.00 | 0.00 |
| ZnO | 0.00 | 0.00 | 0.00 | 0.00 | - | - | 0.02 | 0.03 | 0.03 | 0.00 |
| CuO | 0.03 | 0.00 | - | 0.04 | - | - | 0.00 | 0.02 | 0.00 | 0.00 |
| F | 0.06 | 0.28 | - | 0.10 | - | - | 0.10 | 0.08 | 0.03 | 0.28 |
| Cl | 0.00 | 0.01 | - | 0.00 | - | 0.04 | 0.00 | 0.00 | 0.00 | 0.01 |
| $P_2O_5$ | - | - | - | - | 0.59 | 0.58 | - | - | - | - |
| Total | 100.00 | 100.00 | 100.00 | 100.00 | 100.00 | 100.00 | 100.00 | 100.00 | 99.08 | 100.00 |
| | Cation allocation of major elements on basis of 24 oxygen atoms | | | | | | | | | |
| Si IV | 5.87 | 5.88 | 5.91 | 5.81 | 5.90 | 5.88 | 5.83 | 5.91 | 5.75 | 5.74 |
| Al IV | 0.13 | 0.12 | 0.09 | 0.19 | 0.10 | 0.12 | 0.17 | 0.09 | 0.25 | 0.04 |
| T site | 6.00 | 6.00 | 6.00 | 6.00 | 6.00 | 6.00 | 6.00 | 6.00 | 6.00 | 5.78 |
| Al VI | 1.27 | 0.75 | 0.95 | 1.27 | 0.68 | 1.12 | 1.17 | 0.86 | 0.67 | 0.00 |
| Ti VI | 0.05 | 0.02 | 0.03 | 0.05 | 0.03 | 0.02 | 0.03 | 0.01 | 0.01 | 0.00 |
| Cr | 0.00 | - | - | - | - | - | - | 0.00 | 0.00 | - |
| $Fe^{+3}$ | 2.61 | 3.23 | 3.01 | 2.69 | 3.29 | 2.86 | 2.81 | 3.04 | 3.14 | 4.00 |
| O site | 4.00 | 4.00 | 4.00 | 4.00 | 4.00 | 4.00 | 4.00 | 4.00 | 4.00 | 4.00 |
| $Fe^{+2}$ | 0.00 | 0.00 | 0.00 | 0.00 | 0.00 | 0.00 | 0.00 | 0.00 | 0.00 | 0.00 |
| $Mn^{+2}$ | 0.13 | 0.07 | 0.09 | 0.05 | 0.06 | 0.13 | 0.10 | 0.08 | 0.07 | 0.10 |
| Mg | 0.03 | 0.04 | 0.02 | 0.05 | 0.03 | 0.03 | 0.02 | 0.03 | 0.02 | 0.01 |
| Ca | 5.91 | 5.99 | 5.98 | 6.01 | 6.05 | 5.95 | 5.99 | 5.98 | 6.08 | 6.12 |
| A site | 6.00 | 6.00 | 6.00 | 6.00 | 6.00 | 6.00 | 6.00 | 6.00 | 6.00 | 6.22 |
| O | 23.96 | 23.95 | 23.97 | 23.93 | 23.96 | 23.95 | 23.93 | 23.96 | 23.88 | 23.76 |
| | Garnet components (Mole fraction) | | | | | | | | | |
| sp | 0.02 | 0.01 | 0.02 | 0.01 | 0.01 | 0.02 | 0.02 | 0.01 | 0.01 | 0.02 |
| al | 0.00 | 0.00 | 0.00 | 0.00 | 0.00 | 0.00 | 0.00 | 0.00 | 0.00 | 0.00 |
| py | 0.01 | 0.01 | 0.00 | 0.01 | 0.01 | 0.01 | 0.00 | 0.01 | 0.00 | 0.00 |
| gr | 0.29 | 0.17 | 0.22 | 0.30 | 0.16 | 0.25 | 0.27 | 0.20 | 0.15 | 0.00 |
| ad | 0.65 | 0.81 | 0.75 | 0.67 | 0.82 | 0.72 | 0.70 | 0.76 | 0.79 | 1.00 |
| sp+al+py | 0.03 | 0.02 | 0.02 | 0.02 | 0.02 | 0.03 | 0.02 | 0.02 | 0.02 | 0.00 |

An. No. : Serial number of analysis in a sample.
sp: Spessartine.
al: Almandine.
py: Pyrope.
gr: Grossular.
ad: Andradite.

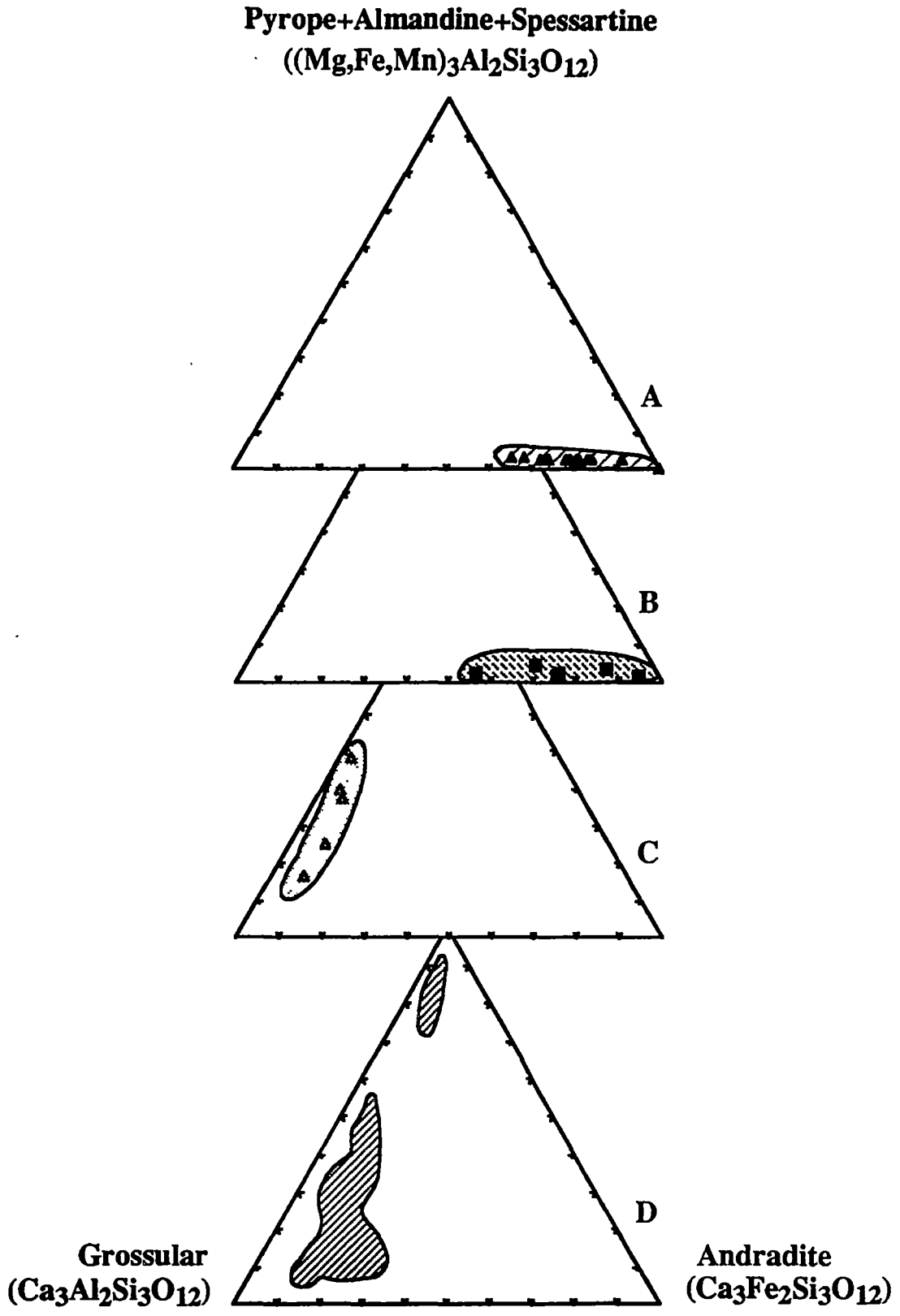


Fig. 5.2. Ternary diagrams showing compositional variation of garnet from the Kara skarn deposit, northwestern Tasmania (A) and other scheelite skarn deposits. **B:** King Island scheelite deposit, Tasmania (from Kwak and Tan, 1981); **C:** Otjua scheelite prospect, Namibia (compositions calculated from data of Steven and Moore, 1994); **D:** MacTung scheelite deposit, Canada (plot adopted from Dick and Hodgson, 1982).

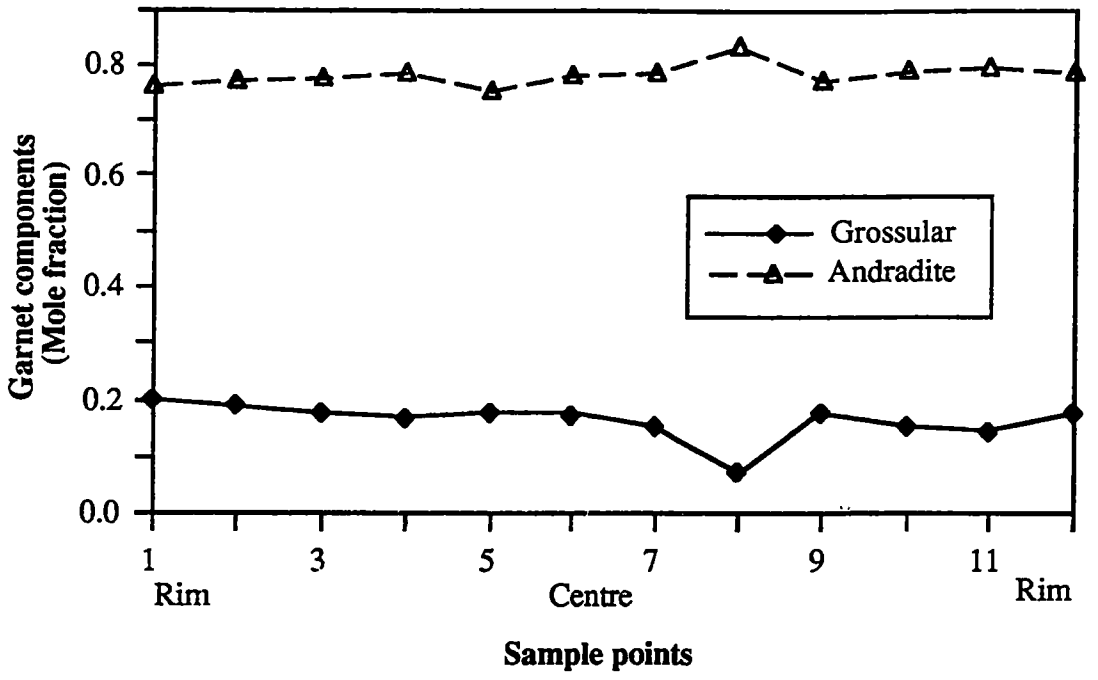


Fig. 5.3. Microprobe traverse showing variation of andradite and grossular across a zoned garnet grain (Stage III). The traverse is about 5mm long. Sample S8 from the Kara deposit, northwestern Tasmania.

grossular garnet. The results reported from the present study are from Stages II and III mineral assemblages. The compositional variation of vesuvianite is very minimal: $SiO_2$ (34.6 - 36.5 wt. % ), CaO (31.3 - 36.9 wt. % C), $Al_2O_3$ (11.5 to 18.8 wt. %), $FeO_{total\ iron}$ (2.7 -7.4 wt. %) and MgO (2.3 - 4.2 wt. %). Late vesuvianite (Stage III) tends to have consistently low magnesium concentrations averaging around 2.5 wt. % MgO. Manganese content in all vesuvianite is very low, <1.0 wt. % MnO. Tin is absent, the highest analysis gaving a value of 0.07 wt. % $SnO_2$. Fluorine and chlorine contents are 1.0-1.8% F and 0.1-0.4% Cl.

### 5.3.4. Amphibole

A range of compositional variations from representative amphibole analyses is given in Table 5.4. The amphibole shows wide compositional variation: $SiO_2$ (34.5 - 43.0 wt. %), $FeO_{total\ iron}$ (18.0 - 33.1 wt. % ), CaO (10.9 - 13.8%), $Al_2O_3$ (6.5 - 14.2 wt. % ), MgO (1.1 - 10.9 wt. %), $Na_20$ and $K_2O$ (1.0 - 2.5 wt. %), and $TiO_2$ (<0.5 wt. % ). The amphibole shows

Table 5.3. Representative microprobe analyses of vesuvianite from Stages II and III mineral assemblages, the Kara skarn deposit. Cation calculations based on procedure of Deer et al. (1980). $H_2O$ content has been inferred to bring oxide total to 100%.

| | Vesuvianite | | | | | | | | | |
|---|---|---|---|---|---|---|---|---|---|---|
| S. No. | 105323 | 105339 | 105341 | S2 | S4A | S8 | S16 | S16 | S32 | S2 |
| An. No. | 3 | 6 | 3 | 1 | 6 | 1 | 1 | 2 | 1 | 6 |
| Stage | II | II | II | II | II | II | II | II | II | III |
| | Oxide composition (wt. %) | | | | | | | | | |
| $SiO_2$ | 35.09 | 34.77 | 35.55 | 34.89 | 35.01 | 36.13 | 35.39 | 35.57 | 35.42 | 35.44 |
| $TiO_2$ | 0.27 | 0.10 | 1.06 | 0.44 | 1.09 | 1.36 | 0.35 | 1.86 | 0.80 | 1.56 |
| $SnO_2$ | 0.04 | 0.00 | 0.00 | 0.00 | 0.04 | 0.00 | 0.01 | 0.00 | 0.00 | 0.04 |
| $WO_3$ | 0.00 | 0.00 | 0.00 | 0.00 | 0.00 | 0.00 | 0.00 | 0.00 | 0.00 | 0.00 |
| $Al_2O_3$ | 13.80 | 12.82 | 14.48 | 11.85 | 14.09 | 17.19 | 13.71 | 14.67 | 12.69 | 14.31 |
| $Cr_2O_3$ | 0.00 | 0.00 | 0.00 | 0.00 | 0.00 | 0.00 | 0.00 | 0.00 | 0.00 | 0.00 |
| FeO | 5.83 | 6.90 | 4.42 | 7.19 | 6.33 | 2.27 | 6.50 | 5.07 | 6.22 | 5.93 |
| CuO | 0.03 | 0.00 | 0.00 | 0.00 | 0.00 | 0.02 | 0.06 | 0.04 | 0.00 | 0.01 |
| ZnO | 0.00 | 0.00 | 0.00 | 0.00 | 0.00 | 0.08 | 0.09 | 0.05 | 0.07 | 0.02 |
| MnO | 0.66 | 0.61 | 0.24 | 0.55 | 0.66 | 0.12 | 0.49 | 0.42 | 0.83 | 1.55 |
| MgO | 2.95 | 3.30 | 3.27 | 4.15 | 2.84 | 3.08 | 3.47 | 2.53 | 3.10 | 2.56 |
| CaO | 35.42 | 35.60 | 36.13 | 35.67 | 35.31 | 36.86 | 36.27 | 35.80 | 31.30 | 34.74 |
| $Na_2O$ | 0.02 | 0.01 | 0.01 | 0.01 | 0.01 | 0.01 | 0.00 | 0.01 | 0.02 | 0.00 |
| $K_2O$ | 0.01 | 0.00 | 0.00 | 0.01 | 0.00 | 0.00 | 0.00 | 0.01 | 0.02 | 0.00 |
| F | 0.76 | 0.00 | 0.00 | 0.97 | 0.65 | 0.67 | 1.43 | 1.08 | 0.92 | 1.82 |
| Cl | 0.25 | 0.16 | 0.18 | 0.13 | 0.23 | 0.29 | 0.24 | 0.39 | 0.16 | 0.14 |
| Total (T) | 95.14 | 94.27 | 95.34 | 95.85 | 96.26 | 98.08 | 98.01 | 97.50 | 91.55 | 98.12 |
| $H_2O$ | 4.87 | 5.73 | 4.66 | 4.15 | 3.74 | 1.92 | 1.99 | 2.50 | 8.45 | 1.88 |
| O=F | 0.32 | 0.00 | 0.00 | 0.41 | 0.27 | 0.28 | 0.60 | 0.45 | 0.39 | 0.76 |
| O=Cl | 0.06 | 0.04 | 0.04 | 0.03 | 0.05 | 0.07 | 0.05 | 0.09 | 0.04 | 0.03 |
| Calc. T | 99.62 | 99.96 | 99.96 | 99.56 | 99.67 | 99.65 | 99.34 | 99.46 | 99.58 | 99.20 |
| | No. of cations based on 76 (O, OH) | | | | | | | | | |
| Si | 16.67 | 16.42 | 16.73 | 16.89 | 16.86 | 17.35 | 17.50 | 17.28 | 16.06 | 17.50 |
| Ti | 0.10 | 0.04 | 0.38 | 0.16 | 0.39 | 0.49 | 0.13 | 0.68 | 0.27 | 0.58 |
| Sn | 0.01 | 0.00 | 0.00 | 0.00 | 0.01 | 0.00 | 0.00 | 0.00 | 0.00 | 0.01 |
| W | 0.00 | 0.00 | 0.00 | 0.00 | 0.00 | 0.00 | 0.00 | 0.00 | 0.00 | 0.00 |
| Al | 7.73 | 7.14 | 8.03 | 6.76 | 8.00 | 9.73 | 7.99 | 8.40 | 6.78 | 8.33 |
| Cr | 0.00 | 0.00 | 0.00 | 0.00 | 0.00 | 0.00 | 0.00 | 0.00 | 0.00 | 0.00 |
| Fe | 2.32 | 2.73 | 1.74 | 2.91 | 2.55 | 0.91 | 2.69 | 2.06 | 2.36 | 2.45 |
| Cu | 0.01 | 0.00 | 0.00 | 0.00 | 0.00 | 0.01 | 0.02 | 0.02 | 0.00 | 0.00 |
| Zn | 0.00 | 0.00 | 0.00 | 0.00 | 0.00 | 0.03 | 0.03 | 0.02 | 0.02 | 0.01 |
| Mn | 0.27 | 0.24 | 0.10 | 0.23 | 0.27 | 0.05 | 0.21 | 0.17 | 0.32 | 0.65 |
| Mg | 2.09 | 2.32 | 2.29 | 2.99 | 2.04 | 2.20 | 2.56 | 1.83 | 2.10 | 1.88 |
| Ca | 18.03 | 18.02 | 18.22 | 18.50 | 18.22 | 18.97 | 19.21 | 18.63 | 15.21 | 18.38 |
| Na | 0.02 | 0.01 | 0.01 | 0.01 | 0.01 | 0.01 | 0.00 | 0.01 | 0.02 | 0.00 |
| K | 0.01 | 0.00 | 0.00 | 0.01 | 0.00 | 0.00 | 0.00 | 0.01 | 0.01 | 0.00 |
| F | 1.24 | 0.00 | 0.00 | 1.61 | 1.07 | 1.10 | 2.43 | 1.80 | 1.43 | 3.08 |
| Cl | 0.75 | 0.49 | 0.52 | 0.38 | 0.70 | 0.88 | 0.75 | 1.20 | 0.46 | 0.44 |
| OH | 15.26 | 17.86 | 14.50 | 13.25 | 11.89 | 6.10 | 6.50 | 8.01 | 25.31 | 6.13 |
| Total | 64.50 | 65.27 | 62.52 | 63.70 | 62.02 | 57.84 | 60.01 | 60.11 | 70.36 | 59.45 |

An. No.: Serial number of analysis in a sample.

Table 5.4. Representative microprobe results of amphibole from the Stage III mineral assemblage, Kara skarn deposit. Element site allocation based on computer programme by Afifi and Essene, University of Michigan.

| | Amphibole | | | | | | | | | |
|---|---|---|---|---|---|---|---|---|---|---|
| S. No. | S17 | S17 | S17 | 18B | 18B | S38 | S38 | S199 | S202 | S202 |
| An. No. | 1 | 4 | 7 | 3 | 6 | 2 | 11 | 3 | 7 | 9 |
| | Oxide composition (%) | | | | | | | | | |
| $SiO_2$ | 43.05 | 38.49 | 36.32 | 40.43 | 34.54 | 37.21 | 37.24 | 41.44 | 39.28 | 42.67 |
| $TiO_2$ | 0.02 | 0.50 | 0.37 | 0.29 | 0.03 | 0.13 | 0.11 | 0.07 | 0.07 | 0.19 |
| $Al_2O_3$ | 6.54 | 11.96 | 12.93 | 10.75 | 12.65 | 12.47 | 14.01 | 12.42 | 12.90 | 8.81 |
| $Cr_2O_3$ | - | - | 0.10 | 0.02 | 0.02 | - | 0.10 | 0.02 | 0.04 | 0.03 |
| $Fe_2O_3$ | 5.05 | 5.78 | 6.92 | 4.40 | 7.91 | 7.20 | 5.26 | 0.68 | 7.94 | 5.85 |
| FeO | 21.68 | 15.49 | 18.67 | 15.46 | 24.19 | 18.30 | 15.79 | 15.74 | 15.69 | 22.05 |
| MnO | 0.60 | 0.41 | 0.44 | 0.92 | 0.75 | 0.77 | 0.73 | 0.66 | 0.73 | 0.67 |
| MgO | 5.80 | 8.04 | 5.38 | 9.06 | 1.08 | 5.30 | 7.34 | 9.75 | 5.83 | 4.11 |
| CaO | 11.48 | 11.95 | 11.84 | 12.42 | 11.33 | 11.76 | 12.21 | 13.58 | 11.56 | 11.02 |
| $Na_2O$ | 1.24 | 1.46 | 1.43 | 1.84 | 1.25 | 1.48 | 1.63 | 1.60 | 1.67 | 1.11 |
| $K_2O$ | 1.01 | 1.92 | 2.31 | 1.19 | 2.50 | 1.76 | 2.04 | 1.85 | 1.89 | 1.89 |
| $H_2O$ | 1.72 | 1.71 | 1.52 | 1.84 | 1.10 | 1.49 | 1.81 | 1.54 | 1.26 | 1.42 |
| F | - | - | - | - | - | - | - | 0.81 | 0.98 | 0.31 |
| Cl | 0.64 | 0.76 | 1.38 | 0.36 | 2.76 | 1.50 | 0.36 | 0.23 | 0.74 | 1.31 |
| O=F | - | - | - | - | - | - | - | 0.34 | 0.41 | 0.13 |
| O=Cl | 0.14 | 0.17 | 0.31 | 0.08 | 0.62 | 0.34 | 0.08 | 0.05 | 0.17 | 0.30 |
| Total | 98.70 | 98.31 | 99.31 | 98.90 | 99.48 | 99.06 | 98.56 | 100.00 | 100.00 | 100.00 |
| | Cation allocations based on 22 oxygen atoms plus 2 (OH) | | | | | | | | | |
| Si IV | 6.84 | 6.06 | 5.82 | 6.27 | 5.76 | 5.95 | 5.86 | 6.24 | 6.03 | 6.64 |
| Al IV | 1.16 | 1.94 | 2.18 | 1.73 | 2.24 | 2.05 | 2.14 | 1.76 | 1.97 | 1.36 |
| $Fe^{+3}$ | 0.00 | 0.00 | 0.00 | 0.00 | 0.00 | 0.00 | 0.00 | 0.00 | 0.00 | 0.00 |
| Ti IV | 0.00 | - | - | 0.00 | - | - | - | - | - | - |
| T site | 8.00 | 8.00 | 8.00 | 8.00 | 8.00 | 8.00 | 8.00 | 8.00 | 8.00 | 8.00 |
| Al VI | 0.06 | 0.28 | 0.26 | 0.23 | 0.25 | 0.30 | 0.46 | 0.45 | 0.36 | 0.25 |
| $Fe^{+3}$ | 0.60 | 0.68 | 0.83 | 0.51 | 0.99 | 0.87 | 0.62 | 0.08 | 0.92 | 0.68 |
| Ti | 0.00 | 0.06 | 0.04 | 0.03 | 0.00 | 0.02 | 0.01 | 0.01 | 0.01 | 0.02 |
| Cr | 0.00 | - | 0.01 | 0.00 | 0.00 | - | 0.01 | 0.00 | 0.00 | 0.00 |
| Mg | 1.37 | 1.89 | 1.28 | 2.09 | 0.27 | 1.26 | 1.72 | 2.19 | 1.33 | 0.95 |
| $Fe^{+2}$ | 2.88 | 2.04 | 2.50 | 2.00 | 3.38 | 2.45 | 2.08 | 2.19 | 2.28 | 3.00 |
| Mn | 0.08 | 0.06 | 0.06 | 0.12 | 0.11 | 0.10 | 0.10 | 0.08 | 0.10 | 0.09 |
| Ca | 0.00 | - | 0.00 | 0.00 | - | 0.00 | - | - | 0.00 | 0.00 |
| M1,2,3 | 5.00 | 5.00 | 5.00 | 5.00 | 5.00 | 5.00 | 5.00 | 5.00 | 5.00 | 5.00 |
| Mg | 0.00 | 0.00 | 0.00 | 0.00 | 0.00 | 0.00 | 0.00 | 0.00 | 0.00 | 0.00 |
| $Fe^{+2}$ | 0.00 | 0.00 | 0.00 | 0.00 | 0.00 | 0.00 | 0.00 | 0.00 | 0.00 | 0.00 |
| Mn | 0.00 | 0.00 | - | - | 0.00 | - | 0.00 | 0.00 | - | - |
| Ca | 1.95 | 2.00 | 2.00 | 2.00 | 2.00 | 2.00 | 2.00 | 2.00 | 1.90 | 1.84 |
| Na | 0.05 | - | - | - | - | - | - | - | 0.10 | 0.16 |
| M4 site | 2.00 | 2.00 | 2.00 | 2.00 | 2.00 | 2.00 | 2.00 | 2.00 | 2.00 | 2.00 |
| Ca | 0.00 | 0.02 | 0.03 | 0.06 | 0.03 | 0.02 | 0.06 | 0.19 | 0.00 | 0.00 |
| Na | 0.34 | 0.45 | 0.44 | 0.55 | 0.40 | 0.46 | 0.50 | 0.47 | 0.40 | 0.17 |
| K | 0.20 | 0.39 | 0.47 | 0.24 | 0.53 | 0.36 | 0.41 | 0.35 | 0.37 | 0.38 |
| A site | 0.54 | 0.85 | 0.95 | 0.85 | 0.96 | 0.83 | 0.97 | 1.02 | 0.77 | 0.55 |
| O | 22.00 | 22.00 | 22.00 | 22.00 | 22.00 | 22.00 | 22.00 | 22.00 | 22.04 | 22.03 |
| OH | 1.83 | 1.80 | 1.63 | 1.91 | 1.22 | 1.59 | 1.90 | 1.55 | 1.29 | 1.47 |
| F | - | - | - | - | - | - | - | 0.39 | 0.48 | 0.15 |
| Cl | 0.17 | 0.20 | 0.37 | 0.09 | 0.78 | 0.41 | 0.10 | 0.06 | 0.19 | 0.34 |

An. No. : Serial number of analysis in a sample.

volatile compositions of 0.2 - 1.2% F and 0.2 - 2.8% Cl.

Microprobe data show that the amphiboles are calcic, falling largely in the hastingsite and magnesian hastingsite fields, on the diagrams of Leake (1978) (Fig. 5.4). Subordinate amounts show compositions towards hornblende and edentite varieties.

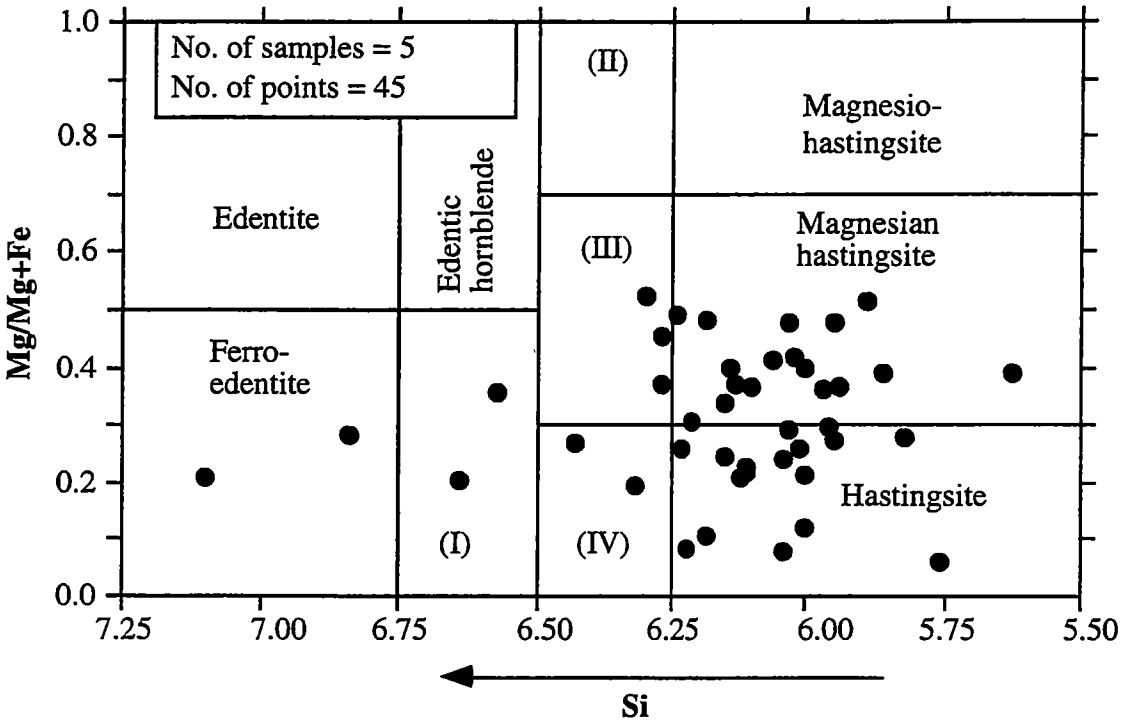


Fig. 5.4. Plot of Mg/(Mg+Fe) against Si (in atomic proportions) of skarn amphibole from the Kara skarn deposit, northwestern Tasmania. Plot based on amphibole classification criteria of Leake (1978). **(I):** Ferro-edentic hornblende; **(II):** Magnesio-hastingsitic hornblende; **(III):** Magnesian hastingsitic hornblende; **(IV):** Hastingsitic hornblende.

### 5.3.5. Epidote and chlorite

***Epidote:*** Typical epidote compositions are given in Table 5.5. Several epidote microprobe analyses have also been reported by Barrett (1980). Epidote shows a narrow compositional range and has average major oxide contents of: 37.0 wt. % $SiO_2$, 24.0 wt. % CaO, 22.9 wt. % $Al_2O_3$, and 12.4% $FeO_{total\ iron}$. It has low chlorine and fluorine concentrations, typically <0.01% F or Cl.

***Chlorite:*** Chlorite compositions are shown in Table 5.5. Many more microprobe analyses of the Kara skarn chlorite have been reported by Barrett (1980) which show higher

Table 5.5. Representative microprobe analyses of epidote and chlorite from Stage III mineral assemblages, Kara skarn deposit. Cation calculations based on procedure of Deer et al. (1980). $H_2O$ content has been inferred to bring oxide total to 100%.

| | Epidote | | | | | | | Chlorite | |
|---|---|---|---|---|---|---|---|---|---|
| S. No. | S8 | S8 | S12 | S12 | S18B | S18B | 105341 | 105328 | 105328 |
| An. No. | 1 | 2 | 1 | 6 | 3 | 4 | 2 | 1 | 2 |
| | | | | Oxide composition (%) | | | | | |
| $SiO_2$ | 36.55 | 36.91 | 39.80 | 39.81 | 37.18 | 36.66 | 36.62 | 28.25 | 30.09 |
| $TiO_2$ | 0.09 | 0.08 | 0.14 | 0.01 | 0.09 | 0.03 | 0.01 | 0.02 | 0.00 |
| $SnO_3$ | 0.09 | 0.06 | 0.00 | 0.00 | 0.00 | 0.00 | 0.00 | 0.05 | 0.01 |
| $WO_3$ | - | - | - | - | - | - | - | 0.00 | 0.00 |
| $Al_2O_3$ | 21.68 | 21.94 | 24.42 | 22.10 | 23.05 | 22.26 | 22.47 | 16.98 | 14.91 |
| $Cr_2O_3$ | 0.00 | 0.00 | 0.00 | 0.00 | 0.00 | 0.00 | 0.00 | 0.00 | 0.00 |
| NiO | 0.00 | 0.00 | 0.00 | 0.00 | 0.00 | 0.00 | 0.00 | - | - |
| FeO | 15.11 | 14.18 | 11.35 | 14.72 | 12.21 | 12.93 | 12.37 | 19.90 | 20.43 |
| CuO | 0.01 | 0.05 | 0.00 | 0.00 | 0.00 | 0.00 | 0.00 | 0.05 | 0.04 |
| ZnO | 0.00 | 0.07 | 0.00 | 0.00 | 0.00 | 0.00 | 0.00 | 0.24 | 0.17 |
| MnO | 0.44 | 0.25 | 0.08 | 0.25 | 0.09 | 0.61 | 0.27 | 1.62 | 1.59 |
| MgO | 0.00 | 0.00 | 0.03 | 0.00 | 0.04 | 0.04 | 0.00 | 19.52 | 18.49 |
| CaO | 23.06 | 23.67 | 23.79 | 22.94 | 23.69 | 23.10 | 23.31 | 0.08 | 0.15 |
| $Na_2O$ | 0.00 | 0.00 | 0.00 | 0.00 | 0.01 | 0.01 | 0.00 | 0.01 | 0.00 |
| $K_2O$ | 0.02 | 0.00 | 0.00 | 0.01 | 0.00 | 0.01 | 0.00 | 0.01 | 0.02 |
| $P_2O_5$ | 0.00 | 0.00 | 0.00 | 0.00 | 0.31 | 0.45 | 0.00 | - | - |
| $SO_3$ | 0.00 | 0.00 | 0.00 | 0.00 | 0.08 | 0.00 | 0.00 | - | - |
| F | 0.01 | 0.03 | 0.05 | 0.02 | 0.00 | 0.00 | 0.00 | 0.38 | 0.20 |
| Cl | 0.00 | 0.00 | 0.00 | 0.00 | 0.10 | 0.00 | 0.01 | 0.01 | 0.01 |
| Total | 97.06 | 97.24 | 99.66 | 99.86 | 96.84 | 96.10 | 95.06 | 87.11 | 86.12 |
| H2O | 2.94 | 2.76 | 0.34 | 0.14 | 3.16 | 3.90 | 4.94 | 12.89 | 13.88 |
| O=F | 0.00 | 0.01 | 0.02 | 0.01 | 0.00 | 0.00 | 0.00 | 0.16 | 0.09 |
| O=Cl | 0.00 | 0.00 | 0.00 | 0.00 | 0.02 | 0.00 | 0.00 | 0.00 | 0.00 |
| Calc T | 100.00 | 99.99 | 99.98 | 99.99 | 99.98 | 100.00 | 100.00 | 99.84 | 99.91 |
| | No. of cations based on 13 (O, OH) for epidote and 36 (O, OH) for chlorite | | | | | | | | |
| Si | 2.99 | 3.01 | 3.25 | 3.31 | 2.98 | 2.93 | 2.89 | 5.75 | 6.05 |
| Ti | 0.01 | 0.00 | 0.01 | 0.00 | 0.01 | 0.00 | 0.00 | 0.00 | 0.00 |
| Sn | 0.00 | 0.00 | 0.00 | 0.00 | 0.00 | 0.00 | 0.00 | 0.00 | 0.00 |
| W | - | - | - | - | - | - | - | 0.00 | 0.00 |
| Al | 2.09 | 2.11 | 2.35 | 2.17 | 2.18 | 2.10 | 2.09 | 4.07 | 3.54 |
| Cr | 0.00 | 0.00 | 0.00 | 0.00 | 0.00 | 0.00 | 0.00 | 0.00 | 0.00 |
| Ni | 0.00 | 0.00 | 0.00 | 0.00 | 0.00 | 0.00 | 0.00 | - | - |
| Fe | 1.03 | 0.97 | 0.77 | 1.02 | 0.82 | 0.86 | 0.82 | 3.39 | 3.44 |
| Cu | 0.00 | 0.00 | 0.00 | 0.00 | 0.00 | 0.00 | 0.00 | 0.01 | 0.01 |
| Zn | 0.00 | 0.00 | 0.00 | 0.00 | 0.00 | 0.00 | 0.00 | 0.04 | 0.03 |
| Mn | 0.03 | 0.02 | 0.01 | 0.02 | 0.01 | 0.04 | 0.02 | 0.28 | 0.27 |
| Mg | 0.00 | 0.00 | 0.00 | 0.00 | 0.00 | 0.00 | 0.00 | 5.92 | 5.55 |
| Ca | 2.02 | 2.07 | 2.08 | 2.04 | 2.03 | 1.98 | 1.97 | 0.02 | 0.03 |
| Na | 0.00 | 0.00 | 0.00 | 0.00 | 0.00 | 0.00 | 0.00 | 0.00 | 0.00 |
| K | 0.00 | 0.00 | 0.00 | 0.00 | 0.00 | 0.00 | 0.00 | 0.00 | 0.01 |
| P | 0.00 | 0.00 | 0.00 | 0.00 | 0.02 | 0.03 | 0.00 | - | - |
| S | 0.00 | 0.00 | 0.00 | 0.00 | 0.00 | 0.00 | 0.00 | - | - |
| F | 0.00 | 0.00 | 0.01 | 0.00 | 0.00 | 0.00 | 0.00 | 0.27 | 0.14 |
| Cl | 0.00 | 0.00 | 0.00 | 0.00 | 0.01 | 0.00 | 0.00 | 0.01 | 0.01 |
| OH | 0.79 | 0.74 | 0.09 | 0.04 | 0.83 | 1.03 | 1.29 | 17.32 | 18.45 |
| Sum | 8.96 | 8.93 | 8.57 | 8.61 | 8.89 | 8.97 | 9.07 | 37.08 | 37.52 |

An. No. : Serial number of analysis in a sample.

magnesium content than the results reported herein. Typical major element oxide concentrations from this study are: 30.0 wt. % $SiO_2$, 20.0 wt. % $FeO_{total\ iron}$, 19.5 wt. % MgO, 15.0 wt. % $Al_2O_3$, <2% wt. MnO, and <0.5 wt. % CaO. Fluorine content is about 0.3 wt. % F, whereas chlorine is distinctly absent. Zinc concentration in chlorite is elevated, averaging 0.20 wt. % ZnO.

**5.3.6. Calcite, apatite and sphene**

***Calcite:*** Analyses of calcite selected from Stages III and IV show narrow compositional variations. Skarn calcite is pure with average oxide proportions of 43.2 wt. % CaO and 0.7 wt. % MgO (analysed) and 54.3 wt. % $CO_2$ (calculated). Iron and manganese are typically absent.

***Apatite and sphene:*** Microprobe analyses of several apatite grains from a selected sample (S35) show that the average skarn apatite composition is 43.0 wt. % $P_2O_5$, 53.5 wt. % CaO, 3.0 wt. % F, and 0.1 wt. % $FeO_{total\ iron}$. Magnesium and manganese are absent in the apatite. Analyses of sphene from the Stage III mineral assemblage (sample S18B) gave average oxide composition of 30.0 wt. % $SiO_2$, 27.8 wt. % CaO, 24.8 wt. % $TiO_2$, 5.9 wt. % $Al_2O3$, 2.7 wt. % $FeO_{total\ iron}$, 0.3 wt. % MgO and 0.04 wt. % MnO.

**5.3. 7. Scheelite and magnetite**

***Scheelite:*** Microprobe analyses of coarse-grained scheelite from the Stages II and III assemblages are shown in Table 5.6. The scheelite shows minor compositional variation within either Stage II or III: $WO_3$ (72.3-77.0 wt. %), CaO (20.0 ±1 wt. %), (0.3-3.1 wt. %, mean 1.8 wt. %), PbO (<0.5 wt %), and FeO and MnO (<0.05 wt. %). Calculated powellite content in scheelite ranges from 1.0 to 7.0 wt. % with an average of ~4.0 wt %. Molybdenum content may vary within a single scheelite grain ( Fig. 5.5). This variation suggests changes in oxidation/reduction conditions or ore fluid content of molybdenum.

***Magnetite:*** Microprobe analyses of Stages II-III magnetite show that mineral is nearly pure, with oxide composition of 97 to 100 wt. % $FeO_{total\ iron}$, <1.5 wt. % MnO. MgO, CaO and $Al_2O_3$ contents are <0.5 wt % . ZnO and NiO concentrations are <0.2 wt. %.

Table 5.6. Selected microprobe results of scheelite from the Stages II and III mineral assemblages, the Kara skarn deposit. Cation calculations based on procedure of Deer et al. (1980).

| S. No. | 105328 | 105323 | 105323 | BS1-1 | BS1-1 | BS1-1 | BS1-1 | BS1-2 | BS1-2 | S202 |
|---|---|---|---|---|---|---|---|---|---|---|
| An. No. | 1 | 2 | 3 | A1 | A5 | A6 | A7 | B2 | B7 | 1 |
| Stage | II | II | III | III | III | III | III | III | III | III |
| | | | | Oxide composition (%) | | | | | | |
| MnO | 0.00 | 0.00 | 0.00 | 0.04 | 0.00 | 0.00 | 0.00 | 0.00 | 0.00 | 0.00 |
| FeO | 0.00 | 0.01 | 0.01 | 0.00 | 0.01 | 0.00 | 0.00 | 0.00 | 0.00 | 0.00 |
| CaO | 20.08 | 19.91 | 19.66 | 20.46 | 13.18 | 20.52 | 20.62 | 20.75 | 20.71 | 20.34 |
| MoO3 | 3.10 | 1.35 | 0.37 | 0.98 | 0.94 | 1.78 | 2.04 | 2.62 | 2.72 | na |
| WO3 | 73.45 | 76.14 | 76.29 | 75.65 | 49.42 | 74.38 | 74.29 | 74.95 | 74.29 | 76.06 |
| PbO | 0.00 | 0.00 | 0.02 | 0.00 | 0.02 | 0.30 | 0.26 | 0.19 | 0.00 | na |
| Total | 96.63 | 97.42 | 96.34 | 97.13 | 63.56 | 96.98 | 97.22 | 98.51 | 97.73 | 96.40 |
| | | | | Allocation of cations based on 4 oxygen atoms | | | | | | |
| Mn | 0.00 | 0.00 | 0.00 | 0.00 | 0.00 | 0.00 | 0.00 | 0.00 | 0.00 | 0.00 |
| Fe | 0.00 | 0.00 | 0.00 | 0.00 | 0.00 | 0.00 | 0.00 | 0.00 | 0.00 | 0.00 |
| Ca | 1.04 | 1.04 | 1.04 | 1.07 | 1.05 | 1.07 | 1.07 | 1.06 | 1.06 | 1.08 |
| Mo | 0.19 | 0.08 | 0.02 | 0.06 | 0.09 | 0.11 | 0.12 | 0.16 | 0.16 | - |
| W | 2.77 | 2.88 | 2.93 | 2.87 | 2.86 | 2.82 | 2.80 | 2.78 | 2.77 | 2.92 |
| Pb | 0.00 | 0.00 | 0.00 | 0.00 | 0.00 | 0.00 | 0.00 | 0.00 | 0.00 | 0.00 |
| | | | | Powellite (mole %) | | | | | | |
| Mo/(Mo+W) | 6.37 | 2.78 | 0.76 | 2.04 | 2.96 | 3.71 | 4.24 | 5.34 | 5.58 | - |

An. No. : Serial number of analysis in a sample.
na: Not analysed

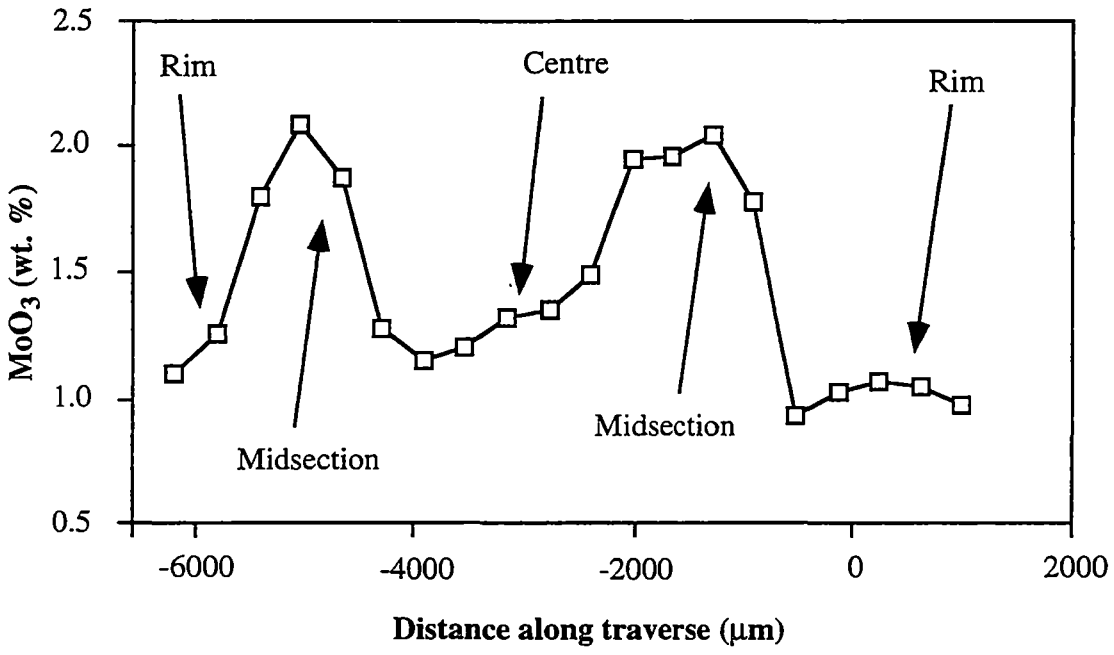


Fig. 5.5. Microprobe traverse showing variation of molybdenum content across a Stage III scheelite grain from the Kara skarn deposit, northwestern Tasmania. Sample BS1.

## 5.4. DISCUSSIONS

Mineral chemical data provide information which can be used to classify the skarn type. Redox conditions prevailing during skarn evolution influence the skarn type formed and can be inferred from the determination of relative ratios of $Fe^{2+}/Fe^{3+}$ in skarn minerals. Sato (1980) and others have shown that reduced skarns typically have relatively high $Fe^{2+}/Fe^{3+}$ ratios, whereas oxidised skarns have relatively low $Fe^{2+}/Fe^{3+}$ ratios. Brown and Essene (1985) have pointed out that redox activities can only be calculated from garnet and pyroxene phases. They argue that other mineral phases are not suitable because either they are end-member in composition (e.g. quartz, wollastonite, fluorite) or have end-member equilibria with insufficient thermodynamic data for redox determination (e.g. vesuvianite, epidote).

Chemical determinations of minerals from the Kara skarn deposit showed that a large proportion of the skarn minerals at Kara are calcium-rich (diopside, andradite, Ca-amphibole, epidote, fluorite, calcite, sphene, apatite, scheelite). This observation suggests high calcium activity during skarn formation, most likely emanating from the dissolution of calcic carbonate protoliths, and thus indicating that the Kara skarn deposit is calcic. There are also skarn minerals with high iron contents (magnetite, andradite, amphibole, epidote, chlorite, hematite) but a bigger proportion of the iron is locked up in magnetite.

Most of the Kara skarn minerals have chemistries that are indicative of oxidising environments of skarn development. The pyroxene at Kara is diopside (Mg-rich, $Fe^{2+}$-poor clinopyroxene) and coexists or is overprinted by andradite garnet ($Fe^{3+}$-rich garnet). Kwak (1994) has pointed out that there is a tendency to produce Mg-rich pyroxene and andradite in oxidised environments, and hedenbergite (plus grossular) in reduced skarns. The occurrence of diopside and andradite with no hedenbergite at Kara suggests that conditions during skarn formation of the Kara deposit were oxidising. Estimation of the log $f(O_2)$ value of skarn formation using garnet composition from temperature-log $f(O_2)$ plots of Gustafson (1974) gave log $f(O_2)$ value of >-25, while garnet-clinopyroxene composition plots of Brown and Essene (1985) showed log $f(O_2)$ values of >-20. The widespread occurrence of magnetite with minor pyrite also tends to support the conclusion of an

oxidising environment of skarn formation. Epidote is believed to suggest oxidising conditions (eg. Kwak, 1994). Its widespread occurrence in the late phases further confirms the oxidised nature of the Kara skarn. Using suggestions of Sato (1980), the observed occurrence of molybdenum within scheelite latices rather than as sulphides (molybdenite) in the skarns at Kara can be construed as indicating an oxidised conditions of formation as opposed to reduced conditions.

Molybdenum contents in scheelite vary from 0.4% to 3.1% $MoO_3$ and can be observed even within one grain and are not spatially associated with molybdenite. These variations in molybdenum contents may be related to availability of molybdenum in the fluids and if they are related changes in oxidation/reduction state of the skarn, then they represent minor fluctuations within a dominantly oxidised skarn. Barrett (1980) concluded that the late stage skarn formation at Kara was reducing from the presence of the rarely encountered molybdenite and low powellite-scheelite. Because molybdenite forms a very insignificant proportion of skarn mineralogy, even in the late stages, it is argued here that the overall late stage oxidation/reduction skarn conditions can not be estimated from this rare molybdenite; it is suggested, instead, that these oxidation/reduction be estimated from more predominant minerals (garnet, clinopyroxene, epidote, scheelite). It is noted that the reducing conditions reported by Barrett (1980) may have existed, but only locally since the predominant skarn minerals from Stages I to IV point to oxidised conditions as discussed above. Calcite coexisting with magnetite carries no iron. This lack of $Fe^{2+}$ (or FeO) in calcite despite abundant iron (magnetite) in calcite facies probably confirms oxidising conditions, whereby most of the iron would be in its oxidised state ($Fe^{3+}$), thus not available for incorporation into the calcite matrix.

The scheelite powellite content of about ~4 wt. % (2 wt. % $MoO_3$) at Kara is lower than the average values of 15 wt. powellite reported in scheelite from the King Island deposit, Tasmania (Wesolowski and Ohmoto, 1986). This difference in the content of molybdenum in scheelite between the two deposits probably indicates that the King Island skarn system represents a relatively molybdenum-rich system in comparison to the Kara system.

In their attempts to classify skarns on the basis of pyroxene compositions, Nakano et al. (1994) reported that Mn/Fe ratios and Zn content of pyroxene in each deposit are relatively constant and that they tend to vary regionally in accordance with metal type. They found that tungsten skarns have pyroxene composition with an intermediate Mn/Fe ratio (averaging around 0.15), Cu-Fe deposits have low Mn/Fe ratios of (<0.1), whereas Zn-Pb deposits contain a high Mn/Fe ratio (>0.2). Using the classification of Nakano et al. (1994), the average clinopyroxene Mn/Fe ratio of 0.17 for the Kara skarn deposit indicates that the deposit is a tungsten skarn deposit.

Stage I and II garnets with relatively high tin levels, averaging 0.25% Sn, appear to be the dominant carriers of the significant tin encountered in the skarn.

# CHAPTER 6: FLUID INCLUSION STUDIES

## 6.1. INTRODUCTION

Fluid inclusion studies supported with detailed paragenetic information provide important information for the understanding of skarn systems (e.g. Einaudi, 1981; Kwak, 1986; Kwak, 1994; Meinert, 1992). Barrett (1980) undertook fluid inclusion studies for the Kara deposit but his studies lacked fluid inclusion data for the minerals from the early phases, and were also not integrated with a detailed skarn paragenetic study. In this study, fluid inclusion studies were undertaken with the following aims:

(1) to understand the thermal history of skarn formation and ore deposition,

(2) to determine the effects of volatile composition on the transport and deposition of scheelite mineralisation, and

(3) to deduce the source of ore fluids and physico-chemical conditions of the skarn system.

## 6.2. METHOD OF STUDY

### 6.2.2. Microthermometric method

The method of collecting microthermometric measurements is similar to that described by Roedder (1984). The method involves obtaining measurements on doubly polished plates prepared from the skarn minerals (and a few from the granite) using a gas-flow USGS heating-freezing stage. The fluid inclusion stage is mounted on a Nikon microscope fitted with a long focal length of x32 power lens. During freezing experiments, the sample chamber is kept fog-free by blowing $N_2$ gas over the chamber. Freezing experiments were carried out first to avoid stretching and decrepitating fluid inclusions. Freezing and heating experiments were restricted to the Types I-III primary fluid inclusions described in the following section. During freezing experiments, freezing point depression and clathration temperature were measured. The clathration temperature was largely shown

by the motion of gas bubbles and a decrease in volume of gas bubbles during the freezing experiments as described in Collins (1979).

These freezing point depressions and clathration temperatures were used to determine salinity data using equation (6.1) of Bodnar (1993) and equation (6.2) of Bozzo et al. (1973).

$$\text{Salinity (equiv. wt. \% NaCl)} = 1.78xT-0.0442xT^2+0.000557xT^3 \quad (6.1)$$

(T: Temperature of depression in °C)

$$\text{Salinity (equiv. wt. \% NaCl)} = 15.5022-1.02342xt-0.05286xt^2 \quad (6.2)$$

(t: Temperature of clathration in °C)

### 6.2.2. Thermal decrepitation mass spectrometry method

Thermal decrepitation mass spectrometry is a technique that has been applied to study volatiles in fluid inclusions by many researchers including Hoffmann et al. (1988). The analytical procedure involves decrepitation of fluid inclusions in a mass spectrometer by steadily increasing heat in the sample chamber of the mass spectrometer.

To determine major volatiles and understand the nature and evolution of the skarn forming fluids, the thermal decrepitation mass spectrometry technique was used on skarn minerals from early to late stage mineral assemblages. A total of 18 samples of clinopyroxene, garnet, vesuvianite, fluorite, calcite, magnetite and scheelite were analysed.

***Method of sample preparation:*** The procedure adopted for sample preparation is similar to that described by many researchers (e.g. Hoffmann, 1988; Norman and Sawkins, 1987). Mineral fragments from crushed/chipped samples were crushed and ground using a hand mortar and pestle, and sieved to retain a -500+211 μm fraction. The sieved fraction was treated with 6M HCl to remove carbonates and sulphides; rinsed with water and acetone to remove carbonaceous material and contamination. For calcite and fluorite, no acid was used. The samples were left to dry at ambient temperatures under an infra-red lamp for about 48 hours for gas determination.

***Volatile determination:*** Determination of gases in fluid inclusions was carried out using the Kratos ISQ Organic Mass Spectrometer at the University of Tasmania Central Science Laboratory. The procedure for the determination was as follows An aluminium Mass Spectrometer sample-cup full of prepared sample (about 7mg) is inserted into the fast response probe and introduced into the Mass Spectrometer sample chamber via the vacuum lock. The probe was heated immediately to 150°C, and the analysis started simultaneously with the commencement of a temperature range of the probe at 20°C per minute to 550°C and held for 10 minutes. The minimum cycle by this method was 400 milliseconds which is too slow to cope with actual length of inclusion bursts, but nevertheless samples sufficiently often to give a representation of major species present. Thus the method is qualitative and also offers semi-quantitative results. Ion profiles for $CH_4^+$ $CH_4$, $OH^+$ and $H_2O^+$ ($H_2O$), $CO_2^+$ ($CO_2$), $H_2S^+$ ($H_2S$), SO, $SO_2^+$ ($SO_2$) and $HCl^+$ (HCl) were determined for each sample.

## 6.3. FLUID INCLUSION PETROGRAPHY

Fluid inclusions were determined from 40 doubly polished sections using a petrographic microscope before commencing the freezing/heating experiments. The fluid inclusions vary in size from <3μm to about 40μm and in shape from equant to rounded, elongated, irregular, and amoeboid.

### 6.3.1. Fluid inclusion types

Four inclusion types can be classified on the basis of observable phases under the microscope and the criteria for relative timing of fluid inclusions from Roedder (1984):

(1) Type I inclusions are primary liquid-vapour inclusions with moderate to high liquid/vapour ratios (Figs. 6.1A-6.1H).

(2) Type II fluid inclusions (Fig. 6.1G) are primary liquid-vapour inclusions containing very fine-grained (<2μm) unidentified daughter minerals that exhibit elongate to equant grain shapes.

(3) Type III inclusions are largely primary inclusions containing liquid and $CO_2$

Fig. 6.1. Photomicrographs of fluid inclusion from skarn minerals, the Kara deposit, northwestern Tasmania. Ty I: Type I; Ty II: Type II; Ty IV: Type IV.

**A.** Abundant Type I fluid inclusions in Stage I clinopyroxene.

**B.** Type I fluid inclusions in Stage III scheelite.

**C.** Triangular-shaped Type I fluid inclusions and trails of Type IV fluid inclusions in Stage III scheelite.

**D.** Equant solitary Type I fluid inclusion in Stage III calcite.

**E.** Elongate and equant Type I fluid inclusions in Stage III quartz.

**F.** Solitary Type I fluid inclusion in Stage III fluorite.

**G.** Types I, II and III fluid inclusions in Stage III fluorite.

**H.** Type I with high vapour/liquid ratios and trails of Type IV fluid inclusions in Stage III fluorite.

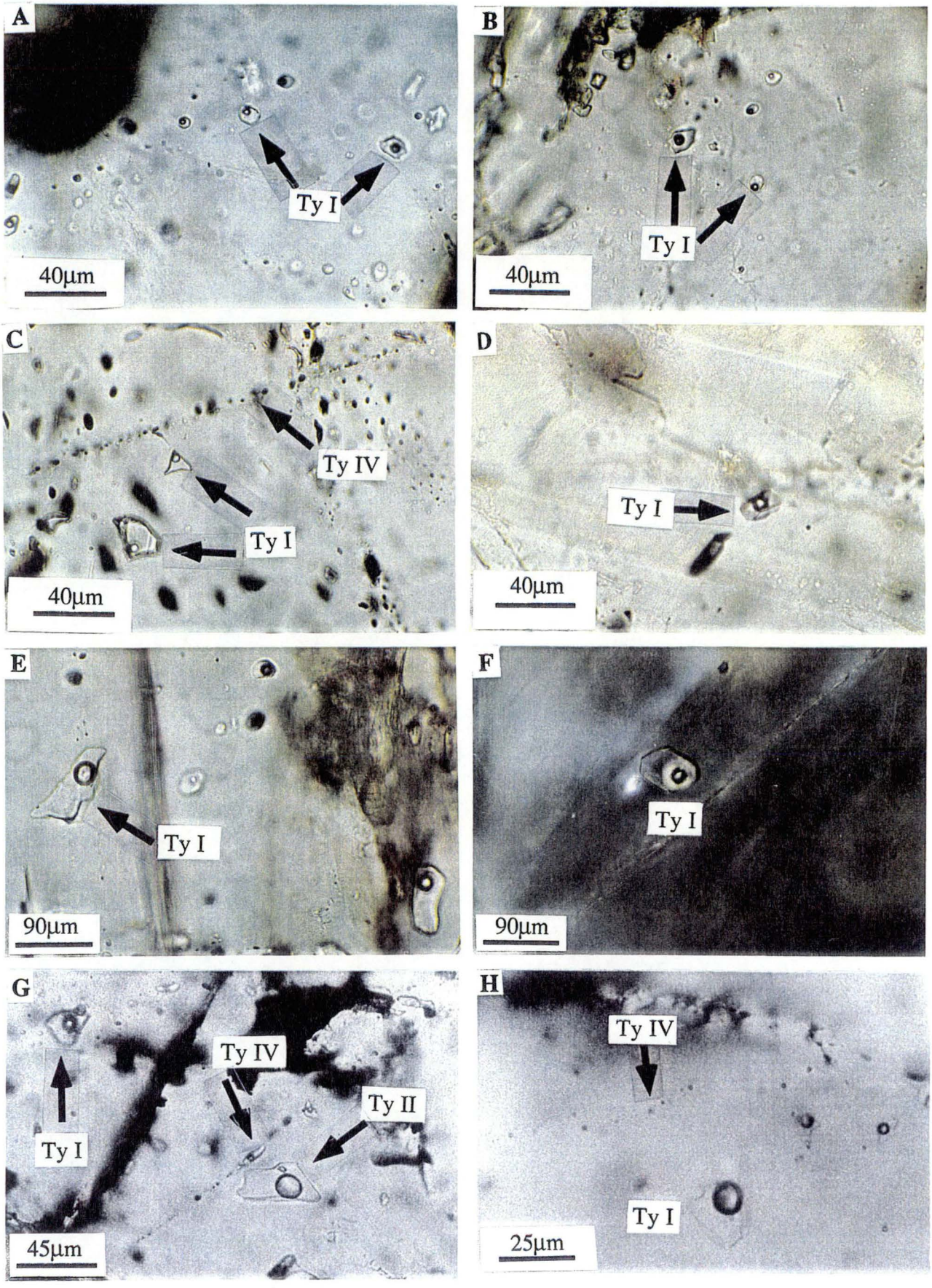
A
Ty I
40μm
B
Ty I
40μm
C
Ty IV
Ty I
40μm
D
Ty I
40μm
E
Ty I
90μm
F
Ty I
90μm
G
Ty IV
Ty II
Ty I
45μm
H
Ty IV
Ty I
25μm

Fig. 6.1

vapour which could not be determined with certainty in many instances and occur rarely.

(4) Type IV fluid inclusions (Figs. 6.1C, 6.1G and 6.1H) are secondary or pseudosecondary liquid-vapour inclusions that contain variable liquid/vapour ratios.

Primary fluid inclusions were identified largely for their solitary occurrence. In places, they form clusters with random spatial distribution. Secondary and pseudosecondary fluid inclusions occur as trails across grain boundaries or within grains and are commonly small, generally <3μm across.

## 6.4. MICROTHERMOMETRY

Microthermometric measurements were acquired from the minerals of Stages I to III comprising clinopyroxene, garnet, vesuvianite, quartz, calcite, fluorite and scheelite. Fluid inclusions in quartz from the granite were also measured.

### 6.4.1 Microthermometric results

Freezing and heating experiments were restricted to the primary fluid inclusions of Types I-III. The results of these experiments are tabulated in Appendix V.

***Homogenisation temperature :*** The Results of the heating experiment are presented graphically in Fig. 6.2. Stage I clinopyroxene yielded a homogenisation temperature range of 460° to 620°C (n = 15), with a bimodal distribution clustering at around 520°C and 600°C (Fig. 6.2A).

The Stage II mineral assemblages gave a wide homogenisation temperature range of 350-570°C with a mode at 500°C (n = 26). The Stage II scheelite gave homogenisation temperatures of 350° to 580°C (n = 15) with a frequency distribution showing a vague bimodal population with modes at about 350°C and 560°C (Fig. 6.2B). Garnet yielded homogenisation temperatures of 460° to 510°C (n = 3), whereas vesuvianite yielded homogenisation temperatures of 360° to 570°C with a mode at 500°C (n = 8).

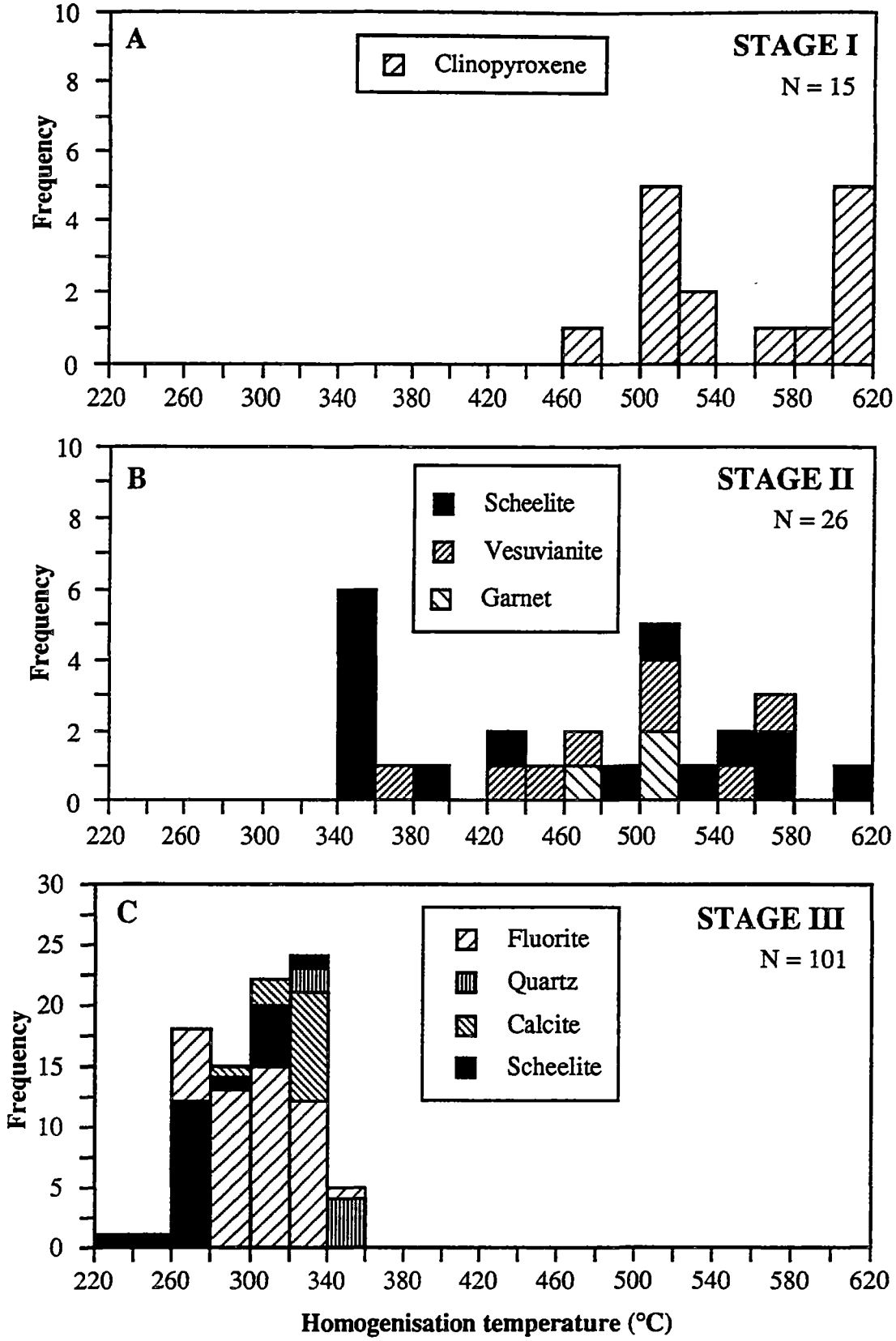


Fig. 6.2. Histograms of homogenisation temperatures from the Stages I-III mineral assemblages, the Kara deposit, northwestern Tasmania.

Quartz, scheelite, calcite and fluorite from the Stage III mineral assemblage yielded a homogenisation temperature range of 240° to 360°C (n = 101) with a general mode at about 300°C (Fig. 6.3C). Individual mineral phases gave homogenisation temperature values as follows: quartz yielded homogenisation temperatures of 296° to 360°C (mode 315°C, n = 20), whereas scheelite gave homogenisation temperatures of 237° to 330°C (mode 280°C, n = 28). Homogenisation temperatures of calcite display values of 294° to 340°C (mode 330°C, n = 12). Fluorite gave a homogenisation temperature range of 262° to 342°C (mode 300°C, n = 41).

Type I fluid inclusions in granite quartz gave homogenisation temperatures above 565°C, whereas Type IV gave homogenisation temperatures ranging from 234.0 to 332.2°C.

***Freezing temperature data:*** Freezing temperature data consisted of first melting point, freezing point depression and clathration temperatures. Only a limited number of first melting point temperature measurements could be obtained. None was measured from the Stage I mineral assemblage. These data show a wide variation from -15.0°C to -56.6°C for Stages II and III mineral assemblages. One measurement from Stage II vesuvianite gave a first melting point of -56.6°C. Stage III mineral assemblages yielded an overall range of first melting points of -15° to -37°C with a median at -32°C (n = 5) from individual measurements of scheelite (-36.6°, -31.5°C), fluorite (-30.0°, -15.0°C) and quartz (-37.0°C). Two measurements of fluid inclusions from granite quartz gave first melting points of -54.9°C and -41.0°C.

The first melting point of -56.6°C is interpreted to be $CO_2$ solid melting while the other first melting point temperatures of down to -37.0°C suggest that the skarn fluids contain salts other than that of sodium (e.g. potassium, calcium and magnesium).

***Salinity:*** The calculated salinity values are presented in histograms in Fig. 6.3 and show a wide variation from as low as 1.0 equiv. wt. % NaCl to 18.0 equiv. wt. % NaCl (Fig. 6.3). Frequency distributions of fluid inclusion salinity data for the skarn assemblage vaguely reveal two populations, one with a mode at about 5 equiv. wt. % NaCl and another at about 12 equiv. wt. % NaCl (Fig. 6.3). Details of salinities for individual minerals and

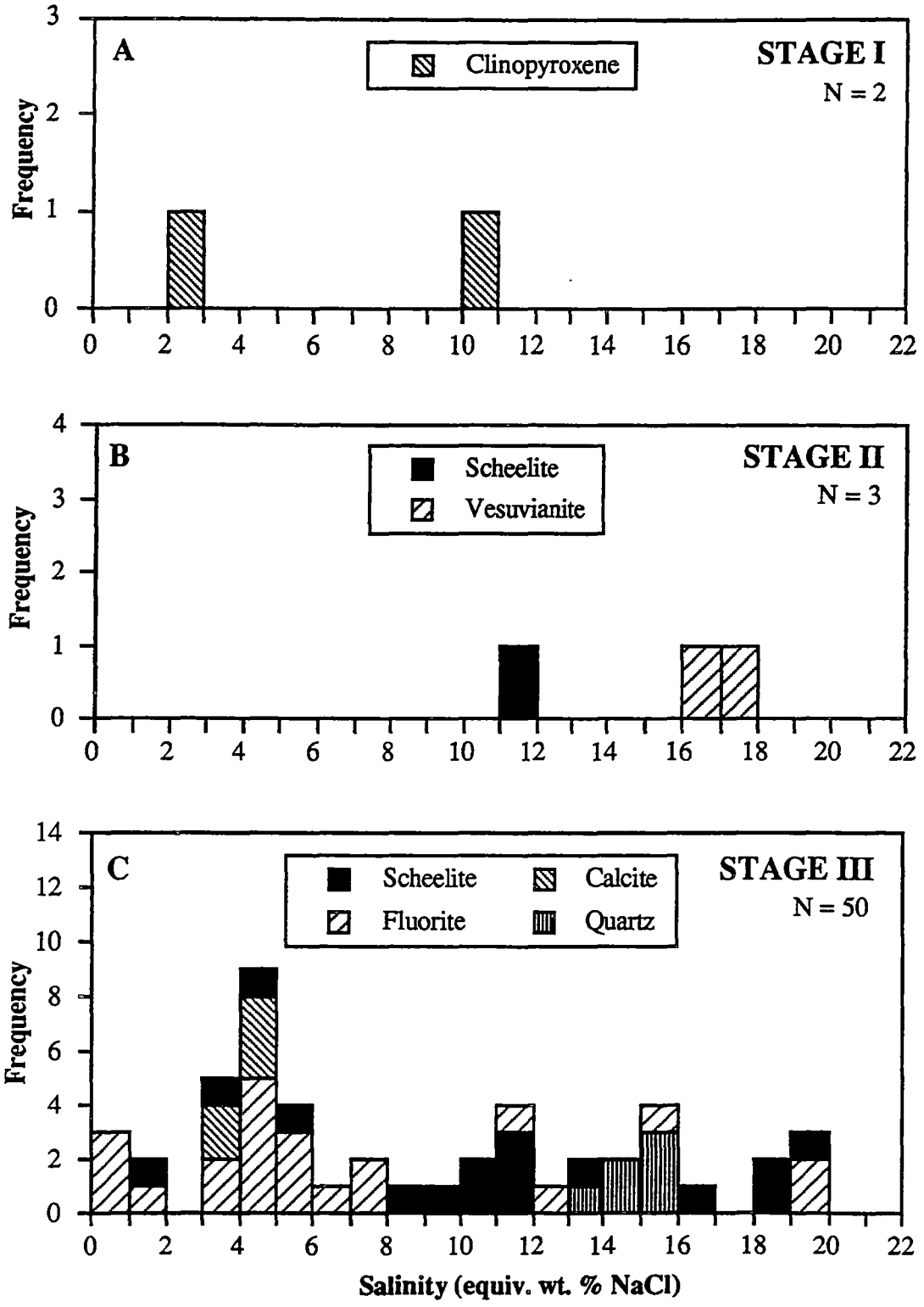


Fig. 6.3. Frequency distribution diagrams of salinity data from Stages I-III skarn mineral assemblages, the Kara deposit, northwestern Tasmania.

mineral assemblages are given below.

Stages I and II consisted of very few measurements (n = 5). Two analyses from Stage I clinopyroxene gave a low salinity value of 2.0 equiv. wt. % NaCl and a higher moderate value of 10.0 equiv. wt. % NaCl (Fig. 6.3A). The Stage II mineral assemblages showed moderate salinities of 12.0 and 17.8 equiv. wt. % NaCl from scheelite and 16.0 equiv. wt. % NaCl from vesuvianite to give a median of 16.0 equiv. wt. % NaCl (Fig. 6.3B).

The Stage III mineral assemblage yielded salinity values of 0.2 to 19.8 equiv. wt. % NaCl and give a bimodal distribution with modes of 5 equiv. wt. % NaCl and 15 equiv. wt. % NaCl (Fig. 6.3C). Individual mineral phases gave salinity values described below. Quartz yielded salinity values of 13.4 to 15.3 equiv. wt. % NaCl (mode 15.0 equiv. wt. % NaCl, n = 7). Scheelite gave a wide salinity range of 1.1- 18.0 equiv. wt % NaCl (mode 11.0 equiv. wt % NaCl, n = 16). Calcite gave salinities of 3.4 to 5.0 equiv. wt. % NaCl (median 5 equiv. wt. % NaCl, n = 5). Fluorite gave salinities of 0.2 to 19.8 equiv. wt. % NaCl (mode 7, n = 22).

Type IV fluid inclusions in granite quartz yielded salinities of 0.2, 23.5 and 25.5 equiv. wt. % NaCl.

Fig. 6.4 is a scatter plot showing the relationship between homogenisation temperature and salinity data for the Stages I to III mineral assemblages from the Kara skarn deposit. There appears to be no systematic relationship between homogenisation temperature and salinity. However, the data show a general cooling trend of skarn and ore fluids from Stages I-II to Stage III, but the salinity data displays variable trends from Stage I (2-10 equiv. wt. % NaCl) and Stage II (12-18 equiv. wt. % NaCl) to Stage III (0.2-20 equiv. wt. % NaCl). This salinity variation is difficult to interpret as variable salinities can be formed by mixing or boiling of fluids.

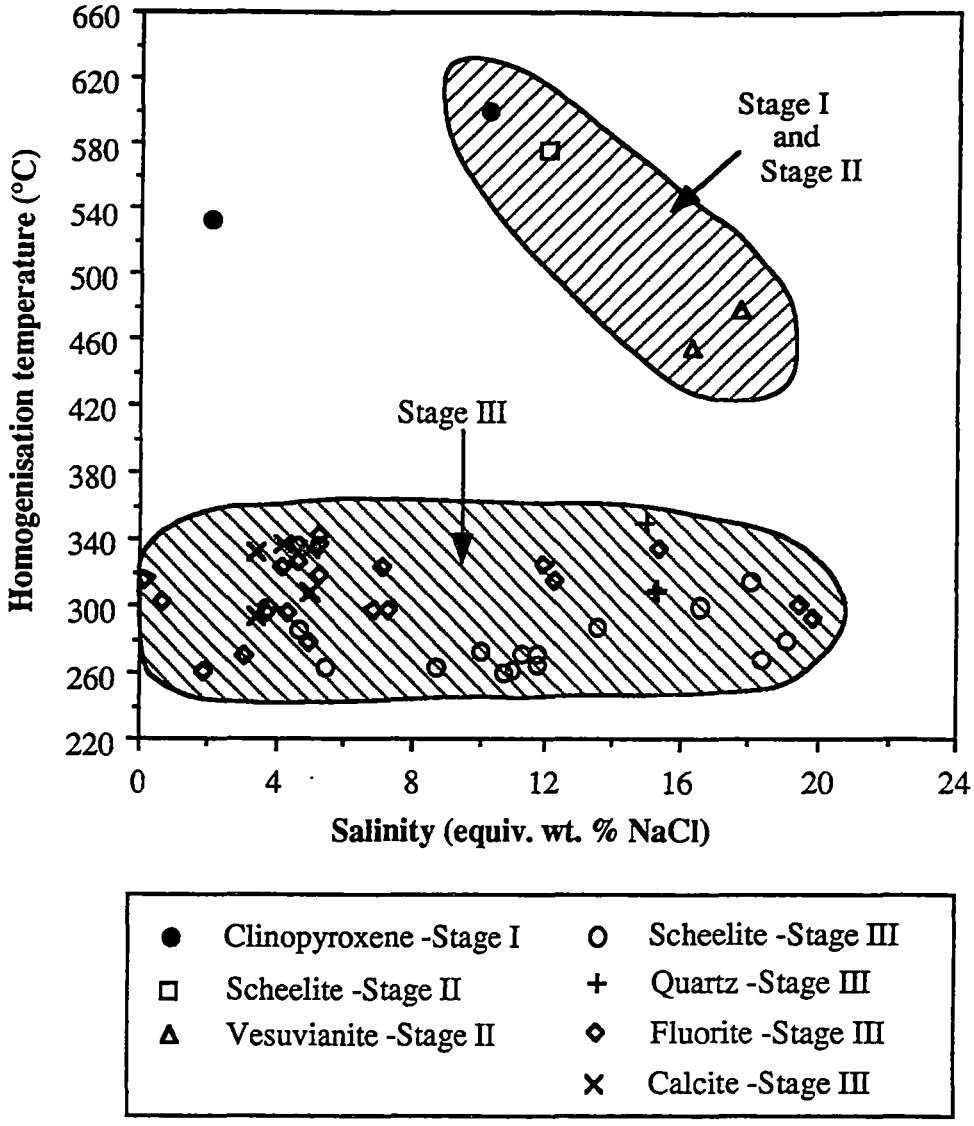


Fig. 6.4. Plot of homogenisation temperatures against salinity values of fluid inclusions from the Stages I-III skarn minerals, Kara deposit, northwestern Tasmania.

## 6..5. THERMAL DECREPITATION MASS SPECTROMETRY

Volatile components in fluid inclusions include $H_2O$, $H_2S$, $O_2$, $CO_2$, CO, Ne, Ar, $CH_4$, $C_nH_n$ and $N_2$. Fluid inclusion gas compositions are considered by many workers (e.g. Norman and Sawkins, 1987; Kesler , 1988; Khin Zaw et al., 1994) to provide useful insights into the chemistry of hydrothermal fluids, fluid-rock interaction and possible mechanism of ore deposition. The interaction of wall rocks and ore fluid may add gas to the fluids to trigger ore deposition. Gilbert et al. (1992) showed that high levels of $N_2$ (up to 10

mole %) in hydrothermal fluids decrease the solubility of scheelite and therefore favour its deposition.

### 6.5.1. Results

Results of the gas analyses are summarised in Table 6.1. Selected fluid inclusion gas chromatographs are presented in Appendix VI. Fig. 6.5 is an example of fluid inclusion gas chromatographs from a Stage II scheelite showing the relative abundances of $CH_4$, $OH^+$

Table 6.1. Fluid inclusion gas composition of skarn minerals from the Kara deposit, northwestern Tasmania.

| S. No. | $H_2O$ | $CO_2$ | $CH_4$ | $H_2S$ | $SO_2$ | $N_2$ | HCl | REMARKS |
|---|---|---|---|---|---|---|---|---|
| Clinopyroxene (Stage I) | | | | | | | | |
| S36 | W | W | nd | nd | | | nd | gas-poor |
| Garnet (Stage II) | | | | | | | | |
| S16 | W | nd | nd | nd | | | nd | gas-poor |
| Vesuvianite (Stage II) | | | | | | | | |
| SII3 | S | nd | nd | S | | | S | $H_2S$-HCl |
| Scheelite (Stage II) | | | | | | | | |
| S159 | S | S | nd | M | nd | nd | S | $CO_2$-$H_2S$-HCl |
| Magnetite (Stage II) | | | | | | | | |
| S82 | S | W | W | nd | | | W | gas-poor |
| Scheelite (Stage III) | | | | | | | | |
| BS1 | S | W | W | M | nd | nd | S | $H_2S$-HCl |
| S127 | S | W | W | M | nd | nd | S | $H_2S$-HCl |
| S189 | S | W | M | M | nd | nd | W | $H_2S$-$CH_4$ |
| S200 | S | W | W | S | nd | nd | M | $H_2S$-HCl |
| S206 | S | W | nd | M | nd | nd | S | $H_2S$-HCl |
| Magnetite (Stage III) | | | | | | | | |
| S35 | M | M | nd | nd | | | nd | $CO_2$ |
| S127 | S | W | nd | W | | | nd | |
| S178 | S | W | nd | nd | | | W | |
| S200 | W | nd | nd | nd | | | W | |
| S202 | S | nd | nd | nd | | | nd | gas-poor |
| Fluorite (Stage III) | | | | | | | | |
| S17 | S | M | W | W | nd | nd | nd | $CO_2$ |
| Quartz-epidote (Stage III) | | | | | | | | |
| S81 | S | nd | nd | W | | | nd | gas-poor |
| Calcite (Stage III) | | | | | | | | |
| S179 | S | M | nd | W | - | - | nd | $CO_2$ |
| S182 | S | S | W | nd | nd | nd | nd | $CO_2$ |

S, strong; M, moderate; W, weak; nd, not detected.

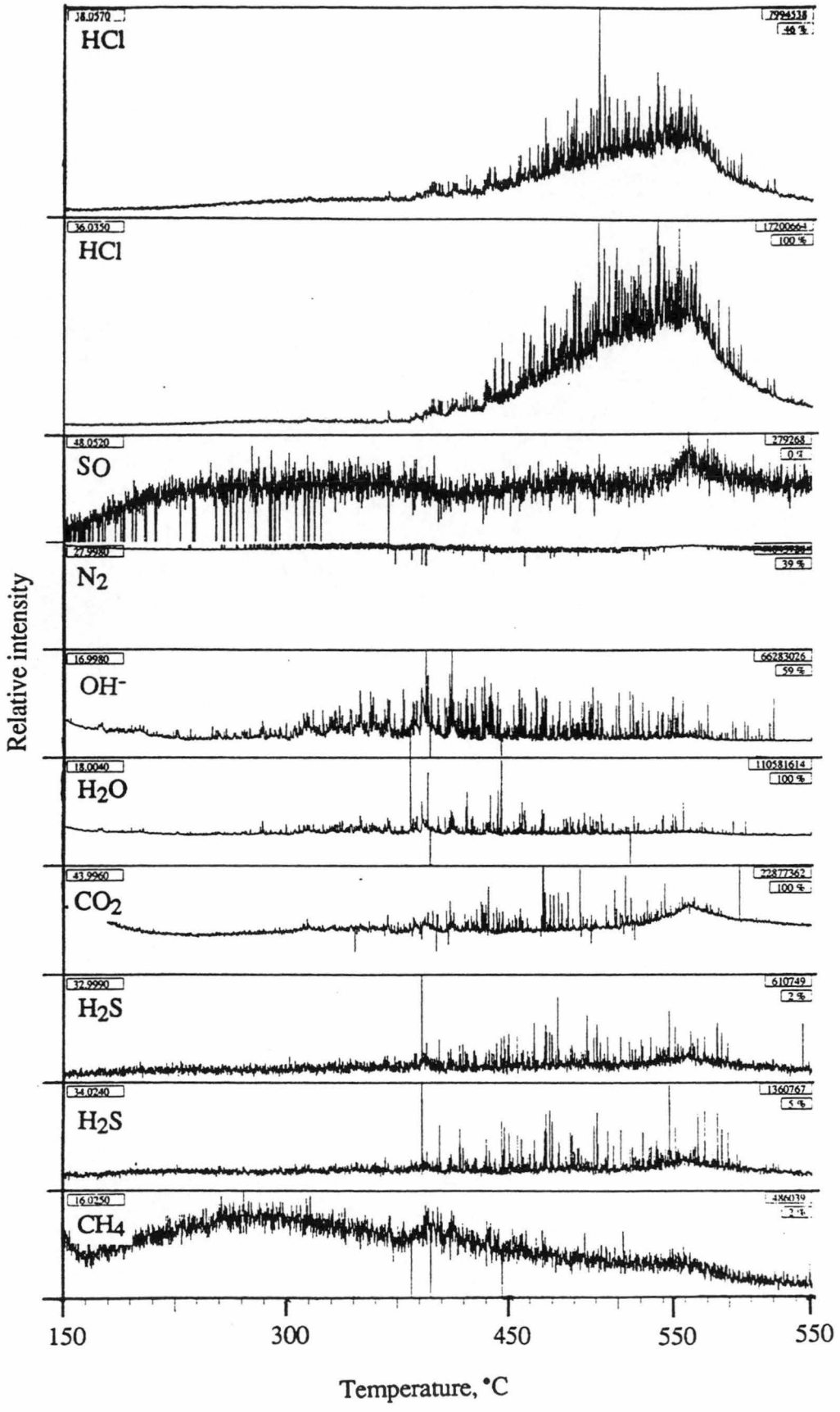


Fig. 6.5. Thermally decrepitated mass spectrometric chromatographs of fluid inclusion volatiles from Stage II scheelite(Sample number S159), the Kara deposit, northwestern Tasmania.

and $H_2O^+$ ($H_2O$), $CO_2^+$ ($CO_2$), $H_2S^+$ ($H_2S$), SO, $SO_2^+$ ($SO_2$) and $HCl^+$ (HCl) . To provide a semi-quantitative result, four categories were used. They represent a combination of 1) the intensity of the species' signal during decrepitation relative to the background signals and 2) the number of such spikes. The four categories in order of decreasing level of importance are: (i) strong, (ii) moderate, (iii) weak, and (iv) not detected.

Spectra from all analyses show that $H_2O$ is the major volatile component of the fluid inclusions. $N_2$ proved difficult to detect mainly because of the inherent high levels of $N_2$ in the analytical system. Fluid inclusions from the early mineral assemblage (clinopyroxene) have negligible amounts of volatiles: typically low $H_2O$, $CO_2$ and no $CH_4$ or $H_2S$. Fluid inclusions from Stage II garnet also show similar gas compositions to those of the Stage I clinopyroxene although they lack $CO_2$.

Other skarn assemblages also show $H_2O$ as a major constituent. Stage II vesuvianite has strong concentrations of $H_2S$, HCl and no $CH_4$. Stage II scheelite also has strong $H_2S$ and HCl but contains high $CO_2$ concentrations as well. Stage III scheelite has similar composition to Stage II scheelite except for the relatively lower concentrations of $CO_2$ and moderate to low $CH_4$. Stage II magnetite shows low $CO_2$, $CH_4$ and HCl, whereas the Stage III magnetite shows moderate to no $CO_2$, weak to no HCl, occasional low $H_2S$ and no $CH_4$. Fluorite (Stage III) has moderate $CO_2$ and weak $CH_4$ and $H_2S$. Stage III calcite shows strong concentrations of $CO_2$ and little to no $CH_4$ and $H_2S$.

## 6.6. DISCUSSIONS

### 6.6.1. Implications of fluid inclusion microthermometry data

Fluid inclusion microthermometry of the Kara skarn minerals reveals a temperature progression from higher homogenisation temperatures (up to >610°C) for early mineral assemblages to lower homogenisation temperatures (down to 240°C) for late mineral assemblages. The early assemblages represented by clinopyroxene, garnet, vesuvianite and scheelite of Stages I-II gave homogenisation temperatures of 350° to >610°C and display more than one population with clusters at about 350°, 500° and 600°.

Late mineral assemblages represented by scheelite, calcite, fluorite and quartz of

Stage III display homogenisation temperatures ranging between 240°C and 350°C, average 300°C. Though scheelite mineralisation occurred throughout much of the skarn-forming phases from early high temperature to late low temperature phases, major scheelite deposition developed during the late phases of skarn formation at around 280°C in association with hydrous-rich minerals. Magnetite mineralisation occurred in a similar manner to scheelite but a reasonably high proportion of the total magnetite appears to have been deposited in the early phases (Stage II) as opposed to scheelite. This type of skarn development and ore deposition of dominantly anhydrous minerals at high temperatures (>500°C) during the early stages followed by the formation of lower temperature hydrous mineral assemblages in association with ore deposition is in agreement with many studies on skarn deposits (e.g. Einaudi et al., 1981; Kwak, 1987, 1994; Meinert, 1992).

Salinity values revealed by the Stages I to III skarn assemblages vary widely from as low as 0.2 eq. wt % to as high as 19.0 equiv. wt. % NaCl. A plot of temperature against salinity shows that Stages I and II salinity data, though limited in number, generally cluster along a line with a negative slope if one low salinity value is ignored, whereas the Stage III salinity data cluster along a line parallel to the salinity axis. Adopting interpretations of Shepherd et al. (1985), the following deductions can be made for the Kara deposit. The negative trend revealed by Stages I and II data probably suggests involvement of high temperature magmatic brines during the early phases of skarn formation, while the horizontal trend for the Stage III assemblages may be related to fluid mixing caused by continued introduction of high saline fluids from the nearby granite and a new source of low saline fluids of possible meteoric origin. Involvement of at least two fluid sources has been suggested for other skarns (e.g. JC tin skarn deposit, Layne and Spooner, 1991). First melting points of down to -37.0°C obtained for the Stages II and III mineral assemblages suggest that skarn fluids were complex NaCl-KCl-$CaCl_2$-$MgCl_2$-$H_2O$ brines.

### 6.6.2. Implications of fluid inclusion gas composition

Gas analyses of samples from early skarn assemblages to late skarn assemblages show that the early anhydrous phases (clinopyroxene and garnet) are poor in volatile gases. They

have weak levels of $H_2O$ and $CO_2$. This low volatile content in these early anhydrous skarn minerals may be explained by 1) lack of fluid decrepitation of inclusions during heating to 550°C due to high temperature of homogenisation (550°C) or 2) deposition of the minerals from fluids that had low concentrations of volatiles. This interpretation is in line with other skarn studies which show that early skarn formation is largely anhydrous (e.g. Meinert, 1992) and tend to support the formation of dominantly anhydrous minerals.

Fluid inclusions in magnetite show $H_2O$ and $CO_2$ as the only significant volatiles. This composition of $H_2O$ and $CO_2$ in fluid inclusions in magnetite would indicate an oxidised environment of formation as indicated by the redox reaction (6.3). Equation (6.4) may also be applied to explain the fluid inclusion composition in magnetite.

$$CH_4 + O_2^- = H_2O + CO_2 \qquad (6.3)$$

$$H^+ + HCO_3^- = H_2O + CO_2 \qquad (6.4)$$

The apparent absence of other species such as $CH_4$ in magnetite fluid inclusions would suggest complete reaction to the right in equations (6.3) and (6.4) at the time of magnetite deposition. Sherlock et al. (1993) have argued that $CO_2$ can exist without $CH_4$ in oxidised environments (>log $f(O_2)$ = -30). The $CO_2$ could partly be emanating from the decomposition of the limestone (Gordon Limestone) as a result of heat from the granite intrusion or fluids thereof as shown in equation (6.5).

$$CaCO_3 = CaO + CO_2 \qquad (6.5)$$

Many studies and models on hydrothermal deposits (e.g. Polya, 1987; Gilbert et al., 1992) have shown that scheelite transportation occurs under low pH, whereas deposition occurs at high pH in saline fluids. Gilbert et al. (1992) further showed that the presence of $CH_4$, $CO_2$ and $N_2$ enhances scheelite deposition. Many workers including Wesolowski et al. (1984) and Wood and Vlassopoulos (1989) have reported that tungsten is transported

chiefly as $WO_4^{2-}$, $HWO4^-$, $H_2WO_4$, $NaHWO_4$ species rather than a chloride (or other halogen) complex in natural solutions. Using this information, equation (6.6) can be proposed to account for the species detected in scheelite. Thus fluids transporting tungsten under low pH (inferred from the presence of HCl gases) would precipitate scheelite upon encountering a favourable site such as one with high salinity and high $Ca^{2+}$ activity. HCl gases detected in scheelite can be interpreted 1) as remnants of the contents of the transporting media and/or 2) as products resulting from the deposition of scheelite as shown in equation (6.6). The relatively strong concentration of $H_2S$ in scheelite fluid inclusions together with HCl is considered to have provided the required acidity (equation 6.7) in the transporting media before deposition.

$$HWO_4^- + Ca^{2+} + NaCl = CaWO_4 + HCl + Na^+ \quad (6.6)$$

$$H^+ + HS^- = H_2S \quad (6.7)$$

Early scheelite (Stage II) has high $CO_2$ as opposed to the low $CO_2$ in later scheelite (Stage III). This change may indicate that most of the $CO_2$ had escaped at the time or where later scheelite was being deposited. The Stage III calcite which is observed to have strong $CO_2$ concentrations is generally not spatially associated with significant scheelite.

Scheelite fluid inclusions generally show low to no $CH_4$ gas. This gas and other organic compounds in granite-related hydrothermal deposits emanate largely from the break-down of organic compounds in sedimentary piles through interaction with hydrothermal fluids as demonstrated by Hoffmann et al. (1988) for the Aberfoyle tin-tungsten deposit in northeastern Tasmania. $CH_4$ can influence oxidation/reduction state as discussed in other studies on metal transport (e.g. Khin Zaw, 1994). The absence or rarity of $CH_4$ suggests that ore deposition at Kara occurred under oxidising conditions, which is in agreement with the conclusion from mineral chemistries given in Chapter 5 of this thesis.

# CHAPTER 7: STABLE ISOTOPE GEOCHEMISTRY

## 7.1. INTRODUCTION

Stable isotope studies provide important constraints for the source(s) of ore fluids responsible for the deposition of mineralisation (eg. Valley, 1986). Source reservoirs generally show characteristic isotopic ranges, and potential sources for ore fluid include: 1) sea water (O, H, S, C), 2) meteoric water (O, H), 3) mantle (O, S, C) and 4) biosphere (C, H, N, S) (Taylor, 1987). The present study involved analyses of carbon and oxygen stable isotopes from skarn minerals and the associated protolith marble of the Gordon Limestone with a view to determining:

(1) the source or sources of skarn- and ore-forming fluids, and

(2) the history of these fluids.

## 7.2. METHOD OF STUDY

Carbon and oxygen isotope measurements on carbonate rocks were performed at the University of Tasmania Central Science laboratory. Samples for analyses were prepared by drilling out calcite material from hand specimens. The analyses were performed by conventional methods and involved reacting the samples at 25°C to produce gases for measurement on a VG micromass 602D mass spectrometer. Nineteen samples of calcite from Stages III and IV and the Gordon limestone were analysed. The isotopic ratios measured were reported in the conventional notation as $\delta$ values in per mil (‰) with an analytical error of ±0.1 ‰. The oxygen isotopic ratios are given as Standard Mean Ocean Water (SMOW) values and carbon as Peedee Belemnite (PDB) values.

Scheelite and magnetite samples were prepared for oxygen isotope analysis in the Geology Department at the University of Tasmania. The oxide materials for oxygen analysis were obtained by grinding and hand picking the mineral grains. Liberation of oxygen was achieved using the method of Clayton and Mayeda (1963) with bromine penta-

fluoride as a reagent. The liberated oxygen was analysed for oxygen isotopic ratios in the University of Tasmania Central Science Laboratory using a SIRA Series II VG Isogas stable isotope ratio mass spectrometer on five magnetite samples and nine scheelite samples from Stages II and III. The results are reported with respect to SMOW with an error of ±0.2 ‰.

## 7.3. CARBON AND OXYGEN ISOTOPIC COMPOSITIONS OF CARBONATES

Carbon and oxygen isotope analyses of carbonates were undertaken to supplement the earlier results of Barrett (1980), who previously analysed isotope compositions of four secondary (vein or vug) calcites and two protolith marble. Barrett's (1980) results are here considered to be Stages III/ IV of the present classification as his studies were not integrated into a detailed paragenesis.

### 7.3.1. Results

Carbon and oxygen isotope results of the protolith marble and Stages III and IV calcite are presented in Table 7.1 together with the earlier results of Barrett (1980).

***$\delta^{13}C$ values:*** Fig. 7.1 shows the frequency distribution of the $\delta^{13}C$ values of carbonate. The $\delta^{13}C$ values for the protolith marble vary from -1.6 to -4.4‰ with a median of -2.4 ‰ ( N= 3). The $\delta^{13}C$ values of Stage III calcite vary from -2.6 to -7.2‰ (PDB) with a mode of -4.5‰ (N = 13), whereas the Stage IV calcite yielded -1.6 to -5.0‰ with a median of -4.8‰ (N = 3). The Stage III/IV secondary calcite results of Barrett (1980) range from -5.2 to -7.3‰ with a mode of -6.5‰ (N = 4). The calcite $\delta^{13}C$ data for late skarn formation gives a range of -1.6 to -7.3‰ (mode at -5.0‰, N = 20).

***$\delta^{18}O$ values:*** Fig. 7.2 shows the frequency distribution of these results. The calcite $\delta^{18}O$ data for the protolith marble from the present studies and Barrett's (1980) work range from 11.7 to 23.4‰ with a median of 13.5‰ (N= 3). The calcite $\delta^{18}O$ values are 3.4 to 14.0‰ (mode at 11.5‰ ) for Stage III calcite; 9.8 to 12.1‰ (median 10.3‰) for Stage IV calcite and 7.8 to 11.7‰ (mode 10.3‰) for Barrett's (1980) calcite results (Stages III/IV). Overall, the calcite $\delta^{18}O$ data for the late skarn assemblages give a range from 3.4 to 14.0‰ (mode 11.2‰).

Table 7.1. Isotopic compositions of protolith marble and Stages III-IV skarn calcites, the Kara deposit, northwestern Tasmania. The associated fluid isotopic compositions were calculated using equations of O'Neil (1969) and Ohmoto and Rye (1979).

| Sample No. | Skarn Stage or marble | $\delta^{13}C_{calcite}$ ‰ (PDB) | $\delta^{18}O_{calcite}$ ‰ (SMOW) | $\delta^{13}C_{CO2}$ ‰ (PDB) | $\delta^{18}O_{H2O}$ ‰ (SMOW) |
|---|---|---|---|---|---|
| 60960# | Marble | -1.60 | 23.40 | 1.21 (at 500°C) | 22.27 (at 500°C) |
| 60961# | Marble | -4.40 | 13.50 | -1.86 (at 500°C) | 12.37 (at 500°C) |
| S184 | Marble | -2.44 | 11.67 | -0.11 (at 330°C) | 7.63 (at 330°C) |
| S46 | III | -7.29 | 12.23 | -4.95 (at 330°C) | 8.19 (at 330°C) |
| S109 | | -4.73 | 13.98 | -2.40 (at 330°C) | 9.95 (at 330°C) |
| S112 | | -4.43 | 11.80 | -2.09 (at 330°C) | 7.77 (at 330°C) |
| S146 | | -4.11 | 6.90 | -1.78 (at 330°C) | 2.87 (at 330°C) |
| S155 | | -6.78 | 10.31 | -4.44 (at 330°C) | 6.27 (at 330°C) |
| S168 | | -5.00 | 7.24 | -2.66 (at 330°C) | 3.20 (at 330°C) |
| S177 | | -5.60 | 12.81 | -3.27 (at 330°C) | 8.77 (at 330°C) |
| S178 | | -5.41 | 3.41 | -3.08 (at 330°C) | -0.63 (at 330°C) |
| S179 | | -2.62 | 12.78 | -0.28 (at 330°C) | 8.74 (at 330°C) |
| S180 | | -4.37 | 11.83 | -2.03 (at 330°C) | 7.80 (at 330°C) |
| S182 | | -4.58 | 10.92 | -2.24 (at 330°C) | 6.88 (at 330°C) |
| S183 | | -5.23 | 11.89 | -2.90 (at 330°C) | 7.86 (at 330°C) |
| S191 | | -5.25 | 11.44 | -2.91 (at 330°C) | 7.41 (at 330°C) |
| 105316# | III/IV | -5.20 | 11.70 | -2.86 (at 330°C) | 7.66 (at 330°C) |
| 105315# | | -7.30 | 8.10 | -4.96 (at 330°C) | 4.06 (at 330°C) |
| 105317# | | -6.60 | 12.10 | -4.26 (at 330°C) | 8.06 (at 330°C) |
| 105318# | | -6.30 | 7.80 | -3.96 (at 330°C) | 3.76 (at 330°C) |
| S39 | IV | -4.99 | 9.83 | -3.83 (at 240°C) | 2.96 (at 240°C) |
| S89 | | -4.79 | 10.37 | -3.63 (at 240°C) | 3.50 (at 240°C) |
| S196 | | -1.67 | 12.07 | -0.51 (at 240°C) | 5.20 (at 240°C) |

# Sample with mineral isotopic compositional data from Barrett (1980), and fluid $\delta^{13}C_{CO2}$ and $\delta^{18}O_{H2O}$ values calculated in the present study.

### 7.3.2 Carbon and oxygen isotopic compositions of fluids

Carbon and oxygen isotopic compositions of fluids responsible for the formation of the protolith marble and the skarn were determined in order to unravel the history of the

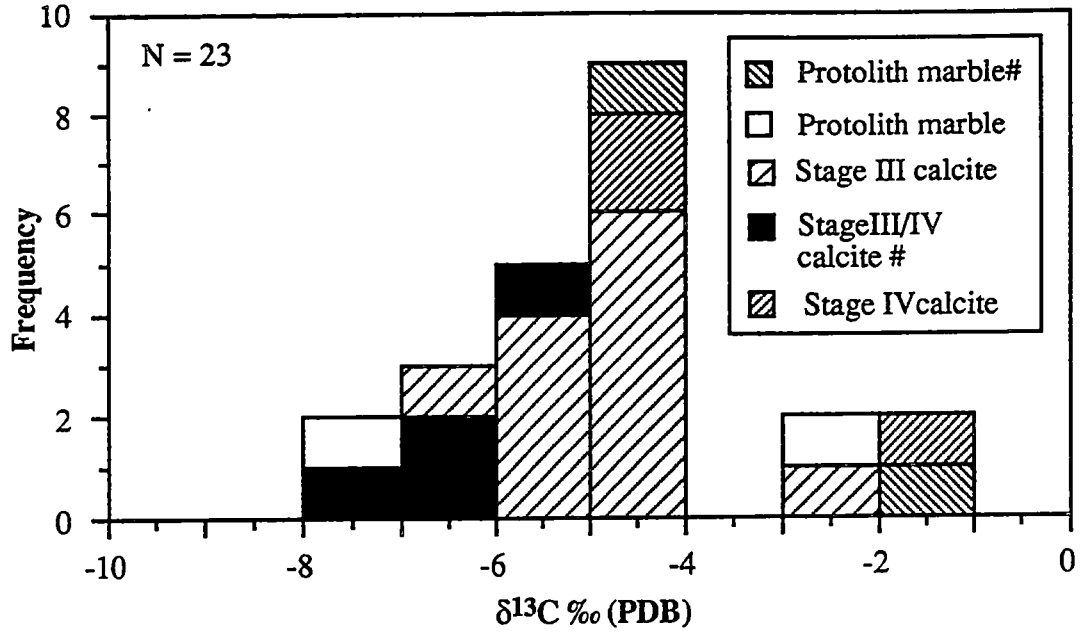


Fig. 7.1. Frequency distribution of $\delta^{13}C$ carbonate values (‰, PDB) of the protolith marble and Stages III-IV skarn calcites from the Kara deposit, northwestern Tasmania. # Data from Barrett (1980).

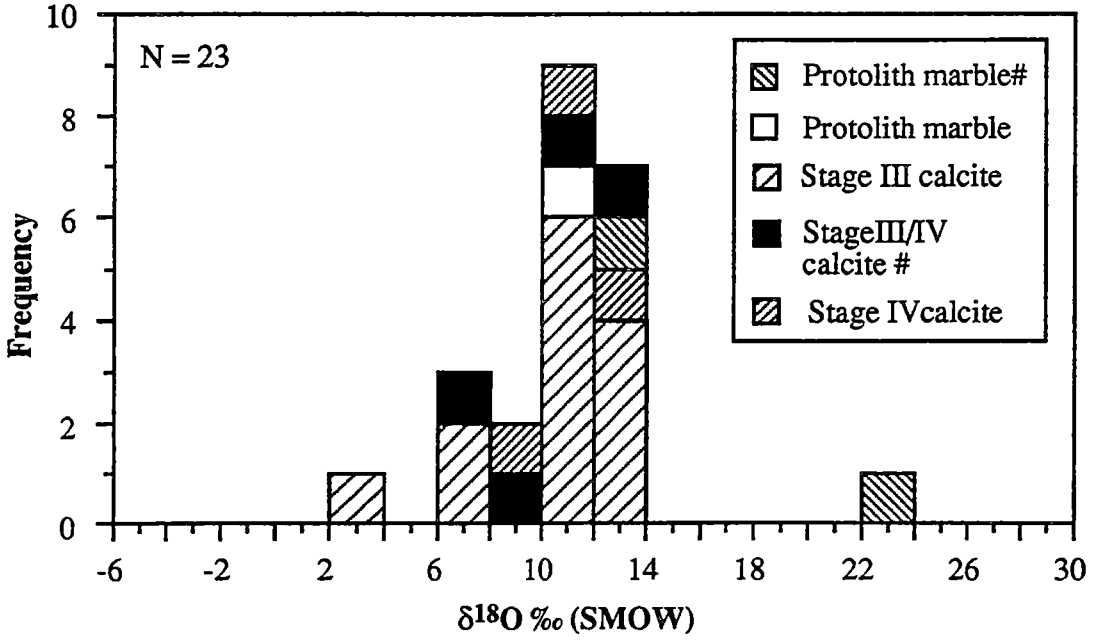


Fig. 7.2. Histogram of $\delta^{18}O$ carbonate values (‰, SMOW) of the protolith marble and Stages III-IV skarn calcites from the Kara deposit, northwestern Tasmania. # Data from Barrett (1980).

fluids associated with the formation of the skarn and the protolith marble. Two methods were applied: (1) plotting a calcite fractionation curve and fitting it on the plot of raw carbonate isotopic data, and (2) calculating fluid isotopic compositions for each mineral isotopic value.

Determination of parent fluid composition during skarn calcite formation using method (1) involved calculating the calcite fractionation curve at temperatures from 100°C to 500°C using equation (7.1) of Ohmoto and Rye (1979) and equation (7.2) of O'Neil et al. (1969).

$$1000\ln a\,(C_{calcite}\text{-}C_{CO2}) = 8.27 - 8.914\times10^{8}\times T^{-3} + 8.557\times10^{6}\times T^{*-2} - 18.11\times10^{3}\times T^{-1} \quad (7.1)$$

$$1000\ln a\,(O_{CaCO3}\text{-}O_{H2O}) = 2.7\times10^{6}\times T^{-2} - 3.39 \quad (7.2)$$

The curve fit shown in Fig. 7.3 indicates a dominant fluid with an initial composition of $\delta^{13}C$ and $\delta^{18}O$ values of -2‰ (PDB) and 7.5‰ (SMOW), respectively. For a few points, the curve fit gives parent fluid compositions with $\delta^{13}C$ and $\delta^{18}O$ values of -2 to -5‰ PDB) and 4 to 10‰ (SMOW), respectively.

Calculation of isotopic fluid compositions using method (2) were obtained using equations (7.1) and (7.2), together with temperatures obtained from fluid inclusion heating experiments (Chapter 6). The analysed protolith marbles contain patches of skarn minerals from Stages I/II (diopside and vesuvianite) and III (amphibole and calcite) for which fluid inclusion homogenisation temperatures have been determined. Sample S184 contains Stage III amphibole and calcite whereas, the marble samples of Barrett (1980) were reported to contain diopside and vesuvianite and therefore presumed to be of Stage I/II. As no fluid inclusion homogenisation temperature data were obtained from Stage IV calcite, the minimum homogenisation temperature of 240°C measured from secondary (Type IV) fluid inclusions in granite quartz from the nearby intrusive were used to calculate the Stage IV isotopic fluid values.

The calculated $\delta^{13}C_{CO2}$ and $\delta^{18}O_{H2O}$ values are shown in Table 7.1 and graphically presented in Figs. 7.4 and 7.5. Two samples of marble in equilibrium with Stage I/II

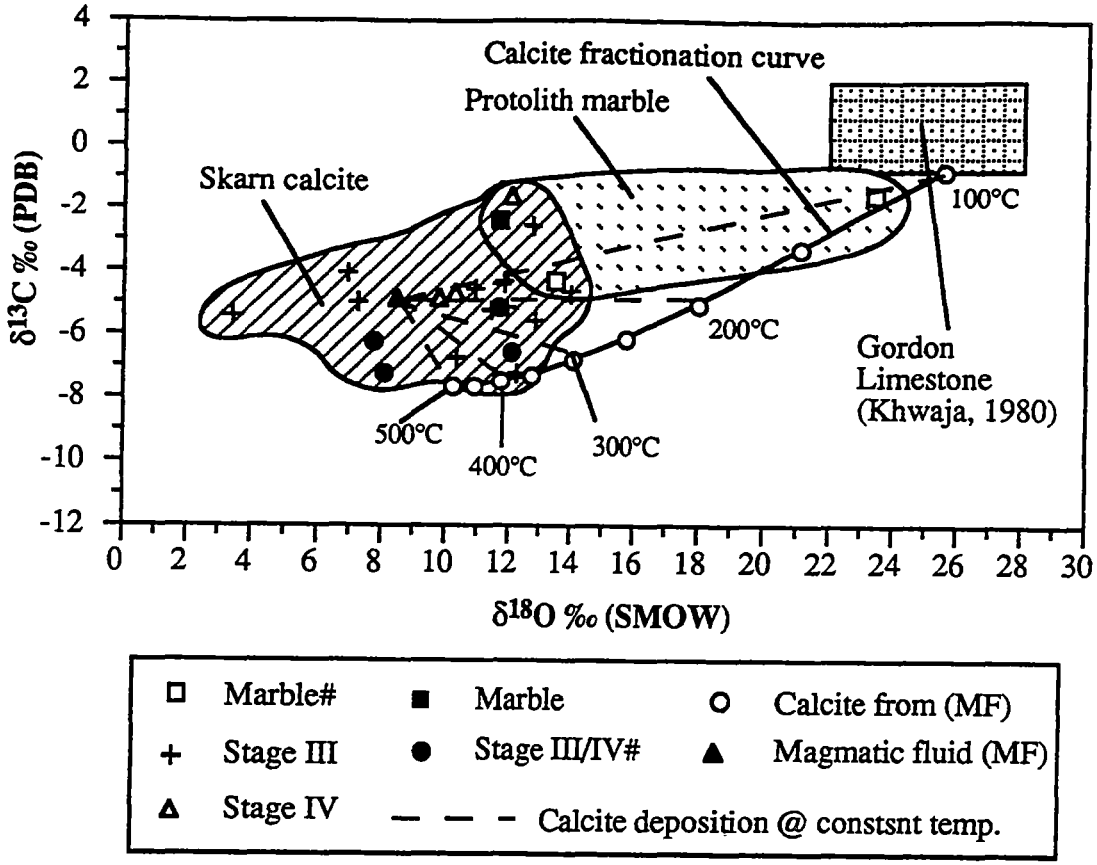


Fig. 7.3. Plot of $\delta^{13}C$ and $\delta^{18}O$ carbonate values (‰) of the protolith marble and Stages III-IV skarn calcite from the Kara skarn deposit, northwestern Tasmania. Included in the plot is data of unmetamorphosed host carbonates (Gordon Limestone) of northwestern Tasmania. The equilibrium isotopic fractionation curve for calcite was determined at 50°C intervals using the equation of O'Neil (1969) and Ohmoto and Rye (1979). # Data from Barrett (1980).

mineral assemblages gave a relatively wide range of $\delta^{13}C_{CO2}$ values of 1.2 and -1.9‰ at a temperature of 500°C estimated from Stages I/II fluid inclusion studies. One protolith marble in equilibrium with Stage III mineral assemblages gave a $\delta^{13}C_{CO2}$ value of -0.1‰ using the average Stage III skarn calcite fluid homogenisation temperature of 330°C. Stages III/IV of Barrett's (1980) skarn carbonate data yielded $\delta^{13}C_{CO2}$ values of -2.9 to -5.0‰ (mode at -4‰) at 330°C. The Stage IV calcite gave -0.5, -3.6 and -3.8‰ at 240°C.

Two samples from the protolith marbles coexisting with Stage I/II mineral assemblages gave $\delta^{18}O_{H2O}$ values of 12.4 and 22.3‰ at 500°, whereas one marble coexisting with Stage III skarn minerals yielded a $\delta^{18}O_{H2O}$ value of 7.3‰ at 330°C.

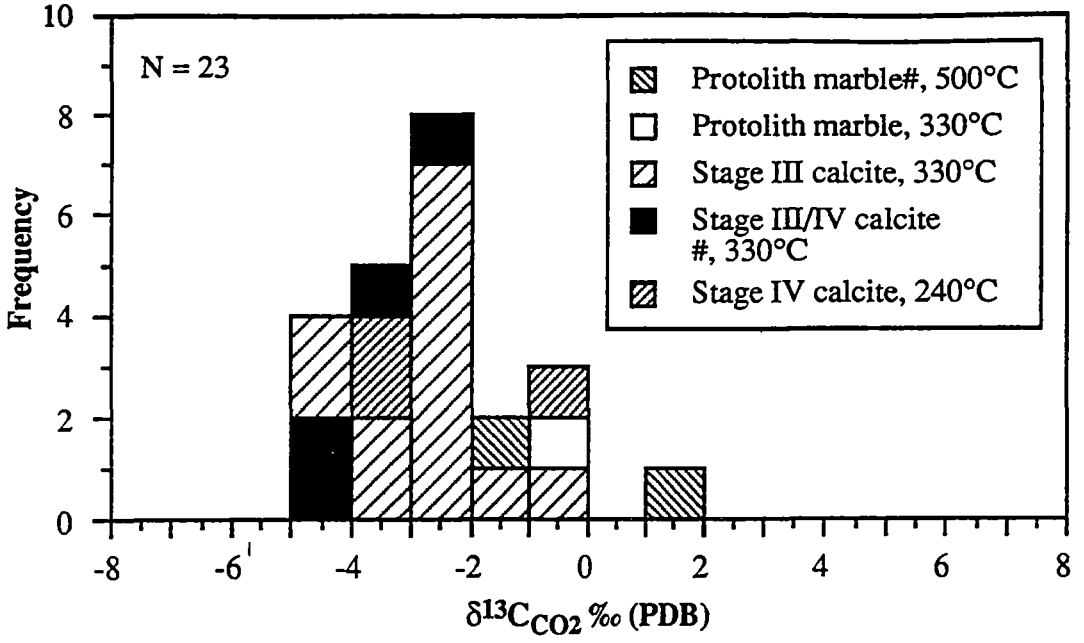


Fig. 7.4. Histogram of $\delta^{13}C_{CO2}$ hydrothermal fluid values (‰, PDB) for the protolith marble and skarn calcite from the Kara deposit, northwestern Tasmania. The temperatures applied were estimated from coexisting mineral fluid inclusion studies (Chapter 6). # Fluid isotopic compositions calculated from raw data of Barrett (1980).

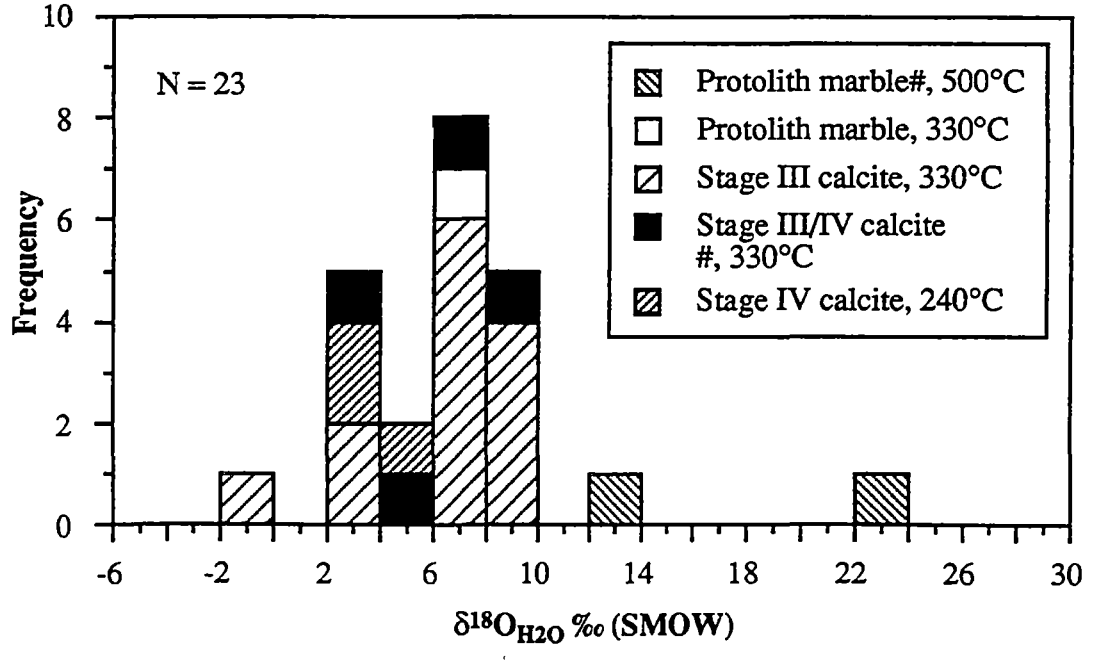


Fig. 7.5. Histogram of $\delta^{18}O_{H2O}$ hydrothermal fluid values (‰, SMOW)for the skarn calcite and marble from the Kara deposit, northwestern Tasmania. The temperatures applied were estimated from coexisting mineral fluid inclusion studies. # Fluid isotopic compositions calculated from raw data of Barrett (1980).

The Stage III calcite from the present study and secondary calcite of Barrett (1980) show a variation of $\delta^{18}O_{H2O}$ values from -0.6 to 10.0‰ (average 7‰) at an average temperature of 330°C. The Stage IV calcite gave $\delta^{18}O_{H2O}$ values of 3.0 to 5.2‰ (average 4‰) at a temperature of 240°C.

Fig. 7.6 shows the relationship between calculated $\delta^{13}C_{CO2}$ and $\delta^{18}O_{H2O}$ data for the skarn- and marble-forming fluids. The plot reveals a broad band with a positive concave down trend.

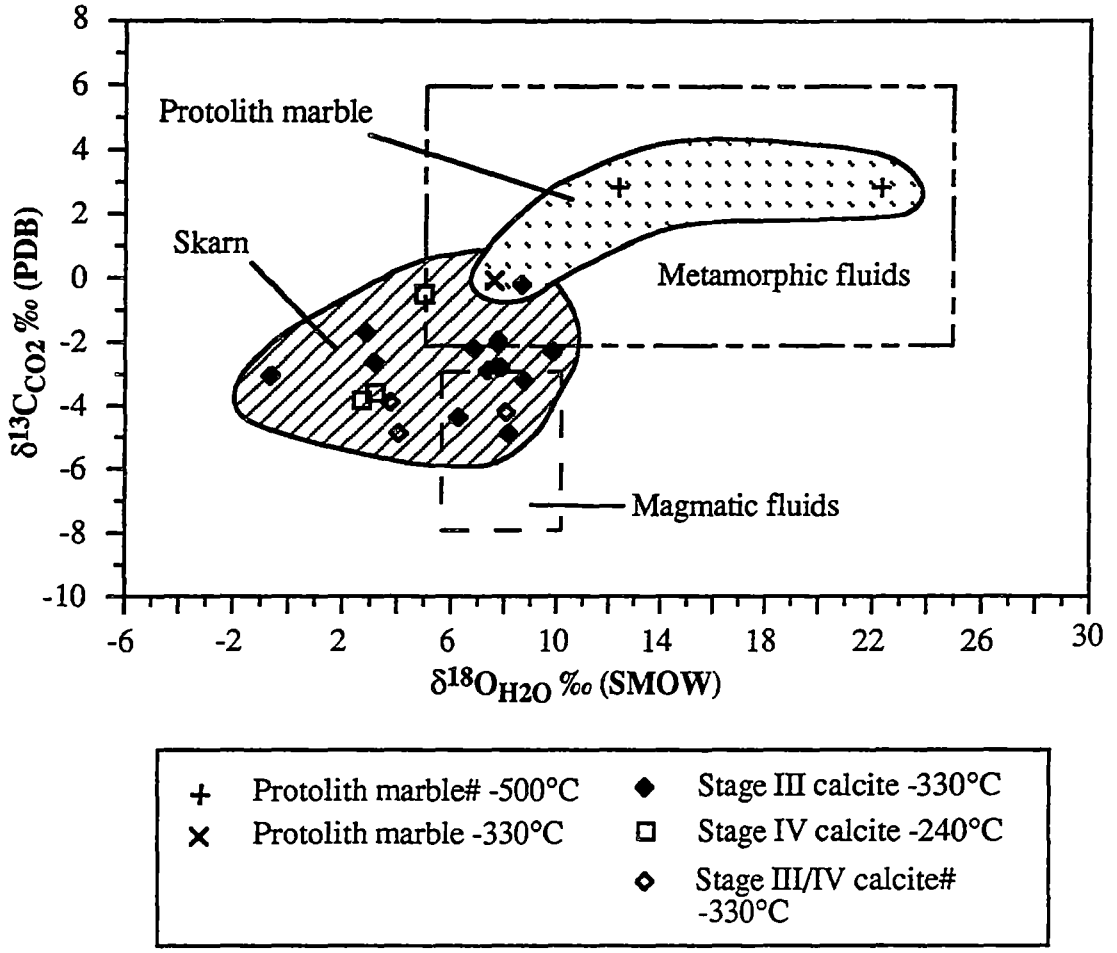


Fig. 7.6. Plot of $\delta^{13}C_{CO2}$ versus $\delta^{18}O_{H2O}$ values of the protolith marble- and skarn calcite-forming fluids for the Kara skarn deposit, northwestern Tasmania.

## 7.4. OXYGEN ISOTOPES OF MAGNETITE AND SCHEELITE

Oxygen isotopic ratios from magnetite and scheelite were measured from both the Stage II and Stage III magnetite and are reported with respect to SMOW.

### 7.4.1. $\delta^{18}O$ values of magnetite

The magnetite $\delta^{18}O$ results are presented in Table 7.2. The Stage II magnetite had one $\delta^{18}O$ value of 4.7 ‰. The Stage III magnetite had $\delta^{18}O$ values of 2.7‰ and 4.7 ‰ (mean 3.3 ‰, N = 4).

Oxygen isotopic compositions of ore fluids were calculated from $\delta^{18}O_{magnetite}$ using a fractionation equation (7.3) of Hoernes (1980) and fluid inclusion temperatures (Chapter 6) and are presented in Table 7.2 and Fig. 7.7.

$$1000\ln a (O_{magnetite}\text{-}O_{H2O}) = 8.342xTx10^{-3} - 12.175 \qquad (7.3)$$

The temperatures used in the isotopic ore fluid calculations were 500°C for Stage II magnetite and 300°C for Stage III magnetite. The calculated Stage II $\delta^{18}O_{H2O}$ value for magnetite is 12.7‰ and the Stage III values range from 12.3‰ to 13.9‰ (mean 12.9‰).

### 7.4.2. $\delta^{18}O$ values of scheelite

Scheelite $\delta^{18}O$ results are shown in Table 7.2. One measurement on Stage II scheelite yielded a $\delta^{18}O$ value of 5.5‰ while Stage III scheelite samples had $\delta^{18}O$ values of 4.3-6.4‰ (mean 5.5 ‰, N = 8).

Oxygen isotopic composition of ore fluids were calculated using a theoretical scheelite-$H_2O$ fractionation equation (7.4) of Wesolowski and Ohmoto (1986).

$$1000\ln a (O_{scheelite}\text{-}O_{H2O}) = 1.39x10^{6}xT^{2} - 5.87 \qquad (7.4)$$

The calculated scheelite $\delta^{18}O_{H2O}$ values are given in Table 7.2 and shown in a frequency

Table 7.2. Mineral and ore fluid oxygen isotopic compositions for Stages II and III magnetite and scheelite. Temperatures estimated from fluid inclusion studies (Chapter 6). Ore fluids (H2O) calculated using equations (7.4) and (7.5).

| S. No. | Stage | $\delta^{18}O$ magnetite ‰ (SMOW) | | $\delta^{18}O$ scheelite ‰ (SMOW) | |
|---|---|---|---|---|---|
| | | Mineral | $H_2O$ | Mineral | $H_2O$ |
| S147 | II | 4.7 | 12.7 (at 500°C) | - | - |
| S159 | | - | - | 5.5 | 9.0 (at 500°C) |
| S47 | III | 2.8 | 12.4 (at 300°C) | 6.2 | 7.8 (at 300°C) |
| S125 | | | | 4.3 | 5.9 (at 300°C) |
| S127 | | 3.5 | 13.1 (at 300°C) | 5.6 | 7.2 (at 300°C) |
| S188 | | - | - | 4.3 | 5.9 (at 300°C) |
| S154 | | 4.3 | 13.9 (at 300°C) | 6.4 | 8.0 (at 300°C) |
| S200 | | - | - | 5.6 | 7.2 (at 300°C) |
| S202 | | - | - | 6.0 | 7.6 (at 300°C) |
| S208 | | 2.7 | 12.3 (at 300°C) | 5.6 | 7.2 (at 300°C) |

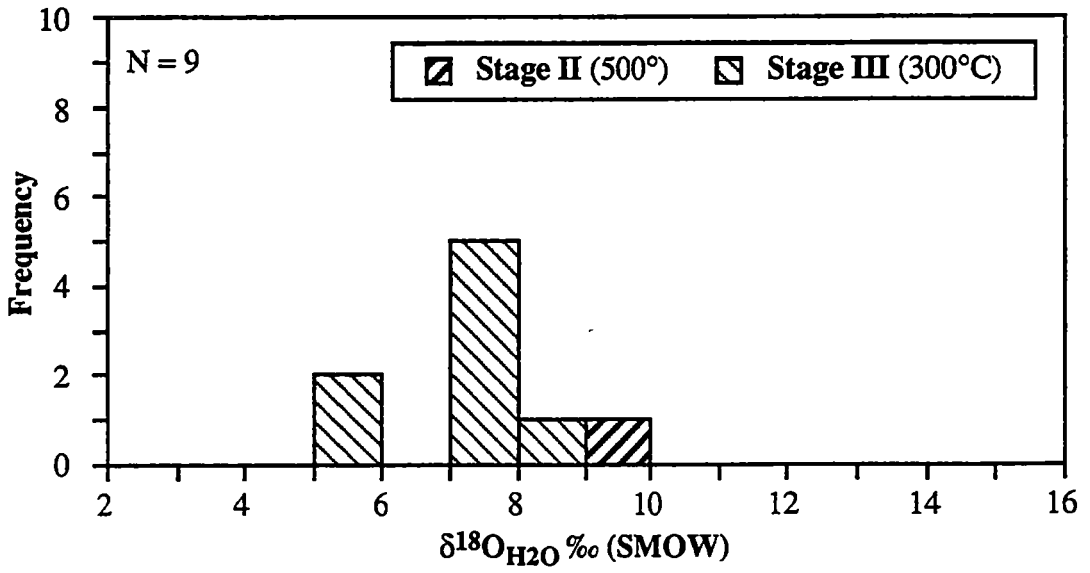


Fig. 7.7. Frequency distribution of magnetite $\delta^{18}O_{H2O}$ values from the Kara deposit, northwestern Tasmania.

distribution diagram in Fig. 7.8. Stage II scheelite gave one ore fluid $\delta^{18}O_{H2O}$ value of 9.0‰ at 500°C, whereas Stage III scheelite gave ore fluid $\delta^{18}O_{H2O}$ values of 5.9-8.0 ‰ (mean 7.2‰) at temperatures of 300°C.

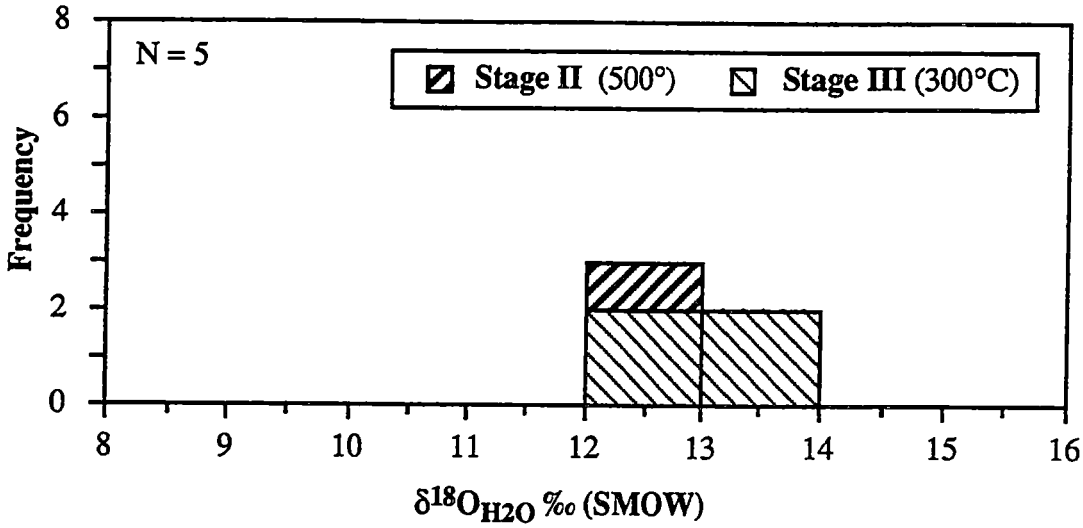


Fig. 7.8. Frequency distribution of $\delta^{18}O_{H2O}$ values of scheelite from the Kara deposit, northwestern Tasmania. Scheelite ore fluid calculations based on equation (7.5) using mean temperatures obtained from fluid inclusion studies (Chapter 6) for Stages II and III mineral assemblages.

## 7.5. DISCUSSION

Taylor (1987) has pointed out that calculated isotopic fluid values are commonly compared with reservoir fluid compositions to infer their origin and history. In this section, an attempt is made to characterise and identify source(s) of skarn-forming fluids from the fluid $\delta^{13}C$ and $\delta^{18}O$ compositional values determined by calculations using mineral isotopic composition measurements, fluid inclusion data and experimental or theoretical fractionation equations. Attempts are also made to relate the skarn calcite and protolith marble isotopic compositions at Kara to isotopic values of the unmetamorphosed host sequence and skarn deposits elsewhere.

### 7.5.1. Implications of carbonate carbon and oxygen isotope data

Khwaja (1980) reported $\delta^{13}C$ values of -1.5 to 1.8‰ (average 0‰, PDB) and $\delta^{18}O$ values of 22.0 to 27.8‰ (SMOW) for unmetamorphosed Gordon Limestone which hosts the Kara skarn deposit. Isotopic measurements of the protolith marble in this study reveal $\delta^{13}C$ compositions of -1.6 to -4.4‰ (mode at -2.4‰) and $\delta^{18}O$ compositions of 10 to 23‰ which are depleted in both carbon and oxygen values relative to the unmetamorphosed Gordon limestone values. The $\delta^{13}C$ compositions are also generally below marine limestone range of -2 to 4‰ (Valley, 1986) but close to the $\delta^{13}C$ values of about -3 to -8‰ for igneous or skarn calcites reported elsewhere (e.g. Taylor, 1987). These $\delta^{13}C$ values are lighter than the $\delta^{13}C$ values of -0.5 to 1.7‰ reported by Bowman et al. (1985) for protolith marbles at the CanTung E Zone scheelite skarn which were interpreted as being depleted in carbon isotopes.

The wide range of $\delta^{18}O_{calcite}$ values of 10 to 23‰ for the marble reflects change from marine limestone values of 22 to 28‰ for the Gordon Limestone values, to magmatic $\delta^{18}O$ values of 5.5 to 10‰ resulting from:

(1) mixing with magmatic fluids, and

(2) decarbonation.

The decarbonation process is considered by many workers including Taylor (1987) to preferentially remove heavy isotopes through the escaping $CO_2$ gas thus rendering carbonates impoverished in the heavy isotopes. Escaping $CO_2$ could be incorporated in metamorphic or magmatic fluids. However, large relative decreases in $\delta^{18}O$ values such as the ones manifested in the Kara marble are believed to be associated with water-rock exchange or infiltration metasomatism (Taylor, 1987)

The $\delta^{13}C_{calcite}$ values of skarn calcite ranging from -1.7‰ to -7.3‰ with a mean at -4.5‰ are much lighter than values obtained in the protolith marble and are comparable to values reported in other skarns (Bowman et al., 1985) and are similarly interpreted as suggesting that the calcite carbon is largely magmatic.

The $\delta^{18}O_{calcite}$ values with a cluster at 11.2‰, from a range of 3.4 to 14.0‰, are generally on the heavier part of the igneous $\delta^{18}O$ spectrum of 5.5-10.0‰ but are within the

wide metamorphic fluid range of 5-25‰ (Taylor, 1979). This wide variation in the oxygen isotopic values and a mean at 11.2‰ suggests there is more than one source for the oxygen. The lighter $\delta^{18}O$ values (<5‰) could indicate meteoric water ($\delta^{18}O$ value of 0‰) involvement and the values between 5 and 10‰ may suggest magmatic input, whereas heavier values (>10‰) may be due to metamorphic waters resulting from interaction between magmatic fluids and wall rocks.

The skarn calcite carbon and oxygen isotope plot does not easily fit on the calcite fraction curve determined at temperatures from 100° to 500°C to give one parent fluid from which the skarn calcite could have precipitated. At skarn calcite temperatures of formation of about 240° to 330°C, parent fluid compositions are variable with $\delta^{13}C_{CO2}$ values of 0 to -5‰ (PDB) and $\delta^{18}O_{H2O}$ values mostly from 4 to 12‰ (SMOW) and occasionally about 0‰. This revelation of variations in parent isotopic compositions suggests:

(1) multiple fluid sources,

(2) heterogeneous source, or

(3) continued water-rock interaction for skarn formation.

These variations are highlighted in the discussion on the calculated $\delta^{13}C_{CO2}$ and $\delta^{18}O_{H2O}$ fluid compositions below.

The calculated $\delta^{13}C_{CO2}$ values during marble formation at temperatures of 330° to 500°C range from 1.2 to -1.9‰ and are within the range for sea water (-2 to 4‰, PDB; Valley, 1986). The calculated fluid $\delta^{13}C_{CO2}$ composition during skarn calcite formation at temperatures of 240° to 330°C average approximately -3‰ from a narrow range of 0 to -5‰. These values are generally within the range of a mantle source which has a cluster at -5‰ to 2‰, and overlap the magmatic range, -3.0 to -5.5‰ (Taylor, 1987).

The calculated $\delta^{18}O_{H2O}$ composition during the formation of the protolith marble at temperatures of 330° to 500°C varies from 22‰ to low 10‰. The heavy oxygen isotopic values revealed by the protolith marble are typical for marine sources which display values of 20‰ to 26‰ (Valley, 1986), whereas the lighter components are within the magmatic range or metamorphic range. The calculated $\delta^{18}O_{H2O}$ values during skarn calcite formation at temperatures of 240° to 330°C have a mean value of around 7‰ and a wide $\delta^{18}O_{H2O}$

range of 0 to 10‰ which may be explained by a diverse range of sources, from: 1) magmatic waters which generally vary from 5.5 to 10.0‰ (Taylor, 1979), 2) metamorphic waters with a wide isotopic composition range of 5 to 25‰ (Taylor, 1979), and 3) meteoric water with $\delta^{18}O_{H2O}$ values of around 0‰.

The plot of calculated $\delta^{18}O_{H2O}$ against $\delta^{13}C_{CO2}$ for the protolith marble and skarn calcite at the Kara deposit reveals a concave down trend which is similar to that displayed at Pine Creek tungsten skarn and is considered to indicate high water-rock interaction (Taylor, 1987). Taylor (1987) and others have proposed several other interpretations to explain such trends :

(1) the nearby granite as the dominant source,

(2) metamorphic fluids resulting from metamorphic transformations of calcareous host rocks now consumed or partly transformed to marble, and

(3) meteoric water.

Other hydrothermal deposits which have been interpreted to form multiple fluid sources but with generally dominant granite fluids include, the JC tin skarn deposit (Layne and Spooner, 1991); CanTung E Zone scheelite skarn deposit (Bowman et al., 1985); Saucelle-Barruecopardo gold-tungsten bearing hydrothermal deposits (Antona et al., 1994).

### 7.5.2. Implications of magnetite $\delta^{18}O$ data

The $\delta^{18}O_{H2O}$ value calculated at 500°C from Stage II magnetite (4.7‰) of 12.7‰ is similar to values of 12.3 to 13.9‰ for the Stage III $\delta^{18}O_{H2O}$ calculated at 300°C from the magnetite III (2.7 to 4.3‰) indicating that oxygen isotopic compositions of hydrothermal fluids probably remained similar from Stage II to Stage III. The mean $\delta^{18}O_{H2O}$ values at a mean of 12.5‰ (SMOW) are slightly heavier than the 5.5‰ to 10‰ igneous fluid range (Taylor, 1987), but below the sedimentary isotopic range of 20‰ to 28‰, and within the metamorphic range (5‰ to 25‰; Valley, 1986). However, Devonian granitoid fluids have been reported with relatively high oxygen isotopic ratios. Khin Zaw (1991) reported Devonian fluids with $\delta^{18}O_{fluid}$ values of 8.5 to 12.6‰ (mode at 10.0‰, SMOW) calculated from magnetite and biotite isotopic compositions at the south end of the Rosebery deposit in

northwestern Tasmania, and attributed their origin to a magmtic source. These magnetite $\delta^{18}O_{H2O}$ data are generally similar to those determined from skarn calcite, indicating that skarn-forming fluids were largely magmatic in origin.

### 7.5.3. Implications of scheelite oxygen isotope data

The calculated ore fluid oxygen isotope compositions of 9.0‰ (Stage II scheelite) and 5.9 to 8.0‰ (Stage III scheelite) show that compositions remained within the typical oxygen isotope composition for magmatic fluids. These values compare well with $\delta^{18}O_{H2O}$ values of 6 to 10 ‰ for the King Island scheelite deposit (Wesolowski et al., 1986) and 7 to 10 ‰ for the Glenorchy Au-W-Sb mineralisation, New Zealand (Paterson, 1982). The King Island values have been interpreted as due to magmatic sources. In contrast, the Glenorchy values which are associated with deposits hosted in metamorphic rocks are considered to be due to metamorphic fluids. Antona et al. (1994) also obtained similar fluid values of 7 to 10.5‰ (SMOW) from gold-scheelite hydrothermal deposits, Saucelle-Barruecopardo Area, and proposed a source resulting from interaction between magmatic fluids and metamorphic rocks.

The scheelite $\delta^{18}O_{H2O}$ values at Kara cluster in the magmatic range and are generally in agreement with $\delta^{18}O_{H2O}$ values from skarn calcite and magnetite described in the preceding sections, and thus confirm a dominantly magmatic source.

Table 7.3 is a summary of mineral and hydrothermal fluid isotopic variations for the skarn minerals and the protolith carbonate of the Kara skarn deposit in comparison with other skarn or granitoid-related deposits.

Table 7.3. Mineral isotopic compositions of the Kara skarn deposit and other granitoid-related deposits.

| SKARN DEPOSIT (REF.) | STAGE | MINERAL | $\delta^{13}C_{mineral}$ ‰ (PDB) | | $\delta^{18}O_{mineral}$ ‰ (SMOW) | |
|---|---|---|---|---|---|---|
| | | | Range | Mean | Range | Mean |
| Kara skarn deposit | Marble | Calcite | -1.6 to -4.4 | -2.4 | 11.6 to 23.4 | 13.5 |
| (this study) | II | Magnetite | | | 4.3 to 4.7 | 4.3 |
| | | Scheelite | | | 5.8 to 6.6 | 6.2 |
| | III | Scheelite | | | 4.3 to 6.0 | 5.6 |
| | | Magnetite | | | 2.7 to 3.5 | 3.1 |
| | | Calcite | -2.6 to -7.3 | -5.0 | 3.4 to 14.0 | 11.0 |
| | IV | Calcite | -1.7 to -5.0 | -4.5 | 9.8 to 12.1 | 10.3 |
| King Island deposit (*) | Skarn | Scheelite | | | 3.6 to 5.7 | |
| CanTung deposit (**) | Marble | Calcite | -5 to 1.7 | | 19.7 to 20 | |
| | Skarn | Calcite | | | 11.7 to 14.2 | |
| | Skarn | Quartz | | | 12.0 to 15.2 | 12.9 |
| Otjua deposit (***) | Marble | | -0.7 to 0.3 | -0.1 | 5.2 to 16.2 | 15.5 |
| | Skarn (Early?) | Calcite | -2.5 to -5.8 | -3.9 | 16.0 to 18.5 | 17.0 |
| | Skarn (Late?) | Calcite | -4.2 to -5.9 | -5.1 | 15.2 to 15.6 | 15.3 |

* King island scheelite skarn deposit, Tasmania (Wesolowski and Ohmoto, 1986).
** CanTung scheelite deposit, Canada (Bowman et al., 1985).
*** Otjua scheelite skarn deposit, Namibia (Steven and Moore, 1994).

# CHAPTER 8: GENETIC MODEL AND EXPLORATION IMPLICATIONS

## 8.1. INTRODUCTION

In this chapter, the genesis of the Kara skarn deposit in comparison with other tungsten skarn deposits will be presented, and exploration implications for the Kara-type skarn deposit will be discussed.

## 8.2. GENETIC MODEL AND COMPARISONS

The Kara deposit shows many similarities and a few differences with other scheelite skarn deposits (e.g. King Island in Tasmania, Otjua in Namibia, CanTung in Canada and Sangdong in Korea) (Table 8.1). The deposits occur in carbonate host lithologies of various ages that are associated with felsic intrusives of varying ages. Other important features associated with these deposits include oxidation state of the skarns, plumbing system or channel ways for fluids, metal source and level of emplacement of the associated intrusive. These deposits are generally characterised by early anhydrous mineral assemblages that are overprinted by later hydrous retrograde mineral assemblages, with the exception of the Otjua deposit where the retrograde phase does not appear to have developed or has not been constrained. One major feature of these scheelite deposits is the variation in oxidation conditions which can be used as a criterion for subdividing scheelite deposits.

The Kara deposit is extremely rich in magnetite, very poor in sulphides, lacks pyrrhotite and seems to be highly oxidised in comparison to the other scheelite deposits. The King Island deposit is moderately oxidised, whereas Otjua, CanTung and Sangdong are relatively reduced (Table 8.1). The differences in oxidation levels of these skarns are revealed by varying $Fe^{2+}/Fe^{3+}$ ratios which are generally manifested in the type of garnet and clinopyroxene formed. Oxidised scheelite skarns are andradite-rich and hedenbergite-poor (e.g. Kara and King Island; Table 8.1) while reduced skarns are commonly andradite-

Table 8.1. Comparison of the Kara deposit with other scheelite deposits; King island deposit in Tasmania, Otjua prospect in Namibia, the CanTung scheelite in Canada and Sangdong in South Korea.

| Features | Kara (Ref: this study) | King Island (Ref: *) | Otjua (Ref: **) | CanTung (Ref: ***) | Sangdong (Ref: ****) |
|---|---|---|---|---|---|
| Host rock | Ordovician calcic marble | Cambrian marble | Late Proterozoic marble | Cambrian calcic marble | Cambrian limestone |
| Intrusion/Age | Highly fractionated Devonian granite | Devonian granodiorite | Highly fractionated Cambrian leucogranite | Cretaceous monzonite | Cretaceous granitoid (inferred) |
| Plumbing system and distance | Via marble contact | Via fault ± marble contact, 0-200m | Possibly via marble contact and fault, ?m | Via marble Contact | Via fracture, >500m |
| Confining Pressure | 1kb (Mills, 1971) | 1-2kb | High (deep level) | 1kb | 800b |
| Zone of skarn development | Contact aureole | Contact aureole | Contact aureole | Contact aureole | Distal (500m) |
| Prograde temperatures | 450° to 600°C | Up to 800°C | _ | 450° to 520°C | Up to 600°C |
| Retrograde temperatures | 350° to 240°C | Down to 180°C | _ | 400° to 270°C | 300°C |
| Salinity (NaCl equiv. wt. %) | 2 to 20 (to 45; Barrett, 1980) | 3 to 65 | _ | 4 to 14 | 1 to 48 |
| Garnet component (mole %) | $Ad_{70-100}$ ($Gr_{0-25}$) | $Ad_{43-98}$ | $Ad_{3-9}$ ($Gr_{50-70}$) | $Ad_{30-50}$ ($Gr_{50-70}$) | $Ad_{10-100}$ ($Gr_{10-90}$) |
| Clinopyroxene component (mole %) | $Hd_{0-25}$ ($Di_{75-100}$) | $Hd_{23-98}$ | $Hd_{50-90}$ | $Hd_{75-100}$ | $Hd_{80-95, 3-25}$ ($Di_{0-17, 75-97}$) |
| Molybdenum content in scheelite | Up to 6% powellite (<3% $MoO_3$) | Mean 15% powellite | nil | <3% powellite (<0.6% Mo) | <4% Mo |
| Pyrite | Minor | Minor | Minor (<1%) | Minor | Minor |
| Pyrrhotite | Absent | Minor | Minor (<2%) | Abundant | Abundant |
| Molybdenite | Absent | Minor | Absent | nil | Minor |
| Magnetite | Abundant | Minor | nil | nil | Minor |
| Oxidation/reduction level | Very oxidised | Moderately oxidised | Reduced | Reduced | Reduced (to moderately oxidised) |
| Fluorine in hydrous minerals | <2 wt % F | _ | _ | <3 wt % F | _ |

Table 8.1. Continued.

| Features | Kara (Ref: this study) | King Island (Ref: *) | Otjua (Ref: **) | CanTung (Ref: ***) | Sangdong (Ref: ****) |
|---|---|---|---|---|---|
| $\delta^{13}C$ ‰, PDB (skarn calcite) | -1.7 to -7.3 (mean -5.0) | _ | -2.5 to -5.9 (mean -4.5) | -5.6 to -7.2 (mean -6.3) | -1.59 to -8.09 (mean -3.92) |
| $\delta^{18}O$ ‰, SMOW (skarn calcite) | 3.4 to 14.0 (mean 11.0) | _ | 15.2 to 18.5 (mean 16) | 11.7 to 14.2 (mean 13.0) | 10.9 to 13.8 (mean 12.2) |

* Kwak and Tan (1981); Wesolowski et al. (1988); Wesolowski and Ohmoto (1986).
** Steven and Moore (1994).
*** Khin Zaw (1976); Mathieson and Clark (1984); Bowman et al. (1985).
**** Moon (1983).

poor and hedenbergite-rich (e.g. CanTung, Otjua and Sangdong; Table 8.1). Though the Sangdong is reduced, it also contains andradite-rich garnets and hedenbergite-poor clinopyroxene (Table 8.1). These deposits also show variations in the nature of the plumbing system, which can be a direct contact between carbonate protoliths or an indirect contact through faults or both (Table 8.1).

The genetic model for the Kara magnetite-scheelite skarn deposit is presented in the context of the geology, paragenesis, fluid inclusion and stable isotope information described in the preceding Chapters and the current knowledge of skarns summarised in Chapter 1.

The genesis of the Kara deposit is demonstrated in a cartoon in Fig. 8.1 which shows the development of the skarn following the Devonian granitoid intrusion into Cambrian and Ordovician rocks that were folded by the preceding the Mid-Palaeozoic Tabberabberan orogenic event. Skarns develop in the calcareous horizons which have a direct contact with the intrusion to act as a permeable connection. The folded Ordovician-Cambrian beds have been overprinted by high-temperature early skarns within carbonate units due to the emanating fluids derived from the emplaced Devonian granite after an initial isochemical metamorphism of contact rocks (Fig. 8.1A). These early skarn assemblages preferentially form in calcareous rocks which are chemically very reactive and have enhanced permeability.

During the early stages (Stages I and II), skarn-forming fluids are largely anhydrous and granite-derived, and no convection cell to focus fluids from meteoric sources from the country rocks has formed. In the late stages (Stages III and IV), deuteric granite fluids

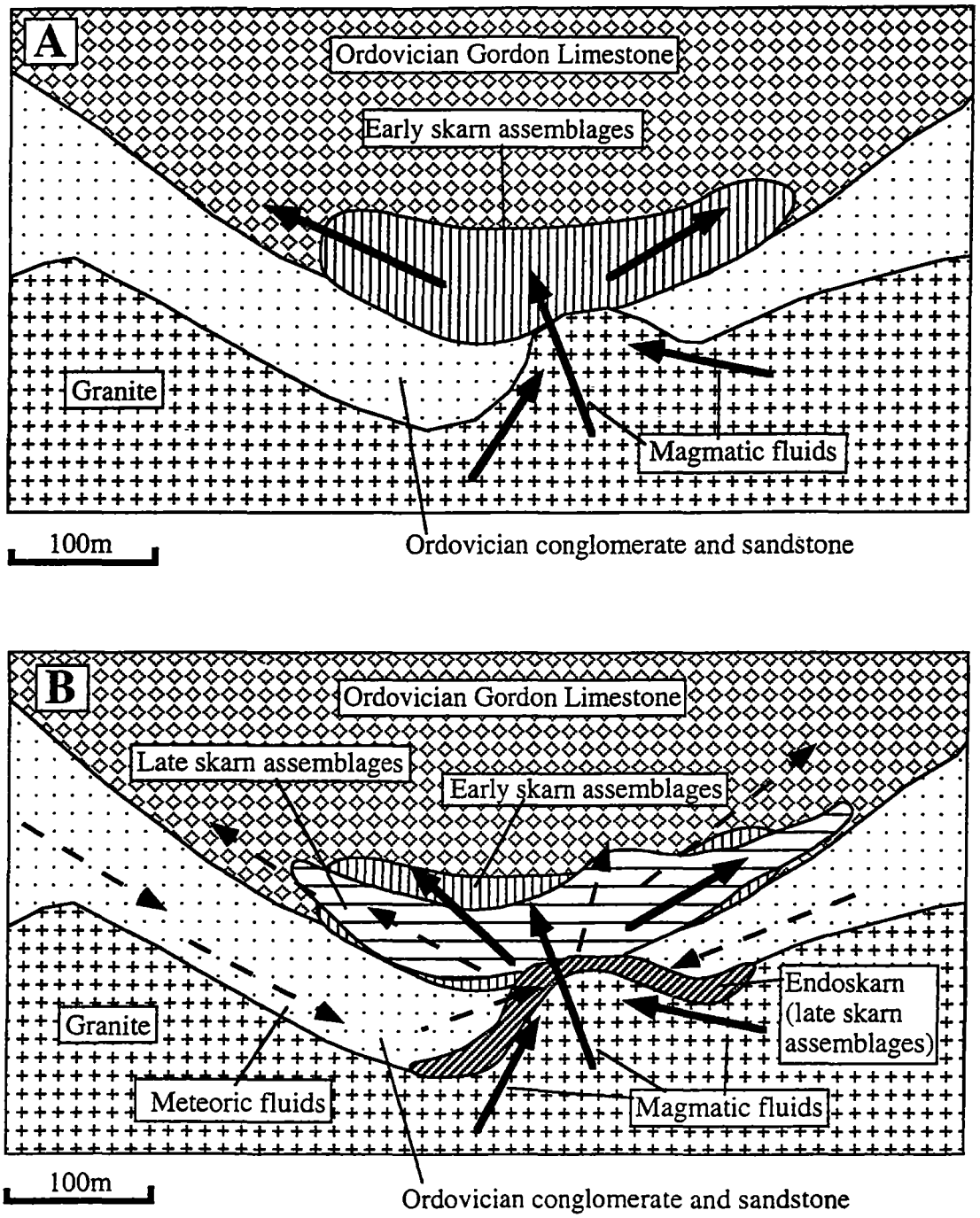


Fig. 8.1. Idealised cross sections showing the genesis of the Kara skarn deposit. **A.** Formation of early skarn assemblages in the Gordon Limestone following Devonian granite emplacement and isochemical metamorphism. **B.** Formation of late skarn assemblages of Stages III and IV due to mixing of magmatic fluids and minor meteoric fluids.

concentrate volatiles, mix with meteoric fluids and are focussed into permeable early-formed skarns and unreplaced carbonate units to form late stage skarns (Fig. 8.1B) which are dominantly hydrous. This late stage is also accompanied by the formation of endoskarns due to metasomatic alteration of the igneous protolith in areas where fluids have permeated intensely. Major scheelite and magnetite mineralisation accompanies hydrous minerals in the late stages of skarn-formation.

## 8.3. EXPLORATION IMPLICATIONS

The exploration model being proposed for the Kara type scheelite-magnetite skarn deposit is based on the genetic considerations outlined in the preceding section together with criteria on geology, geochemistry and geophysics. The model is presented as Fig. 8.2.

### 8.3.1. Geological criteria

Geological criteria involves mainly mapping or locating calcareous rocks that have been intruded by felsic rocks and delineating the contact aureole. As faults and marble-granitoid contacts form channelways for ore fluids, identifying and locating these geological features may lead towards areas of mineralisation. Knowledge of the stratigraphy of the area may be important in estimating the level of emplacement which may indicate whether the geological setting is favourable for scheelite deposition. During geological mapping, special attention should be paid to observe any alterations in the granite as intense alterations along granite margins may suggest areas where hydrothermal ore fluids were focussed which further suggests potential scheelite-magnetite deposition in the vicinity.

### 8.3.2. Geochemical criteria

Undertaking lithogeochemistry of the granitoid involving trace and major element analysis to determine the level of fractionation, highly fractionated granitoids are desirable for scheelite formation. Because magmatic fluid interaction with host rocks results in a general depletion of heavy isotopic compositions of carbonate protolith which generally increases towards skarn bodies, determination of carbon and oxygen isotopic compositions

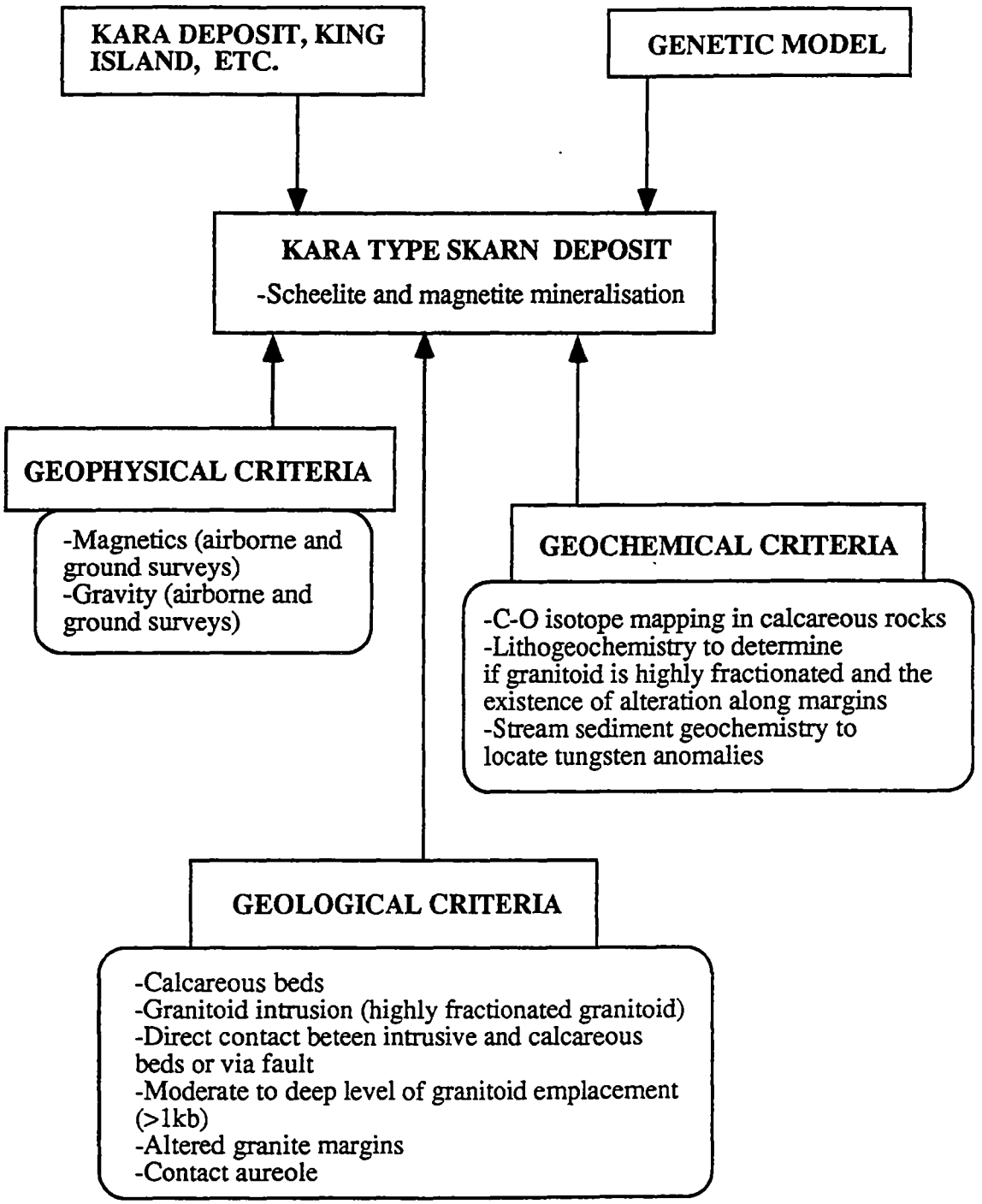


Fig. 8.2. Exploration model for the Kara-type deposit showing important criteria associated with the model.

of carbonates can be an important vector towards skarn deposits. Collection of stream sediment and soil samples for tungsten analysis which may be important in targeting areas for follow-up exploration.

### 8.3.3. Geophysical criteria

Since the target deposit style contains magnetite which has high a magnetic susceptibility and is generally denser than the host limestone and or the granitoid surroundings, geophysical methods will largely hinge on magnetics and gravity. These two methods can both be undertaken by airborne and ground techniques. Because skarns can be relatively small in volume, regional gravity and magnetic surveys may not pick-up the bodies easily as their geophysical signatures may be swamped by regional features. These techniques are therefore more useful at local scales. In the Kara situation where there is a cover of basaltic rocks with relatively high magnetic susceptibility and which is relatively dense, screening may still allow a scheelite-magnetite skarn to be located.

# CHAPTER 9: SUMMARY AND CONCLUSIONS

In this final chapter, the following summary and conclusions can be made on the Kara scheelite-magnetite deposit.

1) The Kara scheelite-magnetite deposit area regionally occurs in a deformed zone between two PreCambrian basement blocks, the Tyennan block exposed to the south and the Rocky Cape block to the north, which are believed to have caused a compressive stress regime during the Mid-Palaeozoic Tabberabbaran Orogeny (e.g. Williams et al., 1989). The deposit is spatially associated with the Devonian Housetop Granite whose origin and those of the other Devonian granitoids of northwestern Tasmanian is not well understood but could be attributed to Mid-Palaeozoic subduction processes to the east of eastern Australia as suggested for Devonian granitoids in the Lachlan belt (Coney, 1992).

2) The Kara skarn deposit consists of several mineralised bodies which are largely developed within folded calcareous rocks of the Ordovician Gordon Limestone Subgroup. The skarns are found at the contact between calcareous units of the Gordon Limestone Subgroup and the granite or may be separated from the granite by the Moina Sandstone. The Moina Sandstone members consist of sandstones and argillite, and may be hornfelsed close to the granite.

3) The deposit is a proximal skarn type that developed in contact with a granite intrusive, and consists of magnetite, garnet, clinopyroxene, vesuvianite, amphibole, epidote as principal minerals and fluorite, scheelite, quartz, hematite, chlorite, wollastonite, sphene, pyrite as subordinate or accessory minerals.

4) Detailed textural and paragenetic studies indicate that the early Stages I and II skarn mineral assemblages consist of clinopyroxene, garnet and vesuvianite. These early skarn mineral assemblages have been overprinted by later skarn assemblages (Stages III and IV) that are characterised by the appearance of abundant hydrous minerals such as amphibole, epidote and chlorite.

5) The early Stage I skarn consists of clinopyroxene, and is devoid of scheelite mineralisation. Magnetite and scheelite ore formation commenced during the Stage II skarn development and increased with the appearance of abundant hydrous mineral phases during the Stage III skarn formation. Magnetite is the principal ore mineral as well as the principal skarn mineral, and thus generally occurs in all skarn zones or mineral facies except the basal epidote-quartz zone. Scheelite mineralisation in the early skarn assemblages is generally associated with vesuvianite, and the scheelite grains are fine-grained (<0.2mm) and isolated, but are coarse-grained (up to 15mm or more) in the late mineral assemblages, comprising hydrous minerals such as amphibole. Though scheelite mineralisation is commonly associated with hydrous minerals, chiefly amphibole and vesuvianite in all skarn zones except the basal epidote-quartz zone, it does occur in anhydrous minerals (e.g. garnet) but these are commonly late phase minerals. Increased amounts of hydrous minerals do not necessarily correspond to increased scheelite mineralisation.

6) The skarns at Kara display a distinct mineral zonation consisting of mineral assemblages dominated by one or two minerals. The mineral zonation changes from an epidote-quartz zone at the contact with the granite to garnet, vesuvianite, clinopyroxene, magnetite, epidote, amphibole and hematite zones away from the granite. The epidote-quartz zone at the base of the skarn appears to have developed largely from the alteration of the granite intrusive and is interpreted as an endoskarn, whereas the skarn zones found away from this zone represent exoskarns that have formed by replacing the Gordon Limestone.

7) Tungsten grades vary from low (<0.01 wt. % $WO_3$) to ore grade (>0.7 wt. % $WO_3$) and show a crude zonation with high grades developed in skarn zones away from the epidote-quartz zone. Molybdenum concentrations are low (<2 wt. % Mo) and accompany tungsten in scheelite. Tin is generally low, <0.10% Sn, but may be high in places (~1.5 wt. % Sn) and appears to be solely confined to garnet from the early skarn phases.

8) The Kara deposit is a calcic type skarn and is characterised by calc-silicate and calcium-rich minerals which include diopside, andradite, Ca-amphibole, epidote, fluorite, calcite, sphene, apatite and scheelite. It is also iron-rich as shown by the widespread

occurrence of magnetite and subordinate hematite and iron-rich silicate minerals such as andradite, amphibole and epidote. The deposit is low in manganese minerals, and appears to be low in magnesium, although magnesium is present in diopside. The widespread occurrence of calcium-rich minerals suggests a high calcium activity which is believed to be important in efficiently precipitating scheelite during skarn formation. This high calcium activity is most likely due to the dissolution of carbonate protolith. Barrett (1980) showed that calcium levels decrease towards granite contact, whereas other elements such as aluminium, silica, titanium and iron increase.

9) Most of the skarn minerals have chemistries that are indicative of an oxidising environment for skarn development. The pyroxene at Kara is diopside-rich ($Fe^{2+}$-poor clinopyroxene) with compositions of $Hd_{0-25}Di_{70-100}Jo_{0-5}$ and coexists or is overprinted by andradite garnet ($Fe^{3+}$-rich garnet) with compositions of $Ad_{0-100}Gr_{0-30}Sp+Al+Py_{0-5}$. The observed clinopyroxene-garnet association together with their composition are indicative of an oxidising skarn forming environment (Kwak, 1994). Garnet temperature-log $f(O_2)$ plots of Gustafson (1974) give oxygen fugacities of log $f(O_2)$ = -27 to -20 at 450° to 550°C. Andradite versus hedenbergite compositional plots with superimposed oxygen fugacities from Brown and Essene (1985) show oxygen fugacities of log $f(O_2)$ >-22 for the Kara deposit. The widespread occurrence of magnetite with minor pyrite also tends to support the conclusion of an oxidising environment of skarn formation. Kwak (1984) has suggested that epidote occurrence indicates an oxidising skarn environment and thus its widespread occurrence at Kara can be considered to further confirm oxidising conditions for the Kara deposit. The occurrence of molybdenum as powellite in scheelite, rather than as a sulphide in form of molybdenite, is suggestive of oxidising environments. This association has been demonstrated in many papers and reviews (e.g. Sato, 1980; Meinert, 1992).

10) Fluid inclusion microthermometry of the Kara skarn minerals reveal that the early anhydrous mineral assemblages were formed at higher temperatures (up to >610°C) and that as temperatures declined to less than 300°C mineral assemblages were dominated by hydrous phases (eg. amphibole, epidote). Major scheelite mineralisation occurred during the cooler period of skarn development, although a subordinate proportion also formed at

higher temperatures during Stage II skarn formation.

11) Salinity values for the Stages I to III skarn assemblages vary widely from 0.2 equiv. wt % to as high as 19.0 equiv. wt. % NaCl. Barrett (1980) reported salinity values from 0.7 to 45.1 equiv. wt. % NaCl for the Kara deposit. Salinity data for Stages I and II generally vary from 10.0 to 17.8 equiv. wt. % NaCl, with an isolated value of 2.0 equiv. wt. % NaCl and show a negative trend on a plot of temperature against salinity. This negative trend probably indicates formation of early skarn assemblages from one source with high salinity concentrations which is presumed to be the nearby granite. The Stage III salinity data are variable (0.2-19.0 equiv. wt. % NaCl) and form a horizontal trend parallel to the salinity axis on the temperature-salinity plot which suggests two possibilities:

(a) mixing between two fluid types or

(b) unmixing of a single fluid during cooling and pressure change (Shepherd et al., 1985).

The possibility of mixing between two fluid types may be explained by high salinity fluids originating from the nearby granite and the low salinity fluids of meteoric origin. Mixing between two fluid types has been suggested as a possible mechanism for the formation of many skarn deposits or parts thereof (e.g. JC tin skarn deposit, Layne and Spooner, 1991). First melting point temperatures suggest the presence of salts of potassium, calcium and magnesium in addition to salts of sodium in the skarn-forming and ore fluids.

12) Fluid inclusions gas composition studies by thermal decrepitation mass spectrometry show most skarn minerals have moderate to strong concentrations of $H_2O$ volatiles and that:

(a) Early anhydrous skarn assemblages (clinopyroxene and garnet) from Stages I and II contain weak or undetectable concentrations of $CO_2$, $H_2S$, HCl and $CH_4$ volatiles.

(b) Later minerals including the early hydrous vesuvianite generally show higher volatile concentrations of $CO_2$, $H_2S$, HCl and $CH_4$.

The occurrence of $CO_2$ in fluid inclusions associated with scheelite is consistent with observations made in other scheelite deposits where the presence of $CO_2$ together with

other volatiles (eg. $N_2$) has been interpreted to trigger or enhance scheelite precipitation (Gilbert et al., 1992). The presence of HCl may have played an important role of providing an acidic environment which is conducive to tungsten transportation.

13) The protolith marble at the Kara skarn shows a wide variation in $\delta^{13}C$ and $\delta^{18}O$ values from -2‰ to -7‰ (PDB) and 3-23‰ (SMOW) respectively. Both the carbon and oxygen values are depleted relative to the unmetamorphosed Gordon Limestone equivalent which has $\delta^{13}C$ and $\delta^{18}O$ values of 0‰ (PDB) and 22-29‰ (SMOW), respectively. The lightest isotopic compositions are recorded in marble in close contact with a skarn body. The depletion towards isotopic igneous values indicates:

(a) interaction of marble with metasomatic fluids derived from the nearby granite and or

(b) decarbonation as suggested for other skarn deposits (e.g. CanTung scheelite skarn, Bowman et al., 1985; JC tin skarn deposit, Layne and Spooner, 1991; Otjua tungsten skarn prospect, Steven and Moore, 1994).

14) The calcite from Stages III and IV skarn assemblages generally has isotopically lighter carbon and oxygen than the protolith marble. $\delta^{13}C$ and $\delta^{13}C$ values of calcite range from -2‰ to -7‰ (PDB) and 3‰ to 12‰ (SMOW), respectively. Magnetite and scheelite $\delta^{18}O_{H2O}$ calculated for hydrothermal fluids from oxygen isotopic values of magnetite and scheelite are generally in agreement with those of fluids calculated from calcite and are consistent with Devonian magmatic hydrothermal fluid composition.

# REFERENCES


Antona, J. F., Fallick, A., E., Garcia sanchez A., 1994 - Fluid inclusion and stable isotope studies of gold-tungsten bearing hydrothermal deposits, Saucella-Barruecopardo Area, Spain. European Journal Mineral 6, 819-835.

Baillie, P. W., Williams, P. R., Seymour, D. R., Lenox, P. G., Green, G. R., 1986 - St. Valentines, Geological Atlas, 1:50 000 series. Geological Survey, Tasmania Department of Mines, Hobart.

Banks, M. R., Baillie, P. W., Brown, 1989 - Late Cambrian to Devonian, in Geology and mineral resources of Tasmania, ed. Burrett, C. F., Martin, E. L. Special publication, Geological Society Australia 15, 182-237.

Barrett, D. E., 1980 - Geology, mineralogy and conditions of formation of the Kara scheelite skarn. Unpublished B.Sc. Honours thesis, Geology Department, University of Tasmania, Hobart.

Bodnar, R. J., 1993 - Revised equation and table for determining the freezing point depression of $H_2O$-NaCl solutions. Geochimica et Cosmochimica Acta 57, 683-684.

Bowman, J. R., Covert, J. J., Clark, A. H., Mathieson, G. A., 1985 - The CanTung E Zone scheelite orebody, Tungsten, Northwest Territories: Oxygen, hydrogen, and carbon isotope studies. Economic geology 80, 1872-1895.

Bozzo, A. T., Chen, R., Burden, A. J., 1973 - The properties of hydrates of chlorite and carbon dioxide, in Fourth International symposium on fresh water from the sea, ed. Delyannis, A. E., 437-451.

Brown, A. V., 1989 - Eo-Cambrian—Cambrian, in Geology and mineral resources of Tasmania, ed. Burrett, C. F., Martin, E. L. Special publication, Geological Society Australia 15, 47-83.

Brown, P. E., Bowman, J. R., Kelly, W. C., 1985 - Petrologic and stable isotope constraints on the source and evolution of skarn-forming fluids at Pine Creek, California. Economic Geology 80, 72-95.

Brown, P. E., Essene, J. E., 1985 - Activity variations attending tungsten skarn formation, Pine Creek, California. Contributions to Mineralogy and Petrology 89, 358-369.

Clayton, R. N., Mayeda, T. K., 1963 - The use of bromide pentafluoride in the extraction of oxygen from oxides and silicates for isotopic analysis. Geochimica et Cosmochimica Acta 27, 43-52.

Collins, P. L. F., 1979 - Gas hydrates in fluid inclusions and the use of freezing temperatures for estimating salinity. Economic Geology 74, 1435-1444.

Collins, P. L. F., 1983 - Geology and mineralisation at Cleveland tin Mine, western Tasmania. Unpublished PhD thesis, University of Tasmania, Hobart.

Collins, P. L. F., Brown, S. G., Dronseika, E. V., Morland, R., 1989 - Mid-Palaeozoic ore deposits, in Geology and mineral resources of Tasmania, ed. Burrett, C. F., Martin, E. L. Special publication 15, Geological Society Australia 15, 270-292.

Coney, P. J., 1992 - The Lachlan belt of eastern Australia and Circum-Pacific tectonic evolution, in The Palaeozoic eastern margin of Gondwanaland: Tectonics of the Lachlan fold belt, southeastern Australia and related orogens, ed. Fergusson, C. F., Glen, R. A. Tectonophysics 214, 1-25.

Cowan, D, 1981 - Report CMS 81/8/22. Unpublished report. Tasmania Mines Limited. Burnie, Tasmania.

Deer, W. A., Howie, R. A., Zussman, J., 1980 - An introduction to rock-forming minerals. Longman Group Limited, London, 528.

Dick, L. A., Hodgson C. J., 1982 - The MacTung W-Cu(-Zn) contact metasomatic and related deposits of the Northwestern Canadian Cordillera. Economic Geology 77, 845-867.

Dobson, C. D., 1982 - Geology and alteration of the Lost River tin-tungsten fluorine deposit, Alaska. Economic Geology 77, 1033 -1052.

Einaudi, M. T., Meinert, D. L., Newberry, R. J., 1981 - Skarn deposits. Economic Geology 75th Anniversary, 317-391.

Fander, H., W., 1972 - Report CMS 79/8/23 - Kara scheelite drill cores. Unpublished report. Tasmania Mines Limited. Burnie, Tasmania.

Fander, H., W., 1979 - Report CMS 72/5/7 - Petrology - Mineralogy of drill cores. Unpublished report. Tasmania Mines Limited. Burnie, Tasmania.

Gee, R. D., Grooves, D. I., 1971 - Structural features and mode of emplacement of part of the Blue Tier Batholith in northeastern Tasmania. Journal of Geological Society of Australia 18, 41-55.

Gibert, F., Moine, B., Schott, J., Dandurand, J., 1992 - Modeling of the transport and deposition of tungsten in the scheelite-bearing calc-silicate gneisses of the Montagne Noire, France., Contributions to Mineralogy and Petrology 112, 371-384.

Green, G. R., 1990 - Palaeozoic geology and mineral deposits of Tasmania, in Geology and mineral deposits of Australia and Papua New Guinea, ed. Hughs, F. E. Australian Institute of Mining and Metallurgy, Melbourne, 1207-1223.

Gustafson, W. I., 1974 - The stability of andradite, hedenbergite, and related minerals in the system Ca-Fe-Si-O-H. Journal of Petrology 15, 455-496.

Hall, D. L., Cohen, L. H., Schiffman, P., 1988 - Hydrothermal alteration associated with the Iron Hat skarn deposit, eastern Majove Desert, San Bernardino County, California. Economic Geology 83, 568-587.

Higgins, N. C., 1980 - Fluid inclusion evidence for the transport of tungsten by carbonate complexes in hydrothermal fluids. Canadian Journal of Earth Sciences 17, 823-830.

Hoernes, S., 1980 - A BASIC-programme for calculations of O-isotope temperatures. Contributions to Mineralogy and Petrology 74, 107-108.

Hoffmann, C. F., Henley, R. W., Higgins, N. C., Solomon, M., Summons, R. E., 1988 - Biogenic hydrocarbons in fluid inclusions from the Aberfoyle tin-tungsten deposit, Tasmania, Australia. Chemical geology 70, 287-299.

Hopwood, T, 1985 - Report on Tasminex E.L. 17/68: Kara scheelite mine area. Unpublished report. Tasmania Mines Limited. Burnie, Tasmania.

Hughes, T. D., 1950 - Tungsten prospect, Hampshire. Unpublished report. Geological Survey, Tasmania Department of Mines, Hobart.

Kesler, S. E., 1988 - Fluid inclusion gas analyses in mineral exploration. Journal of Geochemical Exploration 42, 1-4.

Khin Zaw, 1976 - The CanTung E-Zone orebody, Northwest Territories: A major scheelite skarn deposit. Unpublished MSc thesis, Queen's University, Canada.

Khin Zaw, 1991 - The effect of Devonian metamorphism and metasomatism on the mineralogy and geochemistry of the Cambrian VMS deposits in the Rosebery-Hercules Districts, western Tasmania. Unpublished PhD thesis, University of Tasmania, Hobart.

Khin Zaw, Clark, A. H., 1978 - Fluoride-hydroxyl ratios of skarn silicates, CanTung E-zone scheelite orebody, Tungsten, Northwest Territories. Canadian Mineralogist 16, 207-221.

Khin Zaw, Huston, D. L., Large, R. R., Mernargh, T. P., Ryan, C. G., 1994 - Geothermometry and chemical composition of fluid inclusions from the Tennant Creek gold-copper deposits: Implications for ore genesis and exploration. Special volume on Australian Proterozoic copper-gold deposits, Mineral. Deposita 29, 288-300.

Khwaja, A. Z., 1980 - Depositional and diagenetic environments of the Gordon Subgroup (Ordovician), Gunns Plains, N. W. Tasmania. Unpublished PhD thesis, University of Tasmania.

Kitto, P. A., 1994 - Structural and geochemical controls on mineralisation at Renison, Tasmania. Unpublished PhD thesis, University of Tasmania, Hobart.

Kwak, T. A. P., 1978 - Conditions of formation of King Island scheelite contact skarn, Tasmania, Australia. American Journal of Sciences 278, 968-985.

Kwak, T. A. P., 1983 - The geology and geochemistry of the zoned Sn-W-F-Be skarns at Mt. Lindsay, Tasmania, Australia. Economic Geology 78, 1440-1465.

Kwak, T. A. P., 1986 - Fluid inclusions in skarns (carbonate replacement deposits). Journal Metamorphic Petrology 4, 363-384.

Kwak, T. A. P., 1994 - Hydrothermal alteration in carbonate-replacement deposits; Ore skarns and distal equivalents, in alteration and alteration processes associated with ore-forming systems, ed. Lentz, D. R. Geological Association of Canada, short course notes 11, 381-402.

Kwak, T. A. P., Askins, P. W., 1981 - The nomenclature of carbonate deposits with emphasis on Sn-F (-Be-Zn) wrigglite skarns. Journal Geological Society Australia 28, 123-136.

Kwak, T. A. P., Tan, T. H., 1981 - The geochemistry of zoning in the skarn minerals at the King Island (Dolphin) mine. Economic Geology 76, 468-497.

Large, R. R., 1972 - Metasomatism and scheelite mineralisation at the Bold Head, King Island. Australasian Institute of Mining and Metallurgy Proceedings 238, 31-45..

Layne, G. D., Spooner, E. T. C., 1991 - The JC tin deposit, Southern Yukon Territory: Geology, paragenesis, and fluid inclusion microthermometry. Economic Geology 86, 29-47.

Leake, B. E., 1978 - Nomenclature of amphiboles. American Mineralogist 63, 1023-1058.

Leaman, D. E, Richardson, R. G., 1989 - The granites of west and northwest of Tasmania: a geophysical interpretation. Geological Survey Tasmania Bulletin 66.

Leaman, D. E, Richardson, R. G., Shirley, J. E., 1980 - Tasmania - the gravity field and its interpretation. Unpublished report, Tasmania Department of Mines, Hobart, 1980/36.

Mathieson, G. A. and Clark, A. H., 1984 - The CanTung E Zone scheelite skarn deposit orebody, Tungsten, Northwest Territories: A revised genetic model. Economic Geology 79, 883-901.

McClenaghan, M. P., Calmcho, A., Higgins, N. C., Reid, E. J., 1989 - Mid-Palaeozoic granitoids, in Geology and mineral resources of Tasmania, ed. Burrett, C. F., Martin, E. L. Special publication 15, Geological Society Australia 15, 253-270.

Meinert, L., 1992 - Skarns and skarn deposits. Geoscience Canada 19, No. 4, 145-162.

Mills, D. M., 1971 - The St. Valentine Peak granite-metasediment contact zone. Unpublished B.Sc. Honours thesis, Geology Department, University of Tasmania, Hobart.

Moon, K. J., 1983 - The genesis of the Sangdong tungsten deposit, the Republic of Korea. Unpublished PhD thesis, University of Tasmania, Hobart.

Nakano, T., Yoshino, T., Shimazaki, H., Shimizu, M., 1994 - Pyroxene composition as an indicator in the classification of skarn deposits. Economic Geology 89, 1567-1580.

Newberry, R. J., Swanson, S. E., 1986 - Scheelite skarn granitoids: An evaluation of the rocks of magmatic source and process. Ore Geology Reviews 1, 57-81.

Newberry, R. J., Einaudi, M. T., 1981 - Tectonic and geochemical setting of tungsten skarn mineralisation in Caldillera, in Relations of tectonics to ore deposits in the southern Cordillera, ed. Dickson, W. R., Payne, W. D. Arizona Geological Society Digest XIV, 99-111.

Norman, D. I., Sawkins, F. J., 1987 - Analysis of volatiles in fluid inclusions by mass spectrometry. Chemical geology 61, 1-10.

Ohmoto, H., Rye, R. O., 1979 - Isotopes of sulphur and carbon, in Geochemistry of hydrothermal ore deposits, 2nd edition, ed. Barnes, H. L. New York, Wiley Interscience, 509-567.

O'Neil, J. R., Clayton, R. N., Mayeda, T. K., 1969 - Oxygen isotope fractionation in divalent metal carbonates. Journal Chemical Physics 51, 5547-5558.

Patterson, D. J., Ohmoto, H., Solomon, M., 1981 - Geologic setting and genesis of cassiterite-sulphide mineralisation at Renison Bell, western Tasmania. Economic Geology 76, 393-438.

Paterson, C., J., 1982 - Oxygen isotopic evidence for the origin and evolution of scheelite ore-forming fluid, Glenorchy, New Zealand. Economic Geology 77, 1672-1687.

Plumridge, C., 1986 - Notes of the Kara deposit and surrounding area and its potential for gold mineralisation. Unpublished report, Tasmania Mines Limited, Burnie.

Polya, D. A., 1978 - Chemical behaviour of tungsten in hydrothermal fluids and genesis of the Panasqueira W-Cu-Sn deposit, Portugal: An experimental, theoretical and field study. Unpub. PhD thesis, Victorian University of Manchester.

Richards, D., Jones, M., 1981 - Evaluation of Kara Properties, northwestern Tasmania. Unpublished report. Tasmania Mines Limited. Burnie, Tasmania.

Reid, A. M., 1924 - Deposits of iron ore at Hampshire. Unpublished report, Tasmania Mines Department.

Roedder, E., 1984 - Fluid inclusions. Reviews in Mineralogy 12, Mineralogical Society of America, Washington, D. C., 664.

Sato, K., 1980 - Tungsten skarn deposit of the Fujigatani mine, southwest Japan. Economic Geology 75, 1066-1082.

Sawka, W. N., Heizler, M. T., Kistler, R. W., Chapel, B. W., 1990 - Geochemistry of highly fractionated I- and S-type granites from the tin-tungsten province of western Tasmania. Geological Society of America, Special paper 246, 161-179.

Shepherd, T. J., Rankin, A. H, Alderton, D. H. M., 1985 - A practical guide to fluid inclusion studies. Black & Sons, London. 235.

Sherlock R. L., Jowett, E. C., Smith, B. D., Irish, D. E., 1993 - Distinguishing barren and auriferous veins in the Sigma Mine, Val-d'Or, Quebec. Canadian Journal Earth Sciences 30, 413-419.

Singoyi, B., Khin Zaw, 1994a - Mineral paragenesis, fluid Inclusion and oxygen isotope studies of the magnetite-scheelite skarn deposit, Kara, northwestern Tasmania, in Contentious issues in Tasmania, ed. Cooke, D., Kitto, P. Geological Society of Australian 39, Tasmania Division, Hobart. 3-4 November 1994, 119-120.

Singoyi, B., Khin Zaw, 1994b - Genesis of Magnetite-Scheelite Skarn Mineralisation at Kara, Northwestern Tasmania: Constraints from Mineral Paragenesis, Fluid Inclusion and Oxygen Isotope Studies, in Australian Research On Ore Genesis Symposium. Proceedings, Australian Mineral Foundation, December 12-14, 1994, Adelaide, South Australia, 11.1-11.5.

Steven, N. M., Moore, J. M., 1994 - Pan-African tungsten skarn mineralisation at the Otjua prospect, Central Namibia. Economic Geology 8, No. 7, 1431-1452.

Taylor, B. E., 1987 - Stable isotope geochemistry of ore-forming fluids, in Short course in stable isotope geochemistry of low temperature fluids, ed. Kyser, T. K. Mineralogical Association of Canada 13, 337-445.

Taylor, H. P., Jr., 1979 - Oxygen and hydrogen isotope relationships in hydrothermal ore deposits, in Geochemistry of hydrothermal ore deposits, ed. Barnes, H. L. J. Wiley and Sons, New York, 236-277.

Turnbul, D. G., 1991 - The geology and geochemistry of the Colebrook Hill skarn. Unpublished B.Sc. Honours thesis, CODES, Geology Department, University of Tasmania, Hobart.

Turner, N. J, 1989 - PreCambrian, in Geology and mineral resources of Tasmania, in Geology and mineral resources of Tasmania, ed. Burrett, C. F., Martin, E. L. Special publication, Geological Society Australia 15, 5-46.

Valley, J. W., 1986 - Stable isotope geochemistry of metamorphic rocks, in Stable isotopes of high temperature geological processes, ed. Valley, J. W., Taylor, H. P. Jr., O'Neil , J. R. Reviews in Mineralogy 16, 445-489.

Wesolowski, D., Cramer, J. J., Ohmoto, H., 1988 - Scheelite mineralisation in skarns adjacent to Devonian granitoids at King Island, Tasmania, in Recent advances in the geology of granite related mineral deposits, ed. Taylor, R. O., Strong, D. F. Canadian Institute of Mining and Metallurgy, 235-251.

Wesolowski, D., Drummond, S. E., Mesmer, R. E., Ohmoto, H., 1984 - Hydrolysis of tungsten (IV) in aqueous sodium chloride solutions to 300°C. Inorganic chemistry 23, 1120-1132.

Wesolowski, D., Ohmoto, H., 1986 - Calculated oxygen isotope fractionation factors between water and the minerals scheelite and powellite. Economic Geology 81, 471-477.

Whitehead, C. H.,1985 - Preliminary review of the potential of magnetite resources, Kara

Properties, E. L. 17/68. Unpublished report. Tasmania Mines NL limited. Burnie.

Whitehead, C. H.,1990 - Kara scheelite-magnetite deposit, in Excursion guide E2, Tin and tungsten deposits related to Devonian granitoids. 19th Australian Geological Convention., Hobart.

Whitehead, C. H.,1992 - Scheelite and magnetite ore resources, Kara Properties, Tasmania Mines limited. Unpublished report. Tasmania Mines limited. Burnie.

Williams, E., McClenaghan, M. P., Collins, P. L. F., 1989 - Mid-Palaeozoic deformation, granitoid and ore deposits, in Geology and mineral resources of Tasmania, ed. Burrett, C. F., Martin, E. L. Special publication, Geological Society Australia 15, 238-292.

Wood, S. A., Vlassopoulos, D., 1989 - Experimental determination of the hydrothermal solubility and speciation of tungsten at 500°C and 1 kbar. Geochimica et Cosmochimica Acta 53, 303-312.

# APPENDICES

## APPENDIX I. Catalogue of samples studied from the Kara deposit area.

### A. Samples collected by the present author.

| Cat. No. | S. No. | Drill hole no/ sample depth | Mine coordi-nates | Rock name | Composition | Sample preparation |
|---|---|---|---|---|---|---|
| **Kara No. 1 skarn body** | | | | | | |
| | S1 | DDH230.@ 16.0m | 5840N, | Skarn | Cpx+Mag | R, PS |
| | S2 | DDH230 @ 17.0m | 7540E | Skarn | Cpx+Ves+Mag±Ves | R, PS |
| | S3 | DDH230 @ 21.9m | | Skarn | Ves+Cpx | R, PS |
| | S4 | DDH230 @ 21.6m | | Skarn | Cpx±Ves | R, PS |
| | S113 | DDH230 @ 22.0 | | Skarn | Ves+Mag±Ep | R, PS, CR |
| | S6 | DDH230 @ 25.4m | | Skarn | Ves+Mag±Ep | R, PS |
| | S7 | DDH230 @ 26.0m | | Skarn | Cpx+Mag±Gar±Ves | R, PS |
| | S8 | DDH230 @ 30.7m | | Skarn | Ves±Cpx±Mag | R, PS |
| | S9 | DDH230 @ 34.0m | | Skarn | Mag+Cpx+Amp | R, PS |
| | S10 | DDH230 @ 39.0m | | Skarn | Gar+Mag±Cpx±Ves±Cc | R, PS |
| | S11 | DDH230 @ 45.0m | | Skarn | Gar±Mag | R, PS |
| | S12 | DDH230 @ 47.8m | | Skarn | Ep+Qtz±Sp | R, PS |
| | S13 | DDH230 @ 55.4m | | Skarn | Ep+Qtz | R, PS |
| | S14 | DDH110 @ 12.16m | 5840N, | Skarn | Mag+Cpx | R, PS |
| | S15 | DDH110 @ 24.32m | 7295E | Skarn | Mag+Cpx | R, PS |
| | S16 | DDH110 @ 29.98m | | Skarn | Gar+Cpx+Ves+Mag | R, PS, CR |
| | S17 | DDH110 @ 31.92m | | Skarn | Mag+Amp+Flu+Cpx | R, PS, FI, CR |
| | S18 | DDH110 @ 34.45m | | Skarn | Mag+Amp±Cpx±Gar±Ep | R, PS |
| | S18B | DDH110 @ 34.35m | | Skarn | Gar+Mag+Amp+Flu ±Cpx | R, PS, FI |
| | S19 | DDH110 @ 35.87 | | Skarn | Gar±Mag±Cpx±Qtz ±Amp±Chl±Ap | R, PS, FI |
| | S20 | DDH110 @ 39.82 | | Skarn | Gar+Ep+Qtz+Amp+Flu | R, PS, FI |
| | S21 | DDH110 @ 42.6 | | Skarn | Ep+Qtz | |
| | S22 | DDH125 @ 85.2 | 5865.0N, 7330.0E | Granite | Altered granite | R, TS, FI |
| | S26 | DDH113 @ 38.2 | 5865.0N, | Skarn | Cpx+Gar+±Ep | R, PS, FI |
| | S27 | DDH113 @ 50.16 | 7150.0E | Skarn | Mag+Cpx | R, PS |
| | S28 | DDH113 @ 55.08 | | Skarn | Mag+Ves | R, PS |
| | S29 | DDH113 @ 65.46 | | Skarn | Mag+Cpx | R, PS |
| | S30 | DDH113 @ 68.93 | | Skarn | Cpx+Amp | R, PS |
| | S31 | DDH113 @ 74.17 | | Skarn | Mag+Cpx+Ves | R, PS |
| | S32 | DDH113 @ 77.82 | | Skarn | Ves+Cpx+Gar±Ep | R, PS |
| | S33 | DDH113 @ 86.64 | | Skarn | Ep+Qtz | R, PS, FI |
| | S34 | DDH113 @ 89.68 | | Granite | Altered granite | R, TS |
| | S35 | DDH108 @ 13.26 | 5845.0N, | Skarn | Gar±Mag±Cpx±Amp±Ep | R, PS, FI, CR |
| | S36 | DDH108 @ 30.4 | 7295.0E | Skarn | Cpx+Mag+Amp | R, PS, CR |
| | S37 | DDH108 @ 33.74 | | Skarn | Cpx+Mag±Qtz | R, PS |

**S. No.** Sample number; **R:** Rock or mineral sample; **PS:** Polished/thin section; **FI:** Fluid inclusion section, **CO:** Samples drilled out for carbon-oxygen isotope analysis; **SO:** Samples analysed for oxygen isotope composition; **CR:** Samples crushed/ground for fluid inclusion gas analysis by thermal decrepitation mass spectrometry; **Cpx:** clinopyroxene; **Gar:** garnet; **Ves:** vesuvianite; **Amp:** amphibole; **Ep:** epidote; **Flu:** fluorite; **Ap:** apatite; **Cc:** calcite (or other carbonate mineral); **Chl:** chlorite; **Qtz:** quartz; **Wol:** wollastonite; **Sp:** sphene; **Ser:** Sericite; **Mag:** magnetite; **Sch:** scheelite; **Hm:** hematite; **Py:** pyrite; **Cpy:** chalcopyrite.

## APPENDIX I. Continued.

### A. Continued.

| Cat. No. | S. No. | Drill hole no/ sample depth | Mine coordi-nates | Rock name | Composition | Sample preparation |
|---|---|---|---|---|---|---|
| | S38 | DDH108 @ 37.09 | | Skarn | Mag+Cpx+Ves+Py±Cpy | R, PS |
| | S39 | DDH108 @ 40.23 | | Skarn | Cpx+Mag±Cc±Qtz±Ep | R, PS, CO |
| | S40 | DDH108 @ 42.76 | | Granite | Altered granite | |
| | S52 | DDH207 @ 23.7 | 5976.7N, | Sand-stone | Hornfelsed qtz sandstone | R, TS |
| | S53 | DDH207 @ 35.0 | 7260.3E | Sand-stone | Hornfelsed qtz sandstone | R, TS |
| | S54 | DDH207 @ 43.7 | | Skarn | Ves±Cpx±Mag±Chl±Ep | R, PS |
| | S55 | DDH207 @ 67.4 | | Skarn | Ves+Cpx+Cc | R, PS |
| | S56 | DDH207 @ 68.9 | | Skarn | Ves+Cpx+Mag±Ep | R, PS |
| | S58 | DDH207 @ 83.9 | | Skarn | Cpx+Amp±Flu±Ep | R, PS, FI |
| | S59 | DDH207 @ 86.8 | | Skarn | Cpx+Mag+Amp+Flu +Sch | R, FI |
| | S80 | DDH207 @ 93.5 | | Skarn | Gar+Mag+Ves+Cc±Sch | R |
| | S60 | DDH207 @ 94.9 | | Skarn | Ves+Mag+Qtz+Sch | R, PS, FI |
| | S61 | DDH207 @ 94.7 | | Skarn | Ep+Qtz±Sp | R, PS, FI |
| | S81 | DDH207 @ 98.5 | | | Ep+Qtz±Flu | R, FI, CR |
| | S62 | DDH207 @ 100.0 | | Sand-stone | Hornfelsed qtz sandstone | R, TS |
| | S65 | DDH278 @ 35.1 | 5980.1N, | Skarn | Ves+Ep±Cpx | R, PS, FI |
| | S151 | DDH278 @ 44.3 | 7335.5E | Skarn | Cpx+Gar+Amp+Ep+Cc+ Qtz+Sch | R, FI |
| | S66 | DDH278 @ 44.5 | | Skarn | Ves+Cc+Cpx±Ep | R, PS, FI |
| | S67 | DDH278 @ 74.1 | | Skarn | Mag+Ves+Ep±Cpx±Wol | R, PS |
| | S147 | DDH278 @ 90.6 | | Skarn | Gar+Mag | R, CO |
| | S68 | DDH278 @ 93.2 | | Skarn | Gar | R, FI |
| | S146 | DDH278 @ 94.3 | | Skarn | Gar+Amp+Cc | R, CO |
| | S69 | DDH278 @ 94.5 | | Skarn | Ep+Qtz+Cc±Cpx | R, PS, CO |
| | S191 | DDH281 @ 52.2 | 6105.0N, | Skarn | Gar+Cc+Amp+Mag | R, CO |
| | S196 | DDH281 @ 124.6 | 7312.6E | Skarn | Gar+Mag+Amp+Cc | R, CO |
| | S82 | DDH219 @ 7.8 | 5889.6N, | Skarn | Mag±Gar+Amp±Sch | R, CR |
| | S83 | DDH219 @ 12.5 | 1450.9E | Skarn | Gar+Ves+Mag±Cpx±Sch | R |
| | S85 | DDH219 @ 19.0 | | Skarn | Mag+Ves±Sch±Sch | R |
| | S86 | DDH219 @ 23.4 | | Skarn | Mag+Cpx+Amp+Cc±Sch | R |
| | S87 | DDH219 @ 25.0 | | Skarn | Mag+Cpx+Amp+Cc±Sch | R |
| | S88 | DDH219 @ 25.3 | | Skarn | Mag+Cpx+Amp+Cc | R |
| | S89 | DDH219 @ 26.3 | | Skarn | Mag+Amp±Cpx±Cc±Qtz | R, CO |
| | S92 | DDH219 @ 36.6 | | Skarn | Mag+Gar | R |
| | S93 | DDH219 @ 39.7 | | Granite | Epidotised granite | R |
| | S100 | DDH263 @ 30.8 | 5729.8N, 7401.9E | Skarn | Mag+Ep | R |

**S. No.** Sample number; **R:** Rock or mineral sample; **PS:** Polished/thin section; **FI:** Fluid inclusion section, **CO:** Samples drilled out for carbon-oxygen isotope analysis; **SO:** Samples analysed for oxygen isotope composition; **CR:** Samples crushed/ground for fluid inclusion gas analysis by thermal decrepitation mass spectrometry; **Cpx:** clinopyroxene; **Gar:** garnet; **Ves:** vesuvianite; **Amp:** amphibole; **Ep:** epidote; **Flu:** fluorite; **Ap:** apatite; **Cc:** calcite (or other carbonate mineral); **Chl:** chlorite; **Qtz:** quartz; **Wol:** wollastonite; **Sp:** sphene; **Ser:** Sericite; **Mag:** magnetite; **Sch:** scheelite; **Hm:** hematite; **Py:** pyrite; **Cpy:** chalcopyrite.

## APPENDIX I. Continued.

### A. Continued.

| Cat. No. | S. No. | Drill hole no/ sample depth | Mine coordi-nates | Rock name | Composition | Sample preparation |
|---|---|---|---|---|---|---|
| | BS1 | Open cut | (Centre: 6000N, 7000E) | Skarn | Mag+Sch+Amp±Cpx | R, PS, CR |
| | S199 | Open cut | | Skarn | Mag+Amp+Cpx | R, PS |
| | S200 | Open cut | | Skarn | Mag+Amp+Sch±Flu | R, PS, FI, SO, CR |
| | S201 | Open cut | | Skarn | Mag+Amp+Flu±Sch | R, FI |
| | S202 | Open cut | | Skarn | Mag+Sch+Amp±Cpx | R, PS, FI, SO, CR |
| | S204 | Open cut | | Granite | Altered granite | R, PS, FI |
| | S206 | Open cut | | | Sch | R, CR |
| | S208 | Open cut | | Skarn | Mag+Sch+Amp±Cpx | R, FI, SO |
| | S209 | Open cut | | Skarn | Gar+Amp±Cpx±Ves±Ep | R, FI |
| **Bobs' Bonanza skarn** | | | | | | |
| | S41 | DDH309 @ 3.0 | 5721.1N, 7687.1E | Basalt | Coherent feldspar-olivine-phyric basalt | R, TS |
| | S44 | DDH309 @ 33.45 | | Sand-stone | | R |
| | S45 | DDH309 @ 41.74 | | Skarn | Cpx+Qtz±Gar±Sch | R, FI |
| | S112 | DDH309 @ 44.8 | | Skarn | Gar+Mag+Cc±Sch±Cpx | R, FI, CO |
| | S46 | DDH309 @ 46.0 | | Skarn | Gar+Cc±Mag±Qtz | R, FI, CO |
| | S47 | DDH309 @ 47.22 | | Skarn | Mag+Cpx+±Gar±Chl ±Ves±Sch | R, PS, SO |
| | S109 | DDH309 @ 49.6 | | Skarn | Cpx+Mag+Cc+Ser+Ap | R, FI, CO |
| | S108 | DDH309 @ 50.6 | | Skarn | Gar+Mag+Cc+Amp±Cpx ±Sch | R, FI |
| | S49 | DDH309 @ 50.6 | | Skarn | Mag+Cpx | R, PS |
| | S48 | DDH309 @ 51.2 | | Skarn | Cpx+Mag+Cc+Chl±Ap± Py±Cpy | R, PS |
| | S50 | DDH309 @ 51.3 | | Skarn | Ep+Cpx+Flu±Chl±Amp | R, PS |
| | S51 | DDH309 @ 52.2 | | Granite | Altered coarse-grained granite | R, TS |
| **Eastern Ridge skarn** | | | | | | |
| | S168 | DDH275 @ 53.3 | 6283.4N, | Skarn | Gar+Cc±Cpx | R, FI, CO |
| | S171 | DDH275 @ 75.6 | 7642.6E | Skarn | Gar+Hm | R |
| | S159 | DDH277 @ 174.1 | 6509.0N, | Skarn | Ves+Sch | R, SO, CR |
| | S162 | DDH277 @ 190.1 | 7619.2E | Skarn | Mag+Ves+Cc±Sch | R |

**S. No.** Sample number; **R:** Rock or mineral sample; **PS:** Polished/thin section; **FI:** Fluid inclusion section, **CO:** Samples drilled out for carbon-oxygen isotope analysis; **SO:** Samples analysed for oxygen isotope composition; **CR:** Samples crushed/ground for fluid inclusion gas analysis by thermal decrepitation mass spectrometry; **Cpx:** clinopyroxene; **Gar:** garnet; **Ves:** vesuvianite; **Amp:** amphibole; **Ep:** epidote; **Flu:** fluorite; **Ap:** apatite; **Cc:** calcite (or other carbonate mineral); **Chl:** chlorite; **Qtz:** quartz; **Wol:** wollastonite; **Sp:** sphene; **Ser:** Sericite; **Mag:** magnetite; **Sch:** scheelite; **Hm:** hematite; **Py:** pyrite; **Cpy:** chalcopyrite.

## APPENDIX I. Continued.

### A. Continued.

| Cat. No. | S. No. | Drill hole no/ sample depth | Mine coordi-nates | Rock name | Composition | Sample preparation |
|---|---|---|---|---|---|---|
| **Kara North 266 Zone skarn** | | | | | | |
| | S122 | DDH303 @ 15.5 | 7161.8N, 7176.0E | Skarn | Gar+Mag+Cc | R |
| | S118 | DDH303 @ 24.7 | | Skarn | Gar+Mag+Amp±Mag | R |
| | S120 | DDH303 @ 29.1 | | Skarn | Gar+Mag±Ves±Sch | R |
| | S130 | DDH266 @ 39.0 | 7166.5N, | Skarn | Gar+Cc+Mag±Cpx | FI |
| | S127 | DDH266 @ 49.8 | 7200.7E | Skarn | Mag+Sch+Amp | R, PS, FI, SO, CR |
| | S125 | DDH266 @ 55.5 | | | Gar+Mag+Amp+Sch ±Cpx | R, SO |
| | S133 | DDH293 @ 94.4 | 7172.6N, 7213.1E | Granite | Porphyritic granite | R, PS |
| **Kara North Magnetic Zone skarn** | | | | | | |
| | S177 | DDH287 @ 66.0 | 7153.8N, | Skarn | Gar+Mag+Cc±Cpx | R, PS, FI, CO |
| | S179 | DDH287 @ 68.0 | 7394.3E | | Gar+Cc+Amp±Cpx | R, PS, FI, CO, CR |
| | S178 | DDH287 @ 70.9 | | | Gar+Mag+Cc±Cpx | R, FI, CO, CR |
| | S180 | DDH287 @ 77.0 | | | Mag+Cpx | R, PS, CO |
| | S182 | DDH287 @ 97.0 | | | Gar+Mag+Amp+Cc±Cpx ±Sch | R, PS, FI, CO, CR |
| | S183 | DDH287 @ 108.5 | | | Gar+Mag+Amp+Cc±Cpx | R, PS, FI, CO |
| **L5 skarn** | | | | | | |
| | S154 | DDH327 @ 86.5 | 7677.0N, | Skarn | Amp+Mag+Sch | R, SO |
| | S155 | | 7830.2E | Skarn | Mag+Gar+Cpx+Qtz+Sch ±Hm | R, FI, CO |
| | S184 | DDH327 @ 72.2 | | Marble | Marble with Amp+Mag skarn lenses | R, CO |
| | S188 | DDH327@ 90.7 | | Skarn | Amp+Cc+Sch | R, SO |
| | S189 | DDH327 @ 94.3 | | Skarn | Mag+Amp | R |
| | S190 | DDH327 @ 105.0 | | Granite | | R |

**S. No.** Sample number; **R:** Rock or mineral sample; **PS:** Polished/thin section; **FI:** Fluid inclusion section, **CO:** Samples drilled out for carbon-oxygen isotope analysis; **SO:** Samples analysed for oxygen isotope composition; **CR:** Samples crushed/ground for fluid inclusion gas analysis by thermal decrepitation mass spectrometry; **Cpx:** clinopyroxene; **Gar:** garnet; **Ves:** vesuvianite; **Amp:** amphibole; **Ep:** epidote; **Flu:** fluorite; **Ap:** apatite; **Cc:** calcite (or other carbonate mineral); **Chl:** chlorite; **Qtz:** quartz; **Wol:** wollastonite; **Sp:** sphene; **Ser:** Sericite; **Mag:** magnetite; **Sch:** scheelite; **Hm:** hematite; **Py:** pyrite; **Cpy:** chalcopyrite.

## APPENDIX I. Continued.

### B. Samples collected by Barrett (1980). Details on locations given in Barrett (1980).

| S. No | Skarn body/location | Rock name | Sample preparations |
|---|---|---|---|
| 105323 | Kara No. 1 | Skarn | PS |
| 105328 | Kara No. 1 | Skarn | PS |
| 105337 | Kara No. 1 | Skarn | PS |
| 105339 | Kara No. 1 | Skarn | PS |
| 105341 | Kara No. 1 | Skarn | PS |
| 105308 | Kara No. 1 | Skarn | PS, FI |

S. No. Sample number; PS: Polished/thin section; FI: Fluid inclusion section.

**APPENDIX II. Temporal distribution of skarn minerals based on visual examinations and microscopic study of hand specimens from the Kara deposit, northwestern Tasmania.**

| S. No. | STAGE I | STAGE II | STAGE III | STAGE IV |
|---|---|---|---|---|
| 105323 | Cpx | Ves+Sch | Ep+Mag | |
| 105328 | Cpx+Wol | | Mag+Chl+Amp+Flu+Sch | |
| 105337 | | | Ep+Qtz+Flu | Hm |
| 105339 | Cpx+Wol±Qtz | Ves+Sch | Mag+Ep | |
| 105341 | Cpx | Mag+Ves+Sch | | |
| S1 | Cpx+Qtz | | Ep+Qtz+Mag+Cc | |
| S2 | Cpx | Ves | Ep+Qtz+Mag+Ves+Gt | |
| S3 | Cpx | Ves | Ep+Cc+Ves+Mag | |
| S4a | Cpx | Ves+Sch | Amp+Ep | |
| S6 | | Ves | Mag+Ep | |
| S7 | Cpx | Gar | Mag+Ves | |
| S8 | Cpx | Gar+Ves+Mag | Gar+Mag+Ep+Cc±Ves | |
| S9 | Cpx | | Amp+Mag | |
| S10 | Cpx | Gar+Ves | Flu+Sp+Cc+Qtz+Mag | |
| S11 | | Gar | Mag | |
| S12 | | | Ep+Qtz+Sp | |
| S13 | | | Ep+Qtz | |
| S14 | Cpx | Mag+Ser | Hm | |
| S15 | Cpx | Ves+Mag | | |
| S16 | Cpx | Gar+Ves | Mag | |
| S17 | Cpx | Mag | Amp+Flu+Mag | Flu |
| S18 | Cpx | | Amp+Ep+Mag+Gt+Ep | |
| S18B | | Gar+Mag | Amp+Flu+Mag | |
| S19 | Cpx | Gar | Amp+Chl+Qtz+Cc+Mag+Gt+Ap | |
| S20 | | Gar | Ep+Qtz+Amp+Flu | |
| S21 | | | Ep+Qtz | |
| S26 | Cpx+Gar | | Ep+Cc+Ser | Cc |
| S27 | Cpx | Mag | | |
| S28 | | Ves | Amp+Ep+Cc+Mag+Ves | |
| S29 | Cpx | Mag | | |
| S30 | Cpx | | Amp+Flu+Sp+Mag | |
| S31 | Cpx+Ves | | Amp+Mag+Py+Cpy | |
| S32 | Cpx | Ves+Gt+Mag | Ep+Chl+Mag | |
| S33 | | | Ep+Qtz | |
| S35 | Cpx | Gar | Amp+Ep+Mag | |
| S36 | Cpx | | Mag+Amp | |
| S37 | Cpx | | Mag+Py | |
| S38 | Cpx | Ves | Amp+Mag+Py+Cpy | |
| S39 | Cpx | | Mag | Cc+Qtz+Ep |
| S45 | Cpx+Qtz | Gar | Cc+Qtz+Gt+Cpx | |
| S46 | Cpx | Gar | Mag+Cc+Qtz+Gar+Ser | |
| S47 | Cpx | Gar | Ep+Chl+Cc+Mag+Sch+Ves | |
| S48 | Cpx | | Cc+Chl+Mag+Ap+Py | Cpy |

**Cpx:** clinopyroxene; **Gar:** garnet; **Ves:** vesuvianite; **Amp:** amphibole; **Ep:** epidote; **Flu:** fluorite; **Ap:** apatite; **Cc:** calcite (or other carbonate mineral); **Chl:** chlorite; **Qtz:** quartz; **Wol:** wollastonite; **Sp:** sphene; **Ser:** Sericite; **Mag:** magnetite; **Sch:** scheelite; **Hm:** hematite; **Py:** pyrite; **Cpy:** chalcopyrite.

**APPENDIX II. Continued.**

| S. No. | STAGE I | STAGE II | STAGE III | STAGE IV |
|---|---|---|---|---|
| S49 | Cpx | Mag | | |
| S50 | Cpx | | Amp+Ep+Flu | |
| S54 | Cpx | Ves | Ep+Chl+Mag+Ves | |
| S55 | Cpx | Ves | Ep+Cc+Chl+Mag | |
| S56 | Cpx | | Ves+Mag+Gar+Ep | |
| S58 | Cpx | | Amp+Flu+Ep | |
| S59 | Cpx | | Mag+Amp+Flu+Sch | |
| s60 | Cpx+Gar | Mag | | |
| S61 | | | Ep+Qtz+Sp | |
| S65 | Cpx | Ves | Cc+Ep+Ves | |
| S66 | Cpx | Ves | Cc+Ep+Ves | |
| S67 | Cpx+Wol | Ves | Mag+Ves+Ep | |
| S68 | | | Gar | |
| S69 | Cpx | | Ep+Qtz+Ser | Cc+Qtz |
| S80 | | Gar | Mag+Cc | |
| S81 | | | Ep+Qtz+Flu+Sp | Hm |
| S82 | | Mag | Gar±Ep | |
| S83 | Gt±Cpx | Ves+Mag | | |
| S85 | | Mag+Ves+Sch | | |
| S86 | Cpx | | Mag+Amp | |
| S87 | Cpx | Gar | Mag+Amp | |
| S88 | Cpx | | Mag+Amp | Cc |
| S89 | Cpx | | Mag+Amp | Cc±Qtz |
| S92 | | | Ep+Qtz | Hm |
| S94 | | Gar | Ves+Mag+Ep | |
| S100 | Cpx | Gar | Mag+Ep | |
| S108 | Cpx | | Gt+Cc+Amp+Sch+Qtz | |
| S109 | Cpx | | Mt+Cc+Ser+Amp | |
| S110 | Cpx | | Mag±Amp | |
| S112 | ±Cpx | | Gt+Mag+Sch | |
| S113 | Cpx | Ves+Mag | Ep+Mag | |
| S118 | Gar | Mag | Amp±Mag | |
| S120 | | Gar | Mag±Gar±Ep | |
| S122 | | Gar | Mag+Cc | |
| S125 | ±Cpx | Gar | Amp+Mag+Sch | |
| S127 | Cpx | | Mag+Amp+Sch+Flu | |
| S130 | Cpx | | Gar+Cc | Hm |
| S141 | Cpx | Mag+Py | | |
| S146 | Gar±Cpx | | Amp+Cc | |
| S147 | Gar | Mag | | |
| S148 | | Mag | Ep | |
| S154 | Cpx | | Mag+Amp+Sch+Cc | |
| S155 | Cpx | Gt+Qtz+Sch | Mag | |
| S159 | ±Cpx | Ves+Sch | | |
| S162 | | Mag | Ves+Sch+Cc | |

**Cpx:** clinopyroxene; **Gar:** garnet; **Ves:** vesuvianite; **Amp:** amphibole; **Ep:** epidote; **Flu:** fluorite; **Ap:** apatite; **Cc:** calcite (or other carbonate mineral); **Chl:** chlorite; **Qtz:** quartz; **Wol:** wollastonite; **Sp:** sphene; **Ser:** Sericite; **Mag:** magnetite; **Sch:** scheelite; **Hm:** hematite; **Py:** pyrite; **Cpy:** chalcopyrite.

**APPENDIX II. Continued.**

| S. No. | STAGE I | STAGE II | STAGE III | STAGE IV |
|---|---|---|---|---|
| S168 | | Gar | Gt+Cc | |
| S171 | | Gar | | Hm |
| S177 | Cpx | Gar | Mag+Cc | |
| S178 | Cpx | | Cc+Amp+Mag±Cpx | |
| S179 | Cpx | | Cc+Gt | |
| S180 | Cpx | | Mag+Gt+Cc | |
| S181 | Cpx±Sch | Gar+Ves±Sch | Cc | |
| S182 | ±Cpx | Gar | Amp+Mag+Cc±Gar±Qtz±Sch | |
| S183 | ±Cpx | Gar | Cc+Amp+Mag±Sch | |
| S188 | Cpx | | Mag+Amp+Cc+Sch | |
| S189 | Cpx | | Mag+Amp±Sch±Hm±Qtz | |
| S190 | | Gar | Gar+Mag+Amp+Cc | |
| S196 | Cpx | | Mag+Amp | Cc |
| S199 | Cpx | | Mag+Amp | |
| S200 | ±Cpx | Mag | Mag+Amp+Sch±Flu | |
| S201 | ±Cpx | Mag | Mag+Amp+Flu±Sch | |
| S202 | Cpx | | Mag+Amp+Sch±Flu | |
| S208 | Cpx | Mag | Amp+Mag+Sch | |
| S209 | Cpx | Gar+Ves | Mag+Amp+Ep | |
| BS1 | ±Cpx | | Mag+Amp+Sch±Flu | |

**Cpx:** clinopyroxene; **Gar:** garnet; **Ves:** vesuvianite; **Amp:** amphibole; **Ep:** epidote; **Flu:** fluorite; **Ap:** apatite; **Cc:** calcite (or other carbonate mineral); **Chl:** chlorite; **Qtz:** quartz; **Wol:** wollastonite; **Sp:** sphene; **Ser:** Sericite; **Mag:** magnetite; **Sch:** scheelite; **Hm:** hematite; **Py:** pyrite; **Cpy:** chalcopyrite.

**APPENDIX III. Spatial distribution of skarn minerals and metals, the Kara deposit, northwestern Tasmania.**

**A. Relationship between skarn type and the distribution of tungsten along diamond drill hole DDH110, Kara No. 1 orebody.**

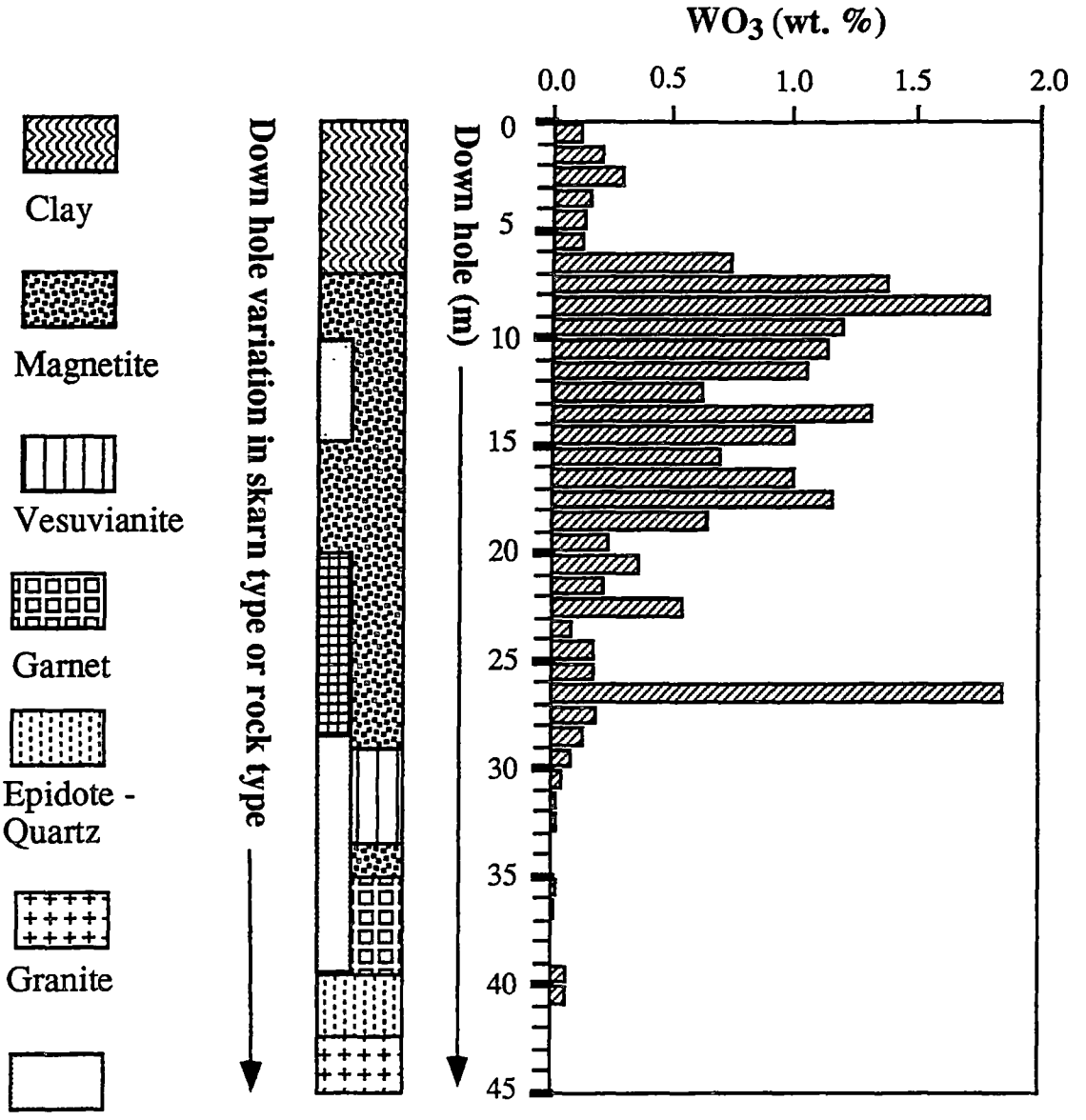

APPENDIX III. Continued.

**B. Relationship between skarn type and the distribution of tungsten along diamond drill hole DDH125, Kara No. 1 orebody.**

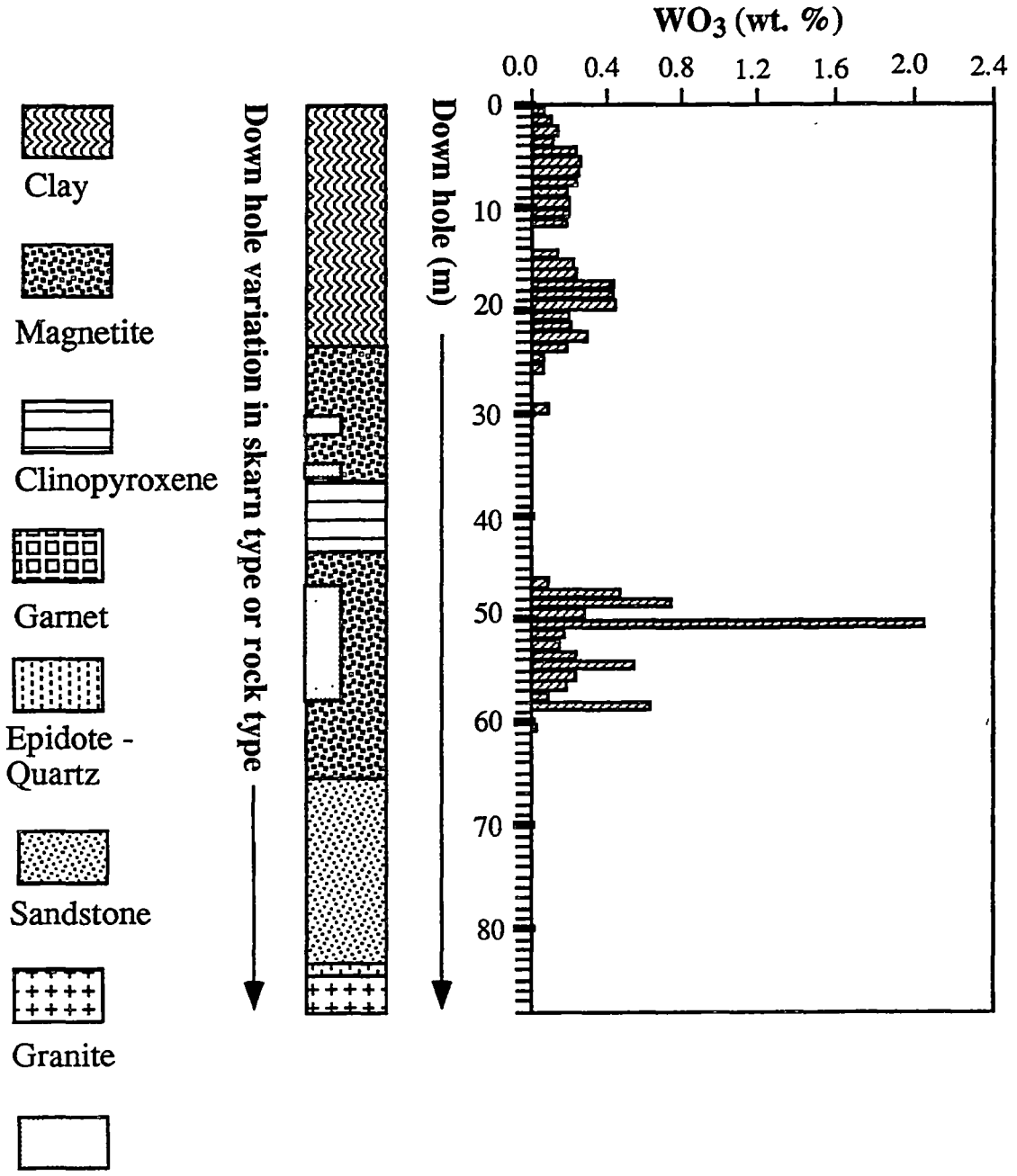

**APPENDIX III. Continued.**

**C. Relationship between skarn type and the distribution of tungsten, tin, lead and bismuth along diamond drill hole DDH219, Kara No. 1 orebody.**

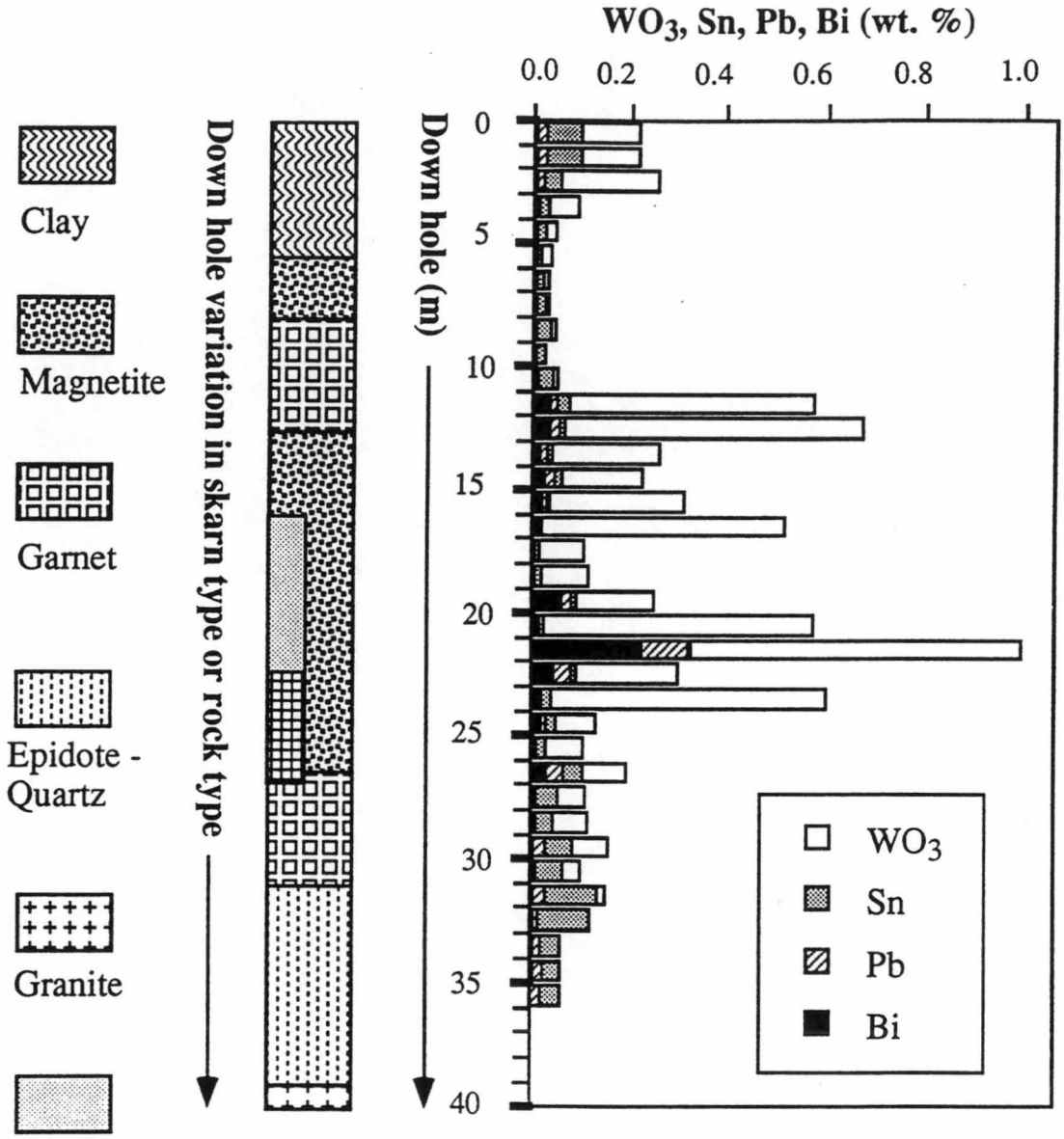


Weak scheeltie mineralisation (<0.5 vol. %)

Strong scheelite mineralisation (>0.5 vol. %)

APPENDIX III. Continued.

**D. Relationship between skarn type and the distribution of tungsten, tin and molybdenum along diamond drill hole DDH230, Kara No. 1 orebody.**

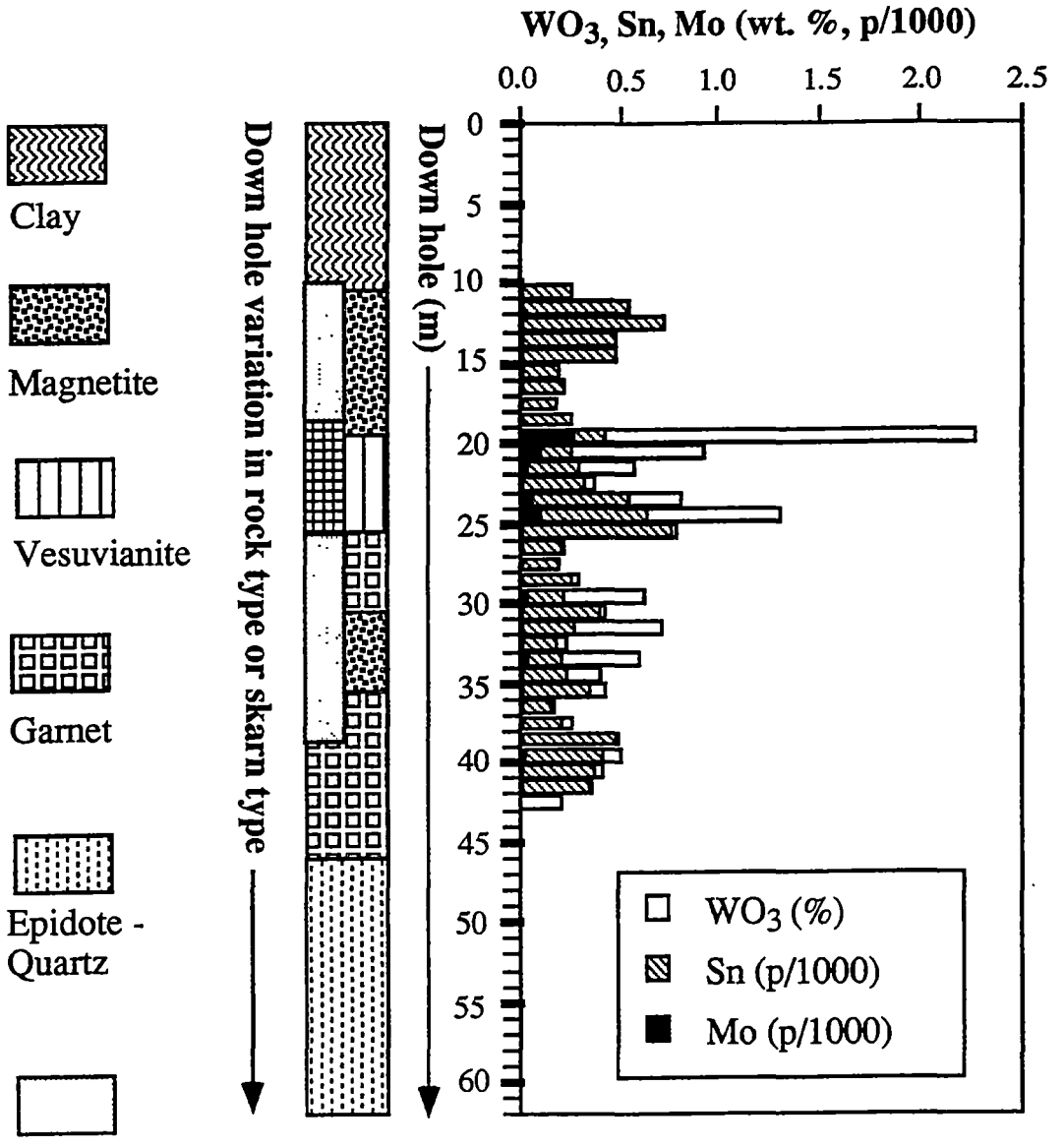

## APPENDIX IV. Microprobe data of skarn minerals from the Kara deposit, northwestern Tasmania.

| Clinopyroxene | | | | | | | | |
|---|---|---|---|---|---|---|---|---|
| S. No. | 105339 | 105339 | 105339 | 105339 | S1 | S1 | S1 | S1 |
| An. No. | 1 | 2 | 3 | 4 | 1 | 2 | 3 | 4 |
| | | | | Oxide composition (wt. %) | | | | |
| $SiO_2$ | 53.15 | 54.02 | 52.99 | 53.52 | 54.07 | 54.43 | 53.91 | 54.10 |
| $TiO_2$ | 0.00 | 0.04 | 0.00 | 0.02 | 0.00 | 0.09 | 0.01 | 0.01 |
| $Al_2O_3$ | 0.52 | 0.36 | 0.57 | 0.45 | 0.15 | 0.85 | 0.39 | 0.26 |
| $Cr_2O_3$ | 0.01 | 0.00 | 0.00 | 0.01 | 0.00 | 0.00 | 0.02 | 0.00 |
| FeOtotal | 4.10 | 3.59 | 5.34 | 4.36 | 2.75 | 0.83 | 3.04 | 2.91 |
| NiO | - | - | - | - | - | - | - | - |
| MnO | 0.47 | 0.39 | 0.68 | 0.61 | 0.63 | 0.07 | 0.62 | 0.74 |
| MgO | 15.63 | 16.10 | 14.74 | 15.67 | 16.31 | 17.98 | 16.32 | 16.65 |
| CaO | 26.19 | 26.12 | 26.16 | 26.13 | 26.21 | 26.18 | 26.09 | 26.47 |
| $Na_2O$ | 0.01 | 0.01 | 0.01 | 0.03 | 0.00 | 0.11 | 0.00 | 0.00 |
| $K_2O$ | 0.00 | 0.01 | 0.00 | 0.01 | 0.00 | 0.00 | 0.00 | 0.00 |
| $P_2O_5$ | - | - | - | - | - | - | - | - |
| S | - | - | - | - | - | - | - | - |
| Cl | - | - | - | - | - | - | - | - |
| TOTAL | 100.08 | 100.64 | 100.49 | 100.81 | 100.12 | 100.54 | 100.40 | 101.14 |
| | | | | Cation allocation based on six oxygen atoms | | | | |
| Si IV | 1.95 | 1.97 | 1.95 | 1.95 | 1.98 | 1.96 | 1.97 | 1.96 |
| Al IV | 0.02 | 0.02 | 0.03 | 0.02 | 0.02 | 0.04 | 0.02 | 0.01 |
| T site | 1.97 | 1.99 | 1.98 | 1.97 | 2.00 | 2.00 | 1.99 | 1.97 |
| Al VI | 0.00 | 0.00 | 0.00 | 0.00 | 0.04 | 0.00 | 0.00 | 0.00 |
| Ti | 0.00 | 0.00 | 0.00 | 0.00 | 0.00 | 0.00 | 0.00 | 0.00 |
| Cr | 0.00 | 0.00 | 0.00 | 0.00 | 0.00 | 0.00 | 0.00 | 0.00 |
| $Fe^{+3}$ | 0.08 | 0.05 | 0.08 | 0.08 | 0.04 | 0.03 | 0.05 | 0.08 |
| $Fe^{+2}$ | 0.05 | 0.06 | 0.09 | 0.06 | 0.04 | 0.00 | 0.04 | 0.01 |
| $Mn^{+2}$ | 0.02 | 0.01 | 0.02 | 0.02 | 0.02 | 0.00 | 0.02 | 0.02 |
| Ni | - | - | - | - | - | - | - | - |
| Mg | 0.86 | 0.87 | 0.81 | 0.85 | 0.89 | 0.96 | 0.89 | 0.90 |
| Ca | 1.03 | 1.02 | 1.03 | 1.02 | 1.03 | 1.01 | 1.02 | 1.03 |
| Na | 0.00 | 0.00 | 0.00 | 0.00 | 0.00 | 0.01 | 0.00 | 0.00 |
| K | - | - | - | - | - | - | - | - |
| M1,M2 | 2.04 | 2.01 | 2.03 | 2.03 | 2.06 | 2.01 | 2.02 | 2.04 |
| Mn/Fe | 0.15 | 0.09 | 0.12 | 0.14 | 0.25 | 0.00 | 0.22 | 0.26 |
| | | | | Clinopyroxene components (mole fraction) | | | | |
| Di | 0.92 | 0.93 | 0.88 | 0.91 | 0.94 | 1.00 | 0.94 | 0.97 |
| Hd | 0.05 | 0.06 | 0.10 | 0.06 | 0.04 | 0.00 | 0.04 | 0.01 |
| Jo | 0.02 | 0.01 | 0.02 | 0.02 | 0.02 | 0.00 | 0.02 | 0.02 |

**S. No.:** sample number; **An. No.:** serial number of analysis
**Di:** diopside
**Hd:** hedenbergite
**Jo:** Johannsenite

## APPENDIX IV. Continued.

**Clinopyroxene**

| S. No. | S2 | S2 | S2 | S4A | S4A | S4A | S16 | S19 |
|---|---|---|---|---|---|---|---|---|
| An. No. | 1 | 2 | 3 | 1 | 2 | 3 | 2 | 1 |
| | | | | Oxide composition (wt. %) | | | | |
| $SiO_2$ | 54.10 | 53.80 | 54.05 | 54.14 | 53.80 | 53.53 | 52.61 | 53.69 |
| $TiO_2$ | 0.00 | 0.03 | 0.00 | 0.05 | 0.02 | 0.06 | 0.10 | 0.00 |
| $Al_2O_3$ | 0.13 | 0.17 | 0.11 | 0.63 | 0.29 | 0.68 | 1.37 | 0.57 |
| $Cr_2O_3$ | 0.01 | 0.01 | 0.00 | 0.02 | 0.02 | 0.00 | 0.03 | 0.03 |
| FeOtotal | 2.75 | 2.91 | 2.56 | 2.51 | 2.89 | 2.75 | 3.78 | 3.03 |
| NiO | - | - | - | - | - | - | 0.02 | 0.16 |
| MnO | 0.62 | 0.68 | 0.63 | 0.58 | 0.72 | 0.49 | 0.70 | 0.58 |
| MgO | 16.39 | 16.40 | 16.71 | 16.56 | 16.33 | 16.43 | 15.43 | 16.35 |
| CaO | 26.29 | 26.03 | 26.26 | 25.94 | 25.85 | 26.06 | 26.23 | 26.03 |
| $Na_2O$ | 0.01 | 0.00 | 0.01 | 0.04 | 0.03 | 0.03 | 0.01 | 0.03 |
| $K_2O$ | - | - | - | - | - | - | 0.02 | 0.00 |
| $P_2O_5$ | - | - | - | - | - | - | 0.41 | 0.40 |
| S | - | - | - | - | - | - | 0.02 | 0.00 |
| Cl | - | - | - | - | - | - | 0.00 | 0.01 |
| Total | 100.30 | 100.03 | 100.33 | 100.47 | 99.95 | 100.03 | 100.72 | 100.87 |
| | | | | Cation allocation based on six oxygen atoms | | | | |
| Si IV | 1.97 | 1.97 | 1.97 | 1.97 | 1.97 | 1.95 | 1.93 | 1.96 |
| Al IV | 0.01 | 0.01 | 0.01 | 0.03 | 0.01 | 0.03 | 0.06 | 0.02 |
| T site | 1.98 | 1.98 | 1.98 | 2.00 | 1.98 | 1.98 | 1.99 | 1.98 |
| Al VI | 0.00 | 0.00 | 0.00 | 0.00 | 0.00 | 0.00 | 0.00 | 0.00 |
| Ti | 0.00 | 0.00 | 0.00 | 0.00 | 0.00 | 0.00 | 0.00 | 0.00 |
| Cr | 0.00 | 0.00 | 0.00 | 0.00 | 0.00 | 0.00 | 0.00 | 0.00 |
| $Fe^{+3}$ | 0.05 | 0.06 | 0.06 | 0.04 | 0.05 | 0.06 | 0.08 | 0.06 |
| $Fe^{+2}$ | 0.04 | 0.03 | 0.02 | 0.04 | 0.04 | 0.02 | 0.04 | 0.03 |
| $Mn^{+2}$ | 0.02 | 0.02 | 0.02 | 0.02 | 0.02 | 0.02 | 0.02 | 0.02 |
| Ni | 0.00 | 0.00 | 0.00 | 0.00 | 0.00 | 0.00 | 0.00 | 0.00 |
| Mg | 0.89 | 0.89 | 0.91 | 0.90 | 0.89 | 0.89 | 0.84 | 0.89 |
| Ca | 1.03 | 1.02 | 1.02 | 1.01 | 1.01 | 1.02 | 1.03 | 1.02 |
| Na | 0.00 | 0.00 | 0.00 | 0.00 | 0.00 | 0.00 | 0.00 | 0.00 |
| K | - | - | - | - | - | - | 0.00 | 0.00 |
| M1,M2 | 2.03 | 2.02 | 2.03 | 2.01 | 2.01 | 2.01 | 2.01 | 2.02 |
| Mn/Fe | 0.22 | 0.22 | 0.25 | 0.25 | 0.22 | 0.25 | 0.17 | 0.22 |
| | | | | Clinopyroxene components (mole fraction) | | | | |
| Di | 0.95 | 0.95 | 0.96 | 0.94 | 0.94 | 0.96 | 0.968085 | 0.95 |
| Hd | 0.03 | 0.03 | 0.02 | 0.04 | 0.04 | 0.02 | 0.010638 | 0.03 |
| Jo | 0.02 | 0.02 | 0.02 | 0.02 | 0.02 | 0.02 | 0.02 | 0.02 |

**S. No.:** sample number; **An. No.:** serial number of analysis
**Di:** diopside
**Hd:** hedenbergite
**Jo:** Johannsenite

## APPENDIX IV. Continued.

**Clinopyroxene**

| S. No. | S19 | S19 | S37 | S37 | S37 | S37 | S199 | S199 |
|---|---|---|---|---|---|---|---|---|
| An. No. | 2 | 4 | 2 | 3 | 4 | 5 | 2 | 3 |
| | | | Oxide composition (wt. %) | | | | | |
| $SiO_2$ | 52.90 | 53.62 | 53.50 | 51.46 | 51.30 | 52.04 | 52.03 | 52.40 |
| $TiO_2$ | 0.03 | 0.00 | 0.04 | 0.03 | 0.10 | 0.02 | 0.04 | 0.06 |
| $Al_2O_3$ | 0.45 | 0.98 | 0.44 | 1.50 | 1.89 | 1.12 | 1.41 | 1.53 |
| $Cr_2O_3$ | 0.00 | 0.06 | 0.09 | 0.00 | 0.04 | 0.00 | 0.04 | 0.00 |
| FeOtotal | 5.41 | 2.76 | 3.01 | 7.68 | 6.86 | 6.14 | 4.61 | 4.74 |
| NiO | 0.00 | 0.02 | 0.00 | 0.00 | 0.00 | 0.07 | 0.00 | 0.00 |
| MnO | 0.54 | 0.54 | 0.17 | 1.15 | 0.81 | 0.92 | 0.76 | 0.71 |
| MgO | 14.85 | 16.71 | 16.78 | 13.22 | 13.56 | 14.34 | 15.30 | 14.94 |
| CaO | 26.04 | 25.92 | 25.98 | 25.53 | 25.62 | 25.57 | 25.78 | 26.65 |
| $Na_2O$ | 0.01 | 0.01 | 0.08 | 0.03 | 0.02 | 0.02 | 0.02 | 0.01 |
| $K_2O$ | 0.01 | 0.00 | 0.01 | 0.00 | 0.00 | 0.01 | 0.00 | 0.00 |
| $P_2O_5$ | 0.41 | 0.43 | 0.52 | 0.37 | 0.53 | 0.45 | 0.00 | 0.00 |
| S | 0.00 | 0.00 | 0.00 | 0.06 | 0.00 | 0.04 | 0.00 | 0.00 |
| Cl | 0.01 | 0.00 | 0.06 | 0.06 | 0.00 | 0.00 | 0.00 | 0.00 |
| Total | 100.65 | 101.04 | 100.66 | 101.08 | 100.73 | 100.75 | 99.99 | 101.04 |
| | | | Cation allocation based on six oxygen atoms | | | | | |
| Si IV | 1.95 | 1.95 | 1.95 | 1.91 | 1.91 | 1.93 | 1.91 | 1.93 |
| Al IV | 0.02 | 0.04 | 0.02 | 0.07 | 0.08 | 0.05 | 0.06 | 0.07 |
| T site | 1.97 | 1.99 | 1.97 | 1.98 | 1.99 | 1.98 | 1.97 | 2.00 |
| Al VI | 0.00 | 0.00 | 0.00 | 0.00 | 0.00 | 0.00 | 0.00 | 0.00 |
| Ti | 0.00 | 0.00 | 0.00 | 0.00 | 0.00 | 0.00 | 0.00 | 0.00 |
| Cr | 0.00 | 0.00 | 0.00 | 0.00 | 0.00 | 0.00 | 0.00 | 0.00 |
| $Fe^{+3}$ | 0.07 | 0.07 | 0.08 | 0.11 | 0.10 | 0.10 | 0.11 | 0.07 |
| $Fe^{+2}$ | 0.05 | 0.02 | 0.01 | 0.12 | 0.11 | 0.09 | 0.03 | 0.08 |
| $Mn^{+2}$ | 0.02 | 0.02 | 0.01 | 0.04 | 0.03 | 0.03 | 0.02 | 0.02 |
| Ni | 0.00 | 0.00 | 0.00 | 0.00 | 0.00 | 0.00 | 0.00 | 0.00 |
| Mg | 0.86 | 0.90 | 0.91 | 0.73 | 0.75 | 0.79 | 0.84 | 0.82 |
| Ca | 1.03 | 1.01 | 1.02 | 1.01 | 1.02 | 1.01 | 1.02 | 1.01 |
| Na | 0.00 | 0.00 | 0.01 | 0.00 | 0.00 | 0.00 | 0.00 | 0.00 |
| K | 0.00 | 0.00 | 0.00 | 0.00 | 0.00 | 0.00 | 0.00 | 0.00 |
| M1,M2 | 2.03 | 2.02 | 2.04 | 2.01 | 2.01 | 2.02 | 2.02 | 2.00 |
| Mn/Fe | 0.17 | 0.22 | 0.11 | 0.17 | 0.14 | 0.16 | 0.14 | 0.13 |
| | | | Clinopyroxene components (mole fraction) | | | | | |
| Di | 0.98 | 0.82 | 0.84 | 0.87 | 0.92 | 0.96 | 0.94 | 0.90 |
| Hd | 0.01 | 0.13 | 0.12 | 0.10 | 0.05 | 0.02 | 0.03 | 0.08 |
| Jo | 0.01 | 0.04 | 0.03 | 0.03 | 0.02 | 0.02 | 0.02 | 0.02 |

**S. No.:** sample number; **An. No.:** serial number of analysis
**Di:** diopside
**Hd:** hedenbergite
**Jo:** Johannsenite

## APPENDIX IV. Continued.

**Garnet**

| S. No. | S8 | S8 | S8 | S8 | S8 | S8 | S8 | S8 | S8 | S8 |
|---|---|---|---|---|---|---|---|---|---|---|
| An. No. | A1 | A2 | A3 | A4 | A5 | A6 | A7 | A8 | A9 | A10 |
| | | | | | Oxide composition (wt. %) | | | | | |
| $SiO_2$ | 35.94 | 35.58 | 35.62 | 35.37 | 33.48 | 35.49 | 34.42 | 27.60 | 35.51 | 35.41 |
| $TiO_2$ | 0.09 | 0.09 | 0.10 | 0.13 | 0.13 | 0.12 | 0.10 | 0.17 | 0.16 | 0.16 |
| $Al_2O_3$ | 4.94 | 4.90 | 4.66 | 4.52 | 5.21 | 4.61 | 4.65 | 4.51 | 4.71 | 4.36 |
| $SnO_2$ | 0.23 | 0.25 | 0.20 | 0.15 | 0.13 | 0.21 | 0.12 | 0.13 | 0.15 | 0.11 |
| $Cr_2O_3$ | 0.00 | 0.00 | 0.00 | 0.00 | 0.00 | 0.00 | 0.00 | 0.00 | 0.00 | 0.00 |
| $Fe_2O_3$ | 24.66 | 24.91 | 25.31 | 25.37 | 23.57 | 25.31 | 25.16 | 23.15 | 25.05 | 25.69 |
| FeO | 0.00 | 0.00 | 0.00 | 0.00 | 0.00 | 0.00 | 0.00 | 0.00 | 0.00 | 0.00 |
| MnO | 0.58 | 0.53 | 0.51 | 0.44 | 0.46 | 0.48 | 0.49 | 0.48 | 0.47 | 0.49 |
| MgO | 0.12 | 0.11 | 0.10 | 0.10 | 0.15 | 0.12 | 0.10 | 0.14 | 0.13 | 0.12 |
| CaO | 33.94 | 33.92 | 34.30 | 34.16 | 33.32 | 34.02 | 33.98 | 29.78 | 34.20 | 34.17 |
| Total | 100.27 | 100.04 | 100.60 | 100.09 | 96.32 | 100.15 | 98.90 | 85.83 | 100.23 | 100.40 |
| | | | | | Cation allocation based on 24 oxygen | | | | | |
| Si IV | 5.91 | 5.86 | 5.85 | 5.84 | 5.72 | 5.85 | 5.75 | 5.33 | 5.85 | 5.83 |
| Al IV | 0.09 | 0.14 | 0.15 | 0.16 | 0.28 | 0.15 | 0.25 | 0.67 | 0.15 | 0.17 |
| Sn | | | | | | | | | | |
| T site | 6.00 | 6.00 | 6.00 | 6.00 | 6.00 | 6.00 | 6.00 | 6.00 | 6.00 | 6.00 |
| Al VI | 0.86 | 0.82 | 0.75 | 0.72 | 0.77 | 0.75 | 0.67 | 0.36 | 0.76 | 0.68 |
| Ti VI | 0.01 | 0.01 | 0.01 | 0.02 | 0.02 | 0.01 | 0.01 | 0.02 | 0.02 | 0.02 |
| Cr | 0.00 | 0.00 | 0.00 | 0.00 | 0.00 | 0.00 | 0.00 | 0.00 | 0.00 | 0.00 |
| $Fe^{+3}$ | 3.04 | 3.08 | 3.11 | 3.14 | 3.01 | 3.13 | 3.14 | 3.34 | 3.09 | 3.17 |
| O site | 4.00 | 4.00 | 4.00 | 4.00 | 4.00 | 4.00 | 4.00 | 4.00 | 4.00 | 4.00 |
| $Fe^{+2}$ | 0.00 | 0.00 | 0.00 | 0.00 | 0.00 | 0.00 | 0.00 | 0.00 | 0.00 | 0.00 |
| $Mn^{+2}$ | 0.08 | 0.07 | 0.07 | 0.06 | 0.07 | 0.07 | 0.07 | 0.08 | 0.07 | 0.07 |
| Mg | 0.03 | 0.03 | 0.02 | 0.02 | 0.04 | 0.03 | 0.02 | 0.04 | 0.03 | 0.03 |
| Ca | 5.98 | 5.99 | 6.03 | 6.04 | 6.10 | 6.01 | 6.08 | 6.16 | 6.03 | 6.03 |
| A site | 6.00 | 6.00 | 6.00 | 6.00 | 6.00 | 6.00 | 6.00 | 6.00 | 6.00 | 6.00 |
| O | 23.96 | 23.94 | 23.93 | 23.93 | 23.87 | 23.93 | 23.88 | 23.68 | 23.93 | 23.93 |
| | | | | | Garnet components in mole fraction | | | | | |
| sp | 0.01 | 0.01 | 0.01 | 0.01 | 0.01 | 0.01 | 0.01 | 0.01 | 0.01 | 0.01 |
| al | 0.00 | 0.00 | 0.00 | 0.00 | 0.00 | 0.00 | 0.00 | 0.00 | 0.00 | 0.00 |
| py | 0.01 | 0.01 | 0.00 | 0.00 | 0.01 | 0.01 | 0.00 | 0.01 | 0.01 | 0.01 |
| gr | 0.20 | 0.19 | 0.17 | 0.17 | 0.17 | 0.17 | 0.15 | 0.07 | 0.17 | 0.15 |
| an | 0.76 | 0.77 | 0.78 | 0.79 | 0.75 | 0.78 | 0.79 | 0.84 | 0.77 | 0.79 |
| sp+al+py | 0.02 | 0.02 | 0.02 | 0.01 | 0.02 | 0.02 | 0.02 | 0.02 | 0.02 | 0.02 |

**sp:** spessartine, **al:** almandine, **py:** pyrope, **gr:** grossular, **an:** andradite.

## APPENDIX IV. Continued.

**Garnet**

| S. No. | S8 | S8 | S10 | S10 | S10 | S10 | S10 | S10 | S10 | S10 |
|---|---|---|---|---|---|---|---|---|---|---|
| An. No. | A11 | A12 | 1 | 2 | 3 | 4 | 5 | 6 | 7 | 8 |
| | | | | | Oxide composition (wt. %) | | | | | |
| $SiO_2$ | 35.16 | 35.55 | 35.62 | 35.64 | 35.96 | 35.84 | 35.60 | 35.44 | 36.07 | 35.90 |
| $TiO_2$ | 0.11 | 0.07 | 0.03 | 0.00 | 0.19 | 0.33 | 1.14 | 0.25 | 0.27 | 0.26 |
| $Al_2O_3$ | 4.05 | 4.80 | 5.23 | 5.08 | 5.99 | 4.14 | 5.84 | 4.76 | 5.64 | 5.40 |
| $SnO_2$ | 0.11 | 0.21 | - | - | - | - | - | - | - | - |
| $Cr_2O_3$ | 0.00 | 0.00 | 0.00 | 0.00 | 0.03 | 0.00 | 0.02 | 0.09 | 0.00 | 0.00 |
| $Fe_2O_3$ | 25.67 | 25.47 | 25.20 | 25.49 | 24.11 | 25.29 | 23.30 | 25.97 | 24.02 | 24.33 |
| FeO | 0.00 | 0.00 | 0.00 | 0.00 | 0.00 | 0.00 | 0.00 | 0.00 | 0.00 | 0.00 |
| MnO | 0.40 | 0.62 | 0.72 | 0.56 | 1.08 | 0.60 | 0.62 | 0.59 | 0.71 | 0.61 |
| MgO | 0.11 | 0.07 | 0.09 | 0.05 | 0.07 | 0.14 | 0.27 | 0.07 | 0.12 | 0.06 |
| CaO | 34.39 | 33.88 | 33.80 | 34.05 | 33.66 | 33.50 | 33.96 | 34.05 | 33.84 | 33.94 |
| Total | 99.89 | 100.46 | 100.69 | 100.87 | 101.09 | 99.84 | 100.75 | 101.22 | 100.67 | 100.50 |
| | | | | | Cation allocation based on 24 oxygen | | | | | |
| Si IV | 5.83 | 5.84 | 5.86 | 5.86 | 5.86 | 5.97 | 5.85 | 5.82 | 5.91 | 5.91 |
| Al IV | 0.17 | 0.16 | 0.14 | 0.14 | 0.14 | 0.03 | 0.15 | 0.18 | 0.09 | 0.09 |
| Sn | | | | | | | | | | |
| T site | 6.00 | 6.00 | 6.00 | 6.00 | 6.00 | 6.00 | 6.00 | 6.00 | 6.00 | 6.00 |
| Al VI | 0.62 | 0.78 | 0.88 | 0.85 | 1.01 | 0.79 | 0.98 | 0.75 | 1.00 | 0.95 |
| Ti VI | 0.01 | 0.01 | 0.00 | - | 0.02 | 0.04 | 0.14 | 0.03 | 0.03 | 0.03 |
| Cr | 0.00 | 0.00 | - | - | 0.00 | 0.00 | 0.00 | 0.01 | - | - |
| $Fe^{+3}$ | 3.18 | 3.14 | 3.12 | 3.15 | 2.96 | 3.17 | 2.88 | 3.21 | 2.96 | 3.01 |
| O site | 4.00 | 4.00 | 4.00 | 4.00 | 4.00 | 4.00 | 4.00 | 4.00 | 4.00 | 4.00 |
| $Fe^{+2}$ | 0.00 | 0.00 | 0.00 | 0.00 | 0.00 | 0.00 | 0.00 | 0.00 | 0.00 | 0.00 |
| $Mn^{+2}$ | 0.06 | 0.09 | 0.10 | 0.08 | 0.15 | 0.08 | 0.09 | 0.08 | 0.10 | 0.09 |
| Mg | 0.03 | 0.02 | 0.02 | 0.01 | 0.02 | 0.03 | 0.07 | 0.02 | 0.03 | 0.02 |
| Ca | 6.11 | 5.97 | 5.96 | 6.00 | 5.88 | 5.98 | 5.98 | 5.99 | 5.94 | 5.98 |
| A site | 6.00 | 6.00 | 6.00 | 6.00 | 6.00 | 6.00 | 6.00 | 6.00 | 6.00 | 6.00 |
| O | 23.92 | 23.93 | 23.93 | 23.93 | 23.94 | 24.01 | 23.99 | 23.93 | 23.97 | 23.97 |
| | | | | | Garnet components in mole fraction | | | | | |
| sp | 0.01 | 0.02 | 0.02 | 0.01 | 0.03 | 0.01 | 0.02 | 0.01 | 0.02 | 0.02 |
| al | 0.00 | 0.00 | 0.00 | 0.00 | 0.00 | 0.00 | 0.00 | 0.00 | 0.00 | 0.00 |
| py | 0.01 | 0.00 | 0.00 | 0.00 | 0.00 | 0.01 | 0.01 | 0.00 | 0.01 | 0.00 |
| gr | 0.14 | 0.18 | 0.20 | 0.20 | 0.22 | 0.18 | 0.22 | 0.17 | 0.23 | 0.22 |
| an | 0.80 | 0.79 | 0.78 | 0.79 | 0.74 | 0.79 | 0.72 | 0.80 | 0.74 | 0.75 |
| sp+al+py | 0.02 | 0.02 | 0.02 | 0.02 | 0.03 | 0.02 | 0.03 | 0.02 | 0.02 | 0.02 |

**sp:** spessartine, **al:** almandine, **py:** pyrope, **gr:** grossular, **an:** andradite.

## APPENDIX IV. Continued.

Garnet

| S. No. | S10 | S10 | S11 | S11 | S11 | S11 | S11 | S11 | S11 | S11 |
|---|---|---|---|---|---|---|---|---|---|---|
| An. No. | 9 | 10 | 1 | 2 | 3 | 4 | 5 | 6 | 7 | 8 |
| | | | | | Oxide composition (wt. %) | | | | | |
| $SiO_2$ | 36.02 | 35.91 | 35.85 | 35.84 | 35.35 | 34.71 | 35.63 | 35.13 | 35.57 | 35.57 |
| $TiO_2$ | 0.02 | 0.00 | 0.23 | 0.20 | 0.24 | 0.15 | 0.21 | 0.13 | 0.18 | 0.24 |
| $Al_2O_3$ | 4.60 | 4.81 | 6.74 | 6.50 | 6.45 | 5.50 | 7.06 | 4.81 | 6.01 | 6.01 |
| $SnO_2$ | - | - | - | - | - | - | - | - | - | - |
| $Cr_2O_3$ | 0.00 | 0.00 | 0.00 | 0.00 | 0.00 | 0.00 | 0.00 | 0.00 | 0.00 | - |
| $Fe_2O_3$ | 26.29 | 25.53 | 23.21 | 23.67 | 23.65 | 25.67 | 22.95 | 26.32 | 24.46 | 24.04 |
| FeO | 0.00 | 0.00 | 0.00 | 0.27 | 0.00 | 0.00 | 0.00 | 0.00 | 0.00 | -1.00 |
| MnO | 0.60 | 0.55 | 0.64 | 0.83 | 0.57 | 0.88 | 0.81 | 0.78 | 0.45 | 0.47 |
| MgO | 0.03 | 0.00 | 0.17 | 0.04 | 0.11 | 0.06 | 0.09 | 0.00 | 0.14 | 0.13 |
| CaO | 33.93 | 33.76 | 34.12 | 33.50 | 33.94 | 33.68 | 33.68 | 33.89 | 34.13 | 34.50 |
| Total | 101.49 | 100.56 | 100.96 | 100.85 | 100.31 | 100.65 | 100.43 | 101.06 | 100.94 | 99.77 |
| | | | | | Cation allocation based on 24 oxygen | | | | | |
| Si IV | 5.88 | 5.91 | 5.84 | 5.83 | 5.80 | 5.73 | 5.80 | 5.79 | 5.81 | 5.84 |
| Al IV | 0.12 | 0.09 | 0.16 | 0.17 | 0.20 | 0.27 | 0.20 | 0.21 | 0.19 | 0.16 |
| Sn | | | | | | | | | | |
| T site | 6.00 | 6.00 | 6.00 | 6.00 | 6.00 | 6.00 | 6.00 | 6.00 | 6.00 | 6.00 |
| Al VI | 0.77 | 0.84 | 1.13 | 1.08 | 1.05 | 0.80 | 1.16 | 0.72 | 0.97 | 1.00 |
| Ti VI | 0.00 | - | 0.03 | 0.02 | 0.03 | 0.02 | 0.03 | 0.02 | 0.02 | 0.03 |
| Cr | 0.00 | - | - | - | - | - | - | - | - | - |
| $Fe^{+3}$ | 3.23 | 3.16 | 2.84 | 2.90 | 2.92 | 3.19 | 2.81 | 3.26 | 3.01 | 2.97 |
| O site | 4.00 | 4.00 | 4.00 | 4.00 | 4.00 | 4.00 | 4.00 | 4.00 | 4.00 | 4.00 |
| $Fe^{+2}$ | 0.00 | 0.00 | 0.00 | 0.00 | 0.00 | 0.00 | 0.00 | 0.00 | 0.00 | 0.00 |
| $Mn^{+2}$ | 0.08 | 0.08 | 0.09 | 0.11 | 0.08 | 0.12 | 0.11 | 0.11 | 0.06 | 0.07 |
| Mg | 0.01 | 0.00 | 0.04 | 0.01 | 0.03 | 0.01 | 0.02 | 0.00 | 0.03 | 0.03 |
| Ca | 5.94 | 5.95 | 5.95 | 5.84 | 5.97 | 5.95 | 5.88 | 5.98 | 5.98 | 6.07 |
| A site | 6.00 | 6.00 | 6.00 | 6.00 | 6.00 | 6.00 | 6.00 | 6.00 | 6.00 | 6.00 |
| O | 23.94 | 23.95 | 23.93 | 23.93 | 23.92 | 23.87 | 23.92 | 23.90 | 23.92 | 23.93 |
| | | | | | Garnet component in mole fraction | | | | | |
| sp | 0.01 | 0.01 | 0.02 | 0.02 | 0.01 | 0.02 | 0.02 | 0.02 | 0.01 | 0.01 |
| al | 0.00 | 0.00 | 0.00 | 0.00 | 0.00 | 0.00 | 0.00 | 0.00 | 0.00 | 0.00 |
| py | 0.00 | 0.00 | 0.01 | 0.00 | 0.01 | 0.00 | 0.00 | 0.00 | 0.01 | 0.01 |
| gr | 0.18 | 0.20 | 0.26 | 0.25 | 0.24 | 0.18 | 0.27 | 0.16 | 0.23 | 0.23 |
| an | 0.81 | 0.79 | 0.71 | 0.73 | 0.73 | 0.80 | 0.70 | 0.82 | 0.75 | 0.74 |
| sp+al+py | 0.02 | 0.01 | 0.02 | 0.02 | 0.02 | 0.02 | 0.02 | 0.02 | 0.02 | 0.02 |

**sp:** spessartine, **al:** almandine, **py:** pyrope, **gr:** grossular, **an:** andradite.

**APPENDIX IV. Continued.**

**Garnet**

| S. No. | S11 | S11 | S11 | S16 | S16 | S18B | S18B | S19 | S19 | S19 |
|---|---|---|---|---|---|---|---|---|---|---|
| An. No. | 9 | 10 | 11 | 1 | 2 | 1 | 2 | 1 | 2 | 3 |
| | | | | Oxide composition (wt. %) | | | | | | |
| $SiO_2$ | 35.86 | 35.60 | 35.98 | 35.81 | 35.75 | 36.12 | 36.07 | 36.19 | 36.19 | 36.50 |
| $TiO_2$ | 0.38 | 0.24 | 0.24 | 0.21 | 0.19 | 0.20 | 0.22 | 0.38 | 0.26 | 0.22 |
| $Al_2O_3$ | 7.63 | 6.90 | 7.34 | 4.06 | 4.37 | 6.46 | 6.92 | 7.19 | 6.83 | 7.26 |
| $SnO_2$ | - | - | - | - | - | - | - | 0.08 | 0.11 | 0.08 |
| $Cr_2O_3$ | - | - | - | - | - | - | - | - | - | - |
| $Fe_2O_3$ | 22.03 | 23.35 | 22.73 | 26.55 | 26.02 | 23.34 | 22.37 | 22.12 | 22.77 | 22.44 |
| FeO | -0.80 | -0.70 | -0.90 | -1.00 | -0.80 | 0.00 | 0.00 | 0.00 | 0.00 | 0.00 |
| MnO | 0.35 | 0.96 | 0.41 | 0.43 | 0.40 | 0.95 | 1.09 | 0.87 | 0.76 | 0.84 |
| MgO | 0.19 | 0.07 | 0.16 | 0.11 | 0.11 | 0.14 | 0.11 | 0.09 | 0.08 | 0.11 |
| CaO | 34.61 | 34.15 | 34.82 | 34.28 | 34.12 | 34.14 | 33.98 | 33.89 | 34.20 | 34.16 |
| Total | 100.30 | 100.54 | 100.79 | 100.48 | 100.14 | 100.49 | 99.85 | 100.47 | 100.54 | 101.28 |
| | | | | Cation allocation based on 24 oxygen | | | | | | |
| Si IV | 5.81 | 5.79 | 5.81 | 5.90 | 5.90 | 5.88 | 5.89 | 5.88 | 5.88 | 5.88 |
| Al IV | 0.19 | 0.21 | 0.19 | 0.10 | 0.10 | 0.12 | 0.11 | 0.12 | 0.12 | 0.12 |
| Sn | | | | | | | | | | |
| T site | 6.00 | 6.00 | 6.00 | 6.00 | 6.00 | 6.00 | 6.00 | 6.00 | 6.00 | 6.00 |
| Al VI | 1.27 | 1.11 | 1.21 | 0.68 | 0.75 | 1.12 | 1.22 | 1.25 | 1.18 | 1.25 |
| Ti VI | 0.05 | 0.03 | 0.03 | 0.03 | 0.02 | 0.02 | 0.03 | 0.05 | 0.03 | 0.03 |
| Cr | - | - | - | - | - | - | - | - | - | - |
| $Fe^{+3}$ | 2.69 | 2.86 | 2.76 | 3.29 | 3.23 | 2.86 | 2.75 | 2.70 | 2.78 | 2.72 |
| O site | 4.00 | 4.00 | 4.00 | 4.00 | 4.00 | 4.00 | 4.00 | 4.00 | 4.00 | 4.00 |
| $Fe^{+2}$ | 0.00 | 0.00 | 0.00 | 0.00 | 0.00 | 0.00 | 0.00 | 0.00 | 0.00 | 0.00 |
| $Mn^{+2}$ | 0.05 | 0.13 | 0.06 | 0.06 | 0.06 | 0.13 | 0.15 | 0.12 | 0.10 | 0.11 |
| Mg | 0.05 | 0.02 | 0.04 | 0.03 | 0.03 | 0.03 | 0.03 | 0.02 | 0.02 | 0.03 |
| Ca | 6.01 | 5.95 | 6.03 | 6.05 | 6.03 | 5.95 | 5.95 | 5.89 | 5.95 | 5.89 |
| A site | 6.00 | 6.00 | 6.00 | 6.00 | 6.00 | 6.00 | 6.00 | 6.00 | 6.00 | 6.00 |
| O | 23.93 | 23.91 | 23.92 | 23.96 | 23.96 | 23.95 | 23.96 | 23.96 | 23.95 | 23.95 |
| | | | | Garnet components in mole fraction | | | | | | |
| sp | 0.01 | 0.02 | 0.01 | 0.01 | 0.01 | 0.02 | 0.03 | 0.02 | 0.02 | 0.02 |
| al | 0.00 | 0.00 | 0.00 | 0.00 | 0.00 | 0.00 | 0.00 | 0.00 | 0.00 | 0.00 |
| py | 0.01 | 0.00 | 0.01 | 0.01 | 0.01 | 0.01 | 0.01 | 0.00 | 0.00 | 0.01 |
| gr | 0.30 | 0.25 | 0.29 | 0.16 | 0.17 | 0.25 | 0.28 | 0.29 | 0.28 | 0.29 |
| an | 0.67 | 0.72 | 0.69 | 0.82 | 0.81 | 0.72 | 0.69 | 0.68 | 0.70 | 0.68 |
| sp+al+py | 0.02 | 0.03 | 0.02 | 0.02 | 0.02 | 0.03 | 0.03 | 0.02 | 0.02 | 0.02 |

**sp:** spessartine, **al:** almandine, **py:** pyrope, **gr:** grossular, **an:** andradite.

## APPENDIX IV. Continued.

**Garnet**

| S. No. | S19 | S19 | S19 | S19 | S19 | S19 | S19 | S19 | S32 | S32 |
|---|---|---|---|---|---|---|---|---|---|---|
| An. No. | 4 | 5 | 6 | 7 | 8 | 9 | 10 | 11 | 1 | 2 |
| | | | | | Oxide composition (wt. %) | | | | | |
| $SiO_2$ | 36.60 | 33.79 | 35.30 | 36.36 | 36.17 | 35.95 | 36.22 | 35.93 | 36.58 | 36.53 |
| $TiO_2$ | 0.27 | 0.20 | 0.10 | 0.25 | 0.22 | 0.23 | 0.23 | 0.21 | 0.35 | 0.31 |
| $Al_2O_3$ | 6.83 | 6.64 | 5.47 | 7.22 | 7.56 | 7.18 | 7.60 | 6.98 | 7.46 | 7.84 |
| $SnO_2$ | 0.04 | 0.13 | 0.38 | 0.15 | 0.10 | 0.07 | 0.12 | 0.10 | - | - |
| $Cr_2O_3$ | 0.00 | 0.00 | 0.00 | 0.00 | 0.10 | 0.00 | 0.00 | 0.00 | 0.00 | 0.00 |
| $Fe_2O_3$ | 22.34 | 24.64 | 24.96 | 22.10 | 21.60 | 22.37 | 21.89 | 22.97 | 21.10 | 20.97 |
| FeO | 0.00 | 0.00 | 0.00 | 0.00 | 0.58 | 0.00 | 0.00 | 0.00 | 0.00 | 0.00 |
| MnO | 0.68 | 0.81 | 0.95 | 0.86 | 1.05 | 0.76 | 0.78 | 0.70 | 0.80 | 0.88 |
| MgO | 0.16 | 0.01 | 0.06 | 0.18 | 0.10 | 0.13 | 0.25 | 0.08 | 0.21 | 0.16 |
| CaO | 33.96 | 34.66 | 33.51 | 34.03 | 33.02 | 34.06 | 34.02 | 34.45 | 34.41 | 34.19 |
| Total | 100.60 | 98.78 | 99.83 | 100.47 | 100.30 | 100.68 | 100.99 | 101.32 | 100.91 | 100.88 |
| | | | | | Cation allocation based on 24 oxygen | | | | | |
| Si IV | 5.94 | 5.60 | 5.82 | 5.89 | 5.88 | 5.85 | 5.86 | 5.83 | 5.89 | 5.88 |
| Al IV | 0.06 | 0.40 | 0.18 | 0.11 | 0.12 | 0.15 | 0.14 | 0.17 | 0.11 | 0.12 |
| Sn | | | | | | | | | | |
| T site | 6.00 | 6.00 | 6.00 | 6.00 | 6.00 | 6.00 | 6.00 | 6.00 | 6.00 | 6.00 |
| Al VI | 1.24 | 0.90 | 0.89 | 1.27 | 1.33 | 1.23 | 1.31 | 1.17 | 1.31 | 1.37 |
| Ti VI | 0.03 | 0.02 | 0.01 | 0.03 | 0.03 | 0.03 | 0.03 | 0.03 | 0.04 | 0.04 |
| Cr | - | - | - | - | - | - | - | - | 0.00 | 0.00 |
| $Fe^{+3}$ | 2.73 | 3.07 | 3.10 | 2.70 | 2.64 | 2.74 | 2.66 | 2.81 | 2.55 | 2.54 |
| O site | 4.00 | 4.00 | 4.00 | 4.00 | 4.00 | 4.00 | 4.00 | 4.00 | 4.00 | 4.00 |
| $Fe^{+2}$ | 0.00 | 0.00 | 0.00 | 0.00 | 0.08 | 0.00 | 0.00 | 0.00 | 0.00 | 0.00 |
| $Mn^{+2}$ | 0.09 | 0.11 | 0.13 | 0.12 | 0.14 | 0.10 | 0.11 | 0.10 | 0.11 | 0.12 |
| Mg | 0.04 | 0.00 | 0.01 | 0.04 | 0.02 | 0.03 | 0.06 | 0.02 | 0.05 | 0.04 |
| Ca | 5.90 | 6.16 | 5.92 | 5.91 | 5.75 | 5.94 | 5.90 | 5.99 | 5.94 | 5.90 |
| A site | 6.00 | 6.00 | 6.00 | 6.00 | 6.00 | 6.00 | 6.00 | 6.00 | 6.00 | 6.00 |
| O | 23.98 | 23.81 | 23.92 | 23.96 | 23.95 | 23.94 | 23.94 | 23.93 | 23.97 | 23.96 |
| | | | | | Garnet components in mole fraction | | | | | |
| sp | 0.02 | 0.02 | 0.02 | 0.02 | 0.02 | 0.02 | 0.02 | 0.02 | 0.02 | 0.02 |
| al | 0.00 | 0.00 | 0.00 | 0.00 | 0.01 | 0.00 | 0.00 | 0.00 | 0.00 | 0.00 |
| py | 0.01 | 0.00 | 0.00 | 0.01 | 0.00 | 0.01 | 0.01 | 0.00 | 0.01 | 0.01 |
| gr | 0.29 | 0.21 | 0.20 | 0.29 | 0.29 | 0.29 | 0.30 | 0.27 | 0.30 | 0.32 |
| an | 0.68 | 0.77 | 0.78 | 0.68 | 0.66 | 0.69 | 0.67 | 0.70 | 0.64 | 0.64 |
| sp+al+py | 0.02 | 0.02 | 0.02 | 0.03 | 0.04 | 0.02 | 0.03 | 0.02 | 0.03 | 0.03 |

**sp:** spessartine, **al:** almandine, **py:** pyrope, **gr:** grossular, **an:** andradite.

## APPENDIX IV. Continued.

**Garnet**

| S. No. | S32 | S32 | S35 | S35 | S35 | S35 | S35 | S35 | S35 | S35 |
|---|---|---|---|---|---|---|---|---|---|---|
| An. No. | 7 | 8 | 1 | 2 | 3 | 4 | 5 | 6 | 7 | 8 |
| | | | | | Oxide composition (wt. %) | | | | | |
| $SiO_2$ | 35.99 | 36.20 | 35.91 | 35.90 | 35.44 | 35.51 | 35.80 | 35.72 | 33.96 | 33.99 |
| $TiO_2$ | 0.33 | 0.37 | 0.22 | 0.17 | 0.28 | 0.24 | 0.22 | 0.18 | 0.01 | 0.02 |
| $Al_2O_3$ | 6.33 | 6.38 | 4.26 | 4.51 | 5.06 | 4.83 | 4.68 | 5.18 | 0.17 | 0.20 |
| $SnO_2$ | - | - | 0.24 | 0.27 | 0.34 | 0.24 | 0.37 | 0.28 | 0.04 | 0.01 |
| $Cr_2O_3$ | 0.00 | 0.00 | - | - | - | - | - | - | - | - |
| $Fe_2O_3$ | 22.87 | 22.50 | 26.29 | 26.16 | 25.82 | 25.40 | 25.95 | 25.32 | 31.53 | 31.48 |
| FeO | 0.00 | 0.00 | -0.70 | -0.70 | -1.00 | -0.80 | 0.00 | 0.00 | 0.00 | 0.00 |
| MnO | 0.53 | 0.60 | 0.47 | 0.47 | 0.63 | 0.62 | 0.55 | 0.59 | 0.97 | 0.70 |
| MgO | 0.17 | 0.23 | 0.13 | 0.17 | 0.12 | 0.11 | 0.15 | 0.16 | 0.06 | 0.02 |
| CaO | 34.59 | 34.14 | 34.11 | 34.10 | 34.40 | 33.89 | 34.42 | 34.19 | 33.75 | 33.86 |
| Total | 100.81 | 100.42 | 100.66 | 100.80 | 100.62 | 99.77 | 100.62 | 100.43 | 100.43 | 100.24 |
| | | | | | Cation allocation based on 24 oxygen | | | | | |
| Si IV | 5.84 | 5.89 | 5.90 | 5.88 | 5.81 | 5.87 | 5.87 | 5.85 | 5.72 | 5.74 |
| Al IV | 0.16 | 0.11 | 0.10 | 0.12 | 0.19 | 0.13 | 0.13 | 0.15 | 0.03 | 0.04 |
| Sn | | | | | | | | | | |
| T site | 6.00 | 6.00 | 6.00 | 6.00 | 6.00 | 6.00 | 6.00 | 6.00 | 5.76 | 5.78 |
| Al VI | 1.05 | 1.12 | 0.72 | 0.75 | 0.78 | 0.81 | 0.77 | 0.86 | 0.00 | 0.00 |
| Ti VI | 0.04 | 0.05 | 0.03 | 0.02 | 0.03 | 0.03 | 0.03 | 0.02 | 0.00 | 0.00 |
| Cr | 0.00 | 0.00 | - | - | - | - | - | - | - | - |
| $Fe^{+3}$ | 2.78 | 2.75 | 3.25 | 3.23 | 3.18 | 3.16 | 3.20 | 3.12 | 4.00 | 4.00 |
| O site | 4.00 | 4.00 | 4.00 | 4.00 | 4.00 | 4.00 | 4.00 | 4.00 | 4.00 | 4.00 |
| $Fe^{+2}$ | 0.00 | 0.00 | 0.00 | 0.00 | 0.00 | 0.00 | 0.00 | 0.00 | 0.00 | 0.00 |
| $Mn^{+2}$ | 0.07 | 0.08 | 0.07 | 0.07 | 0.09 | 0.09 | 0.08 | 0.08 | 0.14 | 0.10 |
| Mg | 0.04 | 0.06 | 0.03 | 0.04 | 0.03 | 0.03 | 0.04 | 0.04 | 0.02 | 0.01 |
| Ca | 6.01 | 5.95 | 6.00 | 5.99 | 6.04 | 6.00 | 6.04 | 6.00 | 6.09 | 6.12 |
| A site | 6.00 | 6.00 | 6.00 | 6.00 | 6.00 | 6.00 | 6.00 | 6.00 | 6.24 | 6.22 |
| O | 23.94 | 23.97 | 23.96 | 23.95 | 23.92 | 23.95 | 23.95 | 23.94 | 23.74 | 23.76 |
| | | | | | Garnet components in mole fraction | | | | | |
| sp | 0.01 | 0.01 | 0.01 | 0.01 | 0.02 | 0.02 | 0.01 | 0.01 | 0.02 | 0.02 |
| al | 0.00 | 0.00 | 0.00 | 0.00 | 0.00 | 0.00 | 0.00 | 0.00 | 0.00 | 0.00 |
| py | 0.01 | 0.01 | 0.01 | 0.01 | 0.01 | 0.01 | 0.01 | 0.01 | 0.00 | 0.00 |
| gr | 0.24 | 0.26 | 0.16 | 0.17 | 0.18 | 0.18 | 0.17 | 0.20 | 0.00 | 0.00 |
| an | 0.70 | 0.69 | 0.81 | 0.81 | 0.80 | 0.79 | 0.80 | 0.78 | 1.00 | 1.00 |
| sp+al+py | 0.02 | 0.02 | 0.02 | 0.02 | 0.02 | 0.02 | 0.02 | 0.02 | 0.00 | 0.00 |

**sp:** spessartine, **al:** almandine, **py:** pyrope, **gr:** grossular, **an:** andradite.

## APPENDIX IV. Continued.

**Vesuvianite**

| S. No. | 105323 | 105323 | 105323 | 105323 | 105323 | 105339 | 105339 | 105339 | 105339 | 105339 |
|---|---|---|---|---|---|---|---|---|---|---|
| An. No. | 1 | 2 | 3 | 4 | 5 | 1 | 2 | 3 | 4 | 5 |
| | | | | Oxide composition (wt. %) | | | | | | |
| SiO2 | 35.74 | 35.27 | 35.09 | 35.05 | 34.88 | 35.13 | 34.82 | 34.90 | 34.75 | 34.71 |
| TiO2 | 0.23 | 0.30 | 0.27 | 0.19 | 0.31 | 0.13 | 0.11 | 0.08 | 0.15 | 0.13 |
| SnO2 | 0.00 | 0.18 | 0.04 | 0.02 | 0.07 | 0.00 | 0.00 | 0.00 | 0.00 | 0.00 |
| WO3 | 0.00 | 0.00 | 0.00 | 0.00 | 0.00 | 0.00 | 0.00 | 0.00 | 0.00 | 0.00 |
| Al2O3 | 14.59 | 14.14 | 13.80 | 13.99 | 13.98 | 13.32 | 13.34 | 14.63 | 12.50 | 12.57 |
| Cr2O3 | 0.00 | 0.00 | 0.00 | 0.00 | 0.00 | 0.00 | 0.00 | 0.00 | 0.00 | 0.00 |
| FeO | 5.90 | 5.54 | 5.83 | 6.05 | 5.54 | 6.25 | 5.98 | 5.93 | 7.21 | 7.13 |
| CuO | 0.00 | 0.00 | 0.03 | 0.00 | 0.00 | 0.00 | 0.00 | 0.00 | 0.00 | 0.00 |
| ZnO | 0.04 | 0.01 | 0.00 | 0.02 | 0.00 | 0.00 | 0.00 | 0.00 | 0.00 | 0.00 |
| MnO | 0.71 | 0.52 | 0.66 | 0.64 | 0.62 | 0.49 | 0.54 | 0.58 | 0.49 | 0.65 |
| MgO | 3.05 | 3.08 | 2.95 | 2.66 | 2.86 | 3.51 | 3.50 | 3.20 | 3.39 | 3.38 |
| CaO | 35.43 | 35.35 | 35.42 | 34.66 | 35.90 | 35.76 | 35.54 | 34.77 | 35.79 | 35.66 |
| Na2O | 0.01 | 0.02 | 0.02 | 0.01 | 0.02 | 0.01 | 0.01 | 0.01 | 0.00 | 0.00 |
| K2O | 0.00 | 0.03 | 0.01 | 0.00 | 0.01 | 0.01 | 0.01 | 0.08 | 0.00 | 0.00 |
| F | 0.85 | 0.79 | 0.76 | 0.83 | 0.78 | 0.00 | 0.00 | 0.00 | 0.00 | 0.00 |
| Cl | 0.19 | 0.35 | 0.25 | 0.26 | 0.28 | 0.46 | 0.40 | 0.20 | 0.13 | 0.15 |
| H2O | 3.26 | 4.42 | 4.87 | 5.62 | 4.75 | 4.93 | 5.75 | 5.62 | 5.59 | 5.62 |
| Total | 96.74 | 95.58 | 95.14 | 94.38 | 95.25 | 95.07 | 94.25 | 94.38 | 94.41 | 94.38 |
| H2O | 3.26 | 4.42 | 4.87 | 5.62 | 4.75 | 4.93 | 5.75 | 5.62 | 5.59 | 5.62 |
| O=F | 0.36 | 0.33 | 0.32 | 0.35 | 0.33 | 0.00 | 0.00 | 0.00 | 0.00 | 0.00 |
| O=Cl | 0.04 | 0.08 | 0.06 | 0.06 | 0.06 | 0.10 | 0.09 | 0.04 | 0.03 | 0.03 |
| | | | | Allocation of cations based on 76 (O, OH) | | | | | | |
| Si | 17.25 | 16.80 | 16.67 | 16.49 | 16.60 | 16.66 | 16.36 | 16.35 | 16.47 | 16.45 |
| Ti | 0.08 | 0.11 | 0.10 | 0.07 | 0.11 | 0.05 | 0.04 | 0.03 | 0.05 | 0.05 |
| Sn | 0.00 | 0.03 | 0.01 | 0.00 | 0.01 | 0.00 | 0.00 | 0.00 | 0.00 | 0.00 |
| W | 0.00 | 0.00 | 0.00 | 0.00 | 0.00 | 0.00 | 0.00 | 0.00 | 0.00 | 0.00 |
| Al | 8.30 | 7.94 | 7.73 | 7.76 | 7.84 | 7.45 | 7.39 | 8.08 | 6.98 | 7.02 |
| Cr | 0.00 | 0.00 | 0.00 | 0.00 | 0.00 | 0.00 | 0.00 | 0.00 | 0.00 | 0.00 |
| Fe | 2.38 | 2.21 | 2.32 | 2.38 | 2.20 | 2.48 | 2.35 | 2.32 | 2.86 | 2.83 |
| Cu | 0.00 | 0.00 | 0.01 | 0.00 | 0.00 | 0.00 | 0.00 | 0.00 | 0.00 | 0.00 |
| Zn | 0.01 | 0.00 | 0.00 | 0.01 | 0.00 | 0.00 | 0.00 | 0.00 | 0.00 | 0.00 |
| Mn | 0.29 | 0.21 | 0.27 | 0.26 | 0.25 | 0.20 | 0.21 | 0.23 | 0.20 | 0.26 |
| Mg | 2.19 | 2.19 | 2.09 | 1.87 | 2.03 | 2.48 | 2.45 | 2.24 | 2.40 | 2.39 |
| Ca | 18.32 | 18.04 | 18.03 | 17.47 | 18.31 | 18.18 | 17.89 | 17.46 | 18.18 | 18.10 |
| Na | 0.01 | 0.02 | 0.02 | 0.01 | 0.02 | 0.01 | 0.01 | 0.01 | 0.00 | 0.00 |
| K | 0.00 | 0.02 | 0.01 | 0.00 | 0.01 | 0.01 | 0.01 | 0.05 | 0.00 | 0.00 |
| F | 1.41 | 1.29 | 1.24 | 1.34 | 1.27 | 0.00 | 0.00 | 0.00 | 0.00 | 0.00 |
| Cl | 0.58 | 1.05 | 0.75 | 0.77 | 0.84 | 1.37 | 1.19 | 0.58 | 0.39 | 0.44 |
| OH | 10.38 | 13.90 | 15.26 | 17.46 | 14.92 | 15.45 | 17.83 | 17.40 | 17.50 | 17.60 |
| Total | 61.21 | 63.82 | 64.50 | 65.88 | 64.41 | 64.33 | 65.73 | 64.74 | 65.02 | 65.12 |

## APPENDIX IV. Continued.

**Vesuvianite**

| S. No. | 105339 | 105339 | 105339 | 105339 | 105341 | 105341 | 105341 | 105341 | 105341 | 105341 |
|---|---|---|---|---|---|---|---|---|---|---|
| An. No. | 6 | 7 | 8 | 9 | 1 | 2 | 3 | 4 | 5 | 6 |
| | | | | Oxide composition (wt. %) | | | | | | |
| SiO2 | 34.77 | 34.85 | 34.32 | 34.46 | 35.34 | 35.91 | 35.55 | 35.73 | 34.56 | 35.18 |
| TiO2 | 0.10 | 0.06 | 0.12 | 0.12 | 0.07 | 1.18 | 1.06 | 0.52 | 0.41 | 0.47 |
| SnO2 | 0.00 | 0.00 | 0.00 | 0.00 | 0.00 | 0.00 | 0.00 | 0.00 | 0.00 | 0.00 |
| WO3 | 0.00 | 0.00 | 0.00 | 0.00 | 0.00 | 0.00 | 0.00 | 0.00 | 0.00 | 0.00 |
| Al2O3 | 12.82 | 13.74 | 13.05 | 12.89 | 14.84 | 16.14 | 14.48 | 16.10 | 12.40 | 14.37 |
| Cr2O3 | 0.00 | 0.00 | 0.00 | 0.00 | 0.00 | 0.00 | 0.00 | 0.00 | 0.00 | 0.00 |
| FeO | 6.90 | 6.21 | 7.37 | 7.12 | 4.99 | 2.61 | 4.42 | 3.13 | 6.00 | 4.86 |
| CuO | 0.00 | 0.00 | 0.00 | 0.00 | 0.00 | 0.00 | 0.00 | 0.00 | 0.00 | 0.00 |
| ZnO | 0.00 | 0.00 | 0.00 | 0.00 | 0.00 | 0.00 | 0.00 | 0.00 | 0.00 | 0.00 |
| MnO | 0.61 | 0.58 | 0.79 | 0.56 | 0.63 | 0.11 | 0.24 | 0.15 | 0.62 | 0.47 |
| MgO | 3.30 | 3.17 | 3.25 | 3.19 | 2.87 | 3.09 | 3.27 | 3.22 | 3.94 | 3.14 |
| CaO | 35.60 | 35.55 | 35.11 | 35.75 | 35.71 | 36.06 | 36.13 | 36.17 | 35.66 | 35.51 |
| Na2O | 0.01 | 0.00 | 0.01 | 0.00 | 0.00 | 0.00 | 0.01 | 0.01 | 0.02 | 0.00 |
| K2O | 0.00 | 0.00 | 0.00 | 0.00 | 0.00 | 0.00 | 0.00 | 0.00 | 0.01 | 0.00 |
| F | 0.00 | 0.00 | 0.00 | 0.00 | 0.00 | 0.00 | 0.00 | 0.00 | 0.00 | 0.00 |
| Cl | 0.16 | 0.10 | 0.21 | 0.15 | 0.15 | 0.22 | 0.18 | 0.16 | 0.07 | 0.74 |
| H2O | 5.73 | 5.74 | 5.77 | 5.76 | 5.40 | 4.68 | 4.66 | 4.81 | 6.31 | 5.26 |
| Total | 94.27 | 94.26 | 94.23 | 94.24 | 94.60 | 95.32 | 95.34 | 95.19 | 93.69 | 94.74 |
| H2O | 5.73 | 5.74 | 5.77 | 5.76 | 5.40 | 4.68 | 4.66 | 4.81 | 6.31 | 5.26 |
| O=F | 0.00 | 0.00 | 0.00 | 0.00 | 0.00 | 0.00 | 0.00 | 0.00 | 0.00 | 0.00 |
| O=Cl | 0.04 | 0.02 | 0.05 | 0.03 | 0.03 | 0.05 | 0.04 | 0.04 | 0.02 | 0.17 |
| | | | | Allocation of cations based on 76 (O, OH) | | | | | | |
| Si | 16.42 | 16.38 | 16.24 | 16.30 | 16.54 | 16.70 | 16.73 | 16.64 | 16.19 | 16.48 |
| Ti | 0.04 | 0.02 | 0.04 | 0.04 | 0.02 | 0.41 | 0.38 | 0.18 | 0.14 | 0.17 |
| Sn | 0.00 | 0.00 | 0.00 | 0.00 | 0.00 | 0.00 | 0.00 | 0.00 | 0.00 | 0.00 |
| W | 0.00 | 0.00 | 0.00 | 0.00 | 0.00 | 0.00 | 0.00 | 0.00 | 0.00 | 0.00 |
| Al | 7.14 | 7.61 | 7.28 | 7.19 | 8.19 | 8.85 | 8.03 | 8.84 | 6.85 | 7.94 |
| Cr | 0.00 | 0.00 | 0.00 | 0.00 | 0.00 | 0.00 | 0.00 | 0.00 | 0.00 | 0.00 |
| Fe | 2.73 | 2.44 | 2.92 | 2.82 | 1.95 | 1.01 | 1.74 | 1.22 | 2.35 | 1.90 |
| Cu | 0.00 | 0.00 | 0.00 | 0.00 | 0.00 | 0.00 | 0.00 | 0.00 | 0.00 | 0.00 |
| Zn | 0.00 | 0.00 | 0.00 | 0.00 | 0.00 | 0.00 | 0.00 | 0.00 | 0.00 | 0.00 |
| Mn | 0.24 | 0.23 | 0.32 | 0.22 | 0.25 | 0.04 | 0.10 | 0.06 | 0.25 | 0.19 |
| Mg | 2.32 | 2.22 | 2.29 | 2.25 | 2.00 | 2.14 | 2.29 | 2.24 | 2.75 | 2.19 |
| Ca | 18.02 | 17.90 | 17.81 | 18.12 | 17.91 | 17.97 | 18.22 | 18.05 | 17.90 | 17.83 |
| Na | 0.01 | 0.00 | 0.01 | 0.00 | 0.00 | 0.00 | 0.01 | 0.01 | 0.02 | 0.00 |
| K | 0.00 | 0.00 | 0.00 | 0.00 | 0.00 | 0.00 | 0.00 | 0.00 | 0.01 | 0.00 |
| F | 0.00 | 0.00 | 0.00 | 0.00 | 0.00 | 0.00 | 0.00 | 0.00 | 0.00 | 0.00 |
| Cl | 0.49 | 0.28 | 0.63 | 0.46 | 0.44 | 0.65 | 0.52 | 0.46 | 0.20 | 2.20 |
| OH | 17.86 | 17.83 | 18.03 | 17.99 | 16.70 | 14.37 | 14.50 | 14.81 | 19.52 | 16.26 |
| Total | 65.27 | 64.92 | 65.57 | 65.40 | 64.01 | 62.14 | 62.52 | 62.51 | 66.17 | 65.17 |

## APPENDIX IV. Continued.

**Vesuvianite**

| S. No. | 105341 | S2 | S2 | S2 | S2 | S2 | S2 | S2 | S2 | S4A-1 |
|---|---|---|---|---|---|---|---|---|---|---|
| An. No. | 7 | 1 | 2 | 3 | 4 | 5 | 6 | 7 | 8 | 1 |
| | | | | Oxide composition (wt. %) | | | | | | |
| SiO2 | 34.72 | 34.89 | 35.52 | 34.68 | 34.83 | 35.77 | 35.44 | 35.98 | 35.85 | 35.73 |
| TiO2 | 0.25 | 0.44 | 0.16 | 0.72 | 0.27 | 0.12 | 1.56 | 0.16 | 0.50 | 1.52 |
| SnO2 | 0.00 | 0.00 | 0.01 | 0.01 | 0.00 | 0.00 | 0.04 | 0.00 | 0.00 | 0.00 |
| WO3 | 0.00 | 0.00 | 0.00 | 0.00 | 0.00 | 0.00 | 0.00 | 0.00 | 0.00 | 0.00 |
| Al2O3 | 13.40 | 11.85 | 13.92 | 12.04 | 12.27 | 14.06 | 14.31 | 14.30 | 14.20 | 14.03 |
| Cr2O3 | 0.00 | 0.00 | 0.00 | 0.00 | 0.00 | 0.00 | 0.00 | 0.00 | 0.00 | 0.00 |
| FeO | 5.82 | 7.19 | 6.36 | 7.70 | 7.43 | 6.52 | 5.93 | 6.83 | 6.76 | 5.74 |
| CuO | 0.00 | 0.00 | 0.00 | 0.03 | 0.05 | 0.00 | 0.01 | 0.00 | 0.00 | 0.05 |
| ZnO | 0.00 | 0.00 | 0.04 | 0.01 | 0.00 | 0.00 | 0.02 | 0.00 | 0.00 | 0.00 |
| MnO | 0.65 | 0.55 | 0.57 | 0.63 | 0.57 | 0.58 | 1.55 | 0.53 | 0.52 | 0.55 |
| MgO | 3.39 | 4.15 | 3.34 | 3.46 | 3.64 | 3.12 | 2.56 | 2.66 | 2.78 | 2.88 |
| CaO | 34.80 | 35.67 | 35.95 | 35.64 | 35.72 | 35.65 | 34.74 | 35.70 | 35.56 | 35.37 |
| Na2O | 0.01 | 0.01 | 0.01 | 0.01 | 0.00 | 0.01 | 0.00 | 0.00 | 0.01 | 0.01 |
| K2O | 0.00 | 0.01 | 0.01 | 0.00 | 0.00 | 0.00 | 0.00 | 0.00 | 0.00 | 0.01 |
| F | 0.00 | 0.97 | 1.42 | 1.01 | 1.06 | 1.44 | 1.82 | 1.75 | 0.99 | 0.77 |
| Cl | 0.13 | 0.13 | 0.24 | 0.19 | 0.11 | 0.23 | 0.14 | 0.30 | 0.29 | 0.37 |
| H2O | 6.83 | 4.15 | 2.45 | 3.85 | 4.06 | 2.50 | 1.88 | 1.78 | 2.54 | 2.97 |
| Total | 93.17 | 95.85 | 97.55 | 96.15 | 95.94 | 97.50 | 98.12 | 98.22 | 97.46 | 97.03 |
| H2O | 6.83 | 4.15 | 2.45 | 3.85 | 4.06 | 2.50 | 1.88 | 1.78 | 2.54 | 2.97 |
| O=F | 0.00 | 0.41 | 0.60 | 0.43 | 0.44 | 0.61 | 0.76 | 0.74 | 0.42 | 0.32 |
| O=Cl | 0.03 | 0.03 | 0.06 | 0.04 | 0.02 | 0.05 | 0.03 | 0.07 | 0.07 | 0.08 |
| | | | | Allocation of cations based on 76 (O, OH) | | | | | | |
| Si | 16.09 | 16.89 | 17.42 | 16.89 | 16.90 | 17.51 | 17.50 | 17.79 | 17.51 | 17.28 |
| Ti | 0.09 | 0.16 | 0.06 | 0.26 | 0.10 | 0.04 | 0.58 | 0.06 | 0.18 | 0.55 |
| Sn | 0.00 | 0.00 | 0.00 | 0.00 | 0.00 | 0.00 | 0.01 | 0.00 | 0.00 | 0.00 |
| W | 0.00 | 0.00 | 0.00 | 0.00 | 0.00 | 0.00 | 0.00 | 0.00 | 0.00 | 0.00 |
| Al | 7.32 | 6.76 | 8.05 | 6.91 | 7.02 | 8.11 | 8.33 | 8.33 | 8.17 | 8.00 |
| Cr | 0.00 | 0.00 | 0.00 | 0.00 | 0.00 | 0.00 | 0.00 | 0.00 | 0.00 | 0.00 |
| Fe | 2.26 | 2.91 | 2.61 | 3.14 | 3.01 | 2.67 | 2.45 | 2.82 | 2.76 | 2.32 |
| Cu | 0.00 | 0.00 | 0.00 | 0.01 | 0.02 | 0.00 | 0.00 | 0.00 | 0.00 | 0.02 |
| Zn | 0.00 | 0.00 | 0.01 | 0.00 | 0.00 | 0.00 | 0.01 | 0.00 | 0.00 | 0.00 |
| Mn | 0.26 | 0.23 | 0.24 | 0.26 | 0.23 | 0.24 | 0.65 | 0.22 | 0.22 | 0.23 |
| Mg | 2.34 | 2.99 | 2.44 | 2.51 | 2.63 | 2.28 | 1.88 | 1.96 | 2.02 | 2.08 |
| Ca | 17.28 | 18.50 | 18.90 | 18.60 | 18.57 | 18.70 | 18.38 | 18.91 | 18.61 | 18.33 |
| Na | 0.01 | 0.01 | 0.01 | 0.01 | 0.00 | 0.01 | 0.00 | 0.00 | 0.01 | 0.01 |
| K | 0.00 | 0.01 | 0.01 | 0.00 | 0.00 | 0.00 | 0.00 | 0.00 | 0.00 | 0.01 |
| F | 0.00 | 1.61 | 2.39 | 1.70 | 1.76 | 2.42 | 3.08 | 2.97 | 1.66 | 1.28 |
| Cl | 0.38 | 0.38 | 0.76 | 0.59 | 0.33 | 0.71 | 0.44 | 0.94 | 0.90 | 1.13 |
| OH | 20.90 | 13.25 | 7.93 | 12.40 | 13.00 | 8.07 | 6.13 | 5.83 | 8.19 | 9.49 |
| Total | 66.91 | 63.70 | 60.82 | 63.30 | 63.57 | 60.78 | 59.45 | 59.83 | 60.24 | 60.73 |

## APPENDIX IV. Continued.

**Vesuvianite**

| S. No. | S4A-2 | S4A-3 | S4A-4 | S8-1 | S16 | S16 | S16 | S16 | S32 | S32 |
|---|---|---|---|---|---|---|---|---|---|---|
| An. No. | 2 | 3 | 4 | 1 | 1 | 2 | 3 | 4 | 1 | 2 |
| | | | | Oxide composition (wt. %) | | | | | | |
| SiO2 | 35.01 | 35.62 | 35.60 | 36.13 | 35.39 | 35.57 | 35.00 | 34.78 | 35.42 | 34.90 |
| TiO2 | 1.09 | 1.20 | 1.24 | 1.36 | 0.35 | 1.86 | 0.54 | 0.42 | 0.80 | 0.73 |
| SnO2 | 0.04 | 0.00 | 0.00 | 0.00 | 0.01 | 0.00 | 0.04 | 0.00 | 0.00 | 0.00 |
| WO3 | 0.00 | 0.00 | 0.00 | 0.00 | 0.00 | 0.00 | 0.00 | 0.00 | 0.00 | 0.00 |
| Al2O3 | 14.09 | 14.25 | 14.32 | 17.19 | 13.71 | 14.67 | 14.77 | 14.06 | 12.69 | 12.09 |
| Cr2O3 | 0.00 | 0.00 | 0.00 | 0.00 | 0.00 | 0.00 | 0.00 | 0.00 | 0.00 | 0.00 |
| FeO | 6.33 | 6.54 | 5.96 | 2.27 | 6.50 | 5.07 | 6.22 | 6.48 | 6.22 | 6.74 |
| CuO | 0.00 | 0.02 | 0.02 | 0.02 | 0.06 | 0.04 | 0.00 | 0.00 | 0.00 | 0.00 |
| ZnO | 0.00 | 0.03 | 0.00 | 0.08 | 0.09 | 0.05 | 0.00 | 0.00 | 0.07 | 0.00 |
| MnO | 0.66 | 0.56 | 0.51 | 0.12 | 0.49 | 0.42 | 0.57 | 0.49 | 0.83 | 1.05 |
| MgO | 2.84 | 2.54 | 2.82 | 3.08 | 3.47 | 2.53 | 2.52 | 3.28 | 3.10 | 2.81 |
| CaO | 35.31 | 35.20 | 35.58 | 36.86 | 36.27 | 35.80 | 35.47 | 36.18 | 31.30 | 30.39 |
| Na2O | 0.01 | 0.02 | 0.01 | 0.01 | 0.00 | 0.01 | 0.01 | 0.01 | 0.02 | 0.04 |
| K2O | 0.00 | 0.00 | 0.00 | 0.00 | 0.00 | 0.01 | 0.00 | 0.00 | 0.02 | 0.01 |
| F | 0.65 | 0.87 | 0.77 | 0.67 | 1.43 | 1.08 | 2.05 | 1.38 | 0.92 | 1.03 |
| Cl | 0.23 | 0.36 | 0.33 | 0.29 | 0.24 | 0.39 | 0.56 | 0.27 | 0.16 | 0.15 |
| H2O | 3.74 | 2.79 | 2.84 | 1.92 | 1.99 | 2.50 | 2.25 | 2.65 | 8.45 | 10.06 |
| Total | 96.26 | 97.21 | 97.16 | 98.08 | 98.01 | 97.50 | 97.75 | 97.35 | 91.55 | 89.94 |
| H2O | 3.74 | 2.79 | 2.84 | 1.92 | 1.99 | 2.50 | 2.25 | 2.65 | 8.45 | 10.06 |
| O=F | 0.27 | 0.37 | 0.32 | 0.28 | 0.60 | 0.45 | 0.86 | 0.58 | 0.39 | 0.43 |
| O=Cl | 0.05 | 0.08 | 0.07 | 0.07 | 0.05 | 0.09 | 0.13 | 0.06 | 0.04 | 0.03 |
| | | | | Allocation of cations based on 76 (O, OH) | | | | | | |
| Si | 16.86 | 17.32 | 17.26 | 17.35 | 17.50 | 17.28 | 17.22 | 17.06 | 16.06 | 15.61 |
| Ti | 0.39 | 0.44 | 0.45 | 0.49 | 0.13 | 0.68 | 0.20 | 0.15 | 0.27 | 0.25 |
| Sn | 0.01 | 0.00 | 0.00 | 0.00 | 0.00 | 0.00 | 0.01 | 0.00 | 0.00 | 0.00 |
| W | 0.00 | 0.00 | 0.00 | 0.00 | 0.00 | 0.00 | 0.00 | 0.00 | 0.00 | 0.00 |
| Al | 8.00 | 8.17 | 8.19 | 9.73 | 7.99 | 8.40 | 8.56 | 8.13 | 6.78 | 6.37 |
| Cr | 0.00 | 0.00 | 0.00 | 0.00 | 0.00 | 0.00 | 0.00 | 0.00 | 0.00 | 0.00 |
| Fe | 2.55 | 2.66 | 2.42 | 0.91 | 2.69 | 2.06 | 2.56 | 2.66 | 2.36 | 2.52 |
| Cu | 0.00 | 0.01 | 0.01 | 0.01 | 0.02 | 0.02 | 0.00 | 0.00 | 0.00 | 0.00 |
| Zn | 0.00 | 0.01 | 0.00 | 0.03 | 0.03 | 0.02 | 0.00 | 0.00 | 0.02 | 0.00 |
| Mn | 0.27 | 0.23 | 0.21 | 0.05 | 0.21 | 0.17 | 0.24 | 0.20 | 0.32 | 0.40 |
| Mg | 2.04 | 1.84 | 2.04 | 2.20 | 2.56 | 1.83 | 1.85 | 2.40 | 2.10 | 1.87 |
| Ca | 18.22 | 18.34 | 18.49 | 18.97 | 19.21 | 18.63 | 18.70 | 19.02 | 15.21 | 14.56 |
| Na | 0.01 | 0.02 | 0.01 | 0.01 | 0.00 | 0.01 | 0.01 | 0.01 | 0.02 | 0.03 |
| K | 0.00 | 0.00 | 0.00 | 0.00 | 0.00 | 0.01 | 0.00 | 0.00 | 0.01 | 0.01 |
| F | 1.07 | 1.45 | 1.28 | 1.10 | 2.43 | 1.80 | 3.46 | 2.32 | 1.43 | 1.58 |
| Cl | 0.70 | 1.11 | 1.01 | 0.88 | 0.75 | 1.20 | 1.74 | 0.84 | 0.46 | 0.42 |
| OH | 11.89 | 8.97 | 9.11 | 6.10 | 6.50 | 8.01 | 7.31 | 8.58 | 25.31 | 29.70 |
| Total | 62.02 | 60.57 | 60.47 | 57.84 | 60.01 | 60.11 | 61.86 | 61.39 | 70.36 | 73.33 |

## APPENDIX IV. Continued.

**Ampibole**

| S. No. | S17 | S17 | S17 | S17 | S17 | S17 | S17 | S17 | S17 | S17 |
|---|---|---|---|---|---|---|---|---|---|---|
| An. No. | 1 | 2 | 3 | 4 | 5.00 | 6 | 7.00 | 8 | 9 | 10 |
| | | | | | Oxide composition (wt. %) | | | | | |
| $SiO_2$ | 43.05 | 3.44 | 38.73 | 38.49 | 38.72 | 37.81 | 36.32 | 40.34 | 37.26 | 37.70 |
| $TiO_2$ | 0.02 | 0.33 | 0.14 | 0.50 | 0.36 | 0.42 | 0.37 | 0.38 | 0.37 | 0.34 |
| $Al_2O_3$ | 6.54 | 10.68 | 10.51 | 11.96 | 11.57 | 12.16 | 12.93 | 8.91 | 12.20 | 11.82 |
| $Cr_2O_3$ | - | 0.06 | - | - | - | 0.02 | 0.10 | 0.02 | 0.06 | - |
| $Fe_2O_3$ | 5.05 | 26.93 | 5.79 | 5.78 | 5.68 | 5.98 | 6.92 | 5.23 | 5.77 | 5.60 |
| FeO | 21.68 | -1.00 | 20.44 | 15.49 | 17.22 | 17.02 | 18.67 | 21.44 | 21.42 | 17.61 |
| MnO | 0.60 | 0.52 | 0.77 | 0.41 | 0.53 | 0.45 | 0.44 | 0.65 | 0.57 | 0.36 |
| MgO | 5.80 | 6.93 | 4.99 | 8.04 | 7.18 | 7.19 | 5.38 | 5.39 | 4.01 | 7.06 |
| ZnO | - | - | - | - | - | - | - | - | - | - |
| CaO | 11.48 | 11.99 | 11.88 | 11.95 | 11.90 | 11.99 | 11.84 | 11.62 | 11.63 | 12.08 |
| $Na_2O$ | 1.24 | 1.47 | 1.16 | 1.46 | 1.61 | 1.61 | 1.43 | 1.51 | 1.48 | 1.51 |
| $K_2O$ | 1.01 | 1.84 | 1.67 | 1.92 | 1.85 | 2.12 | 2.31 | 1.56 | 1.95 | 2.17 |
| $H_2O$ | 1.72 | 0.85 | 1.58 | 1.71 | 1.76 | 1.66 | 1.52 | 1.61 | 1.59 | 1.59 |
| F | - | - | - | - | - | - | - | - | - | - |
| Cl | 0.64 | 0.84 | 1.11 | 0.76 | 0.58 | 0.92 | 1.38 | 1.08 | 1.07 | 1.16 |
| O=F | - | - | - | - | - | - | - | - | - | - |
| O=Cl | 0.14 | 0.19 | 0.25 | 0.17 | 0.13 | 0.21 | 0.31 | 0.24 | 0.24 | 0.26 |
| Total | 98.70 | 64.37 | 98.54 | 98.31 | 98.83 | 99.13 | 99.31 | 99.49 | 99.13 | 98.74 |
| | | | | | Cation allocation based on 22 oxygen, 2 (OH) | | | | | |
| Si IV | 6.84 | 0.97 | 6.23 | 6.06 | 6.10 | 5.97 | 5.82 | 6.43 | 6.00 | 6.00 |
| Al IV | 1.16 | 3.54 | 1.77 | 1.94 | 1.90 | 2.03 | 2.18 | 1.57 | 2.00 | 2.00 |
| $Fe^{+3}$ | 0.00 | 3.49 | 0.00 | 0.00 | 0.00 | 0.00 | 0.00 | 0.00 | 0.00 | 9.00 |
| Ti IV | 0.00 | - | - | - | - | - | - | - | - | - |
| Al VI | 0.06 | - | 0.23 | 0.28 | 0.25 | 0.24 | 0.26 | 0.10 | 0.32 | 0.22 |
| $Fe^{+3}$ | 0.60 | 2.20 | 0.70 | 0.68 | 0.67 | 0.71 | 0.83 | 0.63 | 0.70 | 0.67 |
| Ti | 0.00 | 0.07 | 0.02 | 0.06 | 0.04 | 0.05 | 0.04 | 0.05 | 0.05 | 0.04 |
| Cr | 0.00 | 0.01 | - | - | - | 0.00 | 0.01 | 0.00 | 0.01 | - |
| Mg | 1.37 | 2.72 | 1.20 | 1.89 | 1.69 | 1.69 | 1.28 | 1.28 | 0.96 | 1.68 |
| $Fe^{+2}$ | 2.88 | 0.00 | 2.75 | 2.04 | 2.27 | 2.25 | 2.50 | 2.86 | 2.89 | 2.35 |
| Zn | - | - | - | - | - | - | - | - | - | - |
| Mn | 0.08 | - | 0.11 | 0.06 | 0.07 | 0.06 | 0.06 | 0.09 | 0.08 | 0.05 |
| Ca | 0.00 | - | 0.00 | - | - | 0.00 | 0.00 | - | 0.00 | 0.00 |
| M1,2,3 | 5.00 | 5.00 | 5.00 | 5.00 | 5.00 | 5.00 | 5.00 | 5.00 | 5.00 | 5.00 |
| Mg | 0.00 | 0.19 | 0.00 | 0.00 | 0.00 | 0.00 | 0.00 | 0.00 | 0.00 | 0.00 |
| $Fe^{+2}$ | 0.00 | 0.00 | 0.00 | 0.00 | 0.00 | 0.00 | 0.00 | 0.00 | 0.00 | 0.00 |
| Zn | - | - | - | - | - | - | - | - | - | - |
| Mn | 0.00 | 0.12 | - | 0.00 | 0.00 | - | - | 0.00 | - | - |
| Ca | 1.95 | 2.00 | 2.00 | 2.00 | 2.00 | 2.00 | 2.00 | 1.98 | 2.00 | 2.00 |
| Na | 0.05 | - | - | - | - | - | - | 0.02 | - | - |
| M4 site | 2.00 | 2.00 | 2.00 | 2.00 | 2.00 | 2.00 | 2.00 | 2.00 | 2.00 | 2.00 |
| Ca | 0.00 | 1.61 | 0.05 | 0.02 | 0.01 | 0.03 | 0.03 | - | 0.01 | 0.06 |
| Na | 0.34 | 0.80 | 0.36 | 0.45 | 0.49 | 0.49 | 0.44 | 0.45 | 0.46 | 0.47 |
| K | 0.20 | 0.66 | 0.34 | 0.39 | 0.37 | 0.43 | 0.47 | 0.32 | 0.40 | 0.44 |
| O | 22.00 | 22.00 | 22.00 | 22.00 | 22.00 | 22.00 | 22.00 | 22.00 | 22.00 | 22.00 |
| OH | 1.83 | 1.60 | 1.70 | 1.80 | 1.85 | 1.75 | 1.63 | 1.71 | 1.71 | 1.69 |
| F | - | - | - | - | - | - | - | - | - | - |
| Cl | 0.17 | 0.40 | 0.30 | 0.20 | 0.15 | 0.25 | 0.37 | 0.29 | 0.29 | 0.31 |

## APPENDIX IV. Continued.

**Ampibole**

| S. No. | S17 | S17 | S18B | S18B | S18B | S18B | S18B | S18B | S38 | S38 |
|---|---|---|---|---|---|---|---|---|---|---|
| An. No. | 11 | 12 | 1 | 2 | 3 | 4 | 5 | 6 | 1 | 2 |
| | | | | Oxide composition (wt. %) | | | | | | |
| $SiO_2$ | 37.87 | 39.57 | 36.63 | 37.64 | 40.43 | 42.42 | 37.97 | 34.54 | 39.12 | 37.21 |
| $TiO_2$ | 0.37 | 0.29 | 0.19 | 0.19 | 0.29 | 0.04 | 0.10 | 0.03 | 0.11 | 0.13 |
| $Al_2O_3$ | 10.28 | 9.81 | 10.41 | 9.63 | 10.75 | 9.34 | 10.20 | 12.65 | 10.64 | 12.47 |
| $Cr_2O_3$ | 0.04 | 0.06 | - | - | 0.02 | 0.14 | 0.04 | 0.02 | 0.14 | - |
| $Fe_2O_3$ | 6.72 | 5.15 | 8.26 | 6.29 | 4.40 | 5.10 | 8.27 | 7.91 | 6.24 | 7.20 |
| FeO | 21.56 | 18.26 | 24.81 | 26.23 | 15.46 | 18.15 | 23.77 | 24.19 | 18.69 | 18.30 |
| MnO | 0.52 | 0.38 | 0.75 | 0.61 | 0.92 | 1.07 | 0.66 | 0.75 | 0.94 | 0.77 |
| MgO | 4.57 | 7.49 | 1.50 | 1.60 | 9.06 | 7.01 | 2.09 | 1.08 | 5.98 | 5.30 |
| ZnO | - | - | - | - | - | - | - | - | - | - |
| CaO | 11.74 | 12.03 | 11.31 | 11.48 | 12.42 | 12.15 | 10.91 | 11.33 | 11.82 | 11.76 |
| $Na_2O$ | 1.51 | 1.53 | 1.40 | 1.33 | 1.84 | 0.89 | 1.93 | 1.25 | 1.63 | 1.48 |
| $K_2O$ | 1.92 | 1.88 | 1.84 | 1.77 | 1.19 | 1.21 | 1.11 | 2.50 | 1.37 | 1.76 |
| $H_2O$ | 1.57 | 1.58 | 1.31 | 1.30 | 1.84 | 1.93 | 1.51 | 1.10 | 1.58 | 1.49 |
| F | - | - | - | - | - | - | - | - | - | - |
| Cl | 1.15 | 1.23 | 1.99 | 2.03 | 0.36 | 0.03 | 1.33 | 2.76 | 1.21 | 1.50 |
| O=F | - | - | - | - | - | - | - | - | - | - |
| O=Cl | 0.26 | 0.28 | 0.45 | 0.46 | 0.08 | 0.01 | 0.30 | 0.62 | 0.27 | 0.34 |
| Total | 99.55 | 98.99 | 99.94 | 99.65 | 98.90 | 99.48 | 99.58 | 99.48 | 99.19 | 99.06 |
| | | | | Cation based on 22 oxygen, 2(OH, F, Cl) | | | | | | |
| Si IV | 6.11 | 6.27 | 6.04 | 6.22 | 6.27 | 6.57 | 6.18 | 5.76 | 6.21 | 5.95 |
| Al IV | 1.89 | 1.73 | 1.96 | 1.78 | 1.73 | 1.43 | 1.82 | 2.24 | 1.79 | 2.05 |
| $Fe^{+3}$ | 0.00 | 0.00 | 0.00 | 0.00 | 0.00 | 0.00 | 0.00 | 0.00 | 0.00 | 0.00 |
| Ti IV | - | - | - | 0.00 | 0.00 | 0.00 | - | - | - | - |
| Al VI | 0.06 | 0.10 | 0.06 | 0.09 | 0.23 | 0.27 | 0.14 | 0.25 | 0.20 | 0.30 |
| $Fe^{+3}$ | 0.82 | 0.61 | 1.02 | 0.78 | 0.51 | 0.59 | 1.01 | 0.99 | 0.75 | 0.87 |
| Ti | 0.04 | 0.03 | 0.02 | 0.02 | 0.03 | 0.00 | 0.01 | 0.00 | 0.01 | 0.02 |
| Cr | 0.01 | 0.01 | - | - | 0.00 | 0.02 | 0.01 | 0.00 | 0.02 | - |
| Mg | 1.10 | 1.77 | 0.37 | 0.39 | 2.09 | 1.62 | 0.51 | 0.27 | 1.42 | 1.26 |
| $Fe^{+2}$ | 2.91 | 2.42 | 3.42 | 3.62 | 2.00 | 2.35 | 3.24 | 3.38 | 2.48 | 2.45 |
| Zn | - | - | - | - | - | - | - | - | - | - |
| Mn | 0.07 | 0.05 | 0.10 | 0.09 | 0.12 | 0.14 | 0.09 | 0.11 | 0.13 | 0.10 |
| Ca | 0.00 | - | - | - | 0.00 | 0.00 | - | - | - | 0.00 |
| M1,2,3 | 5.00 | 5.00 | 5.00 | 5.00 | 5.00 | 5.00 | 5.00 | 5.00 | 5.00 | 5.00 |
| Mg | 0.00 | 0.00 | 0.00 | 0.00 | 0.00 | 0.00 | 0.00 | 0.00 | 0.00 | 0.00 |
| $Fe^{+2}$ | 0.00 | 0.00 | 0.00 | 0.00 | 0.00 | 0.00 | 0.00 | 0.00 | 0.00 | 0.00 |
| Zn | - | - | - | - | - | - | - | - | - | - |
| Mn | - | 0.00 | 0.00 | 0.00 | - | - | 0.00 | 0.00 | 0.00 | - |
| Ca | 2.00 | 2.00 | 2.00 | 2.00 | 2.00 | 2.00 | 1.90 | 2.00 | 2.00 | 2.00 |
| Na | - | - | 0.00 | - | - | - | 0.10 | - | - | - |
| M4 site | 2.00 | 2.00 | 2.00 | 2.00 | 2.00 | 2.00 | 2.00 | 2.00 | 2.00 | 2.00 |
| Ca | 0.03 | 0.04 | - | 0.03 | 0.06 | 0.02 | - | 0.03 | 0.01 | 0.02 |
| Na | 0.47 | 0.47 | 0.45 | 0.43 | 0.55 | 0.27 | 0.51 | 0.40 | 0.50 | 0.46 |
| K | 0.40 | 0.38 | 0.39 | 0.37 | 0.24 | 0.24 | 0.23 | 0.53 | 0.28 | 0.36 |
| O | 22.00 | 22.00 | 22.00 | 22.00 | 22.00 | 22.00 | 22.00 | 22.00 | 22.00 | 22.00 |
| OH | 1.69 | 1.67 | 1.44 | 1.43 | 1.91 | 1.99 | 1.63 | 1.22 | 1.68 | 1.59 |
| F | - | - | - | - | - | - | - | - | - | - |
| Cl | 0.31 | 0.33 | 0.56 | 0.57 | 0.09 | 0.01 | 0.37 | 0.78 | 0.32 | 0.41 |

## APPENDIX IV. Continued.

**Ampibole**

| S. No. | S38 | S38 | S38 | S38 | S38 | S38 | S38 | S38 | S38 | S38 |
|---|---|---|---|---|---|---|---|---|---|---|
| An. No. | 3 | 4 | 5 | 6 | 7 | 8 | 9 | 10 | 11 | 12 |
| | | | | Oxide composition (wt. %) | | | | | | |
| $SiO_2$ | 37.40 | 38.98 | 38.95 | 39.01 | 37.87 | 38.14 | 38.65 | 38.40 | 37.24 | 37.87 |
| $TiO_2$ | 0.13 | 0.03 | 0.06 | 0.07 | 0.16 | 0.05 | 0.10 | 0.01 | 0.11 | 0.08 |
| $Al_2O_3$ | 12.38 | 11.81 | 11.59 | 11.71 | 12.63 | 12.35 | 12.23 | 14.08 | 14.01 | 12.30 |
| $Cr_2O_3$ | 0.02 | 0.10 | 0.02 | 0.02 | 0.04 | 0.16 | - | - | 0.10 | - |
| $Fe_2O_3$ | 5.80 | 5.16 | 6.30 | 5.16 | 6.56 | 5.72 | 6.43 | 5.85 | 5.26 | 7.00 |
| FeO | 18.98 | 18.13 | 16.39 | 16.54 | 16.30 | 15.89 | 14.90 | 11.77 | 15.79 | 16.28 |
| MnO | 0.83 | 0.80 | 0.74 | 0.42 | 0.79 | 0.73 | 0.91 | 0.56 | 0.73 | 0.72 |
| MgO | 5.70 | 6.53 | 7.32 | 7.84 | 7.21 | 7.78 | 8.26 | 10.06 | 7.34 | 7.09 |
| ZnO | - | - | - | - | - | - | - | - | - | - |
| CaO | 12.20 | 12.17 | 11.98 | 12.16 | 12.14 | 12.29 | 12.20 | 12.44 | 12.21 | 11.96 |
| $Na_2O$ | 1.71 | 1.73 | 1.86 | 1.67 | 1.66 | 1.63 | 1.68 | 1.77 | 1.63 | 1.73 |
| $K_2O$ | 1.59 | 1.20 | 1.16 | 1.58 | 1.94 | 1.84 | 1.88 | 1.90 | 2.04 | 1.79 |
| $H_2O$ | 1.58 | 1.75 | 1.71 | 1.76 | 1.75 | 1.75 | 1.77 | 1.88 | 1.81 | 1.75 |
| F | - | - | - | - | - | - | - | - | - | - |
| Cl | 1.18 | 0.61 | 0.76 | 0.58 | 0.64 | 0.63 | 0.63 | 0.29 | 0.36 | 0.60 |
| O=F | - | - | - | - | - | - | - | - | - | - |
| O=Cl | 0.27 | 0.14 | 0.17 | 0.13 | 0.14 | 0.14 | 0.14 | 0.07 | 0.08 | 0.14 |
| Total | 99.22 | 98.86 | 98.67 | 98.40 | 99.54 | 98.83 | 99.50 | 98.94 | 98.56 | 99.04 |
| | | | | Cation allocation based on 22 oxygen, 2(OH) | | | | | | |
| Si IV | 5.96 | 6.15 | 6.13 | 6.14 | 5.94 | 6.00 | 6.02 | 5.89 | 5.86 | 5.97 |
| Al IV | 2.04 | 1.85 | 1.87 | 1.86 | 2.06 | 2.00 | 1.98 | 2.11 | 2.14 | 2.03 |
| $Fe^{+3}$ | 0.00 | 0.00 | 0.00 | 0.00 | 0.00 | 0.00 | 0.00 | 0.00 | 0.00 | 0.00 |
| Ti IV | - | - | - | - | - | - | - | - | - | - |
| Al VI | 0.29 | 0.34 | 0.27 | 0.31 | 0.27 | 0.29 | 0.26 | 0.44 | 0.46 | 0.25 |
| $Fe^{+3}$ | 0.70 | 0.61 | 0.75 | 0.61 | 0.77 | 0.68 | 0.75 | 0.68 | 0.62 | 0.83 |
| Ti | 0.02 | 0.00 | 0.01 | 0.01 | 0.02 | 0.01 | 0.01 | 0.00 | 0.01 | 0.01 |
| Cr | 0.00 | 0.01 | 0.00 | 0.00 | 0.01 | 0.02 | - | - | 0.01 | - |
| Mg | 1.35 | 1.53 | 1.72 | 1.84 | 1.69 | 1.82 | 1.92 | 2.30 | 1.72 | 1.67 |
| $Fe^{+2}$ | 2.53 | 2.39 | 2.16 | 2.18 | 2.14 | 2.09 | 1.94 | 1.51 | 2.08 | 2.15 |
| Zn | - | - | - | - | - | - | - | - | - | - |
| Mn | 0.11 | 0.11 | 0.10 | 0.06 | 0.11 | 0.10 | 0.12 | 0.07 | 0.10 | 0.10 |
| Ca | - | - | - | - | - | - | 0.00 | 0.00 | - | 0.00 |
| M1,2,3 | 5.00 | 5.00 | 5.00 | 5.00 | 5.00 | 5.00 | 5.00 | 5.00 | 5.00 | 5.00 |
| Mg | 0.00 | 0.00 | 0.00 | 0.00 | 0.00 | 0.00 | 0.00 | 0.00 | 0.00 | 0.00 |
| $Fe^{+2}$ | 0.00 | 0.00 | 0.00 | 0.00 | 0.00 | 0.00 | 0.00 | 0.00 | 0.00 | 0.00 |
| Zn | - | - | - | - | - | - | - | - | - | - |
| Mn | 0.00 | 0.00 | 0.00 | 0.00 | 0.00 | 0.00 | - | - | 0.00 | - |
| Ca | 2.00 | 2.00 | 2.00 | 2.00 | 2.00 | 2.00 | 2.00 | 2.00 | 2.00 | 2.00 |
| Na | - | - | - | - | - | - | - | - | - | - |
| M4 site | 2.00 | 2.00 | 2.00 | 2.00 | 2.00 | 2.00 | 2.00 | 2.00 | 2.00 | 2.00 |
| Ca | 0.08 | 0.06 | 0.02 | 0.05 | 0.04 | 0.07 | 0.03 | 0.05 | 0.06 | 0.02 |
| Na | 0.53 | 0.53 | 0.57 | 0.51 | 0.51 | 0.50 | 0.51 | 0.53 | 0.50 | 0.53 |
| K | 0.32 | 0.24 | 0.23 | 0.32 | 0.39 | 0.37 | 0.37 | 0.37 | 0.41 | 0.36 |
| O | 22.00 | 22.00 | 22.00 | 22.00 | 22.00 | 22.00 | 22.00 | 22.00 | 22.00 | 22.00 |
| OH | 1.68 | 1.84 | 1.80 | 1.85 | 1.83 | 1.83 | 1.83 | 1.92 | 1.90 | 1.84 |
| F | - | - | - | - | - | - | - | - | - | - |
| Cl | 0.32 | 0.16 | 0.20 | 0.15 | 0.17 | 0.17 | 0.17 | 0.08 | 0.10 | 0.16 |

## APPENDIX IV. Continued.

**Ampibole**

| S. No. | S199 | S199 | S199 | S199 | S199 | S199 | S202 | S202 | S202 | S202 |
|---|---|---|---|---|---|---|---|---|---|---|
| An. No. | 1 | 2 | 3 | 4 | 5 | 6 | 1 | 2 | 3 | 4 |
| | | | | | Oxide composition (wt. %) | | | | | |
| $SiO_2$ | 42.33 | 41.15 | 41.44 | 40.81 | 40.40 | 39.89 | 38.61 | 38.43 | 39.41 | 41.10 |
| $TiO_2$ | 0.14 | 0.16 | 0.07 | 0.24 | 0.23 | 0.09 | 0.36 | 0.37 | 0.36 | 0.25 |
| $Al_2O_3$ | 11.20 | 12.56 | 12.42 | 13.01 | 12.98 | 14.18 | 12.91 | 13.14 | 1.93 | 9.76 |
| $Cr_2O_3$ | - | - | 0.02 | - | - | 0.02 | 0.04 | 0.05 | 0.02 | 4.00 |
| $Fe_2O_3$ | 5.74 | 4.27 | 0.68 | 0.74 | 7.51 | 6.86 | 5.74 | 4.98 | - | 3.14 |
| FeO | 12.67 | 14.73 | 17.35 | 16.37 | 12.34 | 12.44 | 20.37 | 20.78 | 28.18 | 19.34 |
| MnO | 0.65 | 0.67 | 0.66 | 0.72 | 0.74 | 0.72 | 0.79 | 0.69 | 0.48 | 0.51 |
| MgO | 10.93 | 9.65 | 9.75 | 9.74 | 9.80 | 9.57 | 4.97 | 4.54 | 4.13 | 4.96 |
| ZnO | - | - | - | - | - | - | - | - | - | |
| CaO | 12.11 | 12.34 | 13.58 | 12.22 | 12.04 | 12.16 | 11.87 | 11.59 | 11.28 | 11.37 |
| $Na_2O$ | 2.03 | 1.91 | 1.60 | 1.92 | 1.84 | 1.79 | 1.63 | 1.74 | 1.43 | 1.49 |
| $K_2O$ | 1.71 | 1.93 | 1.85 | 1.97 | 1.96 | 2.13 | 2.08 | 1.83 | 2.22 | 1.74 |
| $H_2O$ | 1.33 | 1.27 | 1.54 | 1.32 | 1.37 | 1.39 | 1.28 | 1.23 | 1.19 | 1.28 |
| F | 1.20 | 1.30 | 0.81 | 1.17 | 1.06 | 1.10 | 0.77 | 0.78 | 0.63 | 0.73 |
| Cl | 0.35 | 0.38 | 0.23 | 0.40 | 0.38 | 0.26 | 1.00 | 1.17 | 1.52 | 1.05 |
| O=F | 0.51 | 0.55 | 0.34 | 0.49 | 0.45 | 0.46 | 0.32 | 0.33 | 0.27 | 0.31 |
| O=Cl | 0.08 | 0.09 | 0.05 | 0.09 | 0.09 | 0.06 | 0.22 | 0.26 | 0.34 | 0.24 |
| Total | 101.81 | 101.69 | 101.61 | 100.07 | 102.13 | 102.08 | 101.86 | 100.73 | 92.19 | 100.19 |
| | | | | | Cation allocation based on 22 oxygen, 2(OH) | | | | | |
| Si IV | 6.30 | 6.18 | 6.24 | 5.63 | 6.03 | 5.95 | 6.01 | 6.04 | 7.10 | 6.15 |
| Al IV | 1.70 | 1.82 | 1.76 | 2.12 | 1.97 | 2.05 | 1.99 | 1.96 | 0.41 | 1.72 |
| $Fe^{+3}$ | 0.00 | 0.00 | 0.00 | 0.25 | 0.00 | 0.00 | 0.00 | 0.00 | 0.00 | 0.13 |
| Ti IV | - | - | - | - | - | - | - | - | 0.05 | - |
| Al VI | 0.26 | 0.40 | 0.45 | - | 0.31 | 0.44 | 0.37 | 0.47 | - | - |
| $Fe^{+3}$ | 0.64 | 0.48 | 0.08 | 0.76 | 0.84 | 0.77 | 0.67 | 0.59 | 0.00 | 0.90 |
| Ti | 0.02 | 0.02 | 0.01 | 0.03 | 0.03 | 0.01 | 0.04 | 0.04 | - | 0.03 |
| Cr | - | - | 0.00 | - | - | 0.00 | 0.00 | 0.01 | 0.00 | 0.47 |
| Mg | 2.42 | 2.16 | 2.19 | 2.01 | 2.18 | 2.13 | 1.15 | 1.06 | 1.11 | 1.11 |
| $Fe^{+2}$ | 1.58 | 1.85 | 2.19 | 2.12 | 1.54 | 1.55 | 2.65 | 2.73 | 3.89 | 2.42 |
| Zn | - | - | - | - | - | - | - | - | - | - |
| Mn | 0.08 | 0.09 | 0.08 | 0.08 | 0.09 | 0.09 | 0.10 | 0.09 | - | 0.07 |
| Ca | 0.00 | - | - | 0.00 | - | 0.00 | - | 0.00 | - | - |
| M1,2,3 | 5.00 | 5.00 | 5.00 | 5.00 | 5.00 | 5.00 | 5.00 | 5.00 | 5.00 | 5.00 |
| Mg | 0.00 | 0.00 | 0.00 | 0.00 | 0.00 | 0.00 | 0.00 | 0.00 | 0.00 | 0.00 |
| $Fe^{+2}$ | 0.00 | 0.00 | 0.00 | 0.00 | 0.00 | 0.00 | 0.00 | 0.00 | 0.36 | 0.00 |
| Zn | - | - | - | - | - | - | - | - | - | - |
| Mn | - | 0.00 | 0.00 | - | 0.00 | - | 0.00 | - | 0.07 | 0.00 |
| Ca | 1.93 | 1.99 | 2.00 | 1.81 | 1.93 | 1.94 | 1.98 | 1.95 | 1.56 | 1.82 |
| Na | 0.07 | 0.01 | - | 0.19 | 0.07 | 0.06 | 0.02 | 0.05 | - | 0.18 |
| M4 site | 2.00 | 2.00 | 2.00 | 2.00 | 2.00 | 2.00 | 2.00 | 2.00 | 2.00 | 2.00 |
| Ca | 0.00 | - | 0.19 | 0.00 | - | 0.00 | - | 0.00 | 0.61 | - |
| Na | 0.52 | 0.54 | 0.47 | 0.32 | 0.46 | 0.46 | 0.47 | 0.48 | 0.50 | 0.26 |
| K | 0.32 | 0.37 | 0.35 | 0.35 | 0.37 | 0.41 | 0.41 | 0.37 | 0.51 | 0.33 |
| O | 22.03 | 22.02 | 22.00 | 22.18 | 22.04 | 22.03 | 22.03 | 22.01 | 21.75 | 22.11 |
| OH | 1.32 | 1.27 | 1.55 | 1.22 | 1.37 | 1.38 | 1.33 | 1.29 | 1.43 | 1.28 |
| F | 0.57 | 0.62 | 0.39 | 0.51 | 0.50 | 0.52 | 0.38 | 0.39 | 0.36 | 0.35 |
| Cl | 0.09 | 0.10 | 0.06 | 0.09 | 0.10 | 0.07 | 0.26 | 0.31 | 0.46 | 0.27 |

## APPENDIX IV. Continued.

**Ampibole**

| S. No. | S202 | S202 | S202 | S202 | S202 | S202 |
|---|---|---|---|---|---|---|
| An. No. | 5.00 | 6.00 | 7.00 | 8.00 | 9.00 | 10.00 |
| | | | Oxide composition (wt. %) | | | |
| $SiO_2$ | 38.94 | 39.12 | 39.28 | 39.24 | 42.67 | 40.27 |
| $TiO_2$ | 0.33 | 0.16 | 0.07 | 0.39 | 0.19 | 0.27 |
| $Al_2O_3$ | 11.19 | 13.26 | 12.90 | 11.81 | 8.81 | 9.86 |
| $Cr_2O_3$ | 0.04 | 0.05 | 0.04 | 0.07 | 0.03 | 0.04 |
| $Fe_2O_3$ | 7.48 | 8.58 | 7.94 | 7.57 | 5.85 | 7.43 |
| FeO | 21.59 | 18.11 | 17.75 | 20.82 | 23.06 | 22.37 |
| MnO | 0.45 | 0.66 | 0.73 | 0.58 | 0.67 | 0.52 |
| MgO | 4.16 | 5.10 | 5.83 | 4.30 | 4.11 | 3.98 |
| ZnO | - | - | - | - | - | - |
| CaO | 11.29 | 11.23 | 11.56 | 11.36 | 11.02 | 11.15 |
| $Na_2O$ | 1.41 | 1.56 | 1.67 | 1.58 | 1.11 | 1.43 |
| $K_2O$ | 2.38 | 2.01 | 1.89 | 1.85 | 1.89 | 1.97 |
| $H_2O$ | 1.24 | 1.42 | 1.26 | 1.29 | 1.42 | 1.25 |
| F | 0.46 | 0.55 | 0.98 | 0.72 | 0.31 | 0.51 |
| Cl | 1.61 | 0.91 | 0.74 | 1.00 | 1.31 | 1.51 |
| O=F | 0.20 | 0.23 | 0.41 | 0.30 | 0.13 | 0.21 |
| O=Cl | 0.36 | 0.21 | 0.17 | 0.22 | 0.30 | 0.34 |
| Total | 101.99 | 102.27 | 102.06 | 102.05 | 102.01 | 101.99 |
| | | | Cation allocation based on 22 oxygen, 2(OH) | | | |
| Si IV | 6.12 | 6.01 | 6.03 | 6.11 | 6.64 | 6.32 |
| Al IV | 1.88 | 1.99 | 1.97 | 1.89 | 1.36 | 1.68 |
| $Fe^{+3}$ | 0.00 | 0.00 | 0.00 | 0.00 | 0.00 | 0.00 |
| Ti IV | - | - | - | - | - | - |
| Al VI | 0.20 | 0.41 | 0.36 | 0.27 | 0.25 | 0.15 |
| $Fe^{+3}$ | 0.88 | 0.99 | 0.92 | 0.89 | 0.68 | 0.88 |
| Ti | 0.04 | 0.02 | 0.01 | 0.05 | 0.02 | 0.03 |
| Cr | 0.00 | 0.01 | 0.00 | 0.01 | 0.00 | 0.00 |
| Mg | 0.98 | 1.17 | 1.33 | 1.00 | 0.95 | 0.93 |
| $Fe^{+2}$ | 2.84 | 2.33 | 2.28 | 2.71 | 3.00 | 2.94 |
| Zn | - | - | - | - | - | - |
| Mn | 0.06 | 0.09 | 0.10 | 0.08 | 0.09 | 0.07 |
| Ca | 0.00 | 0.00 | 0.00 | - | 0.00 | 0.00 |
| M1,2,3 | 5.00 | 5.00 | 5.00 | 5.00 | 5.00 | 5.00 |
| Mg | 0.00 | 0.00 | 0.00 | 0.00 | 0.00 | 0.00 |
| $Fe^{+2}$ | 0.00 | 0.00 | 0.00 | 0.00 | 0.00 | 0.00 |
| Zn | - | - | - | - | - | - |
| Mn | - | - | - | 0.00 | - | - |
| Ca | 1.90 | 1.85 | 1.90 | 1.89 | 1.84 | 1.88 |
| Na | 0.10 | 0.15 | 0.10 | 0.11 | 0.16 | 0.12 |
| M4 site | 2.00 | 2.00 | 2.00 | 2.00 | 2.00 | 2.00 |
| Ca | 0.00 | 0.00 | 0.00 | - | 0.00 | 0.00 |
| Na | 0.33 | 0.31 | 0.40 | 0.37 | 0.17 | 0.31 |
| K | 0.48 | 0.39 | 0.37 | 0.37 | 0.38 | 0.39 |
| O | 22.04 | 22.04 | 22.04 | 22.04 | 22.03 | 22.04 |
| OH | 1.30 | 1.45 | 1.29 | 1.34 | 1.47 | 1.31 |
| F | 0.23 | 0.27 | 0.48 | 0.35 | 0.15 | 0.25 |
| Cl | 0.43 | 0.24 | 0.19 | 0.26 | 0.34 | 0.40 |

## APPENDIX IV. Continued.

**Calcite**

| S. No. | S19 | S19 | S19 | S19 | S19 | S19 |
|---|---|---|---|---|---|---|
| An. No. | 1 | 2 | 3 | 4 | 5 | 6 |
| | | | Oxide composition (wt. %) | | | |
| MgO | 0.57 | 0.59 | 0.58 | 0.69 | 0.65 | 0.67 |
| CaO | 54.33 | 53.13 | 54.38 | 54.34 | 54.25 | 54.42 |
| MnO | 0.00 | 0.00 | 0.04 | 0.00 | 0.00 | 0.00 |
| FeO | 0.03 | 0.07 | 0.06 | 0.03 | 0.00 | 0.02 |
| ZnO | 0.09 | 0.00 | 0.04 | 0.00 | 0.00 | 0.10 |
| SrO | 0.00 | 0.02 | 0.00 | 0.03 | 0.00 | 0.00 |
| BaO | 0.05 | 0.02 | 0.00 | 0.00 | 0.00 | 0.08 |
| $CO_2$* | 43.33 | 42.39 | 43.39 | 43.43 | 43.28 | 43.52 |
| Total* | 98.39 | 96.22 | 98.49 | 98.52 | 98.18 | 98.80 |

* Calculated

| | Apatite | | | | | Sphene | |
|---|---|---|---|---|---|---|---|
| S. No. | S35 | S35 | S12 | S12 | S12 | S18B | S18B |
| An. No. | 1 | 2 | 1 | 2 | 3 | 1 | 2 |
| | | | Oxide composition (wt. %) | | | | |
| $SiO_2$ | 0.27 | 0.36 | 29.48 | 29.55 | 29.08 | 29.90 | 30.08 |
| $TiO_2$ | - | - | 32.76 | 32.12 | 32.10 | 24.83 | 29.09 |
| $Al_2O_3$ | - | - | 2.07 | 2.35 | 2.35 | 5.91 | 5.01 |
| $Cr_2O_3$ | - | - | 0.04 | 0.00 | 0.01 | 0.00 | 0.00 |
| FeO | 0.07 | 0.06 | 2.20 | 2.60 | 2.60 | 2.72 | 1.78 |
| NiO | - | - | 0.00 | 0.00 | 0.01 | 0.07 | 0.19 |
| MnO | - | - | 0.09 | 0.09 | 0.22 | 0.04 | 0.00 |
| MgO | 0.00 | 0.00 | 0.05 | 0.10 | 0.11 | 0.28 | 0.11 |
| CaO | 53.82 | 53.29 | 27.36 | 27.06 | 27.02 | 27.83 | 28.63 |
| SrO | 0.00 | 0.00 | - | - | - | - | - |
| BaO | 0.03 | 0.04 | - | - | - | - | - |
| $Na_2O$ | - | - | 0.04 | 0.02 | 0.03 | 0.00 | 0.01 |
| $K_2O$ | - | - | 0.02 | 0.00 | 0.03 | 0.00 | 0.01 |
| $P_2O_5$ | 42.81 | 43.38 | 0.38 | 0.57 | 0.50 | 0.57 | 0.55 |
| $SO_3$ | - | - | 0.00 | 0.00 | 0.00 | 0.11 | 0.11 |
| $H_2O$ | - | - | - | - | - | - | - |
| Cl | 0.03 | 0.06 | 0.00 | 0.01 | 0.01 | 0.02 | 0.01 |
| F | 5.15 | 4.88 | - | - | - | - | - |
| Total | 102.17 | 102.07 | 94.50 | 94.48 | 94.07 | 92.16 | 95.47 |
| O=F | -2.17 | -2.06 | - | - | - | - | - |
| O=Cl | -0.01 | -0.01 | - | - | - | - | - |
| Calc. Total | 100.00 | 100.00 | - | - | - | - | - |

## APPENDIX IV. Continued.

**Scheelite**

| S. No. | BS1 | BS1 | BS1 | BS1 | BS1 | BS1 | BS1 | BS1 | BS1 | BS1 |
|---|---|---|---|---|---|---|---|---|---|---|
| An. No. | A1 (rim) | A2 | A3 | A4 | A5 | A6 | A7 | A8 | A9 | A10 |
| | | | | | Oxide composition (wt. %) | | | | | |
| MnO | 0.04 | 0.00 | 0.00 | 0.01 | 0.00 | 0.00 | 0.00 | 0.04 | 0.01 | 0.00 |
| FeO | 0.00 | 0.00 | 0.02 | 0.00 | 0.01 | 0.00 | 0.00 | 0.00 | 0.01 | 0.05 |
| CaO | 20.46 | 20.19 | 20.53 | 20.44 | 13.18 | 20.52 | 20.62 | 20.80 | 20.82 | 20.54 |
| $MoO_3$ | 0.98 | 1.06 | 1.07 | 1.03 | 0.94 | 1.78 | 2.04 | 1.96 | 1.95 | 1.50 |
| $WO_3$ | 75.65 | 75.20 | 75.63 | 74.87 | 49.42 | 74.38 | 74.29 | 74.57 | 74.49 | 75.07 |
| PbO | 0.00 | 0.00 | 0.37 | 0.04 | 0.02 | 0.30 | 0.26 | 0.00 | 0.00 | 0.00 |
| Total | 97.13 | 96.45 | 97.62 | 96.40 | 63.56 | 96.98 | 97.22 | 97.36 | 97.28 | 97.15 |
| | | | | | Number of cations based on 4 oxygen | | | | | |
| Mn | 0.00 | 0.00 | 0.00 | 0.00 | 0.00 | 0.00 | 0.00 | 0.00 | 0.00 | 0.00 |
| Fe | 0.00 | 0.00 | 0.00 | 0.00 | 0.00 | 0.00 | 0.00 | 0.00 | 0.00 | 0.00 |
| Ca | 1.07 | 1.06 | 1.07 | 1.08 | 1.05 | 1.07 | 1.07 | 1.08 | 1.08 | 1.07 |
| Mo | 0.06 | 0.06 | 0.07 | 0.06 | 0.09 | 0.11 | 0.12 | 0.12 | 0.12 | 0.09 |
| W | 2.87 | 2.87 | 2.86 | 2.86 | 2.86 | 2.82 | 2.80 | 2.80 | 2.80 | 2.84 |
| Pb | 0.00 | 0.00 | 0.00 | 0.00 | 0.00 | 0.00 | 0.00 | 0.00 | 0.00 | 0.00 |
| | | | | | Powellite (mole %) | | | | | |
| Mo/Mo+W | 2.04 | 2.21 | 2.23 | 2.17 | 2.96 | 3.71 | 4.24 | 4.06 | 4.05 | 3.12 |

**Scheelite**

| S. No. | BS1 | BS1 | BS1 | BS1 | BS1 | BS1 | BS1 | BS1 | BS1 | BS1 |
|---|---|---|---|---|---|---|---|---|---|---|
| An. No. | A11 | A12 | A13 | A14 | A15 | A16 | A17 | A18 | A19 | A20 (rim) |
| | | | | | Oxide composition (%) | | | | | |
| MnO | 0.00 | 0.00 | 0.04 | 0.00 | 0.05 | 0.00 | 0.00 | 0.00 | 0.00 | 0.00 |
| FeO | 0.00 | 0.00 | 0.00 | 0.01 | 0.00 | 0.01 | 0.00 | 0.00 | 0.00 | 0.00 |
| CaO | 20.77 | 20.52 | 20.60 | 20.66 | 20.11 | 20.25 | 20.82 | 20.55 | 20.59 | 20.67 |
| $MoO_3$ | 1.35 | 1.32 | 1.21 | 1.16 | 1.28 | 1.88 | 2.09 | 1.81 | 1.27 | 1.10 |
| $WO_3$ | 75.61 | 75.54 | 75.64 | 75.42 | 74.26 | 72.28 | 73.80 | 75.01 | 75.24 | 75.70 |
| PbO | 0.12 | 0.22 | 0.22 | 0.00 | 0.00 | 0.00 | 0.00 | 0.01 | 0.19 | 0.00 |
| Total | 97.85 | 97.06 | 97.70 | 97.25 | 95.70 | 94.41 | 96.71 | 97.38 | 97.29 | 97.47 |
| | | | | | Number of cations based on 4 oxygen | | | | | |
| Mn | 0.00 | 0.00 | 0.00 | 0.00 | 0.00 | 0.00 | 0.00 | 0.00 | 0.00 | 0.00 |
| Fe | 0.00 | 0.00 | 0.00 | 0.00 | 0.00 | 0.00 | 0.00 | 0.00 | 0.00 | 0.00 |
| Ca | 1.08 | 1.07 | 1.07 | 1.08 | 1.06 | 1.08 | 1.08 | 1.07 | 1.07 | 1.08 |
| Mo | 0.08 | 0.08 | 0.07 | 0.07 | 0.08 | 0.12 | 0.13 | 0.11 | 0.08 | 0.07 |
| W | 2.84 | 2.85 | 2.85 | 2.85 | 2.85 | 2.80 | 2.79 | 2.82 | 2.85 | 2.86 |
| Pb | 0.00 | 0.00 | 0.00 | 0.00 | 0.00 | 0.00 | 0.00 | 0.00 | 0.00 | 0.00 |
| | | | | | Powellite (mole %) | | | | | |
| Mo/Mo+W | 2.80 | 2.74 | 2.50 | 2.42 | 2.71 | 4.01 | 4.36 | 3.73 | 2.64 | 2.29 |

## APPENDIX IV. Continued.

**Scheelite**

| S. No. | BS1 | BS1 | BS1 | BS1 | BS1 | BS1 | BS1 | BS1 | BS1 | BS1 |
|---|---|---|---|---|---|---|---|---|---|---|
| An. No. | B1(rim) | B2 | B3 | B4 | B5 | B6 | B7 | B8 | B9 | B10 |
| | | | | | Oxide composition (wt. %) | | | | | |
| MnO | 0.00 | 0.00 | 0.00 | 0.00 | 0.00 | 0.01 | 0.00 | 0.00 | 0.00 | 0.02 |
| FeO | 0.02 | 0.00 | 0.00 | 0.00 | 0.01 | 0.00 | 0.00 | 0.00 | 0.02 | 0.00 |
| CaO | 20.93 | 20.75 | 20.96 | 20.94 | 20.74 | 20.62 | 20.71 | 20.86 | 20.86 | 20.81 |
| $MoO_3$ | 2.55 | 2.62 | 2.57 | 2.37 | 2.26 | 2.38 | 2.72 | 2.62 | 2.88 | 2.47 |
| $WO_3$ | 74.54 | 74.95 | 74.91 | 74.84 | 74.91 | 74.43 | 74.29 | 74.77 | 74.73 | 74.64 |
| PbO | 0.00 | 0.19 | 0.03 | 0.06 | 0.00 | 0.00 | 0.00 | 0.00 | 0.31 | 0.00 |
| Total | 98.04 | 98.51 | 98.47 | 98.22 | 97.92 | 97.44 | 97.73 | 98.25 | 98.79 | 97.93 |
| | | | | | Number of cations based on 4 oxygen | | | | | |
| Mn | 0.00 | 0.00 | 0.00 | 0.00 | 0.00 | 0.00 | 0.00 | 0.00 | 0.00 | 0.00 |
| Fe | 0.00 | 0.00 | 0.00 | 0.00 | 0.00 | 0.00 | 0.00 | 0.00 | 0.00 | 0.00 |
| Ca | 1.07 | 1.06 | 1.07 | 1.07 | 1.07 | 1.07 | 1.06 | 1.07 | 1.06 | 1.07 |
| Mo | 0.15 | 0.16 | 0.15 | 0.14 | 0.14 | 0.14 | 0.16 | 0.16 | 0.17 | 0.15 |
| W | 2.77 | 2.78 | 2.78 | 2.78 | 2.80 | 2.79 | 2.77 | 2.78 | 2.76 | 2.78 |
| Pb | 0.00 | 0.00 | 0.00 | 0.00 | 0.00 | 0.00 | 0.00 | 0.00 | 0.00 | 0.00 |
| | | | | | Powellite (mole %) | | | | | |
| Mo/Mo+W | 5.21 | 5.34 | 5.23 | 4.85 | 4.64 | 4.89 | 5.58 | 5.34 | 5.84 | 5.06 |

**Scheelite**

| S. No. | BS1 | BS1 | BS1 | BS1 | BS1 | BS1 | BS1 | BS1 | BS1 | BS1 |
|---|---|---|---|---|---|---|---|---|---|---|
| An. No. | B11 | B12 | B13 | B14 | B15 (centre) | B16 | B17 | B18 | B19 | B20 |
| | | | | | Oxide composition (wt. %) | | | | | |
| MnO | 0.00 | 0.00 | 0.02 | 0.00 | 0.00 | 0.00 | 0.00 | 0.00 | 0.00 | 0.00 |
| FeO | 0.00 | 0.00 | 0.00 | 0.00 | 0.01 | 0.00 | 0.00 | 0.00 | 0.00 | 0.01 |
| CaO | 20.89 | 20.81 | 20.80 | 20.71 | 20.59 | 20.77 | 20.72 | 20.77 | 20.74 | 20.68 |
| $MoO_3$ | 2.73 | 2.69 | 2.80 | 2.64 | 1.73 | 2.40 | 2.13 | 2.11 | 1.97 | 2.18 |
| $WO_3$ | 74.79 | 74.53 | 74.59 | 74.60 | 75.79 | 75.00 | 75.19 | 74.94 | 74.87 | 75.09 |
| PbO | 0.00 | 0.04 | 0.08 | 0.15 | 0.23 | 0.00 | 0.35 | 0.00 | 0.00 | 0.04 |
| Total | 98.42 | 98.07 | 98.28 | 98.11 | 98.35 | 98.17 | 98.38 | 97.82 | 97.59 | 98.01 |
| | | | | | Number of cations based on 4 oxygen | | | | | |
| Mn | 0.00 | 0.00 | 0.00 | 0.00 | 0.00 | 0.00 | 0.00 | 0.00 | 0.00 | 0.00 |
| Fe | 0.00 | 0.00 | 0.00 | 0.00 | 0.00 | 0.00 | 0.00 | 0.00 | 0.00 | 0.00 |
| Ca | 1.07 | 1.07 | 1.06 | 1.06 | 1.06 | 1.07 | 1.06 | 1.07 | 1.07 | 1.06 |
| Mo | 0.16 | 0.16 | 0.17 | 0.16 | 0.10 | 0.14 | 0.13 | 0.13 | 0.12 | 0.13 |
| W | 2.77 | 2.77 | 2.77 | 2.78 | 2.83 | 2.79 | 2.80 | 2.80 | 2.81 | 2.80 |
| Pb | 0.00 | 0.00 | 0.00 | 0.00 | 0.00 | 0.00 | 0.00 | 0.00 | 0.00 | 0.00 |
| | | | | | Powellite (mole %) | | | | | |
| Mo/Mo+W | 5.56 | 5.50 | 5.71 | 5.40 | 3.55 | 4.90 | 4.36 | 4.33 | 4.06 | 4.47 |

## APPENDIX IV. Continued.

**Scheelite**

| S. No. | BS1 | BS1 | BS1 | BS1 | BS1 | BS1 | BS1 | BS1 | BS1 | BS1 |
|---|---|---|---|---|---|---|---|---|---|---|
| An. No. | B21 (centre) | B22 | B23 | B24 | B25 | B26 | B27 | B28 | B29 | B30 (rim) |
| | | | | Oxide composition (wt. %) | | | | | | |
| MnO | 0.02 | 0.00 | 0.00 | 0.00 | 0.00 | 0.01 | 0.00 | 0.00 | 0.00 | 0.00 |
| FeO | 0.00 | 0.01 | 0.00 | 0.02 | 0.00 | 0.02 | 0.01 | 0.00 | 0.06 | 0.27 |
| CaO | 20.65 | 20.72 | 20.92 | 20.71 | 20.34 | 20.55 | 20.56 | 20.78 | 20.06 | 19.73 |
| $MoO_3$ | 2.06 | 2.01 | 2.20 | 2.13 | 0.61 | 1.72 | 2.52 | 2.16 | 0.42 | 0.16 |
| $WO_3$ | 75.28 | 75.09 | 74.88 | 75.13 | 76.87 | 75.46 | 74.76 | 75.16 | 75.42 | 75.31 |
| PbO | 0.27 | 0.00 | 0.00 | 0.49 | 0.00 | 0.33 | 0.00 | 0.00 | 0.20 | 0.00 |
| Total | 98.28 | 97.83 | 97.99 | 98.47 | 97.81 | 98.09 | 97.84 | 98.10 | 96.15 | 95.46 |
| | | | | Number of cations based on 4 oxygen | | | | | | |
| Mn | 0.00 | 0.00 | 0.00 | 0.00 | 0.00 | 0.00 | 0.00 | 0.00 | 0.00 | 0.01 |
| Fe | 0.00 | 0.00 | 0.00 | 0.00 | 0.00 | 0.00 | 0.00 | 0.00 | 0.00 | 0.01 |
| Ca | 1.06 | 1.07 | 1.08 | 1.06 | 1.06 | 1.06 | 1.06 | 1.07 | 1.06 | 1.06 |
| Mo | 0.12 | 0.12 | 0.13 | 0.13 | 0.04 | 0.10 | 0.15 | 0.13 | 0.03 | 0.01 |
| W | 2.81 | 2.81 | 2.79 | 2.80 | 2.90 | 2.83 | 2.79 | 2.80 | 2.90 | 2.92 |
| Pb | 0.00 | 0.00 | 0.00 | 0.01 | 0.00 | 0.00 | 0.00 | 0.00 | 0.00 | 0.00 |
| | | | | Powellite (mole %) | | | | | | |
| Mo/Mo+W | 4.23 | 4.13 | 4.52 | 4.37 | 1.26 | 3.54 | 5.15 | 4.43 | 0.88 | 0.34 |

**Scheelite**

| S. No. | 105323 | 105323 | 105323 | 105328 | 105328 | S202 | S202 | S202 | S202 |
|---|---|---|---|---|---|---|---|---|---|
| An. No. | 1 | 2 | 3 | 1 | 2 | 1 | 2 | 3 | 4 |
| | | | | Oxide composition (wt. %) | | | | | |
| MnO | 0.00 | 0.00 | 0.00 | 0.00 | 0.00 | 0.00 | 0.03 | 0.05 | 0.04 |
| FeO | 0.00 | 0.01 | 0.01 | 0.00 | 0.00 | 0.00 | 0.02 | 0.00 | 0.00 |
| CaO | 19.92 | 19.91 | 19.66 | 20.08 | 20.11 | 20.34 | 20.60 | 19.96 | 19.88 |
| $MoO_3$ | 0.30 | 1.35 | 0.37 | 3.10 | 2.74 | | | | |
| $WO_3$ | 76.14 | 76.14 | 76.29 | 73.45 | 74.83 | 76.06 | 76.10 | 76.97 | 76.86 |
| PbO | 0.21 | 0.00 | 0.02 | 0.00 | 0.33 | | | | |
| Total | 96.56 | 97.42 | 96.34 | 96.63 | 98.02 | 96.40 | 96.76 | 96.98 | 96.78 |
| | | | | Number of cations based on 4 oxygen | | | | | |
| Mn | 0.00 | 0.00 | 0.00 | 0.00 | 0.00 | 0.00 | 0.00 | 0.00 | 0.00 |
| Fe | 0.00 | 0.00 | 0.00 | 0.00 | 0.00 | 0.00 | 0.00 | 0.00 | 0.00 |
| Ca | 1.05 | 1.04 | 1.04 | 1.04 | 1.04 | 1.08 | 1.09 | 1.05 | 1.05 |
| Mo | 0.02 | 0.08 | 0.02 | 0.19 | 0.16 | 0.00 | 0.00 | 0.00 | 0.00 |
| W | 2.92 | 2.88 | 2.93 | 2.77 | 2.80 | 2.92 | 2.91 | 2.95 | 2.95 |
| Pb | 0.00 | 0.00 | 0.00 | 0.00 | 0.00 | 0.00 | 0.00 | 0.00 | 0.00 |
| | | | | Powellite (mole %) | | | | | |
| Mo/Mo+W | 0.63 | 2.78 | 0.76 | 6.37 | 5.57 | 0.00 | 0.00 | 0.00 | 0.00 |

## APPENDIX IV. Continued.

**Magnetite**

| S. No. | 105339 | 105339 | 105339 | 105341 | 105341 | 105341 | S16 | S16 | S17 | S17 |
|---|---|---|---|---|---|---|---|---|---|---|
| An. No. | 1 | 2 | 3 | 1 | 2 | 3 | 1 | 2 | 1 | 2 |
| | | | | | Oxide composition (wt. %) | | | | | |
| MgO | 0.13 | 0.05 | 0.08 | 0.22 | 0.22 | 0.06 | 0.14 | 0.22 | 0.05 | 0.15 |
| CaO | 0.00 | 0.10 | 0.01 | 0.15 | 0.22 | 0.07 | 0.02 | 0.03 | 0.00 | 0.22 |
| $Cr_2O_3$ | 0.01 | 0.00 | 0.01 | 0.04 | 0.02 | 0.00 | 0.00 | 0.03 | 0.00 | 0.00 |
| MnO | 0.51 | 0.45 | 0.44 | 0.76 | 0.72 | 0.79 | 0.69 | 0.76 | 0.33 | 0.20 |
| FeO | 30.22 | 29.18 | 30.51 | 28.24 | 27.89 | 29.78 | 29.80 | 29.57 | 29.97 | 30.32 |
| NiO | 0.00 | 0.00 | 0.00 | 0.00 | 0.00 | 0.01 | 0.05 | 0.00 | 0.01 | 0.03 |
| ZnO | 0.00 | 0.02 | 0.00 | 0.05 | 0.07 | 0.10 | 0.00 | 0.00 | 0.03 | 0.06 |
| $Fe_2O_3$ | 68.80 | 66.07 | 69.09 | 65.30 | 64.44 | 68.17 | 68.32 | 68.27 | 67.54 | 68.44 |
| TOTAL | 99.67 | 95.86 | 100.14 | 94.75 | 93.57 | 98.98 | 99.01 | 98.88 | 97.92 | 99.42 |

**Magnetite**

| S. No. | S17 | S17 | S17 | S17 | S18B | S18B | S18B | S18B | S18B | S18B |
|---|---|---|---|---|---|---|---|---|---|---|
| An. No. | 3 | 4 | 5 | 6 | 1 | 2 | 3 | 4 | 5 | 6 |
| | | | | | Oxide composition (wt. %) | | | | | |
| MgO | 0.06 | 0.04 | 0.30 | 0.06 | 0.19 | 0.17 | 0.31 | 0.16 | 0.23 | 0.28 |
| CaO | 0.04 | 0.04 | 0.37 | 0.01 | 0.00 | 0.01 | 0.01 | 0.00 | 0.02 | 0.03 |
| $Cr_2O_3$ | 0.02 | 0.00 | 0.00 | 0.00 | 0.00 | 0.00 | 0.01 | 0.02 | 0.01 | 0.00 |
| MnO | 0.31 | 0.41 | 0.33 | 0.33 | 1.32 | 1.00 | 0.72 | 0.79 | 0.74 | 0.79 |
| FeO | 30.44 | 30.18 | 29.49 | 30.18 | 29.12 | 29.67 | 29.53 | 29.65 | 29.75 | 29.46 |
| NiO | 0.00 | 0.05 | 0.00 | 0.02 | 0.00 | 0.05 | 0.00 | 0.00 | 0.00 | 0.00 |
| ZnO | 0.00 | 0.06 | 0.04 | 0.10 | 0.25 | 0.15 | 0.19 | 0.23 | 0.07 | 0.24 |
| $Fe_2O_3$ | 68.57 | 68.18 | 67.48 | 68.06 | 68.46 | 68.86 | 68.49 | 68.30 | 68.71 | 68.38 |
| TOTAL | 99.44 | 98.97 | 98.01 | 98.76 | 99.35 | 99.91 | 99.25 | 99.15 | 99.54 | 99.19 |

**Magnetite**

| S. No. | S19 | S19 | S19 | S19 | S35 | S35 | S35 | S35 | S37 | S37 |
|---|---|---|---|---|---|---|---|---|---|---|
| An. No. | 1 | 2 | 3 | 4 | 1 | 2 | 3 | 4 | 1 | 2 |
| | | | | | Oxide composition (wt. %) | | | | | |
| MgO | 0.18 | 0.08 | 0.22 | 0.22 | 0.27 | 0.27 | 0.43 | 0.43 | 0.37 | 0.28 |
| CaO | 0.00 | 0.00 | 0.00 | 0.01 | 0.00 | 0.00 | 0.00 | 0.00 | 0.00 | 0.00 |
| $Cr_2O_3$ | 0.00 | 0.00 | 0.00 | 0.00 | 0.00 | 0.00 | 0.00 | 0.00 | 0.01 | 0.02 |
| MnO | 0.51 | 0.40 | 0.60 | 0.64 | 0.68 | 0.75 | 1.33 | 1.28 | 1.08 | 0.86 |
| FeO | 29.70 | 29.78 | 29.21 | 29.32 | 29.71 | 29.62 | 28.66 | 28.59 | 28.73 | 29.46 |
| NiO | 0.00 | 0.07 | 0.11 | 0.03 | 0.00 | 0.01 | 0.00 | 0.00 | 0.00 | 0.00 |
| ZnO | 0.13 | 0.00 | 0.12 | 0.03 | 0.14 | 0.13 | 0.09 | 0.17 | 0.10 | 0.18 |
| $Fe_2O_3$ | 67.89 | 67.41 | 67.13 | 67.50 | 68.62 | 68.61 | 68.42 | 68.14 | 67.74 | 68.53 |
| TOTAL | 98.42 | 97.73 | 97.38 | 97.76 | 99.42 | 99.40 | 98.93 | 98.62 | 98.02 | 99.33 |

## APPENDIX IV. Continued.

**Magnetite**

| S. No. | S37 | S37 | S38 | S38 | S38 | S38 | S38 | S38 |
|---|---|---|---|---|---|---|---|---|
| An. No. | 3 | 4 | 1 | 2 | 3 | 4 | 5 | 6 |
| | | | Oxide composition (wt. %) | | | | | |
| MgO | 0.84 | 0.37 | 0.07 | 0.11 | 0.08 | 0.32 | 0.28 | 0.16 |
| CaO | 0.05 | 0.00 | 0.04 | 0.05 | 0.02 | 0.21 | 0.08 | 0.03 |
| $Cr_2O_3$ | 0.03 | 0.00 | 0.04 | 0.00 | 0.00 | 0.01 | 0.01 | 0.07 |
| MnO | 0.99 | 0.92 | 0.23 | 0.35 | 0.19 | 0.26 | 0.43 | 0.47 |
| FeO | 28.08 | 29.15 | 29.93 | 29.94 | 30.30 | 29.66 | 29.30 | 29.72 |
| NiO | 0.01 | 0.01 | 0.01 | 0.02 | 0.05 | 0.06 | 0.00 | 0.00 |
| ZnO | 0.17 | 0.00 | 0.02 | 0.12 | 0.06 | 0.04 | 0.00 | 0.12 |
| $Fe_2O_3$ | 67.95 | 68.32 | 67.29 | 67.75 | 68.09 | 67.75 | 67.19 | 67.66 |
| TOTAL | 98.12 | 98.76 | 97.62 | 98.32 | 98.78 | 98.30 | 97.29 | 98.24 |

**APPENDIX V. Fluid inclusion petrographic and microthermometric data for Stages I-III skarn minerals and granite quartz from the Kara deposit, northwestern Tasmania.**

Salinity values are in equiv. wt % NaCl and were calculated from freezing point depressions and clathration melting temperatures using equations of Bodnar (1993) and Bozzo et al. (1973), respectively.

| S. No. | FI No. | Host mineral. | Shape | Length (μm) | Phases | % Vapour | Occurrence | Type | Abundance | Th (°C) | Tm (°C) | Tm-cl (°C) | Tmf (°C) | Salinity |
|---|---|---|---|---|---|---|---|---|---|---|---|---|---|---|
| **STAGE I MINERAL ASSEMBLAGE** | | | | | | | | | | | | | | |
| S36 | 1 | Clinopyroxene | irregular | 8 | L-V | 10 | isolated | I | common | 510.8 | | | | |
| S36 | 2 | Clinopyroxene | equant | 10 | L-V | 15 | isolated | I | common | 532.1 | | 9.0 | | 2.03 |
| S36 | 3 | Clinopyroxene | oval | 4 | L-V | 5 | isolated | I | common | 512.1 | | | | |
| S36 | 4 | Clinopyroxene | triangular | 10 | L-V | 10 | isolated | I | common | 521.8 | | | | |
| S36 | 5 | Clinopyroxene | irregular | 15 | L-V | 5 | isolated | I | common | 572.8 | | | | |
| S36 | 6 | Clinopyroxene | rectangular | 5 | L-V | 10 | isolated | I | common | 515.5 | | | | |
| S36 | 7 | Clinopyroxene | round | 4 | L-V | 10 | isolated | I | common | >585.3 | | | | |
| S60 | 1 | Clinopyroxene | equant | 21 | L-V | 5 | isolated | I | common | >601 | | | | |
| S60 | 2 | Clinopyroxene | elongated | 9 | L-V | 15 | isolated | I | common | 616.0 | | | | |
| S60 | 3 | Clinopyroxene | irregular | 9 | L-V | 15 | isolated | I | common | >616 | | | | |
| S112 | 4 | Clinopyroxene | spherical | 19 | L-V | 80 | isolated | I | common | 611.0 | | | | |
| S112 | 5 | Clinopyroxene | spherical | 5 | L-V | 10 | isolated | I | common | 600.8 | | 4.3 | | 10.14 |
| **STAGE II MINERAL ASSEMBLAGE** | | | | | | | | | | | | | | |
| S4A | 1 | Scheelite | irregular | 3 | L-V | 10 | isolated | I | rare | 488.6 | | | | |
| S4A | 2 | Scheelite | equant | 7 | L-V(-$CO_2$) | 15 | isolated | III | rare | 575.5 | | 3.0 | | 11.97 |
| S4A | 3 | Scheelite | elongate | 10 | L-V(-$CO_2$) | 10 | isolated | III | rare | 575.5 | | | | |
| S4A | 4 | Scheelite | equant | 6 | L-V | 10 | isolated | I | rare | 356.5 | | | | |
| S4A | 5 | Scheelite | oval | 7 | L-V-D | 15 | isolated | II | rare | 356.7 | | | | |
| S4A | 6 | Scheelite | oval | 10 | L-V-D | 10 | isolated | II | rare | 356.7 | | | | |
| S4A | 7 | Scheelite | irregular | 15 | L-V | 25 | isolated | I | rare | 349.6 | | | | |
| S4A | 8 | Scheelite | elongated | 8 | L-V | 25 | isolated | I | rare | 350.8 | | | | |
| S4A | 9 | Scheelite | triangular | 5 | L-V | 25 | isolated | I | rare | 348.9 | | | | |
| S4A | 1 | Vesuvianite | irregular | 7 | L-V | 5 | isolated | I | rare | 503.0 | | | | |
| S4A | 2 | Vesuvianite | oval | 3 | L-V | 10 | isolated | I | rare | 503.5 | | | | |
| S4A | 3 | Vesuvianite | rounded | 10 | L-V | 10 | isolated | I | rare | 478.0 | | -2.5 | | 17.75 |

**S. No:** Sample number; **FI No:** Serial number of fluid inclusion in a mineral; **L:** Liquid; **V:** Vapour; **D:** Daughter mineral; **Th:** Temperature of homogenisation into liquid phase; **Tm:** Temperature of last ice melting; **Tmf:** Temperature of first ice melting; **Tm-cl:** Clathration temperature.

## APPENDIX V. Continued.

| S. No. | FI No. | Host mineral. | Shape | Length (μm) | Phases | % Vapour | Occurrence | Type | Abundance | Th (°C) | Tm (°C) | Tm-cl (°C) | Tmf (°C) | Salinity |
|---|---|---|---|---|---|---|---|---|---|---|---|---|---|---|
| S35 | 1 | Garnet | irregular | 8 | L-V | 5 | isolated | I | rare | 503.0 | | | | |
| S35 | 2 | Garnet | irregular | 12 | L-V | 10 | isolated | I | rare | 508.6 | | | | |
| S35 | 3 | Garnet | irregular | 10 | L-V | 5 | isolated | I | rare | 464.0 | | | | |
| S60 | 1 | Scheelite | triangular | 6 | L-V-D | 25 | isolated | II | common | 433.0 | | | | |
| S60 | 2 | Scheelite | equant | 12 | L-V-D | 20 | isolated | II | common | 510.0 | | | | |
| S60 | 3 | Scheelite | triangular | 7 | L-V-D | 20 | isolated | II | common | 390.0 | | | | |
| S60 | 4 | Scheelite | irregular | 9 | L-V-D | 20 | isolated | II | common | 528.0 | | | | |
| S60 | 5 | Scheelite | irregular | 12 | L-V-D | 15 | isolated | II | common | 541.0 | | | | |
| S60 | 1 | Vesuvianite | elongated | 10 | L-V | 40 | cluster | I | common | 571.0 | | | | |
| S60 | 2 | Vesuvianite | triangular | 6 | L-V | 25 | cluster | I | common | 428.0 | | | | |
| S60 | 3 | Vesuvianite | equant | 6 | L-V | 10 | cluster | I | common | 548.0 | | | | |
| S66 | 1 | Vesuvianite | elongated | 15 | L-V | 20 | isolated | I | common | 454.7 | | -0.8 | -56.6 | 16.31 |
| S66 | 2 | Vesuvianite | elongated | 9 | L-V | 10 | isolated | I | common | 362.0 | | | | |
| **STAGE III MINERAL ASSEMBLAGE** | | | | | | | | | | | | | | |
| 105308 | 1 | Fluorite | round | 20 | L-V | 15 | isolated | I | common | 298.0 | -4.6 | | | 7.31 |
| 105308 | 2 | Fluorite | elongated | 15 | L-V | 5 | isolated | I | common | 296.0 | | | | |
| 105308 | 3 | Fluorite | irregular | 15 | L-V | 10 | isolated | I | common | 298.0 | -4.3 | | | 6.88 |
| S17 | 1 | Fluorite | elongated | 40 | L-V | 15 | isolated | I | common | 303.7 | | | | |
| S17 | 2 | Fluorite | equant | 30 | L-V | 25 | isolated | I | common | 272.8 | | | | |
| S17 | 3 | Fluorite | elongated | 30 | L-V | 20 | isolated | I | rare | 289.0 | | | | |
| S17 | 4 | Fluorite | equant | 15 | L-V | 15 | isolated | I | rare | 261.9 | | | | |
| S17 | 5 | Fluorite | equant | 20 | L-V (-$CO_2$?) | 20 | isolated | III | common | 323.4 | -2.5 | | | 4.18 |
| S17 | 6 | Fluorite | equant | 20 | L-V (-$CO_2$?) | 20 | isolated | III | common | 334.2 | -11.4 | | | 15.37 |
| S17 | 7 | Fluorite | equant | 15 | L-V | 15 | isolated | I | common | 270.0 | -1.8 | | | 3.06 |
| S17 | 8 | Fluorite | elongated | 16 | L-V | 15 | isolated | I | common | 311.3 | | | | |
| S17 | 9 | Fluorite | elongate | 16 | L-V-D | 15 | isolated | II | rare | 299.5 | | | | |
| S17 | 10 | Fluorite | elongated | 9 | L-V | 15 | isolated | I | common | 298.7 | | | | |
| S17 | 11 | Fluorite | elongated | 15 | L-V | 30 | isolated | I | common | 313.2 | | | | |

**S. No:** Sample number; **FI No:** Serial number of fluid inclusion in a mineral; **L:** Liquid; **V:** Vapour; **D:** Daughter mineral; **Th:** Temperature of homogenisation into liquid phase; **Tm:** Temperature of last ice melting; **Tmf:** Temperature of first ice melting; **Tm-cl:** Clathration temperature.

## APPENDIX V. Continued.

| S. No. | FI No. | Host mineral. | Shape | Length (μm) | Phases | % Vapour | Occurrence | Type | Abundance | Th (°C) | Tm (°C) | Tm-cl (°C) | Tmf (°C) | Salinity |
|---|---|---|---|---|---|---|---|---|---|---|---|---|---|---|
| S18B | 1 | Fluorite | elongated | 22 | L-V-D | 15 | isolated | II | common | 295.3 | -2.2 | | | 3.71 |
| S18B | 2 | Fluorite | elongated | 46 | L-V | 20 | isolated | I | common | 296.0 | -2.6 | | | 4.34 |
| S18B | 3 | Fluorite | elongated | 18 | L-V | 15 | isolated | I | common | 278.0 | -3 | | | 4.96 |
| S18B | 4 | Fluorite | irregular | 28 | L-V | 20 | isolated | I | common | 324.0 | -8.2 | | | 11.93 |
| S18B | 5 | Fluorite | equant | 12 | L-V | 20 | isolated | I | common | 260.0 | -1.1 | | | 1.91 |
| S18B | 6 | Fluorite | elongated | 12 | L-V | 30 | isolated | I | common | 322.6 | -4.5 | | | 7.17 |
| S18B | 7 | Fluorite | rounded | 9 | L-V | 20 | isolated | I | common | 337.2 | | | | |
| S66 | 1 | Calcite | triangular | 9 | L-V | 20 | isolated | I | rare | 321.6 | | | | |
| S66 | 2 | Calcite | elongated | 8 | L-V | 15 | isolated | I | rare | 328.0 | | | | |
| S66 | 3 | Calcite | oval | 6 | L-V | 5 | isolated | I | rare | 327.8 | | | | |
| S20 | 1 | Fluorite | equant | 15 | L-V | 20 | isolated | I | common | 304.2 | | | | |
| S20 | 2 | Fluorite | rounded | 20 | L-V | 15 | isolated | I | common | 292.0 | -16.5 | | | 19.84 |
| S20 | 3 | Fluorite | equant | 10 | L-V | 15 | isolated | I | common | 299.9 | -16 | | | 19.45 |
| S20 | 4 | Fluorite | equant | 15 | L-V-D | 40 | isolated | II | common | 315.5 | -8.5 | | | 12.28 |
| S20 | 5 | Fluorite | equant | 12 | L-V | 15 | isolated | I | common | 331.4 | | | | |
| S20 | 6 | Fluorite | elongated | 6 | L-V | 20 | isolated | I | common | 297.8 | | | | |
| S20 | 1 | Quartz | elongated | 18 | L-V | 5 | isolated | I | common | 332.7 | - | | | |
| S20 | 2 | Quartz | spherical | 5 | L-V | 25 | isolated | I | common | 350.4 | - | | | |
| S20 | 3 | Quartz | equant | 9 | L-V | 25 | isolated | I | common | - | - | 1.2 | | 14.22 |
| S20 | 4 | Quartz | equant | 16 | L-V | 25 | cluster | I | common | 350.0 | -11 | | | 14.97 |
| S20 | 5 | Quartz | elongated | 15 | L-V | 30 | isolated | I | common | 357.8 | - | | | |
| S20 | 6 | Quartz | elongated | 12 | L-V | 10 | isolated | I | common | 322.5 | - | | | |
| S20 | 7 | Quartz | elongated | 12 | L-V | 25 | isolated | I | common | - | - | 1.9 | | 13.38 |
| S20 | 8 | Quartz | elongated | 12 | L-V | 20 | isolated | I | common | 359.0 | - | | | |
| S45 | 1 | Quartz | round | 9 | L-V | 20 | cluster | I | common | 295.8 | | | | |
| S45 | 2 | Quartz | round | 12 | L-V | 30 | | I | common | 303.3 | | | | |
| S45 | 3 | Quartz | elongated | 12 | L-V | 15 | cluster | I | common | 322.6 | | | | |
| S45 | 4 | Quartz | elongated | 9 | L-V | 25 | cluster | I | common | 316.6 | | | | |
| S45 | 5 | Quartz | elongated | 10 | L-V | 15 | cluster | I | common | 310.5 | | 0.2 | | 15.31 |
| S45 | 6 | Quartz | triangular | 25 | L-V | 20 | isolated | I | common | 308.8 | | 0.3 | | 15.21 |

**S. No:** Sample number; **FI No:** Serial number of fluid inclusion in a mineral; **L:** Liquid; **V:** Vapour; **D:** Daughter mineral; **Th:** Temperature of homogenisation into liquid phase; **Tm:** Temperature of last ice melting; **Tmf:** Temperature of first ice melting; **Tm-cl:** Clathration temperature.

## APPENDIX V. Continued.

| S. No. | FI No. | Host mineral. | Shape | Length (μm) | Phases | % Vapour | Occurrence | Type | Abundance | Th (°C) | Tm (°C) | Tm-cl (°C) | Tmf (°C) | Salinity |
|---|---|---|---|---|---|---|---|---|---|---|---|---|---|---|
| S45 | 7 | Quartz | rectangular | 15 | L-V | 15 | isolated | I | common | 308.1 | | 0.2 | | 15.31 |
| S45 | 8 | Quartz | round | 6 | L-V | 10 | isolated | I | common | 315.7 | | | | |
| S45 | 9 | Quartz | elongated | 34 | L-V | 10 | isolated | I | common | 322.6 | | | | |
| S45 | 10 | Quartz | equant | 9 | L-V | 20 | isolated | I | common | 327.2 | | | -37.0 | |
| S45 | 11 | Quartz | elongated | 25 | L-V | 15 | isolated | I | common | 303.7 | | | | |
| S45 | 12 | Quartz | rounded | 9 | L-V | 20 | isolated | I | common | 295.8 | | | | |
| S45 | 13 | Quartz | rounded | 15 | L-V | 25 | isolated | I | common | 306.9 | | | | |
| S45 | 14 | Quartz | rounded | 6 | L-V | 25 | isolated | I | common | | | | | |
| S45 | 15 | Quartz | rounded | 6 | L-V | 15 | isolated | I | common | | | | | |
| S45 | 16 | Quartz | rounded | 6 | L-V | 25 | isolated | I | common | | | | | |
| S45 | 17 | Quartz | rounded | 12 | L-V | 30 | isolated | I | common | | | 1.0 | | 14.44 |
| S200 | 1 | Scheelite | elongated | 19 | L-V | 15 | isolated | | common | 305.1 | | | | |
| S127 | 1 | Scheelite | oval | 9 | L-V | 10 | isolated | I | rare | 236.7 | | | | |
| S127 | 2 | Scheelite | equant | 6 | L-V | 15 | isolated | I | rare | | -0.6 | | | 1.05 |
| S127 | 3 | Scheelite | triangular | 6 | L-V | 10 | isolated | I | rare | 262.0 | | | | |
| S201 | 1 | Fluorite | irregular | 12 | L-V | 40 | isolated | I | common | 318.1 | | | | |
| S201 | 2 | Fluorite | spherical | 16 | L-V | 20 | isolated | I | common | 287.3 | | | | |
| S201 | 3 | Fluorite | elongated | 31 | L-V | 15 | isolated | I | common | 271.2 | | | | |
| S201 | 4 | Fluorite | flat | 15 | L-V | 20 | isolated | I | common | 302.6 | -0.4 | | | 0.70 |
| S201 | 5 | Fluorite | amoeboidal | 77 | L-V | 30 | isolated | I | common | 315.8 | -0.1 | | | 0.18 |
| S201 | 6 | Fluorite | elongated | 18 | L-V | 15 | isolated | I | common | 298.8 | | | | |
| S201 | 7 | Fluorite | spherical | 15 | L-V | 15 | isolated | I | common | 305.5 | | | | |
| S201 | 8 | Fluorite | spherical | 15 | L-V | 20 | isolated | I | common | 309.3 | | | | |
| S201 | 9 | Fluorite | elongated | 21 | L-V | 20 | isolated | I | common | 318.5 | -3.2 | | | 5.26 |
| S201 | 10 | Fluorite | spherical | 16 | L-V | 35 | isolated | I | common | 336.6 | -3.2 | | | 5.26 |
| S201 | 11 | Fluorite | spherical | 12 | L-V | 20 | isolated | I | common | 342.2 | -3.2 | | | 5.26 |
| S201 | 12 | Fluorite | elongated | 28 | L-V | 30 | isolated | I | common | 336.6 | -2.8 | | | 4.65 |
| S201 | 13 | Fluorite | amoeboidal | 35 | L-V | 15 | isolated | I | common | 326.7 | -2.8 | | -30.0 | 4.65 |
| S201 | 14 | Fluorite | equant | 45 | L-V | 20 | isolated | I | common | | -0.4 | | -15.0 | 0.70 |

**S. No:** Sample number; **FI No:** Serial number of fluid inclusion in a mineral; **L:** Liquid; **V:** Vapour; **D:** Daughter mineral; **Th:** Temperature of homogenisation into liquid phase; **Tm:** Temperature of last ice melting; **Tmf:** Temperature of first ice melting; **Tm-cl:** Clathration temperature.

## APPENDIX V. Continued.

| S. No. | FI No. | Host mineral. | Shape | Length (μm) | Phases | % Vapour | Occurrence | Type | Abundance | Th (°C) | Tm (°C) | Tm-cl (°C) | Tmf (°C) | Salinity |
|---|---|---|---|---|---|---|---|---|---|---|---|---|---|---|
| S202 | 1 | Scheelite | equant | 6 | L-V | | isolated | I | common | 606.7 | | | | |
| S202 | 2 | Scheelite | equant | 12 | L-V | 15 | isolated | I | common | 264.4 | | | | |
| S202 | 3 | Scheelite | equant | 12 | L-V | 15 | isolated | I | common | 258.8 | | | | |
| S202 | 4 | Scheelite | amoeboidal | 15 | L-V | 10 | isolated | I | common | 272.7 | | | | |
| S202 | 5 | Scheelite | amoeboidal | 6 | L-V | 15 | isolated | I | common | 265.6 | | | | |
| S202 | 6 | Scheelite | elongated | 12 | L-V | 15 | isolated | I | common | 261.8 | | | | |
| S202 | 7 | Scheelite | elongated | 15 | L-V | 15 | isolated | I | common | 265.7 | | | | |
| S202 | 8 | Scheelite | equant | 6 | L-V | 30 | isolated | I | common | 288.5 | -9.6 | | | 13.51 |
| S202 | 9 | Scheelite | elongated | 22 | L-V | 20 | isolated | I | common | 274.1 | -6.6 | | | 9.98 |
| S202 | 10 | Scheelite | elongated | 6 | L-V | 25 | isolated | I | common | 272.2 | -8 | | | 11.70 |
| S202 | 11 | Scheelite | elongated | 6 | L-V | 15 | isolated | I | common | 261.5 | -7.2 | | | 10.73 |
| S202 | 12 | Scheelite | equant | 21 | L-V | 10 | isolated | I | common | 300.3 | -2.2 | | | 3.71 |
| S202 | 13 | Scheelite | elongated | 31 | L-V | 15 | isolated | I | common | 273.2 | -7.6 | | | 11.22 |
| S202 | 14 | Scheelite | equant | 34 | L-V | 20 | isolated | I | common | 263.6 | -7.4 | | -36.6 | 10.98 |
| S202 | 15 | Scheelite | amoeboidal | 16 | L-V | 15 | isolated | I | common | 265.5 | -8 | | | 11.70 |
| S202 | 16 | Scheelite | equant | 19 | L-V | 30 | isolated | I | common | 264.5 | -3.3 | | | 5.41 |
| S202 | 17 | Scheelite | rounded | 28 | L-V | 30 | isolated | I | common | 287.0 | -2.8 | | -31.5 | 4.65 |
| S202 | 18 | Scheelite | equant | 11 | L-V | 5 | isolated | I | common | 264.0 | -5.6 | | | 8.68 |
| S202 | 19 | Scheelite | irregular | 9 | L-V | 15 | isolated | I | common | 269.0 | -14.6 | | | 18.30 |
| S202 | 20 | Scheelite | equant | 5 | L-V | 15 | isolated | I | common | 280.9 | -15.5 | | | 19.05 |
| S202 | 21 | Scheelite | equant | 6 | L-V | 15 | isolated | I | common | 300.5 | -12.6 | | | 16.53 |
| S178 | 1 | Calcite | equant | 13 | L-V (-$CO_2$) | 20 | isolated | III | common | 338.0 | -2.5 | -2.5 | | 4.18 |
| S178 | 2 | Calcite | rounded | 15 | L-V (-$CO_2$) | 20 | isolated | III | common | 335.0 | -3 | -3.0 | | 4.96 |
| S178 | 3 | Calcite | equant | 13 | L-V | 25 | isolated | I | common | 308.0 | -3 | 3.0 | | 4.96 |
| S178 | 4 | Calcite | elongate | 21 | L-V | 15 | isolated | I | common | 319.0 | | | | |
| S178 | 5 | Calcite | irregular | 25 | L-V | 25 | isolated | I | rare | 337.0 | | | | |
| S178 | 6 | Calcite | elongate | 16 | L-V | 20 | isolated | I | common | 334.4 | | | | |
| S182 | 1 | Calcite | rounded | 10 | L-V | 15 | Isolated | I | rare | 331.9 | -2 | -2.0 | | 3.39 |
| S182 | 2 | Calcite | rounded | 4 | L-V | 30 | isolated | I | rare | 293.8 | -2 | -2.0 | | 3.39 |
| S182 | 3 | Calcite | oval | 6 | L-V | 10 | isolated | I | rare | 337.3 | | | | |

**S. No:** Sample number; **FI No:** Serial number of fluid inclusion in a mineral; **L:** Liquid; **V:** Vapour; **D:** Daughter mineral; **Th:** Temperature of homogenisation into liquid phase; **Tm:** Temperature of last ice melting; **Tmf:** Temperature of first ice melting; **Tm-cl:** Clathration temperature.

## APPENDIX V. Continued.

| S. No. | FI No. | Host mineral. | Shape | Length (μm) | Phases | % Vapour | Occurrence | Type | Abundance | Th (°C) | Tm (°C) | Tm-cl (°C) | Tmf (°C) | Salinity |
|---|---|---|---|---|---|---|---|---|---|---|---|---|---|---|
| S208 | 1 | Scheelite | oval | 9 | L-V | 9 | clusters | I | common | 315.0 | -14.3 | | | 18.04 |
| S208 | 2 | Scheelite | spherical | 5 | L-V | 20 | clusters | I | common | 310.0 | | | | |
| S208 | 3 | Scheelite | spherical | 6 | L-V | 20 | clusters | I | common | 331.4 | | | | |
| S208 | 4 | Scheelite | spherical | 5 | L-V | 15 | clusters | I | common | 303.3 | | | | |
| **GRANITE QUARTZ** | | | | | | | | | | | | | | |
| S34 | 1 | Quartz | rounded | 3 | L-V | 5 | isolated | I | rare | >565 | | | | |
| S34 | 2 | Quartz | triangular | 12 | L-V | 10 | trail | IV | common | 234.0 | | | | |
| S34 | 3 | Quartz | elongated | 9 | L-V | 15 | trail | IV | common | 234.6 | -0.1 | | -54.9 | 0.18 |
| S34 | 4 | Quartz | irregular | 7 | L-V | 15 | trail | IV | common | 264.0 | | | | |
| S34 | 5 | Quartz | equant | 12 | L-V | 15 | trail | IV | common | 321.1 | -24.9 | | -41.0 | 25.52 |
| S34 | 6 | Quartz | rounded | 7 | L-V | 10 | trail | IV | common | 332.2 | -21.7 | | | 23.50 |

**S. No:** Sample number; **FI No:** Serial number of fluid inclusion in a mineral; **L:** Liquid; **V:** Vapour; **D:** Daughter mineral; **Th:** Temperature of homogenisation into liquid phase; **Tm:** Temperature of last ice melting; **Tmf:** Temperature of first ice melting; **Tm-cl:** Clathration temperature.

**APPENDIX VI. Thermally decrepitated mass spectrometric chromatographs of fluid inclusion volatiles for Stages I-III skarn minerals from the Kara deposit, northwestern Tasmania.**

**A. Stage I clinopyroxene (sample number S36)**

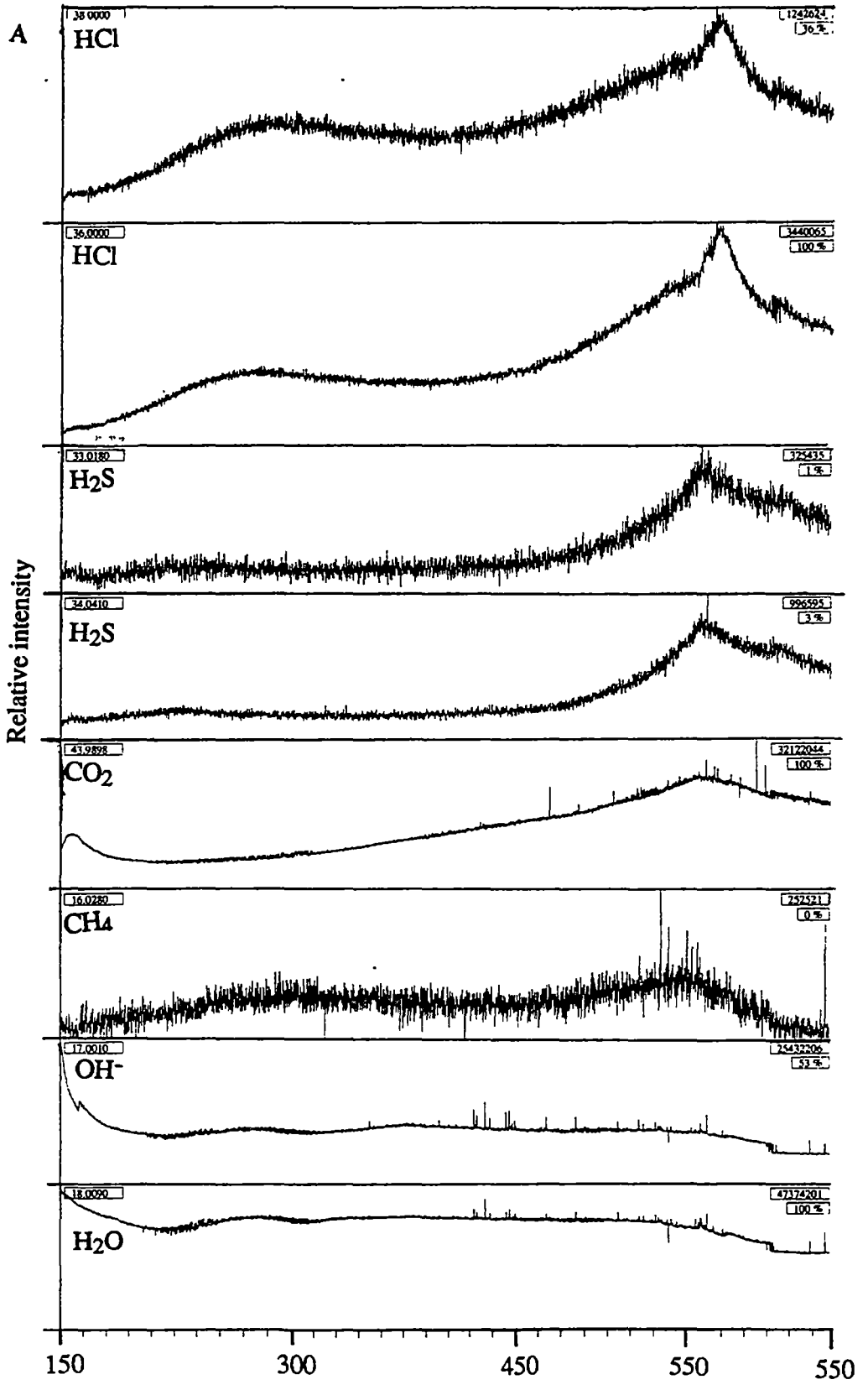

**APPENDIX VI. Continued.**

**B. Stage II garnet (sample number S16).**

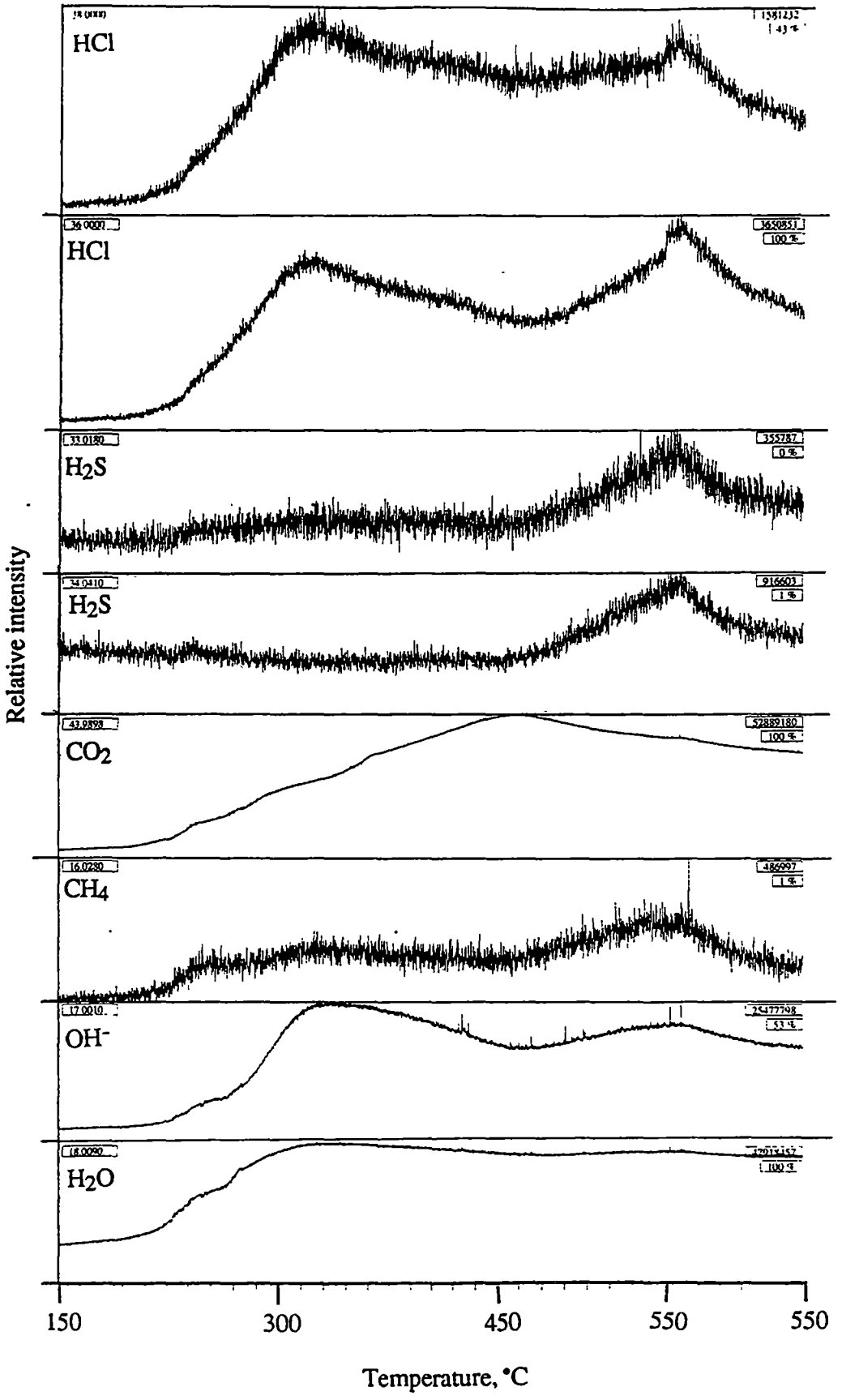

**PENDIX VI. Continued.**

**C. Stage II vesuvianite (sample number S113).**

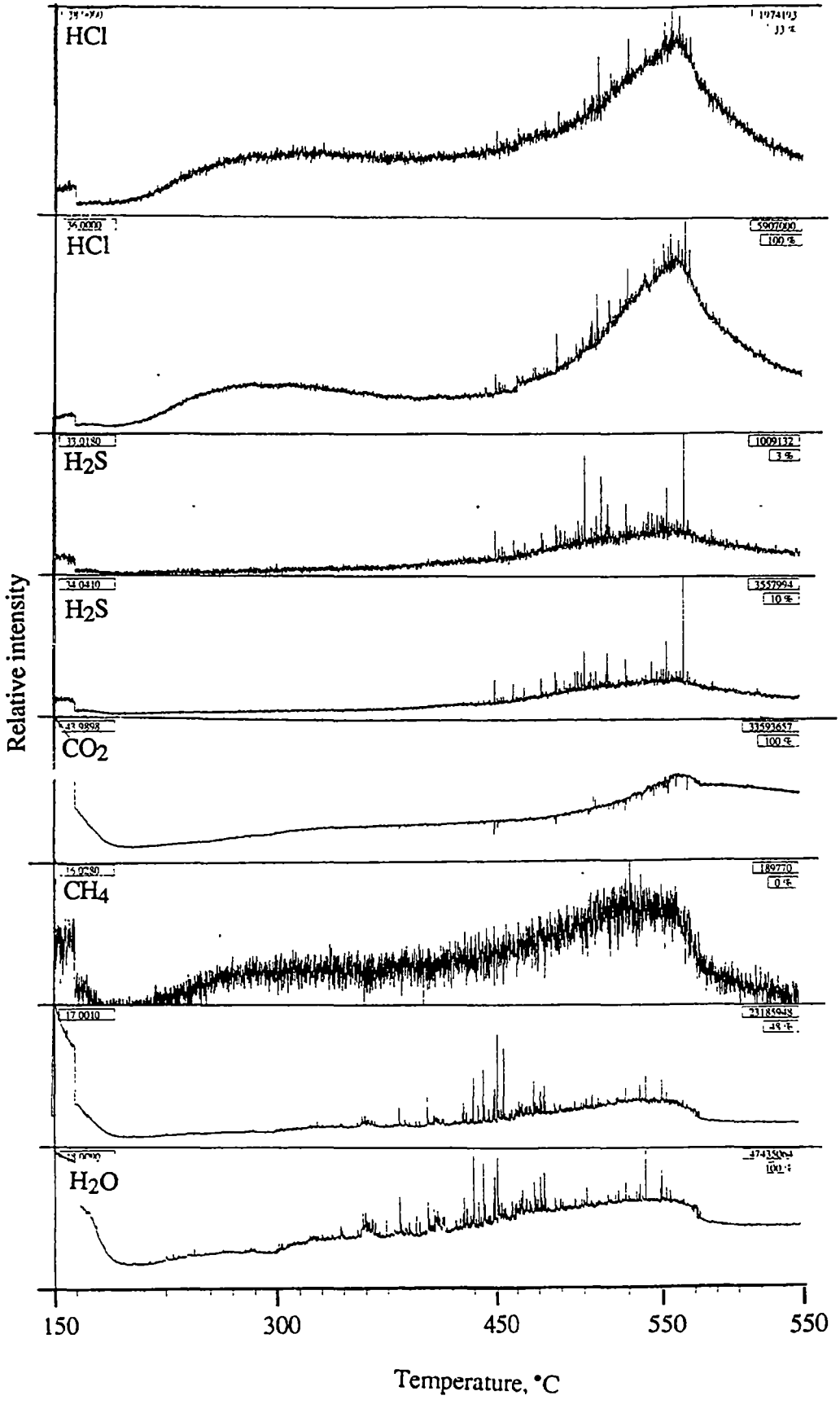

**APPENDIX VI. Continued.**

**D. Stage III magnetite (sample number S82).**

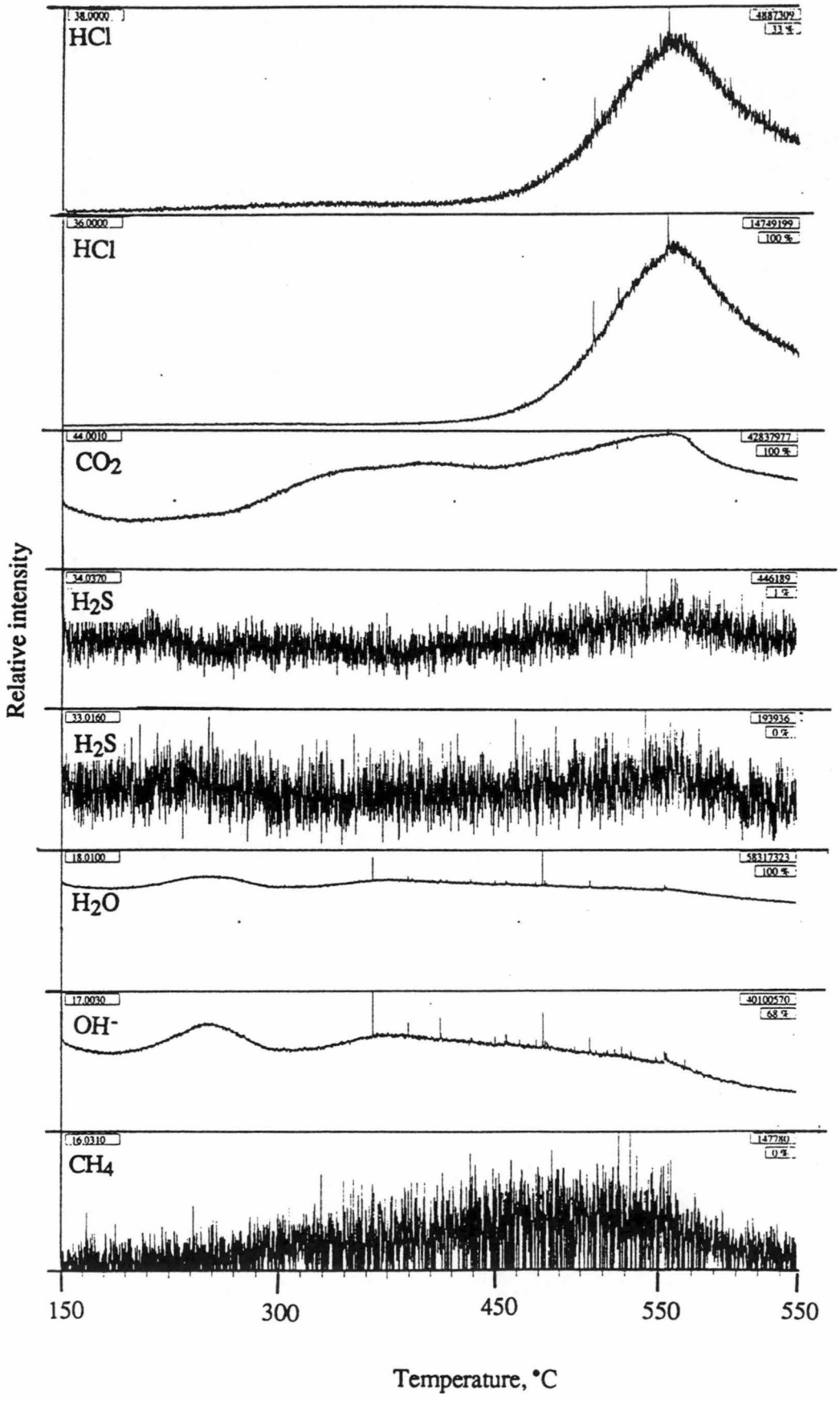

**APPENDIX VI. Continued.**

**E. Stage III scheelite (sample number S127).**

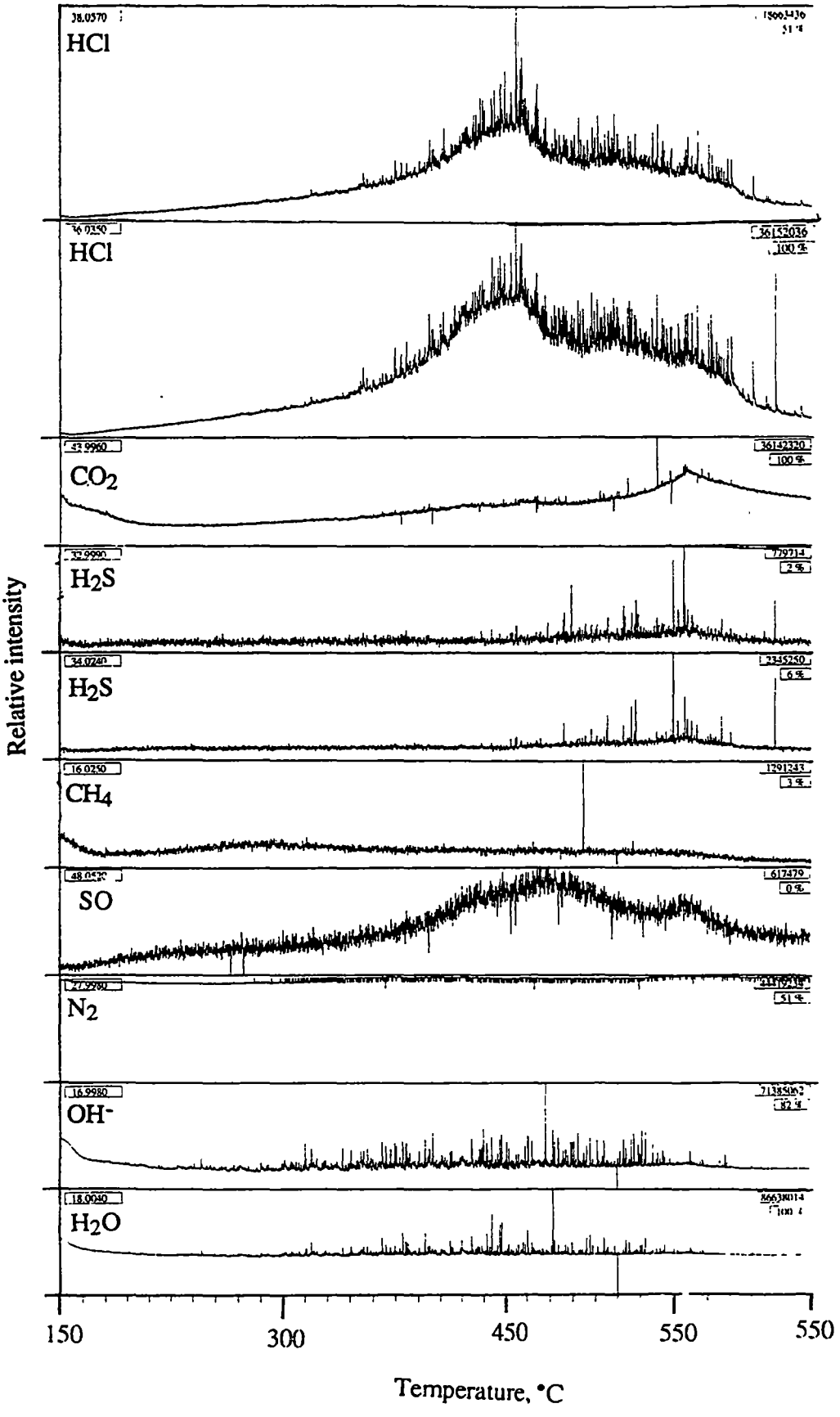

**APPENDIX VI. Continued.**

**F. Stage III calcite (sample number S182).**

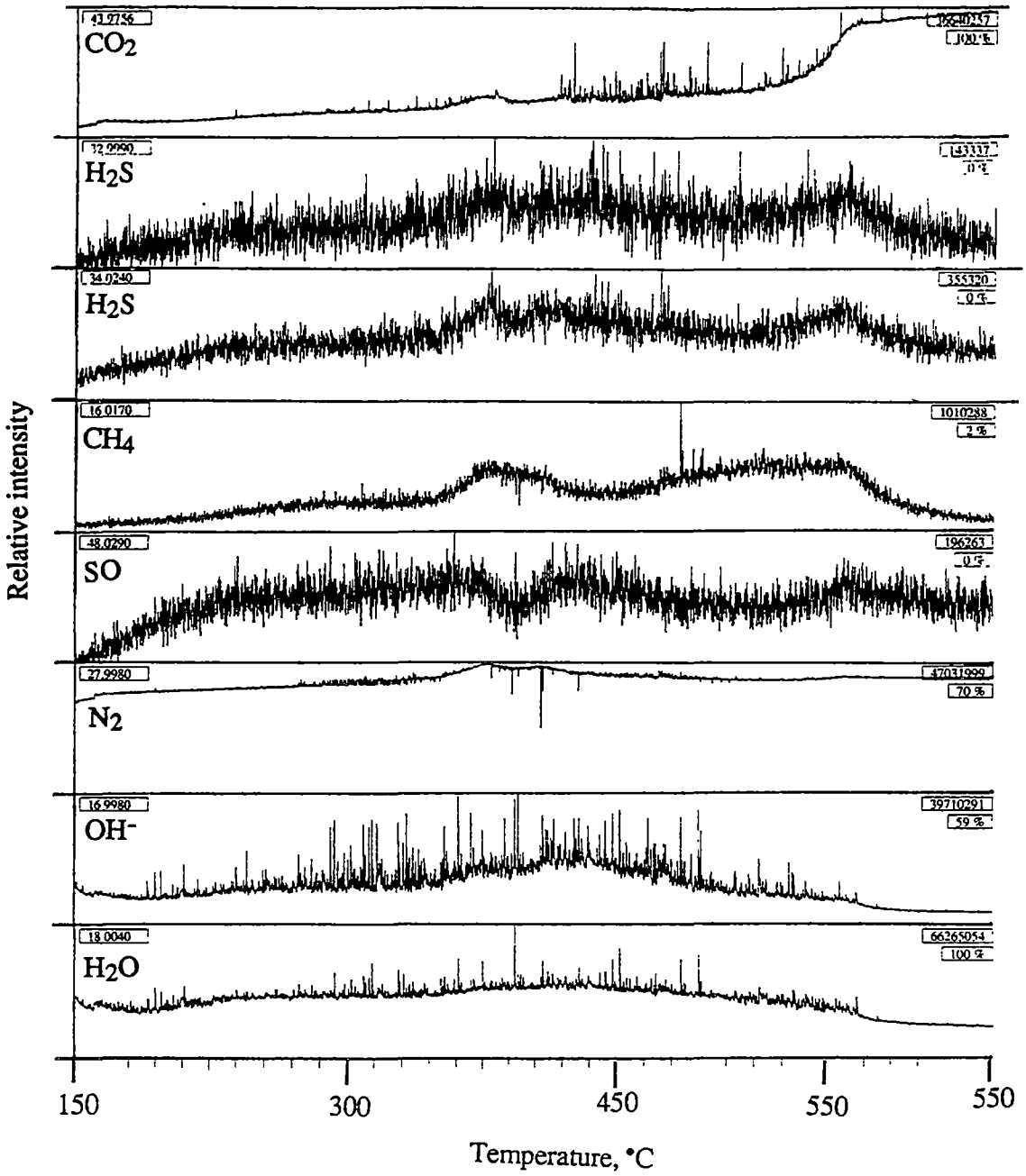

**APPENDIX VI. Continued.**

**G. Stage III fluorite (sample number S17).**

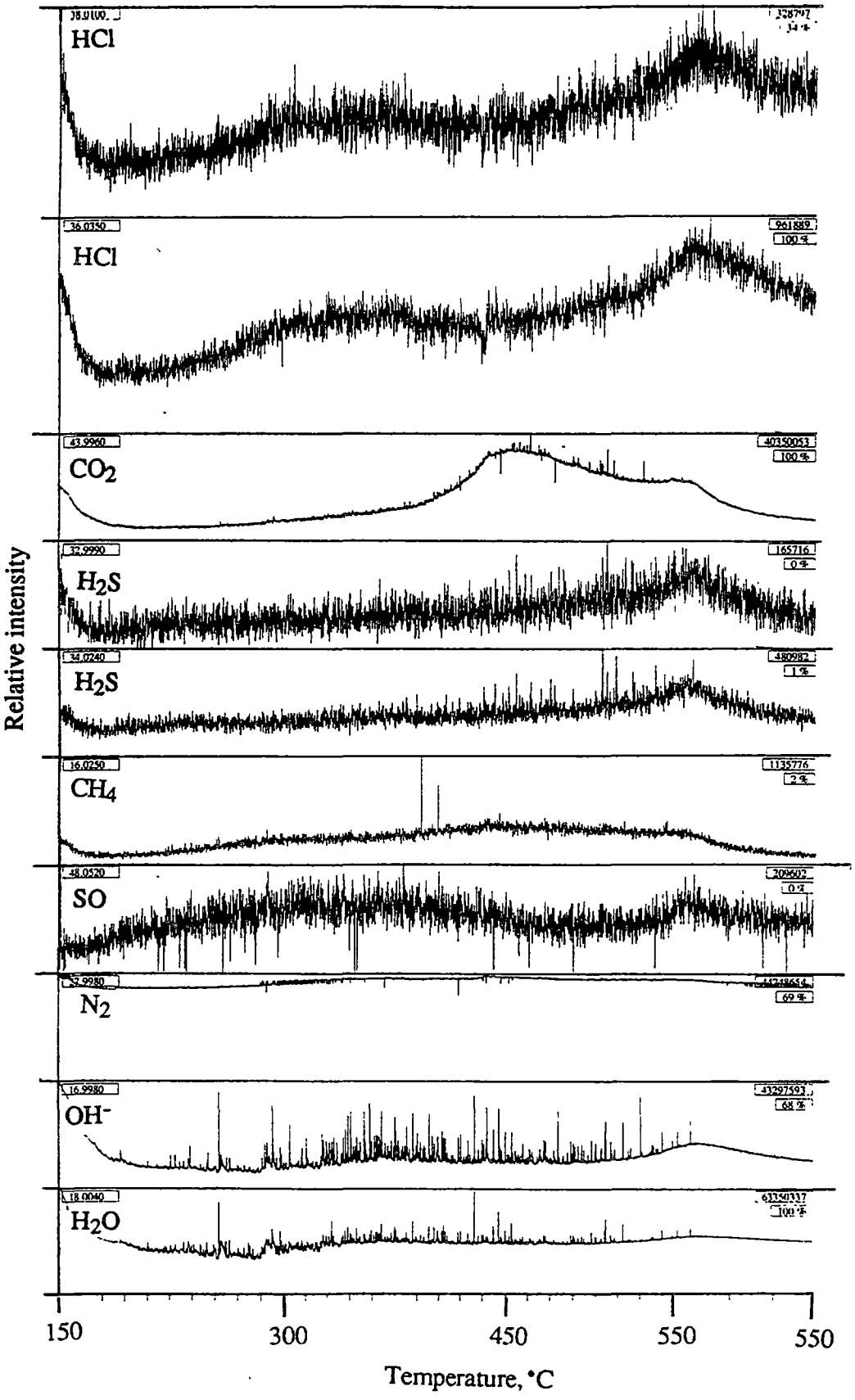

**APPENDIX VI. Continued.**

**H. Stage III quartz-epidote (sample number S18).**